ADAPTIVE TECHNIQUES FOR CYCLOSTATIONARY SPECTRUM SENSING IN COGNITIVE RADIOS

Ph.D. THESIS

by

RIBHU

DEPARTMENT OF ELECTRONICS AND COMMUNICATION ENGINEERING
INDIAN INSTITUTE OF TECHNOLOGY ROORKEE
ROORKEE - 247 667 (INDIA)

JULY, 2015

ADAPTIVE TECHNIQUES FOR CYCLOSTATIONARY SPECTRUM SENSING IN COGNITIVE RADIOS

A THESIS

Submitted in partial fulfillment of the
requirements for the award of the degree
of
DOCTOR OF PHILOSOPHY
in
ELECTRONICS AND COMMUNICATION ENGINEERING

by
RIBHU

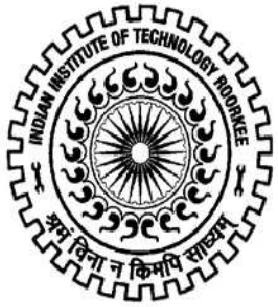

DEPARTMENT OF ELECTRONICS AND COMMUNICATION ENGINEERING
INDIAN INSTITUTE OF TECHNOLOGY ROORKEE
ROORKEE - 247 667 (INDIA)
JULY, 2015

INDIAN INSTITUTE OF TECHNOLOGY ROORKEE
ROORKEE

CANDIDATE'S DECLARATION

I hereby certify that the work which is being presented in the thesis entitled **"Adaptive Techniques for Cyclostationary Spectrum Sensing in Cognitive Radios"** in partial fulfilment of the requirements for the award of the Degree of Doctor of Philosophy and submitted in the Department of **Electronics and Communication Engineering** of Indian Institute of Technology Roorkee, Roorkee is an authentic record of my own work carried out during a period from **December, 2011** to **July, 2015** under the supervision of **Dr. Debashis Ghosh**, Associate Professor, and **Prof. D. K. Mehra**, Professor(Retired), **Department of Electronics and Communication Engineering**, Indian Institute of Technology Roorkee, Roorkee, India.

The matter presented in this thesis has not been submitted by me for the award of any other degree of this or any other Institute.

(RIBHU)

This is to certify that the above statement made by the candidate is correct to the best of our knowledge.

(D.K. Mehra) (Debashis Ghosh)

Supervisor Supervisor

Date:

To Mama Ji,
to my parents,
and
to Mehra Sir.

Acknowledgment

First of all I would like to express my immense gratitude to my supervisors, Prof. D. K. Mehra and Dr. D. Ghosh, for their generous encouragement, insightful comments, and an almost infectious zest for learning. But most of all for showing confidence in me when I had lost it in myself and for slowing me down when I was overconfident of success.

The working facilities provided by the Head I think names of all should be given, Department of Electronics and Communication Engineering IIT Roorkee are highly acknowledged. I also thank Mahendra Ji and Anand Ji, members of Technical staff of signal processing lab for up-to-the-mark maintenance of the lab during six years of my M.Tech and Ph. D. I am obliged to MHRD, Government of India, for the financial support in the form of fellowship.

I am indebted to Mr. S. Chakravorty for all the things technical and non-technical he has taught me during these six years. It is amazing that how every interaction with him can be a great learning experience. I am grateful to my SRC members, Dr. Vinod Pankajakshan, Prof. Manoj Misra, Prof. Dharmendra Singh, and Prof. Tanuja Srivastava for their time and valuable suggestions. I am also beholden to Prof M.J. Nigam, Dr. P. M. Pradhan, and Dr. Brijesh Kumar for all the personal interest they have shown in me and in this thesis.

As for my work, I originally had some wild ideas about spectrum sensing. However, my discussions with my co-spectrum sensors, Hemant, Gaurav, and Aditya made me realize the different ways in which I could look at this problem and made me develop some ideas. A few of these wild ideas were actually tested by Anshuka and Ipsita, who deserve special credit for trusting me with their B. Tech. Project. Also, the lab would have been a considerably duller place without Sudarshan, Giri, Karan, Prateek, and Neeraj; each of whom contributed to making my work more interesting. I would be failing my duty by not listing the commendable support provided by Anupam Sir, Bhawna, Bhuwan, Shravan, Shriya, and Tarlochan outside the lab. This thesis would not have been possible without all the walks, talks and junk food that I had with these people.

This acknowledgment cannot be complete without the mention of all the affection and the great home-cooked food fed to me several times by Mrs. Mehra and Mrs. Ghosh. It was indeed a privilege to be treated as an equal by Abhigyan and as an elder brother by Archishman.

Mobile phones have made this world a small place. One of the best things about these

little devices is that, you can have long pointless conversations with your friends. For this, I would especially like to thank Anu, Jyoti, Kinshuk, Manisha, Neha, Neha (both of them), Paramvir, Rahul, Ruchika, Sakshi, Sameera, Shashikant, Sudheer, Vandana, and Yogeshwar for all their encouraging words, and the food for thought.

Finally, I would like to record my gratefulness to my family, for their love, for allowing me to pursue my dream, and for their support of all my decisions, even the whimsical ones

Ribhu

List of Acronyms

ACS	Adaptive Cross SCORE
ATC	Adapt Then Combine
AWGN	Additive White Gaussian Noise
BEP	Bit Error Probability
BPSK	Binary Phase Shift Keying
BA-FRESH	Blind Adaptive FRESH
C2-LMS	Constrained Doubly adaptive LMS
CAB	Cyclic Adaptive Beamforming
CFAR	Constant False Alarm Rate
CFO	Cyclic Frequency Offset
CR	Cognitive Radio
CRLB	Crammer Rao Lower Bound
CU	Cognitive User
DFT	Discrete Fourier Transform
DTV	Digital Television
ED	Energy detection
FC	Fusion Centre
FCC	Federal Communications Commission
FFT	Fast Fourier Transform
FRESH	FREquency SHift
GLRT	Genralized Liklihood Ratio Test
GMSK	Gaussian Minimum Shift Keying
GSM	Global System for Mobile Communications
IID	Independent and Identically Distributed
LMS	Least Mean Sqaures
LPTV	Linear Perodically Time Varying
LS	Least Squares
LTE	Long-Term Evolution
LU	Licenced User
MIMO	Multiple Input Multiple Output
ML	Maximum Liklihood

MMSE	Minimum Mean Square Error
MTM	Multi Taper Method
OFDM	Orthogonal Frequency Division Multiplexing
OSA	Opeertunistic Spectrum Access
PSD	Power Spectral Density
QAM	Quadrature Amplitude Modulation
QPSK	Quadrature Phase Shift Keying
RAT	Radio Access Technology
RLS	Recursive Least Squares
SCORE	Spectral COherance REstoral
SNR	Signal to Noise Ratio
WiMAX	Worldwide Interoperability for Microwave Access
WLAN	Wireless Local Area Network
WRAN	Wireless Regional Area Networks

Notation

Boldface lowercase letters denote vectors
Boldface uppercase letters denote matrices

$\nabla_{\mathbf{x}}$	Gradient with respect to the vector $\mathbf{x}$
$\Re$	Real part of a complex number
$\Im$	Imaginary part of a complex number
$\lfloor . \rfloor$	Floor operation, returns the greatest integer less than or equal to the argument.
$(.)^*$	Complex conjugate of a complex number
$[.]$	Discrete valued independent variable
$(.)$	Continuous valued independent variable
$((.))_L$	Modulo-L operation, returns the remainder after dividing the argument by L.
$\|.\|$	Returns the absolute value of scaler arguments and Cardinality of sets
$\|\|.\|\|$	The Euclidean norm of a vector
α	Non-conjugate cyclic frequency of a cyclostationary signal, unless specified
β	Conjugate cyclic frequency of a cyclostationary signal, unless specified
$\delta[.]$	The Kronecker Delta function
$\delta(.)$	The Dirac Delta function
γ_i	Input SNR
γ_o	Output SNR
Δ	Cyclic Frequency Offset (CFO)
φ	Rayleigh fading coefficient
$\varphi[n]$	Impulse response of a dispersive multi-path channel
$\boldsymbol{\varphi}$	Vector equivalent of the impulse response of a multi-path channel
λ	The detection threshold
μ	Adaptation step size
$\nu[n]$	Zero Mean Circularly Symmetric Complex Additive white Gaussian noise
σ_x^2	Variance of the random variable x
$a_\alpha[l]$	Regression coefficient of a cyclostationary signal for cyclic frequency α and lag l
$\mathbf{A}^T$	Transpose of a matrix $\mathbf{A}$

$\mathbf{A}^H$	Hermitian (conjugate transpose) of a matrix $\mathbf{A}$
$\mathcal{A}$	The set of cyclic frequencies of a signal.
$e[n]$	The adaptation error
$E[.]$	The Expectation Operation
$\mathcal{H}_0$	The null hypothesis
$\mathcal{H}_1$	The alternate hypothesis
$\mathbf{h}$	The control vector of a multi antenna array, unless specified
$\mathbf{I}_N$	The $N \times N$ identity matrix
$I(x)$	Fisher Information matrix for the variable x
$J(.)$	Cost Function
K	Number of antennas in a Multi-antenna system or The number of collaborating users for collaborative spectrum sensing
L	The number of temporal taps on a FRESH filter branch
L_B	Length of a CFO search block
M	Number of frequency shift branches in a FRESH filter
N	Number of samples being used for sensing
N_c	Cyclic prefix length for an OFDM symbol
N_d	Number of sub-carriers in an OFDM symbol
N_p	Number of pilot sub-carriers in an OFDM symbol
N_s	Overall length of an OFDM symbol
$\mathcal{N}_c(m, \sigma^2)$	Complex Gaussian distribution with mean m and variance σ^2
$\mathcal{O}()$	Of the order of
P_d	Probability of detection
P_{fa}	Probability of false alarm
$Pr.$	Probability of the argument
$Q(.)$	The Marcum Q function
$R_{xx}^{\alpha}[\tau]$	Cyclic autocorrelation function of the signal $x[n]$ at cyclic frequency α and lag τ
$R_{xx^*}^{\beta}[\tau]$	Conjugate Cyclic autocorrelation function of the signal $x[n]$ at cyclic frequency α and lag τ
$\hat{R}_{xx}^{\alpha}[N, \tau]$	Finite time approximate cyclic autocorrelation function of the signal $x[n]$ at cyclic frequency α and lag τ for N samples
$\mathbf{R}_{xx}^{\alpha}[\tau]$	Cyclic autocorrelation matrix of the vector $\mathbf{x}[n]$ at cyclic frequency α and lag τ
$Rice(a, b)$	Rice distribution with a shift a and scaling factor b
$s[n]$	The primary user signal, unless specified
$s^{\alpha}[n]$	$s[n]$ shifted by a frequency α
$\tilde{s}[m]$	The mth sub-carrier of an OFDM symbol

$s^{(p)}[n]$	Pilot component of an OFDM symbol $s[n]$
$s^{(d)}[n]$	Data component of an OFDM symbol $s[n]$
$S_{xx}^{\alpha}(f)$	Cyclic spectral density for the signal x at cyclic frequency α and frequency f
$\mathbf{u}[n]$	The regression vector input to an adaptive filter
$var(.)$	Variance of the argument
$\mathbf{w}$	The weight vector
$\mathbf{w}_o$	The optimal weight vector
$\mathbf{w}[n]$	Adaptive weight vector at the nth iteration
$\tilde{\mathbf{w}}[n]$	weight error vector at the nth iteration

Abstract

Cognitive or environment aware radio has emerged as one of the major technologies to improve the utilization of the limited communication spectrum. The cognition cycle proposed in the literature for an environment aware radio entails the tasks of spectrum sensing, spectrum allocation and reliable transmission. Out of these, spectrum sensing has emerged as an active area of research during the past decade. This involves the detection of primary user or licensed user signals in order to determine the availability of a spectrum band for transmission. Two major challenges faced by spectrum sensing algorithms are very low SNRs of the order of -22 dB; and a limited knowledge about the signal to be sensed.

It is known that the energy detector is the optimal detector for random signals. However, this is known to fail under low SNRs when the noise power is not known correctly. Therefore, it becomes important to look for alternative approaches for spectrum sensing. Several spectrum sensing algorithms based on the cyclostationarity or spectral coherence of the primary user signal have been proposed during the past years. It has been established that cyclostationarity of a signal may be used to detect as well to as enhance it. Optimal filters to enhance cyclostationary signals have also been derived. These filters are observed to exhibit a FRESH (FREquency SHift) structure. Cyclostationarity has also been employed for the purpose of antenna array beam-forming.

In the past, both FRESH filtering as well as cyclostationary beam-forming have been used to enhance cyclostationary signals prior to detection. The first problem that we consider in this thesis is a combination of these two approaches. We propose a Space-Time FRESH filtering structure to enhance the primary user signal by exploiting its spatial, temporal and spectral coherence. The proposed structure is made adaptive to adjust its weights as per the primary signal of interest. The Adaptive Cross SCORE (ACS) algorithm put forward in literature is modified to adapt the proposed structure, and a spectrum sensing algorithm is subsequently developed. However, the resulting algorithm has a complexity of the order of $\mathcal{O}((KLM)^2)$ for K antennas, M frequency shift branches per antenna, and L temporal taps per branch. This is observed to act as a bottleneck in the spectrum sensing procedure. Therefore, we formulate the correlation maximization problem of the ACS algorithm as a constrained MMSE problem to develop a constrained doubly adaptive LMS (C2-LMS) algorithm. It is then shown, using simulation techniques, that the proposed structure, adapted using the proposed algorithm, may result in gains of as much as 10 dB

over conventional Energy and Cyclostationarity detectors.

Following this, we study the performance enhancement achieved in conventional spectrum sensing systems by FRESH filtering the signal prior to the detection stage. A quasi-analytical theory of spectrum sensing based on FRESH filtering is developed. A quasi-analytical approach is required because the variance of the test statistics is found to have an intractable form and should, therefore, be determined empirically. Bounds on this variance have however been derived. It is shown that significant performance gains are achievable in both energy detection and cyclostationarity detection via FRESH filtering of the received signal prior to the detection step. It is observed that FRESH filtering may reduce the number of samples required to achieve a given detection performance by more than 90% in practice, thereby reducing the sensing time in a cognitive radio system. It is also shown that the FRESH filtering before energy detection may reduce the effects of SNR walls caused due to noise uncertainty. The validity of all the derived observations is confirmed via simulations.

It has been shown that multi-path fading and shadowing may affect the performance of a single-user spectrum sensing adversely. It is, however, possible to improve the sensing performance in such cases by employing multi-user diversity, that is, collaboration among multiple sensing nodes. It may be argued that if FRESH filtering leads to performance improvement in a single-user, it should also enhance the detection performance of multiple collaborating users. Hence, we consider the problem of spectrum sensing with multiple collaborating users, each equipped with a FRESH filter. In this case, FRESH filtering or Space-Time FRESH filtering may be used to boost the performance of each individual user, thereby improving the overall detection performance of the system. Here, we consider three models of collaboration viz. centralized, distributed and hierarchical. It is argued that the performance of collaborative FRESH filter-based spectrum sensing can be improved further if the collaborating users adapt their filter weights jointly. It is shown using simulations that joint adaptation results in gains of as much as 2 dB over local adaptation in addition to the gains offered by the FRESH filters. Simulation results are also used to compare the performance of the different collaboration schemes and it is observed that there is a slight degradation in the performance of the proposed sensing technique as the system moves from a purely centralized setting to a purely distributed setting.

In all the problems discussed above, we assume a perfect knowledge of the cyclic frequency at the spectrum sensor. However, this may not always be true. Phenomena such as Doppler shift and sampling clock offset may cause an offset between the true cyclic frequency of the primary user signal and the cyclic frequency known at the receiver. Cyclic Frequency Offset (CFO) is reported to cause severe degradation in the performance of systems exploiting cyclostationarity. In our proposed FRESH filter-based spectrum sensing systems, CFO may manifest at the adaptation stage as well as the sensing stage. In this thesis, we consider these problems separately.

To study the effect of CFO on the sensing stage, we consider the problem of cyclostatioanry spectrum sensing of an OFDM signal with correlated pilots. Spectrum sensing algorithms for OFDM signals are also important because of the popularity of OFDM as a modulation standard as well as it being the most suitable candidate for cognitive radio networks. A detector for the cyclostationary features introduced due to inter-pilot correlation is developed. The performance of the proposed detector is derived and verified in case of AWGN channels. Following this, the effect of an offset in the value of cyclic frequency known at the spectrum sensor is found out, and it is shown that CFO may cause a substantial performance loss in the system. It is then argued that the true cyclic frequency of the received signal may be estimated using the received samples. The Cramer-Rao bound for the true cyclic frequency estimator is then derived. Based on this bound, it is observed that the true cyclic frequency needs to be determined recursively. Therefore, two recursive algorithms, viz. a gradient ascent algorithm and a greedy-search algorithm, to estimate and compensate for the CFO are proposed. The performance of both these algorithms is then evaluated via simulation techniques. It is observed that the proposed cyclic frequency estimation algorithms may compensate the losses caused due to CFO by as much as 15 dB. Simulation results are also used to study the performance of the proposed detection technique under Rayleigh fading both in the presence and the absence of CFO.

A single-branch FRESH filter is considered to study the effects of CFO on the adaptation stage of a FRESH filtering-based spectrum sensor. It is shown that the performances of both the energy detector and the cyclostationarity detector suffer in the presence of a CFO in the adaptation stage. Following this, the greedy search algorithm developed previously is modified to estimate the true cyclic frequency for FRESH filter adaptation. It is observed via simulation techniques that the losses caused due to CFO are reduced by as much as 5 dB for an energy detector and 14 dB for a cyclostationary detector.

Contents

List of Figures

List of Tables

Chapter 1

Introduction

The recent advances in wireless communication technologies have led to an increased demand for the limited communication spectrum. This, under the current static spectrum allocation scheme, has led to a crunch in the availability of the usable spectrum. At the same time, recent studies done by the FCC(Federal Communications Commission) show that the actual utilization of the currently allocated spectrum is less than 40% [39]. This leads to the dual problem of spectrum shortage and underutilization, where on one hand there is an acute shortage of communication spectrum for wireless services, on the other hand the bands licensed to legacy services are unused most of the time.

In order to circumvent these problems, it has been proposed to let the unlicensed users access the vacant licensed spectrum bands opportunistically. That is, a secondary (unlicensed) user may access the primary (licensed) user's band whenever the latter is inactive. This is known as the "Opportunistic Spectrum Access" (OSA) model. However, it is to be noted here that this opportunistic access of the spectrum bands should not be disruptive to the primary users operating in the given bands. Also, the usage patterns of the licensed user may be random and it may not always be possible to prepare a geo-location database to predict the licensed user's activity [16, 116]. Therefore, it becomes necessary for the secondary users to ensure that the band is vacant before transmitting over it.

Cognitive or location aware radio, first proposed by Joseph Mitola, is a key enabling technology for Opportunistic Spectrum Access [87]. A cognitive radio is defined by Haykin in [59] as

> *A Cognitive Radio is an intelligent wireless communication system that is aware of its surrounding environment and uses methodology of understanding by building to learn from the environment and adapt its internal states to statistical variations in the incoming RF signal by making corresponding changes in certain parameters in real time with two primary objectives in mind.*
>
> 1. *Highly reliable communication.*
> 2. *Efficient utilization of the radio spectrum.*

The tasks required to be performed to accomplish these objectives may be identified as

1. **Spectrum Sensing** : Most of the licensed users allowing opportunistic access to their bands are legacy users such as digital television and wireless microphones [59]. These systems already have an infrastructure in place and cannot modify their transmission schemes to ease opportunistic access of the bands in question. It is, therefore, the sole responsibility of the secondary users to ensure that the primary user services remain unaffected by OSA. In other words, the operation of the secondary users must be totally transparent to the licensed or the primary users.

   For this purpose, a secondary user must transmit only when the primary user is quiet, thereby following a listen before talk approach. This requires efficient sensing of the presence of a primary user's signal. This task of the cognitive radio, known as spectrum sensing, becomes challenging because of the fact that the primary user signals to be detected may lie as much as 22 dB below the noise floor [60, 116, 121].

2. **Spectrum Management and Allocation** : It is observed that once a free spectrum resource is detected, there will be multiple secondary users contending to utilize it. Therefore, the design of medium access (MAC) protocols for these users is equally necessary [89]. While designing these protocols, it is to be kept in mind that all the contenders for a given resource are intelligent devices and may "lie" about their requirements. Therefore, based on the nature of the users involved in the scheme, spectrum allocation problems are modelled as collaborative or competitive games for optimal allocation of resources.

   Apart from this, it is also necessary that the secondary users, while transmitting do not exceed certain "interference temperature" limits. Accordingly, it becomes essential to judiciously set a cap for the maximum transmit power in different bands [59]. This limit on the interference temperature is used as a constraint in the game theoretic modeling of the spectrum access problem.

3. **Transmission Schemes** : After a spectrum band is identified by a cognitive user for transmission, the next step is to identify a modulation scheme for the same. While deciding on the modulation scheme, it must be kept in mind that the available spectrum is irregular and may be dis-contiguous. It should also be noted that the transmission by the cognitive user must not interfere with the services in the adjacent bands [23, 84].

   Orthogonal Frequency Division Multiplexing(OFDM), introduced in [12] is a suitable modulation scheme for cognitive radio based systems because of its ease of implementation and flexibility. Also, most modern day wireless systems such as WiMAX (IEEE 802.16) and LTE employ OFDM for transmission.

In this thesis, we focus on the problem of spectrum sensing for cognitive radios. As discussed previously, it is the sole responsibility of the secondary user to prevent interference with the legacy primary user systems and, therefore, it is necessary that it should be sensitive to the presence of a primary user signal. At the same time, it is important that the secondary user should transmit at all possible opportunities. Therefore, the absence of a primary user should be detected as efficiently as its presence. Also, the spectrum sensing operation should be performed before initiating transmission. Since spectrum sensing shares the spectrum opportunity window with the opportunistic transmission operation, it is necessary that the sensing time be minimized in order to maximize the secondary user throughput.

From the above discussion, it is evident that spectrum opportunities may exist in space as well as in time. That is, the secondary users may transmit whenever or wherever no primary user is present. It has been proposed in [137] that transmission opportunities for secondary users may exist in code and angle domains as well. That is, the unused spreading codes as well as MIMO beam-forming directions of the primary user may be used for opportunistic spectrum access. In this thesis, however, we consider only temporal and spatial spectrum sensing.

Also, it may be inferred from the preceding discussion that the problem of spectrum sensing may be viewed as a binary hypothesis testing problem with the null hypothesis corresponding to the absence of a primary user signal and the alternate hypothesis to its presence. It may be observed that a primary user will experience interference if the detection of its presence fails. Therefore, the probability of missed detection for this model may be used as a measure of the interference caused to the primary user. Similarly, the secondary user will transmit only when no primary user is detected and the spectrum sensing operation is over. That is, the throughput of the secondary user system depends on the successful detection of a spectrum hole as well as the time required for sensing. Therefore, the probability of false alarm and the number of samples required for sensing may be used as a measure for the throughput of the cognitive radio system. In view of this, the objective of a spectrum sensing algorithm is to maximize the probability of detection of a primary user signal while minimizing the probability of false alarm and the number of samples required for sensing. The IEEE 802.22 WRAN standards restrict both the probabilities of missed detection and false alarm to 10%.

The simplest approach for spectrum sensing is to detect the energy of the band of interest and compare it against the noise floor. This approach, though optimal for unknown signals, fails if the noise floor is not known precisely [122]. Therefore, it becomes pertinent to look for alternative features that are present in the primary user signal but absent in the ambient noise so as to distinguish the former from the latter.

One such feature is cyclostationarity or spectral coherence [50]. It has been established that most communication signals exhibit distinct cyclostationary signatures [50]. Accord-

ingly, communication signals exhibiting spectral coherence may be enhanced [48] as well as detected [31] by virtue of this property. During the past few years, several methods exploiting the cyclostationary properties of the primary user signals have been proposed for spectrum sensing [60, 92].

In [48], Gardener has shown that the optimal filters for cyclostationary signals have a Linear Periodically Time Varying (LPTV) structure. It has also been shown that LPTV filtering is equivalent to FRESH (FREquency SHift) filtering [50]. Adaptive algorithms for FRESH filtering have been developed in [146] and [135]. It is shown in [105] that optimal FRESH filtering of a sensed signal prior to detection results in significant improvement in the detection performance. Such a spectrum sensor is divided into the FRESH filtering stage and the sensing stage where any detector may be employed to sense the presence of a primary signal after the filtering stage. However, [105] provides only a simulation based study of the effects of FRESH filtering on the detection performance for a fixed length FRESH filter. Cyclostationarity property in signals may also be used for beam-forming [2]. Recently, spectrum sensing methods based on adaptive cyclostationary beam-forming have also been proposed [35].

It may happen that the cyclic frequency known to the cognitive receiver and the actual frequency at which the primary signal embedded in noise exhibits cyclostationarity are different. This difference, known as the cyclic frequency offset (CFO), may be caused due to Doppler shifts in the channel, the inexactness of knowledge of the carrier frequency of the primary user signal or due to an offset in the sampling clock at the receiver [73, 103, 138]. It has been demonstrated that CFO causes severe degradation in the performance of cyclostationarity based systems.

As pointed out above OFDM is the likely modulation standard for cognitive radio based systems owing to its ease of implementation and flexibility. Consequently, the sensing of OFDM signals also becomes important [138, 144]. In this thesis, we explore the problem of the sensing of OFDM signals with correlated pilots. It is shown that pilot correlation in OFDM signals leads to cyclostationarity, which can be detected by the use of cyclostationary spectrum sensing methods. Thus use of cyclostationarity for spectrum sensing is a topic of significant research interest. In the following section we present a brief review of the recent work done in the area of spectrum sensing and in particular cyclostationary spectrum sensing.

1.1 Review of Earlier Work

As stated earlier, the simplest approach for spectrum sensing is the measurement of the energy in the band of interest [65,95]. It is shown in [69] that energy detector is the optimal detector for detecting random signals. The standard energy detector involves band pass of filtering the received signal in the band of interest and comparing its energy against the

noise floor.

In [59] and [60], Haykin considered the problem of temporal windowing in energy detectors. It is observed that due to rectangular windowing the energy contained in one spectral band appears within another band, causing a bias in the observed energy within a band. Also, if some form of windowing is applied then the variance of the detected energy increases. This problem is known as the Bias Variance dilemma in signal processing literature. The author proposed the use of Thomson's multi-taper method(MTM) [124] to overcome this issue. The multitaper method employs the use of multiple windows for estimation of energy and takes their weighted average as an estimate. The windows used here correspond to the eigenvectors of the covariance matrix of the received data and are known as Slepian sequences or Slepian tapers. It has been shown in [60] that Slapian tapers are the optimal windows for energy detection.

An alternative derivation for the MTM is given in [38] and it is noted that MTM is optimal at the cost of a high computational complexity. This implies that the multitaper method being unsuited for the hardware and timing constraints of cognitive radios. Instead [38] describes a filter bank-based spectrum sensor that provides equally good computationally feasible energy estimates using larger filter lengths. It is argued that if filter bank based multicarrier modulation schemes are employed for transmission in cognitive radio systems then the filter-banks may serve the dual purpose of reception of the cognitive radio signal as well as spectrum sensing.

The authors in [28] and [88] independently proposed the use of a generalized ℓ_p norm of the received signal instead of the more conventional ℓ_2 norm for energy detection. This detector has been referred to as the improved energy detector. It is shown in [28] that the probabilities of detection and false alarm are a function of p and may be optimized in its terms for a given number of samples and signal to noise ratio. The optimized value of p is found out to be especially effective under low SNR regimes for the AWGN case. The Rayleigh fading case is considered in [88] and it is shown that p may be optimized in this case as well.

The energy detector, though simple, relies heavily on the knowledge of the ambient noise variance which may not always be exactly available. The authors in [122] considered the problem of energy detector based spectrum sensing under noise uncertainty at low SNRs. It is argued that the spectrum sensing system should be robust to small modeling uncertainties in the signal and noise variances. It is observed that these modeling uncertainties lead to the phenomenon of SNR walls. SNR walls are described as SNRs below which the system will require infinite samples to achieve a desired detection performance. The performance of the improved energy detector under noise uncertainty has been studied in [67]. It is shown that the performance of the energy detector under the worst case noise uncertainty [122] is independent of the exponent p. It is also shown that the conventional energy detector is the best choice under uniform noise uncertainty. Due to the problem of SNR walls in

the energy detector, it becomes necessary to look for alternative detection strategies. It is desirable here to use features present in the primary user signal but absent in the ambient noise. These features mainly stem from the signal and channel properties associated with the primary user.

In [57], the problem of spectrum sensing is formulated as a goodness of fit test against the general class of noise distributions. The test statistic here is based on the number of weighted zero-crossings in the observations. It is observed that this detector is robust to noise uncertainties under the low SNR regime.

It is safe to assume that the primary user signal exhibits some form of temporal correlation either due to the primary user signal structure or due to the multipath channel. Therefore, while the covariance matrix of the received signal will be diagonal in the absence of a primary signal, it will be non-diagonal in case of latter's presence. This will affect the distribution of the eigenvalues of the covariance matrix under the two hypotheses. Based on this fact, several eigenvalue-based tests developed using the generalized likelihood ratio test (GLRT) have been proposed to detect the presence of a primary user [76, 140–142]. It is proposed in [63] to modify the energy detector by using the temporal correlation information about the signal. It is argued that a multipath channel will introduce correlation to a primary user signal thereby improving the detection performance. However, in the absence of temporal correlation in the signal, the standard energy detector performs better in comparison to the modified energy detector.

The method in [143] uses the finite time covariance matrix of the received signal. The authors assumed the channel to be time dispersive and the received signal to be either oversampled or is received by multiple antennas. Oversampling is used to exploit the correlation among the primary signal samples, if present. Again, in the absence of a primary signal the sample covariance matrix becomes diagonal. The test statistic, therefore, is this ratio of the sum of diagonal elements to that of the off-diagonal ones. It may be observed that ideally in the absence of a primary signal the ratio will tend to be infinite. It is observed in [86] that this method may not always perform better in comparison to the energy detector. Therefore, it is proposed therein that the test statistic should be decided based on the correlation properties of the primary user signal. Zeng and Liang put forward in [142] and [141] a test based on eigenvalues of the finite time covariance matrix of the received signal. The ratio of the maximum eigenvalue of this matrix to its minimum is used as a test statistic. It is observed that this ratio will be close to unity in the absence of a primary user signal while it will have a value greater than unity in the presence of a primary user signal.

The idea of employing multiple antennas to detect the presence of a primary user is discussed in [113]. A generalized likelihood ratio test based on the signals received by multiple antennas was developed by the authors to detect the primary user's signal. Only a single primary user is assumed to be present over a time invariant fading channel. It is

argued that the covariance matrix, across multiple receive antennas, would be a sum of a rank-1 matrix with the noise covariance of the form $\sigma^2\mathbf{I}$. This will result in a difference between the largest and the average eigenvalues of the received signal covariance matrix. It is further shown that the GLRT reduces to a test of the ratio of the maximum eigenvalue to the mean of all other eigenvalues. A major drawback of the GLRT based methods is the requirement of a large number of samples. It has been observed that in case where some prior information about the signal is available, the number of samples required may be reduced considerably [41].

The above idea is extended in [6] to the case of primary user employing multiple transmit antennas and using orthogonal space-time block codes for transmission. A test based on the ratio of maximum and minimum eigenvalues of the covariance matrix is proposed and its performance is evaluated. In [37], an optimal Bartlett detector-based sequential probability ratio test is derived for use in multi-antenna array systems. This test is then extended to a MIMO system.

The performance of an eigenvalue-based sensing technique in the presence of correlated noise is analyzed in [111]. The ratio of the maximum to the minimum eigenvalue, known as the standard condition number is used as the test statistic. Bounds on the test statistic under both the hypotheses are derived. It is also shown that the eigenvalues of the sensed signal covariance matrix may also be used to estimate the primary user SNR at the cognitive terminal.

Axell and Larsson used a Bayesian approach in [5] to classify each received sample either as a pure noise sample or as containing a primary user signal. This paper considers the noise variance to be unknown. An optimal soft decision detector is developed for M independent observations. Following this, it is shown that the complexity of this detector grows exponentially with the number of samples. Subsequently, less complex approximations to the detector discussed previously are also proposed.

Another feature of the primary signal that is used for the purpose of sensing is cyclostationarity or spectral coherence [43, 90]. It has been established that most communication signals exhibit distinct cyclostationary signatures [50]and that the signals possessing spectral coherence may be enhanced [48] as well as detected [31] by virtue of this property. The statistical tests for detecting the presence of a cyclostationary signal, first formulated by Dandwate and Giannakis in [31], are employed for the purpose of spectrum sensing by Oner and Jondral in [92]. The authors proposed tests based on cyclostationarity which are used to sense the presence of a GMSK modulated GSM signal for pooling with an OFDM-based WLAN system.

In [104], the relative strengths and variances of the cyclic autocorrelation function at different cyclic frequencies are taken into account. In this paper, weights are derived for optimally combining the values of finite time cyclic autocorrelation function at different cyclic frequencies. These optimal weights are then used to develop a deflection coefficient

based detector [68]. The derived results are verified via simulation.

The eigenvalue properties of the cyclic covariance matrix of the received signal are used for spectrum sensing in [131]. It is shown that all the eigenvalues of the cyclic covariance matrix will tend to zero under the null hypothesis. However, they assume nonzero values under the alternate hypothesis. This paper uses the cyclic correlation significance test to ascertain the presence of a primary user signal. It is to be noted that this test will work in the presence of correlated white noise, whereas the general eigenvalue-based detectors will fail. It is also brought out that the detection threshold is independent of the number of samples.

The problem of selection of cyclic frequencies and cyclic autocorrelation lags that maximize the probability of detection for a given primary signal exhibiting cyclostationarity has been studied in [112]. It is shown that the fourth order cyclic moment of the received signal is required to determine the optimal lags for a given cyclic frequency. Since this knowledge may not always be available, a suboptimal method applicable at low SNRs is also proposed in the paper. The derived results are applied to linearly modulated signals to determine the optimal lag and cyclic frequency sets for these. It turns out, that in general, an increase in the number of feature points being used for detection leads to an improved detection performance.

It is established in [80] that the cyclostationary properties of the signal are preserved if the sign function is used instead of the actual values. This fact is used to derive the cyclostationary features of the sign function of a received signal. It has been shown that tests similar to the ones used to detect the presence of cyclostationary signals may be applied to detect the presence of the signal. The loss of information due to the signal amplitudes is compensated for by the use of larger number of samples. Sequential and cooperative techniques using this scheme have also been proposed in [80]. These detectors are shown to be effective in non-Gaussain impulsive noise in [81].

Apart from detection, the cyclostationarity property of a signal may also be used to enhance it. It was established in [48] that the optimal filter for a cyclostationary signal has a linear periodically time varying structure. It is shown in [50] that a LPTV structure may be interpreted as a FRESH (FREquency SHift) structure. Adaptive algorithms for FRESH filtering have been developed in [146] and [135].

It is shown in [105] that optimal FRESH filtering a signal prior to detection results in significant improvement in the detection performance. Such a spectrum sensor is divided into the FRESH filtering stage and the sensing stage where any detector may be employed to sense the presence of a primary signal after the filtering stage. However, [105] provides only a simulation based study of the effects of FRESH filtering on the detection performance for a fixed length FRESH filter. Hence a detailed analysis of the performance of spectrum sensing aided by FRESH filtering is much required.

Cyclostationarity property in signals may also be used for beam-forming [2, 36, 134].

The first among the cyclostationary beam forming algorithms is the SCORE (Spectral COherence REstoral) class of algorithms presented in [2]. Recently, spectrum sensing methods based on adaptive cyclostationary beam-forming have also been proposed [35].

It is observed that most communication signals exhibit cyclostationarity only for a predefined set of discrete cyclic frequencies. The performance of a cyclostationarity detector, therefore, is dependent on the correct knowledge of these frequencies. Unfortunately, it cannot be ensured that the cyclic frequency known at the cognitive radio terminal and the cyclic frequency of the primary signal are the same. An offset between the actual and the known values of the cyclic frequencies may arise if the channel causes a significant Doppler shift in the primary user signal, or if there is an offset in the sampling clock [72,73,103,138]. The effects of cyclic frequency offset (CFO) on the detection performance are severe as described in [103]. The authors in [103] also proposed a mechanism to bypass the effects of CFO by averaging the test statistics over smaller sample blocks. However, this technique causes a loss in the number of features being used for detection, thereby compromising the detection performance. Therefore, alternative methods for compensation of CFO effects are desirable.

In [72], a recursive greedy search algorithm to find the optimal cyclic frequency maximizing the SCORE objective function is proposed. The performance of this algorithm is studied via simulation and it is found that the proposed algorithm can compensate for the effects of CFO. A gradient ascent based algorithm for cyclic frequency estimation is proposed in [73]. The convergence properties of this algorithm are studied and it is shown using simulation results that this algorithm can compensate for the effects of CFO.

Apart from temporal and spectral correlation, some authors have also advocated the use of methods that rely heavily on the features of primary signals to be detected. These methods include the signature-based methods and the radio access technology (RAT)-based methods. The signature-based methods are employed when the cognitive user has the exact knowledge of some signatures embedded in the primary user waveform. These signatures may be preamble, midamble or the entire signal waveform (matched filtering). It is seen that the matched filter-based methods are optimal for detection of signal waveforms. RAT-based methods, on the other hand, use the knowledge obtained by identifying the transmission technology being employed to access the spectrum. As an example, [136] uses time frequency analysis to distinguish between WLAN and Bluetooth signals. However, the exact knowledge of primary signal waveforms may not be readily available to the cognitive users, thus limiting the use of these methods.

Corderio et. al. in [29] and Chen et. al. in [27] detected digital television signals using signature-based spectrum sensing. They exploited the periodically occurring field sync segments in DTV signals as signature sequences. The received signal is broken into segments equaling the length of frame and correlated with the known pilot sequences. The maximum value of the cross correlation is chosen as the test statistic. In [11], the

performances of the energy detector, the matched filter detector and the cyclostationary detector are compared in terms of their achievable detection rates.

Most of the detectors discussed previously do not take into account channel effects such as fading and shadowing. It is, however, shown in [33] that the performance of feature detectors may degrade considerably under the effect of fading. Also, if the channel between the primary user and the cognitive terminal is in a deep fade then the primary user may become undetectable. This is known as the hidden primary user problem. In order to counter the effects of fading channels, it has been proposed that multiple primary users should sense the spectrum collaboratively [53]. In [66], the authors proposed double threshold based cooperative sensing for the improved energy detector. Here, the exponent p is chosen so as to minimize the sum of probabilities of missed detection and false alarm. The difference between the two thresholds is also optimized to maximize the probability of detection. A k-out-of-N decision rule is used to fuse the decisions in a cooperative setting. This paper also considers the effect of imperfect reporting channels.

The problem of decentralized detection in sensor networks was first considered in [24]. Here, a fusion centre communicating with a set of nodes over a multiple access channel is considered and an optimal sensor configuration is derived. This idea is extended to cognitive radios in [53] and [55].

It is proposed in [30] to perform cooperative sensing using cyclostationary features in the presence of a fusion centre. Here, the cooperating users transmit their test statistics for a single cyclic frequency. These are combined at the fusion centre using equal gain combining. This idea is extended in [82] for a multi-cycle approach. Besides this, the reporting channel constraints are also considered in [82] and a censoring scheme based on the relevance of the data being transmitted by a coopering user is also proposed.

Under the scheme proposed in [149], multiple cognitive radios collaboratively detect the spectrum holes through energy detection in the presence of a fusion centre. It is shown here that reporting from a few and not all sensing nodes is sufficient to detect a primary user in a large cognitive radio network. An optimal voting rule for the sensing nodes is derived along with the optimal thresholds for energy detection-based sensing. This results in the development of fast spectrum sensing algorithms for cognitive radios.

Deflection coefficients are used in [32] for a cooperative multicycle detector. In this paper, multiple secondary users, each sensing a different cyclic frequency collaborate to detect the presence of a primary user signal. The allocation of frequencies to different sensors is either centralized or consensus-based. This paper studies both soft decision-based and hard decision-based collaborations. As a trade-off between soft and hard decisions,quantized test statistics are considered in this paper and the effects of quantization of test statistics on the detection performance is studied.

The problem of limited control channel bandwidth for a large number of cooperating users is considered in [118]. It is proposed here to censor the communication between

individual nodes and the fusion center in order to limit the control channel usage. It is proposed that only the secondary users with strong decisions should report to the fusion center (FC). The performance of this scheme is evaluated for both perfect and imperfect reporting channels and it is seen that the saving in control channel bandwidth outweighs the performance loss due to censoring.

The performance degradation in collaborative sensing techniques due to correlated log normal fading channels is studied in [54]. The noise characteristics of the channel are used to derive a lower bound on the false alarm rate, termed here as the missed opportunity rate. The physical area spanned by the sensing network is taken into account and it is shown that, under correlated fading, a sparse distribution of users over a large area is advantageous as compared to a dense distribution over a small area.

The effects of the errors caused in the control channel are taken into account in [148]. It is shown that errors in the reporting channel limit the performance of cooperative spectrum sensing. As a solution to this problem, a transmit diversity-based cooperative sensing technique is proposed. The different cooperating users are assumed to behave as an antenna array and consequently, space-time and space-frequency codes are used to transmit the sensed information to the fusion centre. Further, a relay-based scheme is also proposed for the sensing nodes in a deep fade. Under this scheme, different sensing nodes act as relays for the nodes whose links with the fusion centre are in a deep fade.

A joint evaluation of soft and hard combination strategies at the fusion center is done in [3]. It is shown that for a small number of cooperating users soft decisions are preferable while hard decisions tend to become a better choice as the number of cooperating users increases. The effect of reporting channel errors on soft and hard combination schemes has been studied in [26]. In this paper, a cooperative detection scheme with a fusion centre is considered. It is assumed that the one-bit hard decisions as well as quantized soft decisions are sent to the fusion centre over a channel that may cause reporting errors. The effects of an improper reporting channel are interpreted in terms of its bit error probability (BEP).

The problem of combination of local test statistics from different cooperating users is studied in [101]. Here, the spectrum sensing problem is remodelled as a constrained non-linear optimization problem. The constraints, in this case, are on the probabilities of detection and false alarm. Apart from algorithms to obtain an optimal solution to the aforementioned problem, this paper also proposes a computationally less intensive solution.

In [108], it is assumed that K collaborating spectrum sensors forward their collected samples to a fusion centre. These samples are used to construct the covariance matrix of the received signal. Based on the covariance matrix, a unified generalized eigenvalue based sensing framework, referred to as the generalized mean detector, is developed. The eigenvalues of the received signal covariance matrix are used to propose three tests based on the ratio of the maximum eigenvalue to the minimum eigenvalue, the arithmetic mean and the geometric mean. Finally closed form expressions for the performance of these tests

are derived.

A Quickest detection-based collaborative spectrum sensing framework is explored in [74]. This paper considers collaborative quickest detection without coordinated communication among the sensing nodes. It is assumed that there exist fixed time slots during which the secondary users can transmit. The cooperating users may transmit randomly during these slots and there is no coordination among them to avoid collisions. Asymptotic analysis is used to obtain the optimal broadcast probability of each sensing user. It is shown that collisions may be avoided if the probability of broadcast at each user is kept proportional to the magnitude of the likelihood function at the respective user.

In [151], a combination scheme minimizing the overall cost of the cooperative sensing system is proposed. The scheme takes into account the time offsets of the local spectrum sensors. The role of the prior probabilities of channel occupancy are taken into account in [106]. This paper considers a fusion center-based cooperation approach with each individual spectrum sensor using GLRT-based statistics. The number of samples required to achieve a given detection performance is also calculated in terms of the instantaneous received SNR. In [58], the individual sensors are assumed to use energy detectors and forward their binary decisions to the FC. The control channel here is considered to be error-free and the fusion center is assumed to use the k-out-of-N rule for combination. Error exponents are introduced and are used as a measure of the system performance.

Collaborative Spectrum sensing based on sequential detection is studied in [152] and [70]. The objective in [152] is to reduce the average sensing time required to reach a decision. In this case, each sensing node transmits its test statistics to the fusion center after each measurement. Based on the accumulated statistics, the fusion center decides on when to stop the detection process. It is assumed that the signal and noise powers are unknown at the sensing nodes and it is shown that the proposed sensing technique is robust to the knowledge of these parameters. The reduction in sensing time is illustrated analytically as well as by the use of simulation results.

A censored truncated sequential cooperation approach has been studied in [85]. It is argued that this approach results in considerable energy savings in the network. The problem is modeled so as to minimize the average energy consumption per sensor subject to constraints on the probabilities of missed detection and false alarm. Under the derived approach, the sensing nodes sense the spectrum and transmit only if they reach a decision before reaching a truncation limit on the number of collected samples.

Most of the cooperative spectrum sensing techniques assume Rayleigh fading channels. As a generalized case, single tap Nakagami channels are considered in [4]. Five new detectors viz. a Neyman Pearson detector, a locally optimum detector for weak signals, a weak signal detector and two GLRT detectors, are proposed here. Optimal detectors are derived when the signal and noise parameters are known. These detectors are then generalized for cases where one or more of the presumed parameters are not known.

Conventional cooperation schemes require a fusion center to arrive at a general decision based on the statistics/decisions of the local nodes. This arrangement is susceptible to node failure as well as requires a high communication overhead. It is also possible that sensing nodes far from the fusion center may not be synchronized to stay silent during the sensing periods. Therefore, it is important to develop distributed cooperation schemes for spectrum sensing. Some of the significant works in this direction are listed below.

Peer-to-peer cooperation for spectrum sensing using distributed detection theory has been discussed in [42]. The classification framework, in this case, is based on time-frequency analysis of the received signal. The short time power spectrum of the signal is used as a feature to detect the air interface of the transmitted signal. It is then shown that the proposed algorithm can distinguish between Bluetooth and 802.11 WLAN operating in the 2.4 GHz ISM band.

A fully distributed and scalable cooperative sensing scheme is developed in [75]. The decision in this case is based on the consensus arrived at by the cooperating users. The test statistic is based on energy detection. This paper considers consensus over both fixed as well as random graphs. The problem of consensus weight design under practical channel conditions and link failures is studied in [147]. A new weighted soft measurement-based combining scheme in the absence of a fusion centre is developed. Each node uses the signal energy as the test statistic and exchanges this information with its local one hop neighbours. The convergence of the weight selection algorithm is also proved in this paper.

A single spectrum slot may not be always available. Therefore, it is an attractive proposition for a spectrum sensing system to monitor multiple primary user bands simultaneously. This can be done in two ways. Either all the primary user bands may be monitored separately, or may be monitored as a single wide band. Under the first strategy, known as multi-band sensing, the occupancy states of different bands are determined separately. The simplest approach for this is presented in [40]. In this paper, it is assumed that the occupancy of different bands is uncorrelated and for an M-band system the composite hypothesis test may be decoupled as M number of independent hypothesis tests.

Hwang et. al. in [64] attempted to address the problem of multi-band sensing by proposing an autoregressive model for the occupancy of different bands. A two-stage spectrum sensing procedure is proposed. The problem of cooperation among multiple secondary users for spectrum sensing over a wideband is dealt with in [102]. The authors modeled the problem as a convex optimization problem to find an optimal scheme called "multiband joint detection". The case of correlated subbands in multiband joint detection is considered in [62] where a frequency coupled optimum linear energy combiner structure is proposed for multiple users. In [40], Segura et. al. proposed the use of generalized likelihood ratio test for the purpose of wideband spectrum sensing. Under the second strategy for wideband spectrum sensing, the entire wide band is sensed as a whole. This also becomes necessary when the primary user is employing a modulation scheme such as wideband OFDM.

The approach discussed by Tian and Giannikis in [126] uses wavelet transforms to separate out the different bands in the received wideband signal spectrum. The PSD of the received signal is first determined using FFT. Following this, wavelet transform is used to detect the edges that separate out the different bands. The PSDs of these bands may then be used to determine their occupancy state.

It is observed that sampling a wideband spectrum band requires very high sampling rate at the spectrum sensor. This leads to higher power consumption by the spectrum sensing equipment. However, recent advances in sub-Nyquist sampling and compressed sensing [34, 128] have led to the development of several compressed sensing-based spectrum sensing algorithms. The sparsity introduced due to the usage pattern of communication spectrum has beenexploited in [139]. It is proposed here to use a consensus-based compressed sensing system to determine the usage pattern of a wideband spectrum. A multi-rate sub-Nyquist spectrum detection system for cooperative wideband sensing is introduced in [119]. The proposed sensing scheme uses only a few sub-Nyquist samples at each cooperating user. It is also proposed to use different sampling rates to improve the overall system efficiency. In [109], a group testing-based spectrum sensing algorithm is proposed. The proposed algorithm tests a group of adjacent sub-bands in a single test, thereby exploiting the inherent sparsity. In [125] and [127], the authors proposed to reconstruct the wideband cyclic spectrum of the signal from the compressed samples. It is shown that the covariance matrix of the channel may be recovered from the covariance matrix of the compressed samples.

As discussed previously, OFDM is the most suitable modualtion scheme for cognitive radio systems. Also, due to its popularity in the current modulation standards, it is necessary for spectrum pooling systems to develop methods to successfully detect these signals. Most of the methods developed for OFDM signal detection are based on the detection of one or more inherent features, such as the cyclic prefix or the pilot tones.

In [25], the authors proposed to use the autocorrelation properties introduced due to the cyclic prefix as features to detect the primary signal. The authors in [8] also used the cyclic prefix as a distinguishing feature in the OFDM system and have developed optimal and suboptimal detectors to detect the non-stationarity caused due to the cyclic prefix. The cyclic autocorrelation function and the sign cyclic autocorrelation function have, respectively, been used to detect the cyclostationary features introduced due to a cyclic prefix in [123] and [130].

The authors in [27] used time-domain symbol cross-correlation to detect the correlation introduced by the pilot tones. This property has also been exploited in [144] where finite time autocorrelation function is used as a test statistic. The authors in [138] use the empirical cyclic spectral density to detect cyclostationarity introduced due to correlated pilots.

The difference in the statistical properties of the pilot and data subcarriers is exploited

in [79] for primary user signal detection. Artificially induced cyclostationary features to assist OFDM signal detection are proposed in [120] and have subsequently been used in [115]. For using the cyclostationary features of OFDM for detection, it is observed that the cyclostationarity introduced due to the cyclic prefix is weak and dependent on the length of the cyclic prefix, whereas the induced cyclostationarity may only be used for detecting secondary user systems.

1.2 Problem Statements and Descriptions

The problems considered in this thesis may be classified into two broad categories, viz. the effect of FRESH filtering on the performance of conventional spectrum sensors, and the effects of CFO on cyclostationary spectrum sensing systems and their prevention.

Under the first set of problems, the performance enhancement offered by the use of FRESH filters in a spectrum sensing system is studied. Firstly, the ideas of cyclostationary beam-forming and FRESH filtering for spectrum sensing are combined to propose a Space-Time FRESH filtering structure for spectrum sensing. A major challenge in this case is the selection of an appropriate algorithm for adapting this structure. Following this, quasi-analytical expressions are derived for performance evaluation of a single-antenna, single-user FRESH filter-based spectrum sensing system for both an energy detector and a cyclostationary detector.

It is found that single user spectrum sensing is inadequate for channels with heavy fading. Similar to conventional spectrum sensing schemes, the performance of FRESH filter based sensing also deteriorates under fading and shadowing. It is, therefore, proposed that multiple users should collaborate to detect the presence of a primary user [53]. Therefore, it is essential to develop collaboration strategies for FRESH filter-based spectrum sensing techniques.

Under the second set of problems, the effect of cyclic frequency offset on cyclostationarity based spectrum sensing systems is studied and methods to counter these effects are proposed. It is observed that CFO may exist either at the filter adaptation stage or at the sensing stage. To elaborate the effects of CFO at the sensing stage a cyclostationary detector for OFDM signals with correlated pilots is developed and the effect on its performance is studied. Following this, methods to compensate for these effects are also developed.

The effect of CFO on the adaptation stage is studied for a single branch FRESH filter based system. The CFO compensation methods developed for the sensing stage are modified for application to this case.

1.3 Thesis Organization

The second chapter introduces the notion of cyclostationarity and reviews some important results regarding cyclostationary signals. The chapter starts with the basic definitions of cyclostationarity and re-develops the expressions for the cyclostationary properties of the continuous-time and discrete-time signals. Following this, the effect of basic signal processing operations on cyclostationary signals is reviewed and based on these, the cyclostationary features of BPSK signals are re-visited.

In Chapter 3, a Space-Time FRESH filtering structure exploiting the spatial, temporal and spectral coherence of the primary user signal is proposed. It is argued that preprocessing the sensed signal using the proposed strucutre prior to the detection step results in an improved primary user detection performance. Following this, the adaptive beam-forming algorithm in [35] is modified to adapt the proposed structure. However, it is found that this algorithm has a complexity of $\mathcal{O}((KML)^2)$ for a K-antenna system with each antenna followed by a FRESH filter containing M number of frequency shift branches and each branch having a length L. This adaptation algorithm therefore acts as a bottleneck in the entire spectrum sensing scheme. Consequently, a linear complexity constrained doubly adaptive LMS algorithm (C2-LMS) is derived to adapt the proposed structure. The performance of the proposed structures and algorithms are then evaluated via simulation.

The performance of FRESH filter-based spectrum sensing in [105] as well as in Chapter 3 is determined mainly on the basis of simulation results. In Chapter 4 we now attempt to develop a mathematical explanation for the performance enhancement caused due to FRESH filtering in a single-user single-antenna system. We derive the statistics for both the energy detector and the cyclostationary detector to show that the performance in both these cases improves significantly due to FRESH filtering. Following this, the number of samples required to achieve a given detection performance are derived and it is shown that FRESH filtering may reduce the number of samples required to achieve a given detection performance by more than one order of magnitude. Further, the effect of noise uncertainty on energy detection-based sensing is studied, and it is observed that FRESH filtering lowers the SNR walls by as much as 14 dB. The validity of these results is then verified via simulations.

In Chapter 5, the single user FRESH filter based spectrum sensors are extended to a multiuser case for flat fading as well as dispersive fading channels. Here, multiple secondary users, each equipped with a FRESH filter, are assumed to collaborate to detect the presence of a primary user signal. All the three models of collaboration, viz. centralized, distributed and hierarchical, are considered here. It is then argued that the performance of collaborative FRESH filter-based spectrum sensing can be improved further if the collaborating users adapt their filter weights jointly. For this purpose, joint adaption algorithms described in [17] are modified to fit the given problem. The validity of these claims is then verified

via simulation.

The problem of spectrum sensing for OFDM signals is considered in Chapter 6. For this purpose, a cyclostationarity detector exploiting inter-pilot correlation in the OFDM signal is developed. The effect of CFO on the performance of this detector is considered and it is shown that the proposed detector fails in the presence of CFO. To counter the effects of CFO, it is proposed to estimate the true cyclic frequency of the sampled signals from its samples. In view of this, the Crammer-Rao bound for the true cyclic frequency estimator is derived and it is argued that the true cyclic frequency should be estimated recursively. Following this, two recursive algorithms, based on greedy search and gradient ascent are developed for estimating the true cyclic frequency.

The effect of cyclic frequency offset on the adaptation stage of a FRESH filter is considered in Chapter 7. Following this, the greedy search algorithm developed in Chapter 6 is modified to estimate the true cyclic frequency for FRESH filter adaptation. The results are again verified via simulation.

Finally, conclusions are drawn in Chapter 8 and directions for future work are identified.

Chapter 2

Cyclostationarity: An Overview

Generation of primary user signal involves various periodic operations such as modulation, sampling, multiplexing and coding. Therefore, the statistical characteristics of the primary user signal determined by these operations are also periodic. Based on the nature and number of periodic phenomena affecting the statistical properties of the data, the parameters of these processes may exhibit single or multiple periodicities. Such processes exhibiting single or multiple periodicities in their statistical parameters are known as cyclostationary processes [47, 90]. Owing to the periodic variation in the statistical properties, the correlation function of a cyclostationary random process will also exhibit periodicity. Cyclostationary processes, are, therefore also referred to as periodically correlated processes. Periodically time varying random processes also find application in biology, radio astronomy and economics. Consequently, starting from the first contributions in Russian literature in 1959, cyclostationarity in random signals has been well researched over the past five and a half decades [46, 51].

This chapter introduces some basic notions of cyclostationarity in communication signals to provide a background for the chapters that follow. The formal definitions of cyclostationary processes and their properties are stated in the first section. The second section looks at the effect of some common signal processing operations on cyclostationary signals. The cyclostationary properties of a BPSK signal are derived in the third section. In the fourth section, linear periodically time-varying filtering is introduced as a method for generating cyclostationary signals.

2.1 Cyclostationarity

A continuous-time real-valued stochastic process $x(t)$, which is a collection of sample functions $\{x(t,\omega)\, t \in \Re, \omega \in \Omega\}$, over the sample space Ω, is said to be Nth-order strict-sense cyclostationary if its distribution function

$$F_{x(t),\, x(t+\tau_1),\ldots,\, x(t+\tau_{N-1})}(\xi_0, \xi_1, \ldots, \xi_{n-1}) = Pr\{x(t) \leq \xi_0, x(t+\tau_1) \leq \xi_1, \ldots x(t+\tau_{N-1}) \leq \xi_{N-1}\} \tag{2.1}$$

is periodic in t with a period T_0, that is,

$$F_{x(t+T_0),\,x(t+\tau_1+T_0),\ldots,\,x(t+\tau_{N-1}+T_0)}(\xi_0,\xi_1,\ldots,\xi_{N-1}) = F_{x(t),\,x(t+\tau_1),\ldots,\,x(t+\tau_{N-1})}(\xi_0,\xi_1,\ldots,\xi_{N-1}) \tag{2.2}$$

Relaxing this definition, $x(t)$ is said to be second-order wide-sense cyclostationary with a period T_0 if its mean and autocorrelation function are periodic in time with period T_0. That is,

$$\begin{aligned} E[x(t+T_0)] &= E[x(t)] \\ R_{xx}(t,\tau) &= E\left[x\left(t+\tfrac{\tau}{2}\right)x\left(t-\tfrac{\tau}{2}\right)\right] \\ &= R_{xx}(t+T_0,\tau) \end{aligned} \tag{2.3}$$

For a complex-valued continuous-time process $x(t)$, the above conditions take the form

$$\begin{aligned} E[x(t+T_0)] &= E[x(t)] \\ R_{xx}(t,\tau) &= E\left[x\left(t+\tfrac{\tau}{2}\right)x^*\left(t-\tfrac{\tau}{2}\right)\right] \\ &= R_{xx}(t+T_0,\tau) \end{aligned} \tag{2.4}$$

If the process $x(t)$ is cyclo-ergodic [15], then

$$x(t+\omega T_0) = x(t,\omega) \tag{2.5}$$

The mean and the autocorrelation function of $x(t)$ may be defined as

$$\begin{aligned} E[x(t)] &= \tfrac{1}{|\Omega|}\textstyle\sum_{\omega\in\Omega} x(t+\omega T_0) && 0 \le t < T_0 \\ R_{xx}(t,\tau) &= E\left[x\left(t+\tfrac{\tau}{2}\right)x^*\left(t-\tfrac{\tau}{2}\right)\right] \\ &= \tfrac{1}{|\Omega|}\textstyle\sum_{\omega\in\Omega}\left(x\left(t+\tfrac{\tau}{2}+\omega T_0\right)x^*\left(t-\tfrac{\tau}{2}+\omega T_0\right)\right) && 0 \le t < T_0 \end{aligned} \tag{2.6}$$

Due to this periodicity, $R_{xx}(t,\tau)$ may be decomposed in the form of a Fourier series as

$$R_{xx}(t,\tau) = \sum_{k=-\infty}^{\infty} R_{xx}^{\frac{k}{T_0}}(\tau)e^{\frac{j2\pi kt}{T_0}} \tag{2.7}$$

where $R_{xx}^{\frac{k}{T_0}}(\tau)$ is the kth Fourier coefficient, defined as

$$R_{xx}^{\frac{k}{T_0}}(\tau) = \lim_{T_0\to\infty}\frac{1}{T_0}\int_{-\frac{T_0}{2}}^{\frac{T_0}{2}} R_{xx}(t,\tau)e^{\frac{-j2\pi kt}{T_0}}dt \tag{2.8}$$

This is also known as the cyclic autocorrelation function at the cyclic frequency $\frac{k}{T_0}$.

As stated earlier, the random process $x(t)$ may be generated due to a plurality of periodic phenomena. The periodicities of these phenomena may or may not be integer multiples of each other. It is, therefore, convenient to define the process as almost cyclostationary. A random process is said to be almost cyclostationary in the wide-sense if its autocorrelation

function is an almost periodic function of t. That is, there exists a countable set $\mathcal{A}$ of cyclic frequencies α such that its autocorrelation function may be expressed in the form

$$R_{xx}(t,\tau) = \sum_{\alpha\in\mathcal{A}} R_{xx}^{\alpha}(\tau)e^{j2\pi\alpha t} \tag{2.9}$$

where

$$R_{xx}^{\alpha}(\tau) = \lim_{T_\alpha\to\infty} \frac{1}{T_\alpha}\int_{-\frac{T_\alpha}{2}}^{\frac{T_\alpha}{2}} R_{xx}(t,\tau)e^{-j2\pi\alpha t}dt \tag{2.10}$$

and

$$T_\alpha = \frac{1}{\alpha} \tag{2.11}$$

Substituting (2.6) into (2.10) and interchanging the order of integration and summation, we get,

$$R_{xx}^{\alpha}(\tau) = \lim_{T_\alpha\to\infty} \frac{1}{T_\alpha|\Omega|}\sum_{\omega\in\Omega}\int_{-\frac{T_\alpha}{2}}^{\frac{T_\alpha}{2}} \left(x\left(t+\frac{\tau}{2}+\omega T_\alpha\right)x^*\left(t-\frac{\tau}{2}+\omega T_\alpha\right)\right)e^{-j2\pi\alpha t}dt \tag{2.12}$$

It may be observed that for $T_\alpha \to \infty$ the integral spans the entire real line. Therefore, it may safely be assumed to have accommodated all the integer shifts of $x\left(t+\frac{\tau}{2}\right)x^*\left(t-\frac{\tau}{2}\right)e^{-j2\pi\alpha t}$ and consequently the above equation may be simplified as

$$R_{xx}^{\alpha}(\tau) = \lim_{T_\alpha\to\infty} \frac{1}{T_\alpha}\int_{-\frac{T_\alpha}{2}}^{\frac{T_\alpha}{2}} \left(x\left(t+\frac{\tau}{2}\right)x^*\left(t-\frac{\tau}{2}\right)\right)e^{-j2\pi\alpha t}dt \tag{2.13}$$

Therefore, $R_{xx}^{\alpha}(\tau)$ may be viewed as the strength of a sinusoid with frequency α hidden in the lag product $z(t,\tau) = x\left(t+\frac{\tau}{2}\right)x^*\left(t-\frac{\tau}{2}\right)$. More generally, a stochastic process $x(t)$ is said to exhibit second-order wide-sense cyclostationarity at a cyclic frequency α if $R_{xx}^{\alpha}(\tau) \not\equiv 0$.

It may be noted that the cyclic autocorrelation function for a cyclostationary random process is independent of time. In other words, said that the random process $z^{\alpha}(t,\tau) := \{z^{\alpha}(t,\tau,\omega)t, \tau\in\Re, \omega\in\Omega\}$, derived out of $x(t)$ as

$$z^{\alpha}(t,\tau) = x\left(t+\frac{\tau}{2}\right)\ x^*\left(t-\frac{\tau}{2}\right)e^{-j2\pi\alpha t}, \tag{2.14}$$

is ergodic. Consequently, the cyclic autocorrelation function at lag τ may also be defined as the mean value of the frequency shifted lag product $z^{\alpha}(t)$ as

$$R_{xx}^{\alpha}(\tau) = E\left[z^{\alpha}(t,\tau)\right] \tag{2.15}$$

Substituting the definition of $z(t)$ in the above, cyclic autocorrelation function may be

defined as

$$R_{xx}^{\alpha}(\tau) = E\left[x\left(t+\frac{\tau}{2}\right)x^{*}\left(t-\frac{\tau}{2}\right)e^{-j2\pi\alpha t}\right] \tag{2.16}$$

Defining the signal $x^{\alpha}(t)$ as

$$x^{\alpha}(t) = x(t)e^{-j2\pi\alpha t}, \tag{2.17}$$

the cyclic autocorrelation function may also be written as [50]

$$R_{xx}^{\alpha}(\tau) = E\left[x^{\frac{\alpha}{2}}\left(t+\frac{\tau}{2}\right)x^{-\frac{\alpha}{2}*}\left(t-\frac{\tau}{2}\right)\right] \tag{2.18}$$

The right side of this equation is the cross correlation between the signals $x^{\frac{\alpha}{2}}(t)$ and $x^{\frac{-\alpha}{2}}(t)$ at lag τ. The cyclic autocorrelation function at a cyclic frequency α may, therefore, be seen as the cross correlation function between two frequency shifted versions of the signals separated by a frequency α. This implies that any signal exhibiting cyclostationarity will be correlated to its frequency shifted version for some discrete frequency shifts $\alpha \in \mathcal{A}$. Consequently, a cyclostationary signal also exhibits spectral coherence [90].

As the autocorrelation function and the power spectral density form a Fourier transform pair, the time-varying power spectral density of $x(t)$ may be expressed as

$$S_{xx}(t,f) = \int_{-\infty}^{\infty} R_{xx}(t,\tau)e^{-j2\pi f\tau}d\tau \tag{2.19}$$

Using the above equation, (2.9) and the linearity property of Fourier transform, the periodically time-varying power spectral density of $x(t)$ may be expressed as

$$S_{xx}(t,f) = \sum_{\alpha\in\mathcal{A}} S_{xx}^{\alpha}(f)e^{j2\pi\alpha t} \tag{2.20}$$

where $S_{xx}^{\alpha}(\tau)$ is defined as

$$\begin{aligned} S_{xx}^{\alpha}(\tau) &= \lim_{T_\alpha\to\infty}\tfrac{1}{T_\alpha}\int_{-\frac{T_\alpha}{2}}^{\frac{T_\alpha}{2}} S_{xx}(t,f)e^{-j2\pi\alpha t}dt \\ &= \int_{-\infty}^{\infty} R_{xx}^{\alpha}(\tau)e^{-j2\pi f\tau}d\tau \\ &= E\left[X(f+\tfrac{\alpha}{2})X^{*}(f-\tfrac{\alpha}{2})\right] \end{aligned} \tag{2.21}$$

Here $X(f)$ is the Fourier transform of $x(t)$ defined as

$$X(f) = \int_{-\infty}^{\infty} x(t)e^{-j2\pi ft}dt \tag{2.22}$$

Thus, the cyclic spectral density may be viewed as the cross-spectral density between two frequency shifted versions of $X(f)$. It may be observed that for a signal exhibiting cyclostationarity at a frequency α, the cyclic spectral density at that frequency must not be uniformly zero.

A wide-sense stationary process may be seen as a special case of a cyclostationary

process with $\alpha = 0$. It may be noted that for $\alpha = 0$, the cyclic spectral density and the cyclic autocorrelation function reduce to the conventional power spectral density and autocorrelation function, respectively.

2.1.1 Conjugate Cyclostationarity

A complex valued random process $x(t)$ is said to be second-order conjugate almost cyclostationary in the wide-sense when its conjugate autocorrelation function, defined as

$$R_{xx^*}(t,\tau) = E\left[x\left(t+\frac{\tau}{2}\right)x\left(t-\frac{\tau}{2}\right)\right], \tag{2.23}$$

is an almost periodic function of t. Consequently, the conjugate cyclic autocorrelation function and the conjugate cyclic spectral density may be defined as

$$R^{\alpha}_{xx^*}(\tau) = E\left[x\left(t+\frac{\tau}{2}\right)x\left(t-\frac{\tau}{2}\right)e^{j2\pi\alpha t}\right] \tag{2.24}$$

$$S^{\alpha}_{xx^*}(f) = E\left[X\left(f+\frac{\alpha}{2}\right)X\left(f-\frac{\alpha}{2}\right)\right] \tag{2.25}$$

2.1.2 Discrete Time Cyclostationary Random Process

A complex-valued discrete time random process $x[n] := \{x[n,\omega], n \in \mathbb{Z}, \omega \in \Omega\}$ is said to be Nth order strict-sense cyclostationary with a period N_0 if

$$F_{x[n+N_0],\,x[n+\tau_1+N_0],\ldots,\,x[n+\tau_{N-1}+N_0]}(\xi_0,\xi_1,\ldots,\xi_{N-1}) = F_{x[n],\,x[n+\tau_1],\ldots,\,x[n+\tau_{N-1}]}(\xi_0,\xi_1,\ldots,\xi_{N-1}) \tag{2.26}$$

Alternatively, It may be said to be wide-sense almost cyclostationary with a cyclic frequency α if its cyclic autocorrelation function $R^{\alpha}_{xx}[\tau]$, defined as

$$R^{\alpha}_{xx}[\tau] = E[x[n]x^*[n-\tau]e^{-j2\pi\alpha n}], \tag{2.27}$$

is nonzero for some $\tau \in \mathbb{Z}$. It may be noted that the definition of the cyclic autocorrelation function for a discrete-time random process is slightly different from that for a continuous-time random process. The cyclic autocorrelation function may, therefore, be interpreted as a cross-correlation between $x^{\alpha}[n]$ and $x[n-\tau]$, where

$$x^{\alpha}[n] = x[n]e^{-j2\pi\alpha n} \tag{2.28}$$

Considering $x[n]$ to be cyclo-ergodic, it may be shown that

$$R^{\alpha}_{xx}[n,\tau] = \lim_{N\to\infty}\frac{1}{2N+1}\sum_{n=-N}^{N} x[n]x^*[n-\tau]e^{-j2\pi\alpha n} \tag{2.29}$$

The cyclic spectral density, in this case, is defined as

$$S_{xx}^{\alpha}(f) = E\left[X\left(f+\frac{\alpha}{2}\right)X^{*}\left(f-\frac{\alpha}{2}\right)\right] \tag{2.30}$$

where

$$X(f) = \sum_{n=-\infty}^{\infty} x[n]e^{-j2\pi fn} \tag{2.31}$$

Similarly, the conjugate cyclic autocorrelation function and the conjugate cyclic spectral density may be defined as

$$R_{xx^{*}}^{\alpha}[\tau] = E[x[n]x[n-\tau]e^{-j2\pi\alpha n}] \tag{2.32}$$

$$S_{xx^{*}}^{\alpha}(f) = E\left[X\left(f+\frac{\alpha}{2}\right)X\left(f-\frac{\alpha}{2}\right)\right] \tag{2.33}$$

It may be noted that for a discrete-time random process, both the frequency f and the cyclic frequency α are normalized to lie between $-\frac{1}{2}$ and $\frac{1}{2}$. Furthermore, discussions pertaining to the effects of sampling on a cyclostationary random process, along with some other standard signal processing operations, is considered in the next section.

2.2 Processing of Cyclostationary Signals

In this section, effects of some simple signal processing operations, viz. convolution, product modulation, and sampling on cyclostationary signals, are discussed. The effects on the cyclic autocorrelation function and the cyclic spectral density in case of both continuous-time and discrete-time random process are considered here.

2.2.1 Linear Convolution

Consider a continuous-time signal $x(t)$ which is a sample function of a cyclostationary process. This signal is passed through a linear time-invariant filter with a known impulse response $h(t)$. The output of this system $y(t)$ may be written as

$$y(t) = \int_{-\infty}^{\infty} x(u)h(t-u)du \tag{2.34}$$

The cyclic autocorrelation function of the filtered signal is given as,

$$\begin{aligned} R_{yy}^{\alpha}(\tau) &= E\left[y\left(t-\tfrac{\tau}{2}\right)y^{*}\left(t-\tfrac{\tau}{2}\right)e^{-j2\pi\alpha t}\right] \\ &= E\left[\int_{-\infty}^{\infty}\int_{-\infty}^{\infty} h(u)x(t+\tfrac{\tau}{2}-u)h^{*}(v)x^{*}(t-\tfrac{\tau}{2}-v)dudve^{-j2\pi\alpha t}\right] \\ &= \int_{-\infty}^{\infty}\int_{-\infty}^{\infty} h(u)E\left[x(t+\tfrac{\tau}{2}-u)x^{*}(t-\tfrac{\tau}{2}-v)e^{-j2\pi\alpha t}\right]h^{*}(v)dudv \\ &= \int_{-\infty}^{\infty}\int_{-\infty}^{\infty} h(u)R_{xx}^{\alpha}(v-u+\tau)h^{*}(v)dudv \end{aligned} \tag{2.35}$$

Since the Fourier transform of the filtered signal is

$$Y(f) = X(f)H(f), \tag{2.36}$$

the cyclic spectral density of $y(t)$ may be written as

$$\begin{aligned} S_{yy}^{\alpha}(f) &= E\left[Y(f+\tfrac{\alpha}{2})Y^*(f+\tfrac{\alpha}{2})\right] \\ &= H\left(f+\tfrac{\alpha}{2}\right) E\left[X(f+\tfrac{\alpha}{2})X^*(f-\tfrac{\alpha}{2})\right] H^*\left(f-\tfrac{\alpha}{2}\right) \\ &= H\left(f+\tfrac{\alpha}{2}\right) S_{xx}^{\alpha}(f) H^*\left(f-\tfrac{\alpha}{2}\right) \end{aligned} \tag{2.37}$$

Similarly, for a discrete time signal $y[n]$ obtained by passing $x[n]$ through an LTI filter with an impulse response $h[n]$, defined as

$$y[n] = \sum_{l=-\infty}^{\infty} h[k]x[n-k], \tag{2.38}$$

the cyclic autocorrelation at cyclic frequency α and lag τ may be written as

$$R_{yy}^{\alpha}[\tau] = \sum_{p=-\infty}^{\infty}\sum_{q=-\infty}^{\infty} h[p]R_{xx}^{\alpha}[\tau-p+q]h^*[q] \tag{2.39}$$

and the cyclic spectral density as

$$S_{xx}^{\alpha}(f) = H\left(f+\frac{\alpha}{2}\right) S_{xx}^{\alpha}(f) H^*\left(f-\frac{\alpha}{2}\right) \tag{2.40}$$

2.2.2 Product Modulation

Consider a signal $y(t)$ defined as

$$y(t) = x(t)w(t) \tag{2.41}$$

with a Fourier transform

$$Y(f) = \int_{-\infty}^{\infty} X(\phi)W(f-\phi)d\phi \tag{2.42}$$

where $x(t)$ and $w(t)$ are independent random signals exhibiting cyclostationarity for cyclic frequencies $\beta \in \mathcal{B}$ and $\gamma \in \Gamma$. The time-varying autocorrelation function of $y(t)$ is given as [50]

$$\begin{aligned} R_{yy}(t,\tau) &= E\left[y\left(t+\tfrac{\tau}{2}\right) y^*(t-\tfrac{\tau}{2})\right] \\ &= E\left[x\left(t+\tfrac{\tau}{2}\right) x^*(t-\tfrac{\tau}{2}) w\left(t+\tfrac{\tau}{2}\right) w^*(t-\tfrac{\tau}{2})\right] \end{aligned} \tag{2.43}$$

By virtue of the independence of $x(t)$ and $w(t)$, it may be shown that

$$R_{yy}(t,\tau) = R_{xx}(t,\tau)R_{ww}(t,\tau) \tag{2.44}$$

Now,

$$R_{xx}(t,\tau) = \sum_{\beta\in\mathcal{B}} R_{xx}^{\beta}(\tau)e^{j2\pi\beta t} \tag{2.45}$$

and

$$R_{ww}(t,\tau) = \sum_{\gamma\in\Gamma} R_{ww}^{\gamma}(\tau)e^{j2\pi\gamma t} \tag{2.46}$$

Therefore,

$$R_{yy}(t,\tau) = \sum_{\beta\in\mathcal{B}}\sum_{\gamma\in\Gamma} R_{ww}^{\gamma}(\tau)R_{xx}^{\beta}(\tau)e^{j2\pi(\beta+\gamma)t} \tag{2.47}$$

Defining $\alpha = \beta + \gamma$ and $\mathcal{A} = \mathcal{B} + \Gamma$, the above may be written as

$$R_{yy}(t,\tau) = \sum_{\alpha\in\mathcal{A}}\sum_{\gamma\in\Gamma} R_{ww}^{\gamma}(\tau)R_{xx}^{\alpha-\gamma}(\tau)e^{j2\pi\alpha t} \tag{2.48}$$

Therefore,

$$R_{yy}^{\alpha}(\tau) = \sum_{\gamma\in\Gamma} R_{ww}^{\gamma}(\tau)R_{xx}^{\alpha-\gamma}(\tau) \;\; \forall\alpha\in\mathcal{A} \tag{2.49}$$

where

$$\mathcal{A} = \{\alpha = \beta + \gamma, (\beta\in\mathcal{B}); (\gamma\in\Gamma)\} \tag{2.50}$$

Invoking the relation between the cyclic spectral density and the cyclic autocorrelation function, we have

$$S_{yy}^{\alpha}(f) = \int_{-\infty}^{\infty}\sum_{\gamma\in\Gamma} R_{ww}^{\gamma}(\tau)R_{xx}^{\alpha-\gamma}(\tau)e^{-j2\pi f\tau}d\tau \;\; \forall\alpha\in\mathcal{A} \tag{2.51}$$

This may be simplified as

$$S_{yy}^{\alpha}(f) = \int_{-\infty}^{\infty}\sum_{\gamma} S_{ww}^{\gamma}(\phi)S_{xx}^{\alpha-\gamma}(f-\phi)d\phi \tag{2.52}$$

Similarly, for a discrete time signal $y[n]$ defined as the product of two discrete time cyclostationary signals $x[n]$ and $w[n]$ and exhibiting cyclostationarity at $\beta\in\mathcal{B}$ and $\gamma\in\Gamma$, respectively, the cyclic autocorrelation function $R_{yy}^{\alpha}[\tau]$ is defined for all $\alpha\in\mathcal{A} = \mathcal{B}+\Gamma$ as

$$R_{yy}^{\alpha}[\tau] = \sum_{\gamma\in\Gamma} R_{ww}^{\gamma}[\tau]R_{xx}^{\alpha-\gamma}[\tau] \tag{2.53}$$

and the cyclic spectral density is given as

$$S_{yy}^{\alpha}(f) = \int_{-\frac{1}{2}}^{\frac{1}{2}}\sum_{\gamma} S_{ww}^{\gamma}(\phi)S_{xx}^{\alpha-\gamma}(f-\phi)d\phi \tag{2.54}$$

2.2.3 Sampling of Continuous-time Signals

Uniform periodic sampling of a continuous time signal $x(t)$ is equivalent to its multiplication with a periodic impulse train $w(t)$ defined as

$$\begin{aligned} w(t) &= \sum_{n=-\infty}^{\infty} \delta(t - nT_s) \\ &= \frac{1}{T_s} \sum_{k=-\infty}^{\infty} e^{j\frac{2\pi kt}{T_s}} \end{aligned} \tag{2.55}$$

The effect of sampling on the second-order cyclostationary properties of a signal $x(t)$ may therefore, be determined by substituting the cyclic autocorrelation function and the cyclic spectral density of $w(t)$ in equations (2.52) and (2.49), respectively. To determine the cyclostationary properties of $w(t)$, consider an almost periodic signal $p(t)$ represented in the form of a Fourier series as

$$p(t) = \sum_{\eta} P_\eta e^{j2\pi\eta t} \tag{2.56}$$

Using (2.13), the cyclic autocorrelation function of $p(t)$ at cyclic frequency α and lag τ is defined as

$$\begin{aligned} R_{pp}^{\alpha}(\tau) &= \int \sum_{\eta} \sum_{\nu} P_\eta P_\nu^* dt e^{j2\pi\eta(t+\frac{\tau}{2})} e^{-j2\pi\nu(t-\frac{\tau}{2})} e^{-j2\pi\alpha t} dt \\ &= \sum_{\eta} \sum_{\nu} P_\eta P_\nu^* e^{j\pi(\eta+nu)\tau} \int e^{-j2\pi(\alpha-\eta+\nu)t} dt \\ &= \sum_{\eta} \sum_{\nu} P_\eta P_\nu^* e^{j\pi(\eta+nu)\tau} \delta(\eta - \alpha + \nu) \end{aligned} \tag{2.57}$$

This may be simplified as [50]

$$R_{pp}^{\alpha}(\tau) = \sum_{\nu} P_\nu P_{\alpha-\nu}^* e^{j\pi(2\nu-\alpha)\tau} \tag{2.58}$$

The cyclic spectral density of $p(t)$ takes the form

$$S_{pp}^{\alpha}(f) = \sum_{\nu} P_\nu P_{\alpha-\nu}^* \delta\left(f - \nu + \frac{\alpha}{2}\right) \tag{2.59}$$

Consequently, the cyclic autocorrelation function and the cyclic spectral density of the sampling wave $w(t)$ may be written as

$$R_{ww}^{\alpha}(\tau) = \frac{1}{T_s^2} \sum_{\nu} e^{j\pi(2\nu-\alpha)} \tag{2.60}$$

$$S_{ww}^{\alpha}(f) = \frac{1}{T_s^2} \sum_{\nu} \delta\left(f - \nu + \frac{\alpha}{2}\right) \tag{2.61}$$

Substituting the expression for cyclic spectral density into (2.52) and simplifying the same, the cyclic spectral density of the signal $y(t) = x(t)w(t)$ may be written as [50]

$$S_{yy}^{\alpha}(f) = \frac{1}{T_s^2} \sum_{m} \sum_{n} S_{xx}^{\alpha+\frac{m}{T_s}}\left(f - \frac{m}{2T_s} - \frac{n}{T_s}\right) \tag{2.62}$$

Hence, it is observed that sampling leads to a repetition of the cyclic spectrum of the signal and, therefore, care must be taken to avoid aliasing of cyclic frequencies.

For a purely stationary $x(t)$ the cyclic spectral density of $y(t)$ will take the form

$$S_{yy}\alpha(f) = \begin{cases} \sum_{m=-\infty}^{\infty} S_{xx}\left(f + \frac{\alpha}{2} - \frac{m}{T_s}\right) & \alpha = \frac{n}{T_0} \\ 0 & \text{otherwise} \end{cases} \tag{2.63}$$

Therefore, sampling a wide-sense stationary signal results in a wide-sense cyclostationary signal.

2.3 Cyclostationarity in BPSK Signals

In this thesis, all the problems involving FRESH filtering use a BPSK signal for simulation-based performance evaluation. In view of this, the cyclostationary characteristics of a BPSK signal [44, 45] are discussed herein. A complex BPSK signal may be defined as

$$x(t) = s(t)e^{j2\pi f_c t} \tag{2.64}$$

with $s(t)$ being the modulating signal, defined as

$$s(t) = \sum_n z_n p(t - nT_0) \tag{2.65}$$

where $\frac{1}{T_0}$ is the baud-rate of the BPSK signal and z_n is the nth information bit. This may be viewed as

$$s(t) = p(t) * \sum_n z_n \delta(t - nT_0) \tag{2.66}$$

where $p(t)$ is the pulse shaping function and the term $\sum_n z_n\delta(t - nT_0)$ corresponds to the sampled version of a continuous time stationary process $z(t)$. Defining

$$\begin{array}{rcl} \check{z}(t) & = & \sum_n z_n \delta(t - nT_0) \\ & = & z(t)\sum_n \delta(t - nT_0) \end{array} \tag{2.67}$$

for a wide sense stationary $z(t)$, the cyclic spectral density of $\check{z}(t)$ is given as

$$S^{\alpha}_{\check{z}\check{z}}(f) = \begin{cases} \frac{1}{T_0}\sum_{m=-\infty}^{\infty} S_{zz}\left(f + \frac{\alpha}{2} - \frac{m}{T_s}\right) & \alpha = \frac{n}{T_0} \\ 0 & \text{otherwise} \end{cases} \tag{2.68}$$

The cyclic spectral density of $s(t)$ may be written as [47]

$$S^{\alpha}_{ss}(f) = P\left(f + \frac{\alpha}{2}\right) S^{\alpha}_{\check{z}\check{z}}(f) P^*\left(f - \frac{\alpha}{2}\right) \tag{2.69}$$

which may in turn be written as

$$S_{ss}^{\alpha}(f) = \begin{cases} \frac{1}{T_0^2} \sum_{m=-\infty}^{\infty} P\left(f+\frac{\alpha}{2}\right) S_{zz}\left(f+\frac{\alpha}{2}-\frac{m}{T_s}\right) P^*\left(f-\frac{\alpha}{2}\right) & \alpha = \frac{n}{T_0} \\ 0 & \text{otherwise} \end{cases} \tag{2.70}$$

This implies that, the baseband component of a BPSK signal exhibits cyclostationarity at multiples of the baud-rate. Accordingly, the cyclic autocorrelation function for the baseband component of a BPSK signal may be written as [47]

$$R_{ss}^{\alpha}(\tau) = \begin{cases} \frac{1}{T_0^2} \sum_{m=-\infty}^{\infty} R_{zz}\left(mT_s\right) r_p^{\alpha}(\tau - mT_s) & \alpha = \frac{n}{T_0} \\ 0 & \text{otherwise} \end{cases} \tag{2.71}$$

where

$$r_p^{\alpha}(\tau - mT_s) = \int_{-\infty}^{\infty} p\left(t+\frac{\tau}{2}\right) p^*\left(t-\frac{\tau}{2}\right) e^{j2\pi\alpha t} dt \tag{2.72}$$

The cyclic autocorrelation function of the modulated signal is given as

$$\begin{aligned} R_{xx}^{\alpha} &= E[x\left(t+\tfrac{\tau}{2}\right) x^*\left(t+\tfrac{\tau}{2}\right) e^{-j2\pi\alpha t}] \\ &= E[s\left(t+\tfrac{\tau}{2}\right) s^*\left(t+\tfrac{\tau}{2}\right) e^{-j2\pi\alpha t}] \\ &= R_{ss}^{\alpha}(\tau) \end{aligned} \tag{2.73}$$

which is same as the cyclic autocorrelation function of the baseband signal. The conjugate cyclic autocorrelation function may be written as

$$\begin{aligned} R_{xx^*}^{\alpha} &= E[s\left(t+\tfrac{\tau}{2}\right) s\left(t+\tfrac{\tau}{2}\right) e^{j2\pi\alpha n} e^{-j4\pi f_c t}] \\ &= E[s\left(t+\tfrac{\tau}{2}\right) s\left(t+\tfrac{\tau}{2}\right) e^{-j2\pi(\alpha-2f_c)t}] \end{aligned} \tag{2.74}$$

As the signal $s[n]$ is real,

$$R_{xx^*}^{\alpha} = R_{ss}^{\alpha-2fc}(\tau) \tag{2.75}$$

That means, a BPSK signal exhibits cyclostationarity at $\frac{k}{T_0}$ and conjugate cyclostationarity at $2f_c \pm \frac{k}{T_0}$.

2.4 Linear Periodically Time Variant Filtering

In this section, it is shown that the second-order cyclostationarity may be generated by passing a purely stationary signal through a Linear Periodically Time-Variant(LPTV) system [47]. It is also seen that many operations such as carrier and pulse modulation may be modeled in the form of equivalent LPTV filters [44, 45]. Therefore, the analysis of LPTV systems helps in determining the cyclostationary characteristics of signals generated via these processes.

For a general linear system, the impulse response $h(t, u)$ is defined as the response of

the system at time t to a time-shifted impulse $\delta(t-u)$. The output $y(t)$ of the system for an input $x(t)$ is given as

$$y(t) = \int_{-\infty}^{\infty} h(t,u)x(u)du \tag{2.76}$$

The system is said to be LPTV if there exists a period T_0 such that for $k \in \mathbb{Z}$

$$h(t,u) = h(t+kT_0, u+kT_0) \tag{2.77}$$

It may be observed that the above function may also be written as $h(t+\tau, t)$ which is periodic in t for all τ. This may, therefore, be expanded in the form of a Fourier series as

$$h(t+\tau,t) = \sum_{k=-\infty}^{\infty} h_k(\tau)e^{j\frac{2\pi kt}{T_0}} \tag{2.78}$$

Generalizing this to a Linear Almost Periodic Time Variant (LAPTV) filter, we have

$$h(t+\tau,t) = \sum_{\eta} h_\eta(\tau)e^{j2\pi\eta t} \tag{2.79}$$

Substituting (2.79) in (2.76) the output of a LAPTV filter may be given as

$$\begin{array}{rcl} y(t) & = & \int_{-\infty}^{\infty} \sum_\eta h_\eta(t-u)e^{j2\pi\eta u}x(u)du \\ & = & \sum_\eta \int_{-\infty}^{\infty} h_\eta(t-u)x(u)e^{j2\pi\eta u}du \end{array} \tag{2.80}$$

Taking Fourier transform on both sides, we have

$$Y(f) = \sum_{\eta} H_\eta(f)X(f-\eta) \tag{2.81}$$

The cyclic spectral density of $y(t)$ at a cyclic frequency α may therefore be written as [50]

$$S_{yy}^{\alpha}(f) = \sum_{\eta}\sum_{\nu} H_\eta\left(f+\frac{\alpha}{2}\right) S_{xx}^{\alpha+\nu-\eta}\left(f-\frac{\eta+\nu}{2}\right) H_\nu\left(f-\frac{\alpha}{2}\right) \tag{2.82}$$

Also, (2.80) may be re-written as

$$y(t) = \sum_{\eta} h_\eta(t) * x^{-\eta}(t) \tag{2.83}$$

where $*$ denotes the convolution operation. Therefore, it may be observed that LAPTV filtering of a signal is equivalent to LTI filtering of frequency shifted versions of that signal. Thus LPTV (or LAPTV) filtering is also known as Frequency shift (FRESH) filtering.

Substituting (2.83) in (2.35), the cyclic autocorrelation function of $y(t)$ takes the form

$$R_{yy}^{\alpha}(\tau) = \sum_{\eta}\sum_{\nu}\int_{-\infty}^{\infty}\int_{-\infty}^{\infty} h_{\eta}(u)R_{xx}^{\alpha+\nu-\eta}(\tau-u+v)h_{\nu}^{*}(v)dudv \tag{2.84}$$

For the discrete time case, the impulse response of a general LAPTV system may be written as

$$h[n+k,n] = \sum_{\eta} h_{\eta}[k]e^{j2\pi\eta n} \tag{2.85}$$

The output $y[n]$ for an input signal $x[n]$ will therefore be given as

$$y[n] = \sum_{\eta}\sum_{k=-\infty}^{\infty} x^{-\eta}[k]h_{\eta}[n-k] \tag{2.86}$$

Consequently, the cyclic autocorrelation function of $y[n]$ may be written as

$$R_{yy}^{\alpha}[\tau] = \sum_{\eta}\sum_{\nu}\sum_{l=-\infty}^{\infty}\sum_{k=-\infty}^{\infty} h_{\eta}[l]R_{xx}^{\alpha+\nu-\eta}[\tau-l+k]h_{\nu}^{*}[k] \tag{2.87}$$

and the cyclic spectral density may be written as

$$S_{yy}^{\alpha}(f) = \sum_{\eta}\sum_{\nu} H_{\eta}\left(f+\frac{\alpha}{2}\right)S_{xx}^{\alpha+\nu-\eta}\left(f-\frac{\eta+\nu}{2}\right)H_{\nu}\left(f-\frac{\alpha}{2}\right) \tag{2.88}$$

From the above expressions it is observed that if the input signal is purely stationary, then the cyclic spectral density of the output signal is non-zero whenever $\alpha+\nu-\eta=0$. Therefore, the output is cyclostationary for $\alpha = \eta-\nu$. Thus, LAPTV filtering of a purely stationary signal results in the generation of a cyclostationary signal. As stated earlier, most modulation systems can be modeled as equivalent LPTV/LAPTV filters and, therefore, the communication signals generated by passing a wide sense stationary (WSS) data signal through these may also be modeled as cyclostationary.

Chapter 3

Space-Time FRESH Filter Based Spectrum Sensing

It has been shown that cyclostationary features may be used to sense the presence of a primary signal embedded in noise [91]. The cyclostationarity property of a signal may also be used to derive an optimal FRESH filter to enhance it [48] as well as form a beam in its direction [2]. The underlying idea in this chapter is to combine the optimal temporal FRESH filter [48] with a cyclostationarity-based beam-former to obtain a generalized Space-Time filtering structure for cyclostationary signals. It is proposed to use this structure, called a Space-Time FRESH filtering structure, to enhance a cyclostationary signal prior to detection. It is argued that the cyclostationary primary component in the received signal, if present, will be enhanced by this process. This enhancement will further result in an improved detection performance of the spectrum sensor.

However, it must be noted that the weights of the optimal space-time FRESH filter will depend on the correlation structure of the primary signal and may not be known at the spectrum sensor. Therefore, it becomes necessary to adapt the weights of this structure so as to obtain the optimal set of weights. For this purpose, the ACS (Adaptive Cross SCORE) beamforming algorithm developed in [36] is modified to adapt a Space-Time structure. However, it is found that the modified ACS algorithm has a computational complexity proportional to the square of the number of elements being adapted. This acts as a bottleneck in the sensing process. To avoid this bottleneck, the correlation maximization problem of the modified SCORE algorithms is reformulated as a constrained MMSE (Minimum Mean Square Error) problem and a stochastic gradient-based algorithm called the C2-LMS algorithm is developed to solve this. It is then shown that the C2-LMS algorithm has a complexity linearly proportional to the number of taps being used for signal enhancement.

Simulation results are used to determine the performance of the proposed structure for

[1]This work has been published in the July 2014 issue of IEEE Transactions on Wireless Communications as "Spectrum Sensing for Cognitive Radios Based on Space-Time FRESH filtering"

both the adaptation algorithms. It is observed that Space-Time FRESH filtering of the received signal prior to energy detection and cyclostationary detection leads to gains of more than 10 dB over the standard energy detector and the cyclostationary detector.

Section 3.1 provides a review of the work done in cyclostationary spectrum sensing, optimal FRESH filtering and SCORE beam-forming, and develops the idea of a space-time FRESH filtering structure. The theories on optimal FRESH filtering and SCORE beam-forming are revisited in Sections 3.2 and 3.3 respectively. The primary signal model along with the standard energy detector is described in Section 3.4. The standard energy detector acts as a baseline to compare the detection performance of the FRESH filters. Section 3.5 details the proposed Space-Time FRESH filtering structure, states the equivalent hypotheses of the spectrum sensing problem for a signal filtered using it and describes a method that may be used to sense the spectrum. Section 3.6 presents the lower complexity constrained doubly adaptive LMS (C2-LMS) algorithm for adapting the filter weights and the related spectrum sensing method. Simulation results in support of the proposed Space-Time FRESH filtering for spectrum sensing are contained in Section 3.7. Finally, the conclusions are drawn in Section 3.8.

3.1 Background and Motivation

In [49] Gardener proposed to use the cyclostationary features of signals for weak signal detection. Here, the spectral correlation theory of cyclostationary detectors is used to relate the different random signal detectors, viz. the spectral line re-generator, the cyclic-spectral analyzer, the likelihood ratio detector and the ML detector. This is followed by arguments in favor of the use of cyclostationary detection in comparison to the energy detection.

Dandawate and Giannakis in [31] derived tests based on cyclic autocorrelation and cyclic spectral density to check for the presence of cyclostationary signals. The proposed method involves an exhaustive search over the possible cyclic frequency for which the cyclic autocorrelation function of the signal of interest is non-zero. The CFAR (constant false alarm rate) tests proposed here use both the cyclic autocorrelation function as well the cyclic spectral density as the test statistics. These tests for the presence of second order cyclostationarity are then extended to detect the presence of kth order cyclostationary signals.

In [92], tests based on cyclostationarity are used to sense the presence of a GMSK modulated GSM signal for spectrum pooling with an OFDM-based WLAN system. Both the cyclic autocorrelation function and the cyclic spectral density are used as test statistics. The performance of the proposed detector is evaluated at different SNRs for AWGN and Rayleigh fading environments. This, however, considers SNRs greater than or equal to -5dB, thereby leaving much scope for improvement in the detection performance.

The single cyclic frequency and single secondary user approach of [91] and [92] is extended to a multiple secondary user, multi-cycle approach in [82]. In this paper, it is proposed to use multiple cyclic frequencies for spectrum sensing. It is argued that the statistics of the received signal at different cyclic frequencies will be independent of each other. Therefore, the statistics derived out of multiple cyclic frequencies may be used to improve the detection performance. The multicycle detector is then extended to a multiple secondary user case where multiple secondary users report to a fusion center. The test statistics are quantized to conserve the control channel bandwidth. The performance of both the single user and the collaborative sensing schemes are studied in AWGN, Rayleigh fading and log normal shadowing. It is shown that increasing the number of cyclic frequencies in the test statistics improves the detection performance.

The work of [82] is further extended in [104]. Here, the relative strengths and variances of the different cyclic frequencies are taken into account. In this paper, weights are derived for optimally combining the finite time cyclic autocorrelation function at different cyclic frequencies, based on its statistics at that given cyclic frequency. These optimal weights are then used to develop a deflection coefficient-based detector [68]. The derived results are verified via simulation.

The problem of cyclostationary spectrum sensing is generalized to a multi-antenna case by Axell and Larsson in [7]. In this paper, the spatial as well as the temporal correlation of the primary component of the received signal is exploited. A GLRT like approach using the eigenvalues of the covariance matrix of the received signal is derived. The proposed method is then used for the detection of an OFDM signal. A similar problem is studied in [131] where the eigenvalues of the cyclic covariance matrix are used instead of the conventional covariance matrix. They derived the expressions for the detection performance under both spatially correlated and uncorrelated noise. This test statistic, similar to the one in [7], requires only the cyclic frequency of the primary signal to develop a CFAR detector. It is observed in both [7] and [131] that a multi-antenna system performs better in comparison to a single-antenna system and the performance improves further with an increase in the number of antennas.

It was shown in [48] that an optimal FRESH filter for cyclostationary signals may be developed on similar lines as an optimal filter for a purely stationary signal. It is also observed that owing to the recent advances in adaptive signal processing [20–22, 56, 93, 98, 99], the weights for these filters may be determined adaptively. It is observed in [145] and [146] that the FRESH filter structure may be adapted blindly by using the original signal as the reference signal and its frequency shifted version as the input to the filter. This is known as the Blind Adpative FRESH (BAFRESH) filter. The convergence properties of this structure have been derived in [146] for the LMS algorithm. The BAFRESH structure, as illustrated in the sequel works for both LMS and the RLS algorithms.

The use of adaptive FRESH filters for BPSK signal was first proposed in [135]. In this

paper, it is shown that adaptive FRESH filters are able to compensate for some amount of error in the known cyclic frequency. This issue is discussed in more detail in the Chapter 7.

FRESH filters are employed for the purpose of spectrum sensing in [105]. It is shown here via simulation results that blind adaptive FRESH filters adapted using both the LMS and the RLS algorithms may be used to adapt the FRESH filter which may then be used to enhance the primary component in a cyclostationary signal prior to detection. This approach is studied only for the cyclostationary detector and it is shown that FRESH filtering a signal prior to detection significantly improves the detection performance.

The cyclostationarity property of signals has also been exploited in [2, 36, 134] for the purpose of beamforming in antenna arrays. These algorithms use the spectral autocoherence of the signal of interest to steer an antenna array in its direction. The first among these is the SCORE (Spectral COherence REstoral) class of algorithms presented in [2]. In this paper, three algorithms, viz. LS-SCORE, cross-SCORE and auto SCORE are developed. All of these algorithms solve the problem of spectral coherence maximization. That is, the weight and control vectors are selected so as to maximize the spectral coherence of the output signal.

The LS-SCORE algorithm derives the optimal steering vector for a fixed control vector. It is shown that in this case the problem of finding an optimal steering vector may be modelled as a least squares problem. In the cross-SCORE problem, both the optimal steering vector and the optimal control vector are determined. It is found here that the maximization problem needs to be solved separately for both these vectors. As a result a recursive solution is obtained. In the auto-SCORE formulation of the SCORE problem, only the optimal steering vector maximizing the cyclic autocorrelation of the filtered signal is obtained. The resulting problem has similar form to Fisher's linear discriminant and may be solved as a generalized eigenvalue problem for the cyclic covariance and the covariance matrices of the received signal.

The Cyclic Adaptive Beamforming (CAB) class of algorithms was proposed in [134] to compensate for the slow convergence speed of the SCORE algorithms. Here again, both the control vector and the steering vector of the antenna array are considered as adaptive and are constrained to a unit norm. It is shown that the optimal steering and control vectors may be obtained as the dominant singular vectors of the cross correlation matrix of the input and control vectors. These are then used to determine the angles of arrival of different signals.

Adaptive versions of both CAB and SCORE classes of algorithms are developed in [36]. It is shown here that recursive computations of the autocorrelation, cyclic autocorrelation and cross correlation matrices of the input signals, and their inverses lead to adaptive implementations of the aforementioned algorithms. The performances of these algorithms are compared under various simulation conditions and it is found that the Adaptive Cross

SCORE (ACS) algorithm outperforms the adaptive CAB algorithm under low SNR conditions.

Cyclostationary beamforming is employed for the purpose of spectrum sensing in [35]. In this paper, both the ACS and the CAB algorithms are used to form a beam in the direction of the signal exhibiting cyclostationarity. The directivity of the resulting beampattern is then used as a test statistic. It is seen that in this case the detectors based on the ACS algorithm outperform the detectors based on CAB algorithms. However, this paper does not compare its proposed detector against the standard energy or cyclostationary detectors, nor does it provide any details on the behaviour of the chosen test statistics.

In the past, Space-Time filtering has been used to improve the capacity, performance and coverage of wireless communication systems [14,52,96,110,132]. The space-time structures exploit the spatial and temporal correlation in the signal to enhance the system performance. It is observed that in multi-antenna cyclostationary spectrum sensing, all three forms of correlation, viz. spatial, temporal, and spectral, will exist. Therefore, in this chapter, we extend the works cited above and propose a Space-Time FRESH filtering structure to enhance and consequently ease the detection of cyclostationary signals.

3.2 Optimal FRESH filtering

If a discrete-time signal $x[n]$ exhibits regular cyclostationarity at cyclic frequencies $\alpha_1, \alpha_2, \ldots \alpha_{M_1} \in \mathcal{A}$ and conjugate spectral coherence at a cyclic frequencies $\beta_1, \beta_2, \ldots \beta_{M_1} \in \mathcal{B}$ then it may be represented as

$$x[n] = \sum_{\alpha_\in \mathcal{A}} \sum_{l=0}^{L_\alpha - 1} a_\alpha[l] x^\alpha[n-l] + \sum_{\beta_\in \mathcal{B}} \sum_{l=0}^{L_\alpha - 1} a_\beta[l] x^{*\beta}[n-l] + \zeta[n] \tag{3.1}$$

where $\zeta[n]$ is the innovation component and, $a_\alpha[l]$ and $a_\beta[l]$ are the regression coefficients at the given cyclic frequencies and lags. Also, $x[n]$ may be estimated using its optionally conjugated time and frequency shifted versions. For a cyclostationary signal corrupted with wide sense stationary noise, this property may be used to denoise it. A linear combination of the time and frequency shifted versions of the noisy signal may be used to enhance the cyclostationary component contained within it. The problem in this case is to find an optimal set of linear combination weights that minimizes the error between the signals of interest and its estimate. In view of this, the problem of optimal FRESH filtering may be stated as, "Given a signal $x[n]$ exhibiting cyclostationarity at M_1 frequencies $\alpha_1, \alpha_2, \ldots, \alpha_{M_1}$ and conjugate cyclostationarity at M_2 frequencies $\beta_1, \beta_2, \ldots, \beta_{M_2}$, find the optimal set of weights $w_{\alpha_m,p}$ and $w_{\beta_m,q}$ so that the mean square value of the error $e[n]$, as defined below, is minimized. [48]" .

$$e[n] = x[n] - v[n] \tag{3.2}$$

where $v[n]$ is the FRESH filtered output, given as

$$v[n] = \sum_{m=1}^{M_1} \sum_{p=0}^{L_{\alpha_m}-1} w^*_{\alpha_m,p} x^{\alpha_m}[n-p] + \sum_{m=1}^{M_2} \sum_{q=0}^{L_{\beta_m}-1} w^*_{\beta_m,q} x^{*\beta_m}[n-q] \tag{3.3}$$

where L_{α_m} and L_{β_m} are the filter lengths corresponding to the frequency shifts α_m and β_m, respectively [48, 105].

Defining

$$\mathbf{w} = [\mathbf{w}^T_{\alpha_1} \dots \mathbf{w}^T_{\alpha_{M_1}} \quad \mathbf{w}^T_{\beta_1} \dots \mathbf{w}^T_{\beta_{M_2}}]^T \tag{3.4}$$

$$\mathbf{u}[n] = \left[\mathbf{x}^{\alpha_1 T}[n] \dots \mathbf{x}^{\alpha_{M_1} T}[n] \quad \mathbf{x}^{\beta_1 T}[n] \dots \mathbf{x}^{\beta_{M_2} T}[n]\right]^T \tag{3.5}$$

where

$$\begin{aligned} \mathbf{w}_{\alpha_i} &= [w_{\alpha_i,1} \dots w_{\alpha_i,L_{\alpha_i}}]^T \\ \mathbf{w}_{\beta_i} &= [w_{\beta_i,1} \dots w_{\beta_i,L_{\beta_i}}]^T \end{aligned} \tag{3.6}$$

and

$$\begin{aligned} \mathbf{x}^{\alpha_i}[n] &= \left[x^{\alpha_i}[n] \dots x^{\alpha_i}[n - L_{\alpha_i} + 1]\right]^T \\ \mathbf{x}^{\beta_i}[n] &= \left[x^{*\beta_i}[n] \dots x^{*\beta_i}[n - L_{\beta_i} + 1]\right]^T \end{aligned} \tag{3.7}$$

equation (3.3) may be rewritten in the form

$$v[n] = \mathbf{w}^H \mathbf{u}[n] \tag{3.8}$$

Mean square value of $e[n]$ may be written as

$$\begin{aligned} J &= E|e[n]|^2 \\ &= E\left[(x[n] - \mathbf{w}^H)(x[n] - \mathbf{w}^H)^*\right] \\ &= \sigma_x^2 - \mathbf{w}^H \mathbf{r}_{ux} - \mathbf{r}_{ux}\mathbf{w}^H + \mathbf{w}^H \mathbf{R}_{uu} \mathbf{w} \end{aligned} \tag{3.9}$$

where

$$\begin{aligned} \mathbf{R}_{uu} &= E\left[\mathbf{u}[n]\mathbf{u}^H[n]\right] \\ \mathbf{r}_{ux} &= E\left[\mathbf{u}[n]x^*[n]\right] \end{aligned} \tag{3.10}$$

This may be solved to obtain

$$\mathbf{w} = \mathbf{R}_{uu}^{-1} \mathbf{r}_{ux} \tag{3.11}$$

In an adaptive setting for FRESH filtering, the original signal may be used as a reference signal to adapt the weight vector $\mathbf{w}$ to their optimal values. This leads to the Blind Adaptive FRESH (BA-FRESH) filtering approach, as described in [145]. The corresponding structure for a BA-FRESH filter is shown in Figure 3.1.

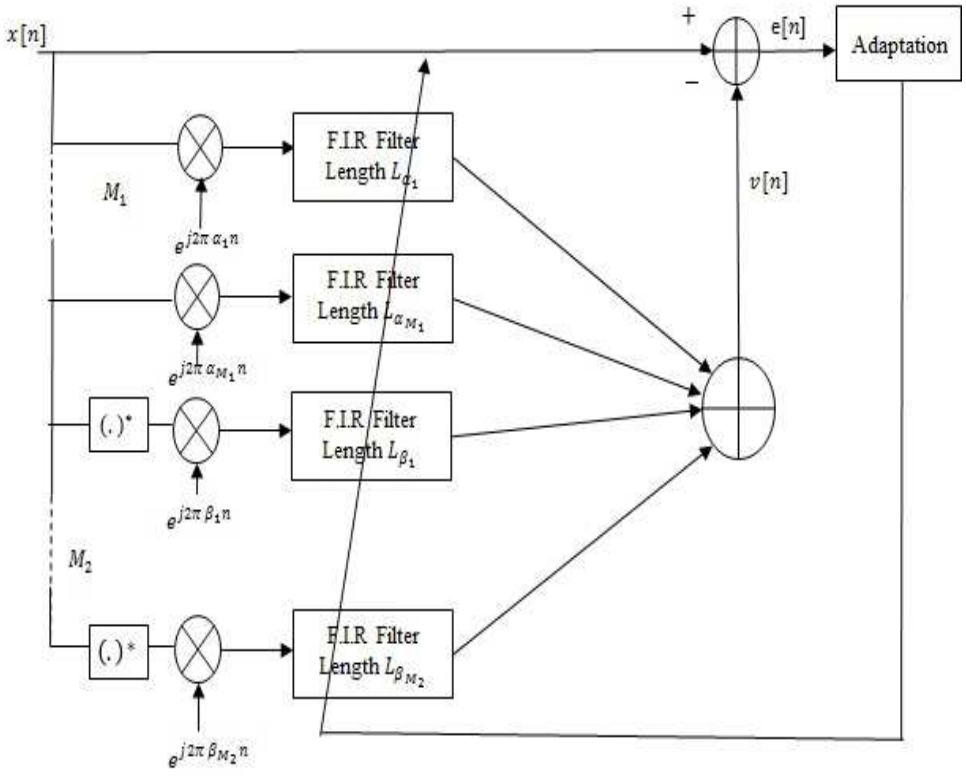

Figure 3.1: The blind adaptive FRESH filtering structure as proposed in [145].

3.3 SCORE Beamforming

It is a well established fact that the use of antenna arrays results in increased directivity as compared to single-antenna systems. Apart from this, it is also known that the direction of the main lobe of an antenna array may be steered electronically. Techniques have been devised to adaptively steer the main lobe of an array, based on the direction of the signal of interest. It has been observed that cyclostationarity exhibited by the signal of interest may also be used to form a beam in the direction of the signal of interest [2].

To describe this technique, consider a signal $s[n]$, exhibiting regular or conjugate cyclostationarity for some cyclic frequency α, incident at an angle θ on an antenna array consisting of K antennas, as shown in Figure 3.2. Also, consider $\mathbf{a}(\theta)$ to be the steering vector of the array for the direction θ and $\boldsymbol{\nu}[n]$ to be the additive zero mean stationary white noise vector whose each component is i.i.d. white circularly symmetric complex Gaussian. Then, the received signal $x[n]$ may be written as

$$\mathbf{x}[n] = \mathbf{a}(\theta)s[n] + \boldsymbol{\nu}[n] \tag{3.12}$$

where

$$\mathbf{a}(\theta) = [1 e^{\frac{j2\pi d sin\theta}{\lambda}} \dots e^{\frac{j(K-1)2\pi d sin\theta}{\lambda}}] \tag{3.13}$$

$$\begin{aligned} \boldsymbol{\nu}[n] &= [\nu_1[n] \dots \nu_K[n]] \\ \nu_k[n] &\sim \mathcal{N}_c(0, \sigma_\nu^2) \end{aligned} \tag{3.14}$$

where d is the spacing between two adjacent elements of the antenna array. It is desired here to steer the main lobe of this array in the direction of $s[n]$. The spatial and spectral coherence of the signal $s[n]$ may be used for this purpose [2]. From the structure in Figure 3.2, the signals $v[n]$ and $y[n]$ may be defined as

$$\begin{aligned} v[n] &= \mathbf{w}^H \mathbf{u}[n] \\ y[n] &= \mathbf{h}^H \mathbf{x}[n] \end{aligned} \tag{3.15}$$

where

$$\begin{aligned} \mathbf{u}[n] &= [u_1[n] u_2[n] \dots u_K[n]]^T \\ u_k[n] &= x_k^{(*)}[n] e^{j2\pi\alpha n} \end{aligned} \tag{3.16}$$

and

$$\begin{aligned} \mathbf{w} &= [w_1, w_2, \dots, w_K]^T \\ \mathbf{h} &= [h_1, h_2, \dots, h_K]^T \end{aligned} \tag{3.17}$$

The outputs of the antenna elements $x_k[n]$ and their frequency shifted versions $u_k[n]$ are linearly combined using weights h_1, $h_2, \dots,$ h_K and w_1, $w_2, \dots,$ w_K. Due to the presence of cyclostationarity in $s[n]$, $y[n]$ is correlated to $v[n]$ and there exist $\mathbf{h}$ and $\mathbf{w}$ maximizing the absolute value of the cross-correlation coefficient ρ_{vy} between $v[n]$ and $y[n]$. The SCORE

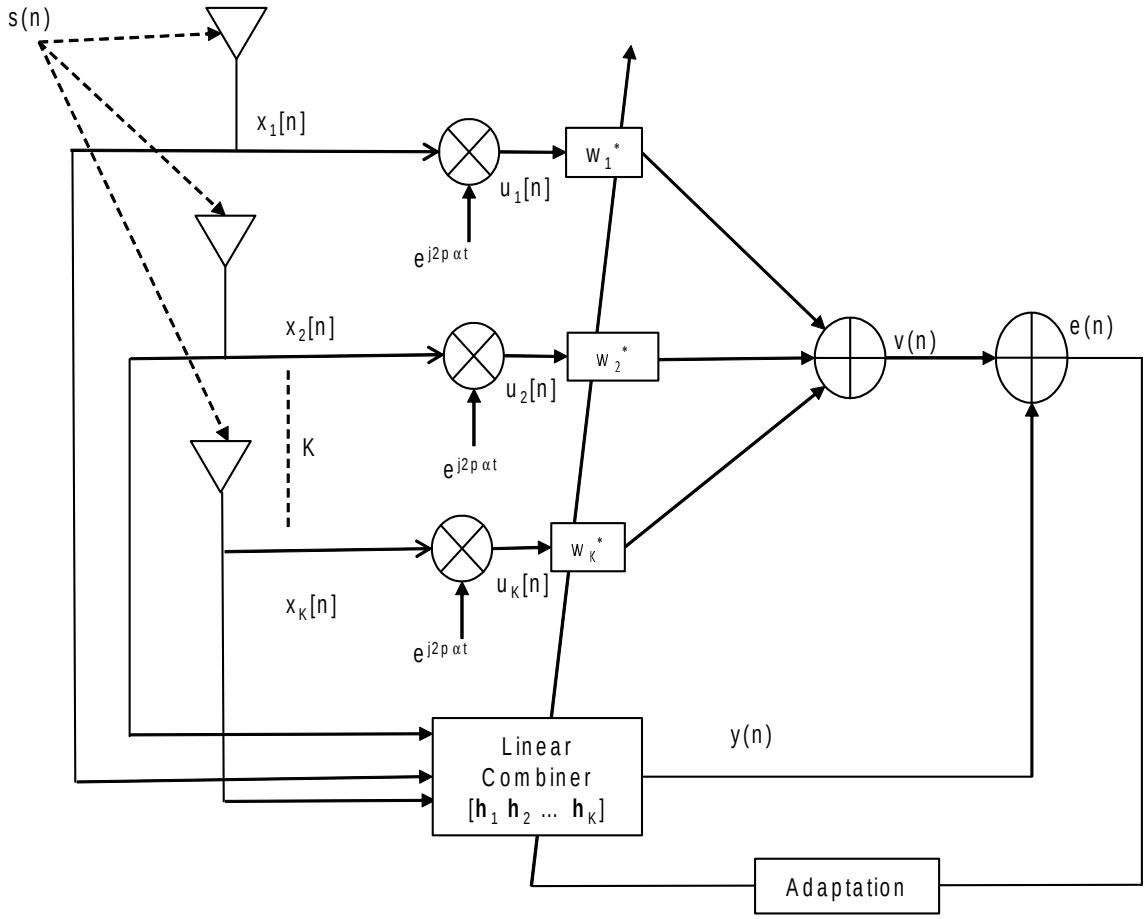

Figure 3.2: The structure for cyclostationary beamforming as used in [2].

beam-forming problem is to find the weight vectors $\mathbf{h}$ and $\mathbf{w}$ maximizing ρ_{vy} defined as

$$|\rho_{vy}|^2 = \frac{|r_{vy}(0)|^2}{\sigma_v^2 \sigma_y^2} = \frac{|\mathbf{w}^H \mathbf{R}_{ux} \mathbf{h}|^2}{\mathbf{w}^H \mathbf{R}_{uu} \mathbf{w} \mathbf{h}^H \mathbf{R}_{xx} \mathbf{h}} \tag{3.18}$$

where

$$\begin{aligned} \mathbf{R}_{xx} &= E\left[\mathbf{x}[n]\mathbf{x}^H[n]\right] \\ \mathbf{R}_{ux} &= E\left[\mathbf{u}[n]\mathbf{x}^H[n]\right] \end{aligned} \tag{3.19}$$

This is a generalized eigenvalue problem and may be solved separately for $\mathbf{w}$ and $\mathbf{h}$ to obtain [2]

$$\begin{aligned} \mathbf{w} &\propto \mathbf{R}_{uu}^{-1} \mathbf{R}_{ux} \mathbf{h} \\ \mathbf{h} &\propto \mathbf{R}_{xx}^{-1} \mathbf{R}_{xu} \mathbf{w} \end{aligned} \tag{3.20}$$

A recursive procedure, the Adaptive Cross SCORE (ACS) algorithm, has been developed in [36] to solve this system of equations.

3.4 The Signal Model and Detectors

The problem of spectrum sensing for a primary signal $s[n]$ in the presence of a noise $\nu[n]$ for a received signal $x[n]$ may be written in the form of a binary hypothesis test as

$$x[n] = \begin{cases} \nu[n] & \mathcal{H}_0 \\ s[n] + \nu[n] & \mathcal{H}_1 \end{cases} \tag{3.21}$$

where the null hypothesis $\mathcal{H}_0$ corresponds to the absence of a primary signal and the alternative hypothesis, $\mathcal{H}_1$ to its presence. Both the primary signal and the noise may be assumed to be zero mean complex Gaussian with variances σ_s^2 and σ_ν^2 respectively. If both the primary signal and the noise variances are known, then the presence of the primary user signal may be detected simply by measuring the energy of $x[n]$ and comparing it against the noise variance [59]. The test statistic in this case for N samples of $x[n]$ becomes

$$\mathcal{E}_x = \frac{1}{N} \sum_{n=0}^{N-1} |x[n]|^2 \tag{3.22}$$

This is the sum square of N number of i.i.d. complex Gaussian terms and, therefore, is Chi-Square distributed with $2N$ degrees of freedom and a scaling factor equal to the variance of $x[n]$. The distribution of $\mathcal{E}_x$ may, therefore, be written as

$$\mathcal{E}_x \sim \begin{cases} \sigma_\nu^2 \chi_{2N}^2 & \mathcal{H}_0 \\ (\sigma_s^2 + \sigma_\nu^2)\chi_{2N}^2 & \mathcal{H}_1 \end{cases} \tag{3.23}$$

Using these distributions and a detection threshold λ, the probabilities of detection and false alarm may be written as

$$P_{fa} = Pr\{\mathcal{E}_x > \lambda | \mathcal{H}_0\} = \frac{\Gamma\left(2N, \sqrt{\frac{\lambda}{2}}\right)}{\Gamma(2N)} \tag{3.24}$$

$$P_d = Pr\{\mathcal{E}_x > \lambda | \mathcal{H}_1\} = \frac{\Gamma\left(2N, \sqrt{\frac{(\sigma_\nu^2+\sigma_s^2)\lambda}{2\sigma_\nu^2}}\right)}{\Gamma(2N)} \tag{3.25}$$

where $\Gamma(.)$ and $\Gamma(.,.)$ are, respectively, the complete and incomplete Γ functions.

Alternatively, as the samples of $x[n]$ are i.i.d. Gaussian, therefore, the central limit theorem may be used on $\mathcal{E}_s$ [122] for a large N, such that the distribution of the test statistic under the two hypotheses may be approximated as

$$\mathcal{E}_x \sim \begin{cases} N_c\left(\sigma_\nu^2, \frac{\sigma_\nu^4}{N}\right) & \mathcal{H}_0 \\ N_c\left((\sigma_s^2+\sigma_\nu^2), \frac{(\sigma_s^2+\sigma_\nu^2)^2}{N}\right) & \mathcal{H}_1 \end{cases} \tag{3.26}$$

In view of this, the probabilities of detection and of false alarm for a threshold λ may be written as

$$P_{fa} = Q\left(\frac{\lambda - \sigma_\nu^2}{\sqrt{\frac{1}{N}}\sigma_\nu^2}\right) \tag{3.27}$$

$$P_d = Q\left(\frac{\lambda - (\sigma_\nu^2+\sigma_s^2)}{\sqrt{\frac{1}{N}}(\sigma_\nu^2+\sigma_s^2)}\right) \tag{3.28}$$

It may be observed that for any given values of σ_ν^2 and σ_s^2 the probabilities of detection and false alarm are functions of the number of samples of $x[n]$. It is therefore possible to determine the number of samples required to achieve a given detection and false alarm performance. Equations (3.27) and (3.28) may be solved to find N as

$$N = \frac{[Q^{-1}(P_{fa}) - Q^{-1}(P_d)(1+\gamma_i)]^2}{\gamma_i^2} \tag{3.29}$$

where $\gamma_i = \frac{\sigma_s^2}{\sigma_\nu^2}$ is the signal to noise ratio at the input of the spectrum sensor.

3.4.1 Noise Uncertainty and SNR walls

The results for the energy detector derived previously correspond to an ideal scenario where the signal and noise variances are exactly known to the spectrum sensor. This may not always be the case.

To explain the effect of noise uncertainty in energy detection, let us assume that the noise variance $\hat{\sigma}_\nu^2$ known at the spectrum sensor is an estimate of the true noise variance σ_ν^2.

Let us also assume that there exists uncertainty in the noise variance by a factor $\rho(\rho > 1)$ that is the value of $\hat{\sigma}_\nu^2$ may lie anywhere in the interval $[\frac{\sigma_\nu^2}{\rho}, \rho\sigma_\nu^2]$.

Considering the worst case while calculating the probabilities of detection and false alarm, i.e. $\hat{\sigma}_\nu^2 = \rho\sigma_\nu^2$ when calculating the probability of false alarm and $\hat{\sigma}_\nu^2 = \frac{\sigma_\nu^2}{\rho}$ when calculating the probability of detection, these may be written as

$$P_{fa} = Q\left(\frac{\lambda - \rho\sigma_\nu^2}{\sqrt{\frac{1}{N}}\sigma_n^2}\right) \tag{3.30}$$

$$P_d = Q\left(\frac{\lambda - (\frac{\sigma_\nu^2}{\rho} + \sigma_s^2)}{\sqrt{\frac{1}{N}}(\frac{\sigma_\nu^2}{\rho} + \sigma_s^2)}\right) \tag{3.31}$$

Solving these, the number of samples required to achieve a given detection performance may be written as

$$N = \frac{[Q^{-1}(P_{fa}) - Q^{-1}(P_d)(1+\gamma_i)]^2}{\left(\gamma_i - \left(\rho - \frac{1}{\rho}\right)\right)^2} \tag{3.32}$$

It may be observed that as $\gamma \to \left(\rho - \frac{1}{\rho}\right)$, $N \to \infty$. In other words, as the uncertainty in noise variance tends to the signal variance, upper bound on the number of samples required to detect a primary user signal will vanish. It may be observed that at an SNR of -20 dB an error as small as 1% may lead to such effects. This phenomenon of the inability of the spectrum sensor to detect a primary user signal at low SNRs was first discusses by Tandra and Sahai in [122] and is known as SNR walls.

3.4.2 The Cyclostationarity Detector

Cyclostationary features of a signal may also be used to distinguish it from WSS-AWGN. To describe this consider the finite time cyclic autocorrelation function of $x[n]$ for N samples at cyclic frequency α and lag τ

$$\hat{R}_{xx}^{\alpha}[N,\tau] = \frac{1}{N-\tau}\sum_{n=\tau}^{N} x[n]x^*[n-\tau]e^{j2\pi\alpha n} \tag{3.33}$$

It may be seen that this is the sum of $(N-\tau)$ frequency shifted lag products of $x[n]$, and $\xi_{xx}^{\alpha}[n,\tau]$ may be defined as

$$\xi^{\alpha}[n,\tau] = x[n]x^*[n-\tau]e^{j2\pi\alpha n} \tag{3.34}$$

The samples of $x[n]$ may be assumed to be to be identically distributed Gaussian and, therefore the terms $\xi_{xx}^{\alpha}[n,\tau]$ may also be assumed to be identically distributed. Hence, $\hat{R}_{xx}^{\alpha}[N,\tau]$ is a sum of a large number of random variables and by the central limit theorem

may be assumed to be Gaussian distributed.

$$E\left[\hat{R}_{xx}^{\alpha}[N,\tau]\right] = \frac{1}{N-\tau}E\left[\sum_{n=\tau}^{N-1}\hat{\xi}_{xx}^{\alpha}[n,\tau]\right] \tag{3.35}$$

Changing the order of summation and expectation and using the fact that $\xi_{xx}^{\alpha}[n,\tau]$ are identically distributed we have,

$$E\left[\hat{R}_{xx}^{\alpha}[N,\tau]\right] = E\left[\hat{\xi}_{xx}^{\alpha}[n,\tau]\right] \tag{3.36}$$

Considering this separately under the two hypotheses, we have

$$\hat{\xi}_{xx}^{\alpha}[n,\tau]|\mathcal{H}_0 = \nu[n]\nu^*[n-\tau]e^{j2\pi\alpha n} \tag{3.37}$$

Therefore,

$$E[\hat{\xi}_{xx}^{\alpha}[n,\tau]|\mathcal{H}_0] = \sigma_\nu^2\delta[\tau]\delta(\alpha) \tag{3.38}$$

where $\delta[.]$ is the Kronecker delta function and $\delta(.)$ is the Dirac delta function. Also,

$$\hat{\xi}_{xx}^{\alpha}[n,\tau]|\mathcal{H}_1 = (s[n]+\nu[n])(s[n-\tau]+\nu[n-\tau])^* e^{j2\pi\alpha n} \tag{3.39}$$

The primary user signal and noise may be assumed to be independent, therefore,

$$\begin{aligned} E[\hat{\xi}_{xx}^{\alpha}[n,\tau]]|\mathcal{H}_1 &= E[s[n]s^*[n-\tau]e^{j2\pi\alpha n}] + E[\nu[n]\nu^*[n-\tau]e^{j2\pi\alpha n}] \\ &= R_{ss}^{\alpha}[\tau] + \sigma_\nu^2\delta[\tau]\delta(\alpha) \end{aligned} \tag{3.40}$$

To determine the variance of $R_{xx}^{\alpha}[N,\tau]$ under the two hypotheses, its mean square value is required. Considering the null hypothesis, we get

$$E\left[|R_{xx}^{\alpha}[N,\tau]|^2\middle|\,\mathcal{H}_0\right] = \frac{1}{(N-\tau)^2}E\left[\sum_{m=\tau}^{N-1}\sum_{n=\tau}^{N-1}\left(\nu[m]\nu^*[m-\tau]e^{j2\pi\alpha m}\right)\left(\nu^*[n]\nu[n-\tau]e^{-j2\pi\alpha n}\right)\right] \tag{3.41}$$

This may be simplified to

$$E\left[|R_{xx}^{\alpha}[N,\tau]|^2|\mathcal{H}_0\right] = \frac{1}{N-\tau}\sigma_\nu^4 + \sigma_\nu^4\delta[\tau]\delta(\alpha) \tag{3.42}$$

The variance $R_{xx}^{\alpha}[N,\tau]$ under the null hypothesis becomes [31]

$$var\left(R_{xx}^{\alpha}[N,\tau]|\mathcal{H}_0\right) = \frac{1}{N-\tau}\sigma_\nu^4 \tag{3.43}$$

Similarly it may be shown that

$$var\left(R_{xx}^{\alpha}[N,\tau]|\mathcal{H}_1\right) = \frac{1}{N-\tau}(\sigma_\nu^2+\sigma_s^2)^2 \tag{3.44}$$

The distribution of $\hat{R}^{\alpha}_{xx}[N,\tau]$ under the two hypotheses for $\alpha \neq 0$, therefore, is

$$\hat{R}^{\alpha}_{xx}[N,\tau] \sim \begin{cases} \mathcal{N}_c\left(0, \frac{\sigma_\nu^2}{N-\tau}\right) & \mathcal{H}_0 \\ \mathcal{N}_c\left(R^{\alpha}_{xx}[\tau], \frac{\sigma_\nu^2}{N-\tau}\right) & \mathcal{H}_1 \end{cases} \tag{3.45}$$

It may be observed that the mean of $\hat{R}^{\alpha}_{xx}[N,\tau]$ is a complex number and the knowledge of its phase is necessary in order to use the finite time cyclic autocorrelation function for detection. If the phase of the cyclic autocorrelation function is known then $\Re\{\hat{R}^{\alpha}_{xx}[\tau]e^{-j\phi}\}$ with ϕ being the said phase, will be a real positive number and may be used as test statistic. The distribution of this test statistic may be given as

$$\Re\{\hat{R}^{\alpha}_{xx}[\tau]e^{j\phi}\} \sim \begin{cases} \mathcal{N}\left(0, \frac{\sigma_\nu^4}{2(N-\tau)}\right) & \mathcal{H}_0 \\ \mathcal{N}\left(|R^{\alpha}_{xx}[\tau]|, \frac{(\sigma_s^2+\sigma_\nu^2)^2}{2(N-\tau)}\right) & \mathcal{H}_1 \end{cases} \tag{3.46}$$

The probabilities of detection and false alarm for a detection threshold λ will be given as

$$P_d = Q\left(\sqrt{2(N-\tau)}\frac{\lambda - |R^{\alpha}_{xx}[\tau]|}{\sigma_s^2+\sigma_\nu^2}\right) \tag{3.47}$$

$$P_{fa} = Q\left(\sqrt{2(N-\tau)}\frac{\lambda}{\sigma_\nu^2}\right) \tag{3.48}$$

In case the phase information of the cyclic autocorrelation function is not available, then absolute value of the finite time cyclic autocorrelation function may be used as a test statistic. The distribution of this test statistic under the two hypotheses is given as [69]

$$|\hat{R}^{\alpha}_{xx}[\tau]e^{j\phi}| \sim \begin{cases} Rice\left(0, \frac{\sigma_\nu^2}{\sqrt{2(N-\tau)}}\right) & \mathcal{H}_0 \\ Rice\left(|R^{\alpha}_{xx}[\tau]|, \frac{\sigma_s^2+\sigma_\nu^2}{\sqrt{2(N-\tau)}}\right) & \mathcal{H}_1 \end{cases} \tag{3.49}$$

In this thesis, both these test statistics have been used for detecting a primary cyclostationary signal embedded in noise

3.5 Proposed Spectrum Sensing Technique

It was earlier shown that if the received signal $x[n]$ contains a primary component $s[n]$ exhibiting regular or conjugate spectral coherence at one or more cyclic frequencies, then it may be estimated as a linear combination of its time and frequency shifted, and conjugated (optional) versions. This estimate of the signal may be used to enhance the cyclostationary component and reduce the noise. Optimal FRESH filtering may, therefore, be used to enhance a primary signal prior to detection.

Similarly, if a primary signal is present and the spectrum sensor consists of multiple antennas then the signal received at different antennas will be correlated. If this signal of interest exhibits cyclostationarity then the spectral coherence properties of the signal may be used to form a beam in the direction of interest.

In view of these, consider the structure shown in Figure 3.3 where each antenna output, in addition to being fed to the linear combiner as in the SCORE beamforming structure, is also fed to an adaptive FRESH filter. Assume that each FRESH filter incorporates M_1 unconjugated and M_2 conjugated frequency shift branches. That is, each FRESH filter has a total of $M(= M_1 + M_2)$ FRESH branches with each branch consisting of an FIR filter containing L delay taps. The number L for each FIR filter is assumed to be same for simplicity, though this may be different for different frequency shifts. The maximum value that L may take is equal to the maximum lag for which the cyclic autocorrelation function is nonzero and/or is limited by the maximum feasible system complexity. Further, it is assumed that the number of frequency shifts that follow each antenna and their values are same. The associated filter weights are, however, assumed to be adaptive. If a signal $s[n]$ exhibiting spectral autocoherence at frequencies $\alpha_1 \dots \alpha_{M_1}$ and conjugate spectral autocoherence at $\beta_1 \dots \beta_{M_2}$ is incident on this array from an angle θ, then the output of the kth antenna may be written as

$$x_k[n] = a_k(\theta)s[n] + \nu_k[n] \tag{3.50}$$

Here $a_k(\theta)$ is the array response of the kth element for the incoming signal incident at an angle θ to the normal, and $\nu_k[n]$ is the additive stationary noise component. Defining

$$\mathbf{u}[n] = \Big[\mathbf{u}_1^T[n], \dots, \mathbf{u}_K^T[n]\Big]^T \tag{3.51}$$

and

$$\mathbf{x}[n] = \Big[x_1[n], \dots, x_K[n]\Big]^T \tag{3.52}$$

where

$$\begin{aligned} \mathbf{u}_k[n] &= \Big[\mathbf{u}_{k1}^T[n], \dots, \mathbf{u}_{kM}^T[n]\Big]^T \\ \mathbf{u}_{km}[n] &= \Big[u_{km}[n], \dots, u_{km}[n-L+1]\Big]^T \\ u_{km}[n] &= x_k^{(*)}[n]e^{j2\pi\alpha_m n} \end{aligned} \tag{3.53}$$

In Figure 3.3,

$$\begin{aligned} v[n] &= \mathbf{w}^H\mathbf{u}[n] \\ y[n] &= \mathbf{h}^H\mathbf{x}[n] \end{aligned} \tag{3.54}$$

Here, $u_{km}[n]$ is the optionally conjugated and frequency shifted version of the received signal at the kth antenna for the mth branch. $\mathbf{u}_{km}[n]$ is the vector containing the input

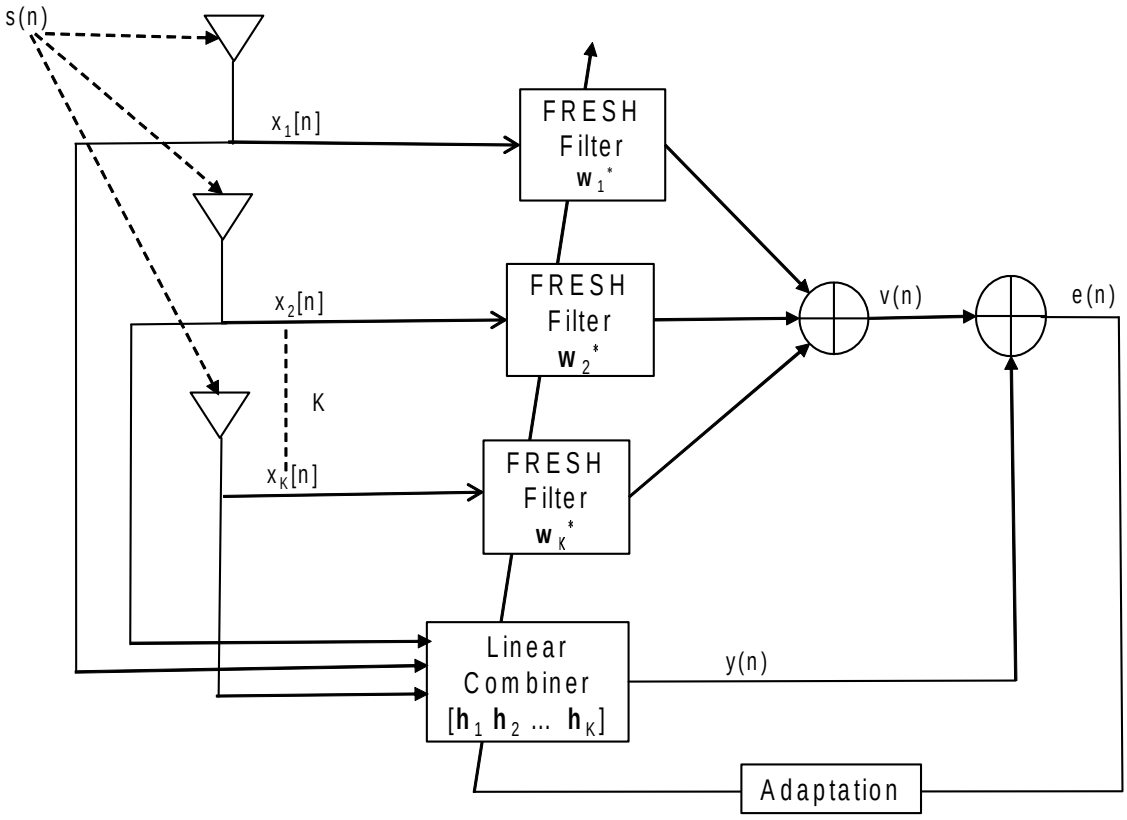

Figure 3.3: The proposed Space-Time FRESH filtering structure.

to the mth FRESH branch of the kth antenna. $\mathbf{u}_k[n]$ is a concatenation of the inputs to the different FRESH branches of the kth antenna and $\mathbf{u}[n]$ is the overall regression vector being fed to the adaptation structure. Similarly, $\mathbf{x}[n]$ is the reference signal vector. The weight vectors maximizing the cross-covariance of the regression and the reference signal vector may be obtained using the optimal Wiener filtering solution as derived in [36]. It may be noted that unlike the case in [36] the dimensions of $\mathbf{x}[n]$ and $\mathbf{u}[n]$ are different. In view of this, the ACS algorithm given in [36] is modified, as follows:

1. Initialize $\mathbf{R}_{uu}[1] = \delta^{-1}\mathbf{I}$, $\mathbf{R}_{xx}[1] = \delta^{-1}\mathbf{I}$, $\mathbf{R}_{ux}[1] = 0$ and $\mathbf{h}[1]$ to any K-dimensional non-zero vector, δ is any arbitrarily small constant.

2. For the kth iteration, update $\mathbf{R}_{uu}[k]$, $\mathbf{R}_{xx}[k]$, $\mathbf{R}_{ux}[k]$, $\mathbf{R}_{xu}[k]$, $\mathbf{w}[k]$ and $\mathbf{h}[k]$ as

$$\mathbf{R}_{ux}[k] = \frac{1}{k}\Big[(k-1)\mathbf{R}_{ux}[k-1] + \mathbf{u}[k]\mathbf{x}^H[k]\Big] \tag{3.55a}$$

$$\mathbf{R}_{xx}^{-1}[k] = \frac{k}{k-1}\Bigg[\mathbf{R}_{xx}^{-1}[k-1] \tag{3.55b}$$

$$- \frac{\mathbf{R}_{xx}^{-1}[k-1]\mathbf{x}[k]\mathbf{x}^H[k]\mathbf{R}_{xx}^{-1}[k-1]}{(k-1) + \mathbf{x}^H[k]\mathbf{R}_{xx}^{-1}[k-1]\mathbf{x}[k]}\Bigg] \tag{3.55c}$$

$$\mathbf{R}_{uu}^{-1}[k] = \frac{k}{k-1}\Bigg[\mathbf{R}_{uu}^{-1}[k-1] \tag{3.55d}$$

$$- \frac{\mathbf{R}_{uu}^{-1}[k-1]\mathbf{u}[k]\mathbf{u}^H[k]\mathbf{R}_{uu}^{-1}[k-1]}{(k-1) + \mathbf{u}^H[k]\mathbf{R}_{uu}^{-1}[k-1]\mathbf{u}[k]}\Bigg] \tag{3.55e}$$

$$\mathbf{R}_{xu}[k] = \mathbf{R}_{ux}^H[k] \tag{3.55f}$$

$$\mathbf{w}[k] = \mathbf{R}_{uu}^{-1}[k]\mathbf{R}_{ux}[k]\mathbf{h}[k-1] \tag{3.55g}$$

$$\mathbf{h}[k] = \mathbf{R}_{xx}^{-1}[k]\mathbf{R}_{xu}[k]\mathbf{w}[k] \tag{3.55h}$$

Assume that the weight attached to the lth delay tap of the mth frequency shift of the k th antenna is represented as $w_{k,m,1}^*$. Then, the output of the filter $v[n]$ may be represented as

$$\begin{aligned} v[n] &= \textstyle\sum_{k=1}^{K}\sum_{m=1}^{M}\sum_{l=1}^{L} w_{k,m,l}^* u_{m,k}[n-l] \\ &= \textstyle\sum_{k=1}^{K}\sum_{m=1}^{M_1}\sum_{l=1}^{L} w_{k,m,l}^* x_k[n-l]e^{j2\pi\alpha_m[n-l]} \\ &\quad + \textstyle\sum_{k=1}^{K}\sum_{m=1}^{M_2}\sum_{l=1}^{L} w_{k,m,l}^* x_k^*[n-l]e^{j2\pi(-\beta_m)[n-l]} \end{aligned} \tag{3.56}$$

The cyclic autocorrelation function of $v[n]$ at cyclic frequency α and lag τ takes the form

$$R_{vv}^{\alpha}[\tau] = \mathbf{w}^H\mathbf{R}_{uu}^{\alpha}[\tau]\mathbf{w} \tag{3.57}$$

where

$$\begin{aligned} \mathbf{w} &= [\mathbf{w}_1, \ldots, \mathbf{w}_K]^T \\ \mathbf{w}_k &= [\mathbf{w}_{k,1} \ldots, \mathbf{w}_{k,M}]^T \\ \mathbf{w}_{k,m} &= [w_{k,m,1}, \ldots, w_{k,m,L}]^T \end{aligned} \tag{3.58}$$

and

$$\mathbf{R}^{\alpha}_{uu}[\tau] = \begin{bmatrix} \mathbf{R}^{\alpha}_{uu;11}[\tau] & \ldots & \mathbf{R}^{\alpha}_{uu;1K}[\tau] \\ \vdots & \ddots & \vdots \\ \mathbf{R}^{\alpha}_{uu;K1}[\tau] & \ldots & \mathbf{R}^{\alpha}_{uu;KK}[\tau] \end{bmatrix} \tag{3.59}$$

$$\mathbf{R}^{\alpha}_{uu;ik}[\tau] = \begin{bmatrix} \mathbf{R}^{\alpha}_{uu;\beta_1\eta_1;ik}[\tau] & \ldots & \mathbf{R}^{\alpha}_{uu;\beta_1\eta_M;ik}[\tau] \\ \vdots & \ddots & \vdots \\ \mathbf{R}^{\alpha}_{uu;\beta_1\eta_1;ik}[\tau] & \ldots & \mathbf{R}^{\alpha}_{uu;\beta_1\eta_M;ik}[\tau] \end{bmatrix} \tag{3.60}$$

$$\mathbf{R}^{\alpha}_{uu;\beta\eta;ik}[\tau] = \begin{bmatrix} (r^{\alpha}_{uu;\beta\eta;ik}[\tau])_{1,1} & \ldots & (r^{\alpha}_{uu;\beta\eta;ik}[\tau])_{1,L} \\ \vdots & \ddots & \vdots \\ (r^{\alpha}_{uu;\beta\eta;ik}[\tau])_{L,1} & \ldots & (r^{\alpha}_{uu;\beta\eta;ik}[\tau])_{L,L} \end{bmatrix} \tag{3.61}$$

where each element of the matrix in (3.61) is defined as

$$(r^{\alpha}_{uu;\beta\eta;ik}[\tau])_{p,q} = (\tilde{r}^{\alpha}_{uu;\beta\eta;ik}[\tau])_{p,q} e^{j2\pi(\eta\tau - \alpha p)} \tag{3.62}$$

$$\begin{aligned} (\tilde{r}^{\alpha}_{uu;\beta\eta;ik}[\tau])_{p,q} &= \left\langle u_{\beta,k}[n-p] u^*_{\eta,i}[n-q-\tau] e^{-j2\pi\alpha n} \right\rangle \\ &= \left\langle x_i[n-p] e^{j2\pi\beta(n-p)} x^*_k[n-q-\tau] e^{-j2\pi\eta(n-q-\tau)} e^{-j2\pi\alpha n} \right\rangle \\ &= R^{\alpha+\eta-\beta}_{x_i x_k}[p-q-\tau] \end{aligned} \tag{3.63}$$

The received signal vector $\mathbf{x}[n]$ in the presence of a primary signal consists of two components; one because of the primary signal $\mathbf{a}(\theta)s[n]$ and the other due to the noise $\boldsymbol{\nu}[n]$. Similarly, the vector $\mathbf{u}[n]$ may also be seen as a linear combination of terms originating due to the primary signal $\mathbf{z}[n]$ and noise $\boldsymbol{\xi}[n]$. Since the terms corresponding to the signal and noise are assumed to be uncorrelated, the terms corresponding to $\mathbf{z}[n]$ and $\boldsymbol{\xi}[n]$ are separated in the cyclic-autocorrelation function of $v[n]$. The hypothesis test may be written as

$$R^{\alpha}_{vv}[\tau] = \begin{cases} \mathbf{w}^H \mathbf{R}^{\alpha}_{\xi\xi}[\tau]\mathbf{w} & \mathcal{H}_0 \\ \mathbf{w}^H \mathbf{R}^{\alpha}_{zz}[\tau]\mathbf{w} + \mathbf{w}^H \mathbf{R}^{\alpha}_{\xi\xi}[\tau]\mathbf{w} & \mathcal{H}_1 \end{cases} \tag{3.64}$$

These estimates assume averaging over infinite samples of the received signal. In practical situations where only a finite number of samples are considered, the estimate of the cyclic autocorrelation function for N samples may be expressed as [31]

$$\hat{R}^{\alpha}_{vv}[N,\tau] = R^{\alpha}_{vv}[\tau] + \hat{\epsilon}^{\alpha}_{vv}[N,\tau] \tag{3.65}$$

where $\hat{\epsilon}^{\alpha}_{vv}[N,\tau]$ is the estimation error due to the finite number of samples. It is shown in [31] that $\hat{\epsilon}^{\alpha}_{vv}[N,\tau]$ may be assumed to be asymptotically normal. That is

$$\lim_{N\to\infty} \hat{\epsilon}^{\alpha}_{vv}[N,\tau] \sim \mathcal{N}\left(0, \frac{\sigma^2_{\epsilon}}{N}\right) \tag{3.66}$$

Consequently, the binary hypothesis test in (3.64) may be modified for a finite number of samples to

$$\hat{R}^{\alpha}_{vv}[N,\tau] = \begin{cases} \mathbf{w}^H \mathbf{R}^{\alpha}_{\xi\xi}[\tau]\mathbf{w} + \hat{\epsilon}^{\alpha}_{vv}[N,\tau] & \mathcal{H}_0 \\ \mathbf{w}^H \mathbf{R}^{\alpha}_{zz}[\tau]\mathbf{w} + \mathbf{w}^H \mathbf{R}^{\alpha}_{\xi\xi}\mathbf{w} + \hat{\epsilon}^{\alpha}_{vv}[N,\tau] & \mathcal{H}_1 \end{cases} \tag{3.67}$$

It is intuitively satisfying to select α and τ such that the strength of the cyclic autocorrelation function of the component due to the primary signal is maximized, thereby making it easier to discriminate between the two hypotheses. From the results derived in [50], it may be seen that the strongest peak of the cyclic autocorrelation function of any cyclostationary signal occurs at $\alpha = 0$ and $\tau = 0$. Detecting this as a feature is same as employing an energy detector at the output of the FRESH filter. In this case, however, the signal is enhanced by virtue of its cyclostationarity. The detection thresholds for the signals filtered by the proposed structure may be determined by the use of the Neyman Pearson criterion via simulation. For a given false alarm rate and a known noise variance, these may also be determined theoretically, as detailed in the next section. The spectrum sensing method based on the proposed adaptive Space-Time FRESH filtering structure may, hence, be summarized as follows.

1. Reset the filter weights.
2. For the nth sample $x[n]$, $n = 1, 2, \cdots, N$, adapt the filter weights using the modified ACS algorithm.
3. After adapting for all the N samples, filter the stored samples using the adapted weights to generate $v[n]$.
4. Calculate the cyclic autocorrelation function for a known cyclic frequency and lag and use it as the test statistic T.
5. Compare T with a pre-determined threshold λ and declare the primary signal as present when $T > \lambda$.

We now give an analysis of the computational complexity of our proposed modified ACS algorithm. Consider that K antennas, each with M branches of the FRESH filter, are to be adapted. Let the length of each branch of the FRESH filter be L. Accordingly, by inspection, the computation of equations (3.55a), (3.55c), (3.55e), (3.55g), (3.55h) require (K^2LM), $(2K^2 + K + 1)$, $(2(KLM)^2 + KLM + 1)$, $((KLM)^2 + K^2\,L\,M)$ and $(K^2LM + K^2)$ complex multiplications, respectively. Therefore, the order of overall computational

complexity of the proposed modified ACS algorithms is $\mathcal{O}((K\,L\,M)^2)$. If N samples are used for adaptation then the order of computational complexity of the adaptation stage becomes $\mathcal{O}(N(K\,L\,M)^2)$. Further, the filtering stage requires $(K\,L\,M)$ multiplications for each sample and therefore, a total of $(N\,K\,L\,M)$ multiplications for N samples. If a simple energy detector is employed then N complex multiplications will be required for calculation of the test statistic. On the other hand, for a cyclostationary detector sensing M cyclic frequencies, the number of complex multiplications required for the calculation of the M dimensional test vector is $2MN$ [31]. Consequently, the entire sensing procedure has a complexity $\mathcal{O}(N(K\,L\,M)^2)$. For $L = 1$ and $M = 1$, our proposed structure in Figure 3.3 reduces to that developed in [36]. Accordingly, the order of computational complexity turns out to be $\mathcal{O}(N\,K^2)$, same as that of the standard ACS algorithm. As we observe, the bottleneck of this procedure is the computationally expensive adaptation algorithm. This calls for the developement of a lower complexity adaptation algorithm so as to make the proposed spectrum sensing approach more effective. The next section describes our proposed approach for reducing the computational cost of the adaptation algorithm.

3.6 A low complexity C2-LMS algorithm for the proposed structure

The ACS and the modified ACS algorithms are designed to maximize the correlation between the filter outputs of the original signal $y[n]$ and its frequency shifted version $v[n]$. Alternatively, the MMSE criterion may be used, minimizing the mean square difference between $y[n]$ and $v[n]$. Here, if the values of $\mathbf{h}$ and $\mathbf{w}$ are optimized separately [2], then it may be shown that the optimal solution for the weight vectors that satisfies the MMSE criterion has a form similar to the optimal solution that maximizes the cross correlation between $v[n]$ and $y[n]$ this has been shown in appendix B. The optimal values $\mathbf{w}_o$ and $\mathbf{h}_o$ of $\mathbf{w}$ and $\mathbf{h}$ that minimize the mean square difference between the respective filter outputs are given as

$$[\mathbf{w}_o, \mathbf{h}_o] = \arg\min_{\mathbf{w},\mathbf{h}} \left\langle |\mathbf{h}^H\mathbf{x}(n) - \mathbf{w}^H\mathbf{u}(n)|^2 \right\rangle \tag{3.68}$$

A similar function has been considered as the objective function for the least squares SCORE beamforming problem in [2] and [36]. However, the methods proposed therein assume either $\mathbf{h}$ or $\mathbf{w}$ to be fixed and not having a null in the direction of incidence of the signal of interest. Here, since only one of the two adaptable weight vectors is being adapted to form a beam that minimizes the MSE, this approach to cyclostationary beamforming is suboptimal. Therefore, it is desired to adapt both $\mathbf{h}$ and $\mathbf{w}$ to achieve an optimal solution to the filtering problem described by (3.68). It may be observed that the global minimum of this function exists at the origin, forcing both the weight vectors to zero. It may also be seen that either of the two weight vectors must always be non-zero to force the other to

take a non-zero value and, consequently, force the system towards a non-trivial solution. The Euclidian norm of either of the two weight vectors may, thus, be constrained to a non-zero constant in order to stop it from converging towards a null vector.

Constraining the Euclidian norm of $\mathbf{h}$ to a constant value g, and invoking the method of Lagrange multipliers, the optimal weight vectors become the ones to minimize the function

$$J(\mathbf{w}, \mathbf{h}) = \left\langle |\mathbf{h}^H \mathbf{x}(n) - \mathbf{w}^H \mathbf{u}(n)|^2 \right\rangle + \lambda \left\langle \|\mathbf{h}\|_2^2 - g^2 \right\rangle \tag{3.69}$$

Analogous to the approach followed in [2], this may be optimized separately for $\mathbf{w}$ and $\mathbf{h}$. Using the method of steepest descent and applying suitable constraints, the weight update equations may be obtained. The adaptation algorithm employing these equations is presented below and its detailed derivation is given in the Appendix A. It is important to note that this algorithm is being derived for applications to very low signal to noise ratio environments. In such cases, it is desired that the step size be dependent on the error variance in order to minimize misadjustment. Accordingly, it is intuitively satisfying to normalize the step size with respect to the norm square of the input signal.

By use of the facts stated above the resulting constrained doubly adaptive LMS algorithm (the C2-LMS algorithm) is given as follows.

1. For input signals $\mathbf{u}[n]$ and $\mathbf{x}[n]$ having weight vectors $\mathbf{w}[n]$ and $\mathbf{h}[n]$, initialize $\mathbf{w}[n] = \mathbf{0}$ and $\mathbf{h}[n] = g\mathbf{i}[k]$ where $\mathbf{i}[k]$ is the kth column of the identity matrix. This choice of the initial antenna pattern ensures the absence of nulls in the direction from which the primary signal is incident.

2. For the nth iteration update $\mathbf{w}$ and $\mathbf{h}$ as

$$\mathbf{w}[n+1] = \mathbf{w}[n] + \mu_w \mathbf{u}[n] e^*[n] \tag{3.70}$$

and

$$\mathbf{h}[n+1] = k[n]\mathbf{h}[n] - \mu_h \mathbf{x}[n] e^*[n] \tag{3.71}$$

where

$$e[n] = y[n] - v[n] \tag{3.72}$$

with

$$v[n] = \mathbf{w}^H[n]\mathbf{u}[n] \tag{3.73}$$

$$y[n] = \mathbf{h}^H[n]\mathbf{x}[n] \tag{3.74}$$

and

$$\mu_h = \frac{\mu}{\left\|\mathbf{x}[n]\right\|_2^2}, \quad \mu_w = \frac{\mu}{\left\|\mathbf{u}[n]\right\|_2^2} \tag{3.75}$$

$$b[n] = \mu_h \Re\{y^*[n]e[n]\} \tag{3.76}$$

$$c[n] = \mu_h^2 \Big\| \mathbf{x}[n] \Big\|_2^2 \Big| e[n] \Big|^2 - g^2 \tag{3.77}$$

$$k[n] = b[n] + \sqrt{(b[n])^2 - c[n]} \tag{3.78}$$

In the above, the symbol $\Re$ denotes the real part of a complex number and the step size μ is normalized w.r.t the inputs $\mathbf{x}[n]$ and $\mathbf{u}[n]$ to accommodate large variations in their values.

Here, the computation of the filtered signal at each stage involves K complex multiplications for $y[n]$ and $K\,L\,M$ complex multiplications for $v[n]$. The calculations of $c[n]$, μ_h and μ_w require K , $K+1$ and $K\,L\,M+1$ multiplications, respectively. All these steps are repeated N times for N samples thereby resulting in computational complexity of order $\mathcal{O}(N\,K\,L\,M)$. Thus, the proposed algorithm provides computational gain compared to the weight adaptation algorithm in [36] (for $L=1$ and $M=1$) and that given in the previous section.

3.6.1 Performance of the proposed Spectrum Sensing method based on energy detector

If, after the adaptation stage, the final weight vector is $\mathbf{w}[N]$ then the n^{th} sample of the filtered output is given as

$$v[n] = \mathbf{w}^H[N]\mathbf{u}[n]$$

The distribution of $v[n]$ under the two hypotheses will be

$$v[n] \sim \begin{cases} \mathcal{N}_c(0, \sigma_\nu^2 \|\mathbf{w}[N]\|^2) & \mathcal{H}_0 \\ \mathcal{N}_c(0, \mathbf{w}^H[N]\mathbf{R}_{zz}[n]\mathbf{w}[N] + \sigma_\nu^2 \|\mathbf{w}[N]\|^2) & \mathcal{H}_1 \end{cases} \tag{3.79}$$

In the presence of a primary user signal, the output signal to noise ratio (γ_o) is given as

$$\gamma_o = \frac{\mathbf{w}^H[N]\mathbf{R}_{zz}[n]\mathbf{w}[N]}{\sigma_\nu^2 \|\mathbf{w}[N]\|^2} \tag{3.80}$$

As the signal is correlated with itself in time, space and frequency, , $\mathbf{R}_{zz}[n] \succ \sigma_s^2\mathbf{I}$, where σ_s^2 is the signal variance. Defining

$$\kappa = \frac{\mathbf{w}^H[N]\mathbf{R}_{zz}[n]\mathbf{w}[N]}{\sigma_s^2 \|\mathbf{w}[N]\|^2} > 1 \tag{3.81}$$

If the noise variance at the receiver has an uncertainty factor ρ, at an input SNR γ_i, then, according to [122], the detector will exhibit SNR walls. Now, as the space-time FRESH filtering will increase the effective SNR of the primary signal, then, for an uncertainty by

a factor ρ in the noise variance the SNR walls are lowered to

$$\gamma_i = \frac{\left(\rho - \frac{1}{\rho}\right)}{\kappa} \tag{3.82}$$

for an input SNR of γ_0.

If the weights $\mathbf{w}[N]$ are normalized such that $\|\mathbf{w}[N]\|_2 = 1$ then, under the null hypothesis, the variance of $v[n]$ will equal the noise variance. In this case, the distribution of the test statistic (T) for the energy detector, defined as $T = \frac{1}{N}\sum_{n=1}^{N}|v[n]|^2$, may be approximated as [122]

$$T|\mathcal{H}_0 \sim \mathcal{N}(\sigma_\nu^2, \sigma_T^2) \tag{3.83}$$

where,

$$\begin{aligned} \sigma_T^2 &= var\left(|\textstyle\sum_{n=0}^{N-1}\mathbf{w}^H[N]\boldsymbol{\xi}[n]|^2\right); \\ &= E[\textstyle\sum_{n=0}^{N-1}\sum_{p=0}^{N-1}|\mathbf{w}[N]\boldsymbol{\xi}[n]|^2|\mathbf{w}[N]\boldsymbol{\xi}[p]|^2] - \sigma_\nu^2 \\ &= \frac{\sigma_\nu^4}{N}\left(\textstyle\sum_{p=0}^{MKL-1}\left(\sum_{l=1}^{MKL}E\left[w_l[N]w_{l-p}^*[N]\right]\right)^2\right) \end{aligned} \tag{3.84}$$

where $\boldsymbol{\xi}[n]$ is the regression vector of the proposed structure under the null hypothesis. In view of these, the probability of false alarm (P_{FA}), given a threshold λ, may be written as

$$P_{FA} = Q\left(\frac{\lambda - \sigma_\nu^2}{\sqrt{\sigma_T^2}}\right) \tag{3.85}$$

where Q denotes the Marcum Q function [122]. It may however be observed that the value of the variance σ_T^2 depends on the values of the adapted filter weights $\mathbf{w}[N]$. Therefore, it is not possible to predict a threshold for a given probability of false alarm and consequently, the detection thresholds need to be determined using simulation. Due to the replacement of the deterministic gradient by the stochastic gradient in the adaption algorithm, misadjustments will occur in the weight vectors. These misadjusted weight vectors $\mathbf{w}[N]$ and $\mathbf{h}[N]$ will limit the SNR gain offered by the FRESH filtering structure and hence the performance of the proposed structure. If the weight vectors $\mathbf{w}[n]$ and $\mathbf{h}[n]$ take their optimal values, $\mathbf{h}_o$ and $\mathbf{w}_o$ respectively, then the error at the n^{th} instant is

$$e_o[n] = \mathbf{h}_o^H\mathbf{x}[n] - \mathbf{w}_o^H\mathbf{u}[n] \tag{3.86}$$

However, in the presence of misadjustment, this will be

$$\begin{aligned} e[n] &= \mathbf{h}^H[n]\mathbf{x}[n] - \mathbf{w}^H[n]\mathbf{u}[n] \\ &= e_o[n] + \tilde{\mathbf{h}}^H[n]\mathbf{x}[n] - \tilde{\mathbf{w}}^H[n]\mathbf{u}[n] \end{aligned} \tag{3.87}$$

where $\tilde{\mathbf{h}}[n] = \mathbf{h}_o - \mathbf{h}[n]$ and $\tilde{\mathbf{w}}[n] = \mathbf{w}_o - \mathbf{w}[n]$. As the two weight error vectors will be

uncorrelated with each other as well as to $e_o[n]$, we have

$$\begin{aligned} E\left[|e[n]|^2\right] &= E\left[|e_o[n]|^2\right] + E\left[\tilde{\mathbf{h}}^H[n]\mathbf{R}_{xx}\tilde{\mathbf{h}}^H[n]\right] \\ &\quad + E\left[\tilde{\mathbf{w}}^H[n]\mathbf{R}_{uu}\tilde{\mathbf{w}}^H[n]\right] \end{aligned} \tag{3.88}$$

where $E[.]$ is the expectation operation. This is done under the assumption that the variations of the weight vectors are slow as compared to those of the signal vectors [61]. Further, writing $J[n] = E\left[|e[n]|^2\right]$ and $J_{min} = E\left[|e_o[n]|^2\right]$ the above equation reduces to

$$J[n] = J_{min} + tr\left(\mathbf{R}_{xx}\boldsymbol{Q}_h[n]\right) + tr\left(\mathbf{R}_{uu}\boldsymbol{Q}_w[n]\right) \tag{3.89}$$

where $\boldsymbol{Q}_h[n] = E\left[\tilde{\mathbf{h}}[n]\tilde{\mathbf{h}}^H[n]\right]$ and $\boldsymbol{\Psi}_w = E\left[\tilde{\mathbf{w}}[n]\tilde{\mathbf{w}}^H[n]\right]$. The excess error may, therefore, be given as

$$J_{ex} = tr\left(\mathbf{R}_{xx}\boldsymbol{\Psi}_h[n]\right) + tr\left(\mathbf{R}_{uu}\boldsymbol{\Psi}_w[n]\right) \tag{3.90}$$

In this case,

$$\begin{aligned} \tilde{\mathbf{w}}[n+1] &= \mathbf{w}_o - \mathbf{w}[n+1] \\ &= \mathbf{w}_o - \mathbf{w}[n] - \mu_w\mathbf{u}[n](\mathbf{h}^H[n]\mathbf{x}[n] - \mathbf{w}^H[n]\mathbf{u}[n])^* \\ &= \tilde{\mathbf{w}}[n] - \mu_w\mathbf{u}[n]e_o^*[n] + \mu_w\mathbf{u}[n]\mathbf{u}^H[n]\tilde{\mathbf{w}}[n] - \\ &\quad \mu_w\mathbf{u}[n]\mathbf{x}^H[n]\tilde{\mathbf{h}}[n] \\ &= (\mathbf{I} - \mu_w\mathbf{u}[n]\mathbf{u}^H[n])\tilde{\mathbf{w}}[n][n] + \mu_w\mathbf{u}[n]e_o^*[n] \\ &\quad + \mu_w\mathbf{u}[n]\mathbf{x}^H[n]\tilde{\mathbf{h}}[n] \end{aligned} \tag{3.91}$$

A similar expression may be derived for $\tilde{\mathbf{h}}[n]$ as

$$\begin{aligned} \tilde{\mathbf{h}}[n+1] &= (\mathbf{I} - \mu_h\mathbf{x}[n]\mathbf{x}^H[n])\tilde{\mathbf{h}}[n] + \mu_h\mathbf{x}[n]e_o^*[n] \\ &\quad + \mu_h\mathbf{x}[n]\mathbf{u}^H[n]\tilde{\mathbf{w}}[n] - \mu\lambda\mathbf{h}[n] \end{aligned} \tag{3.92}$$

It may be observed that the two weight error vectors at any instant are inter-dependent and will increase each other's variance. Therefore, it may be concluded that the mean square value of the excess error will be lower bounded by the sum of the mean square values of the excess errors caused when $\mathbf{h}$ and $\mathbf{w}$ are unknown individually.

3.7 Simulation Results

In this section, simulation results using randomly generated signal are presented. The primary user signal is assumed to be BPSK modulated with a carrier frequency f_c = 125 kHz and a baud rate $f_0 = 10$ kbps. For the purpose of these experiments, the primary user signal variance is kept constant at unity and the variance of the additive noise is varied to achieve input SNRs in the range -22 dB to -2 dB. The sampling rate at the cognitive

receiver is assumed to be 1 MHz. The FRESH filters are assumed to have a single branch at a conjugate frequency shift of $2f_c$. The inter antenna spacing for systems with multiple antennas is fixed at half the wavelength of the input signal. In all the experiments, 500 samples are used to adapt the filter structure using either of the two algorithms discussed earlier. The samples used to adapt the filters are stored and then passed through the adapted filters to obtain a filtered signal. The filtered signal is then subject either to energy detection or to cyclostationary detection.

The performance of the spectrum sensor is evaluated in terms of the probability of detection for different input SNRs. The detection thresholds are set to give a constant false alarm rate P_{FA} of 0.1. For this purpose, test statistics are calculated for 750 independent runs of the system based on the modified ACS algorithm and 1000 independent runs of the system trained by the C2-LMS algorithm. To test the performance of these algorithms 1500 independent trials are run for the modified ACS algorithm-based system and 2000 for the C2-LMS-based system.

3.7.1 Improvement using Space-Time FRESH filter based on the modified ACS algorithm employing energy detection

Figure 3.4 illustrates the performance of the proposed structure adapted using the modified ACS algorithm. Different configurations of the proposed structure are considered and the detection performance is evaluated for the FRESH filter. It may be observed that for a 90% probability of detection a gain of nearly 6.5 dB is achieved over the standard energy detector (mentioned as the 'no enhancement' case) with increase in the detector complexity.

The gains achieved by the proposed structure over the energy detector for a successful detection rate of 95% are summarized in Table 3.1. It may be seen that a proper configuration of the space-time FRESH filter may yield gains as large as 8.5 dB. However, the improvement offered by the structure tends to saturate as the number of antennas and the FRESH filter length is increased.

3.7.2 Improvement using Space-Time FRESH filter adapted using the C2-LMS algorithm with energy detection

In Figure 3.5, we compare the performance of an energy detector-based system for different configurations of the FRESH filter structure adapted using the C2-LMS algorithm. It is observed from Figure 3.5 that for a detection probability of 0.9, gains as much as 9 dB may be achieved by using an appropriate FRESH filter configuration.

The complimentary ROC for different configurations employing two antennas at an SNR of -14 dB is shown in Figure 3.6. It may be observed that in this case, an increase

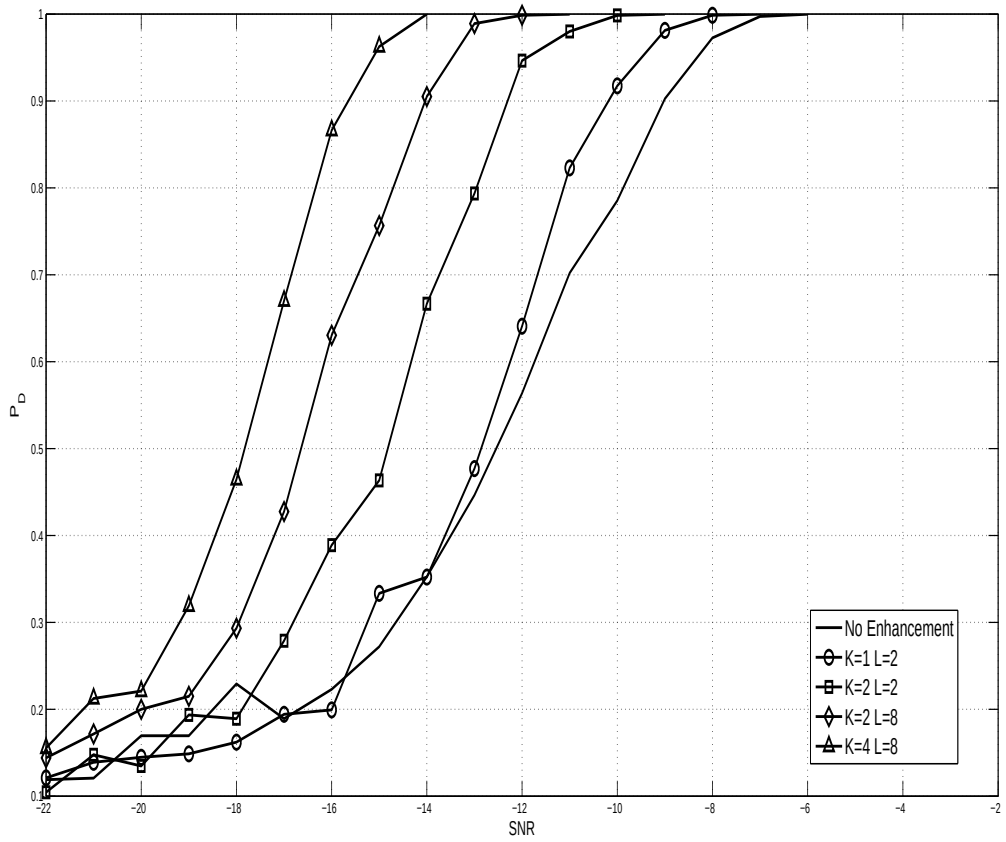

Figure 3.4: Performance using the modified ACS algorithm and the energy detector for different filter lengths for a single-antenna system

Table 3.1: Gains (in decibels) over a simple energy detector for different configurations using the modified ACS algorithm

	L=1	2	4	8	16
K=1	0	0.98	2.19	2.93	3.31
2	1.98	3.10	4.32	4.77	5.12
4	4.02	5.09	5.87	6.5	6.5
8	5.83	6.97	7.76	7.83	7.5
16	6.92	8.57	8.82	8.50	8.45

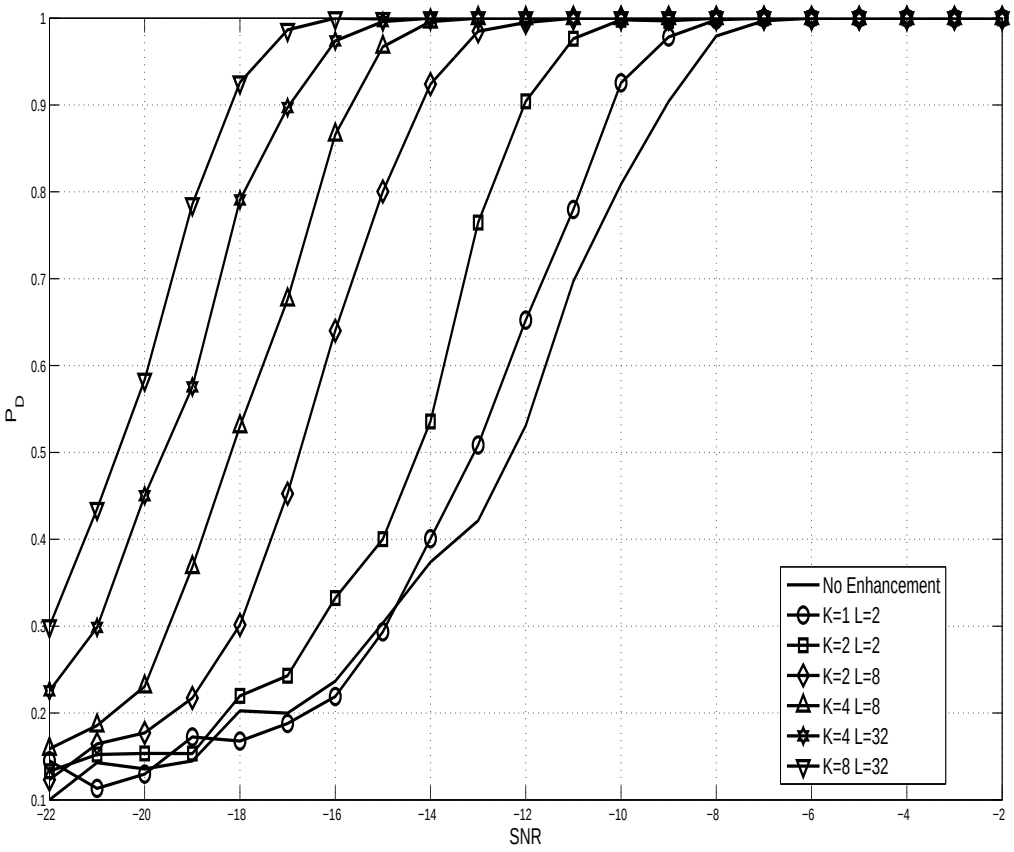

Figure 3.5: Performance using the C2-LMS algorithm and energy detector for different filter configurations

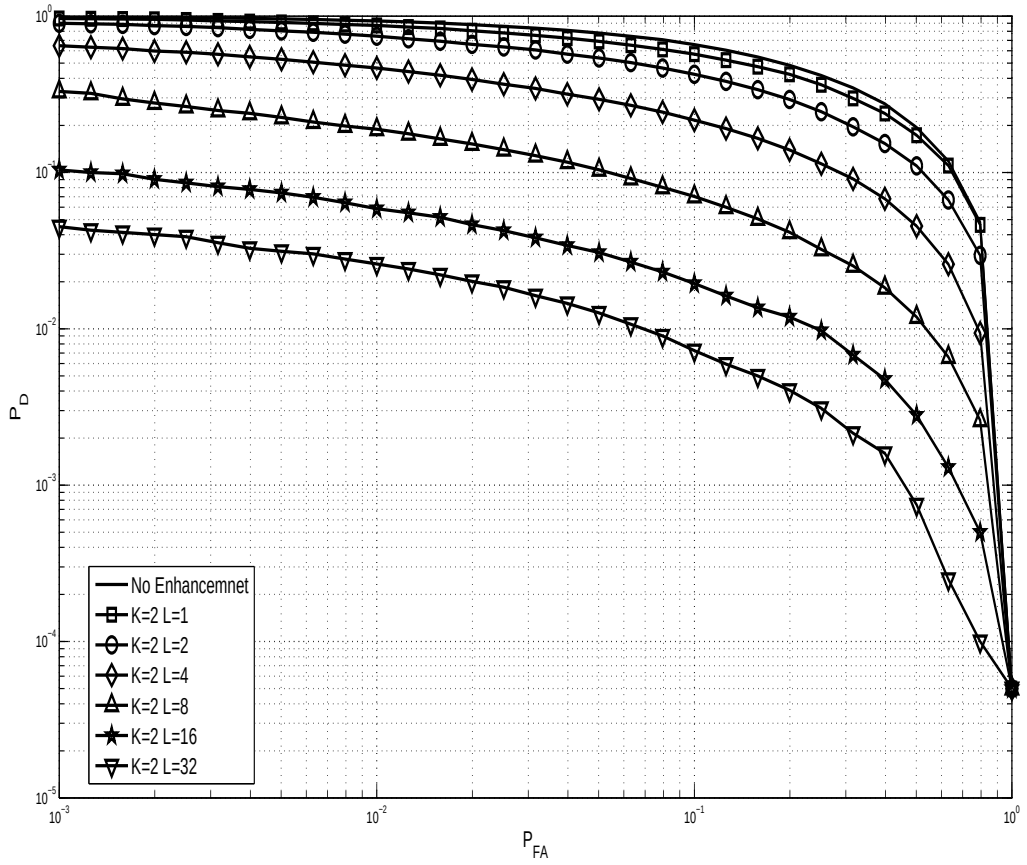

Figure 3.6: Complementary ROC using the C2-LMS algorithm and the energy detector for different FRESH filter lengths in a 2 antenna system at SNR=-14 dB

in FRESH filter length from 1 to 16 reduces the probability of missed detection at a false alarm rate of 1% by more than one order of magnitude. A summary of the gains offered by the C2-LMS algorithm over a standard energy detector for 500 samples and a successful detection rate of 95% is provided in Table 3.2.

3.7.3 The choice of a filter configuration

The performance of different structures having the same value of $(K \times L)$ and hence the same computational complexity is compared in Figure 3.7. For the signal being considered, the correlation coefficient of the signal at two different antennas at the same instant is always greater than the correlation coefficient of the signal and its delayed version at the same antenna. Also, the temporal correlation coefficient of a signal tends to decrease with increasing lag, therefore the additional performance offered by FRESH filters reduces as the filter length increases. On the other hand, as long as the propagation delay between different antennas remains insignificant in comparison to the sampling time, the spatial correlation coefficient will remain unaffected, and therefore the gains offered by increasing the number antennas will be larger. However, more antennas will tend to increase the physical dimensions of the spectrum sensor and also the cost of the sensing node. Therefore, the choice of the space-time configuration for a given computational complexity is also constrained by the physical dimensions of the sensing node.

3.7.4 The lowering of SNR walls

As stated earlier, for the purpose of the simulation experiments, the input signal variance is kept constant and the noise variance is varied according to the input SNR. Therefore, the noise variance may be randomized by adding a random variable with to the input SNR. Consequently, for the purpose of these simulations, a random variable uniformly distributed in the range $[-1, 1]$ is added to the input SNR, thereby introducing a maximum noise uncertainty ± 1 dB relative to the signal variance. In this case as well, the detection performance is calculated by averaging the performance over 2000 independent trials. The effect of noise uncertainty so introduced on the performance of the proposed detector is illustrated in Figure 3.8. It may be seen that under noise uncertainty, the detector performance remains unaffected by the number of samples being used. However, the use of different configurations of the FRESH filter does lower the SNR walls, as predicted by equation (3.82).

3.7.5 Cyclic feature Detector

As a remedy to the effects caused by noise uncertainty, the performance of a cyclostationary detector in conjunction with the proposed filter structure adapted using the C2-LMS

Table 3.2: Gains (in decibels) over a simple energy detector for different configurations using the C2-LMS algorithm for 500 samples

	L=1	2	4	8	16	32
K=1	0	1.038	2.29	3.37	4.7	4.79
2	1.58	2.86	4.2	5.06	6.05	6.6
4	3.05	4.5	5.66	6.66	7.57	7.8
8	4.81	5.89	7.14	7.83	8.58	9.1
16	6.022	7.11	8.1	9.03	9.74	9.96

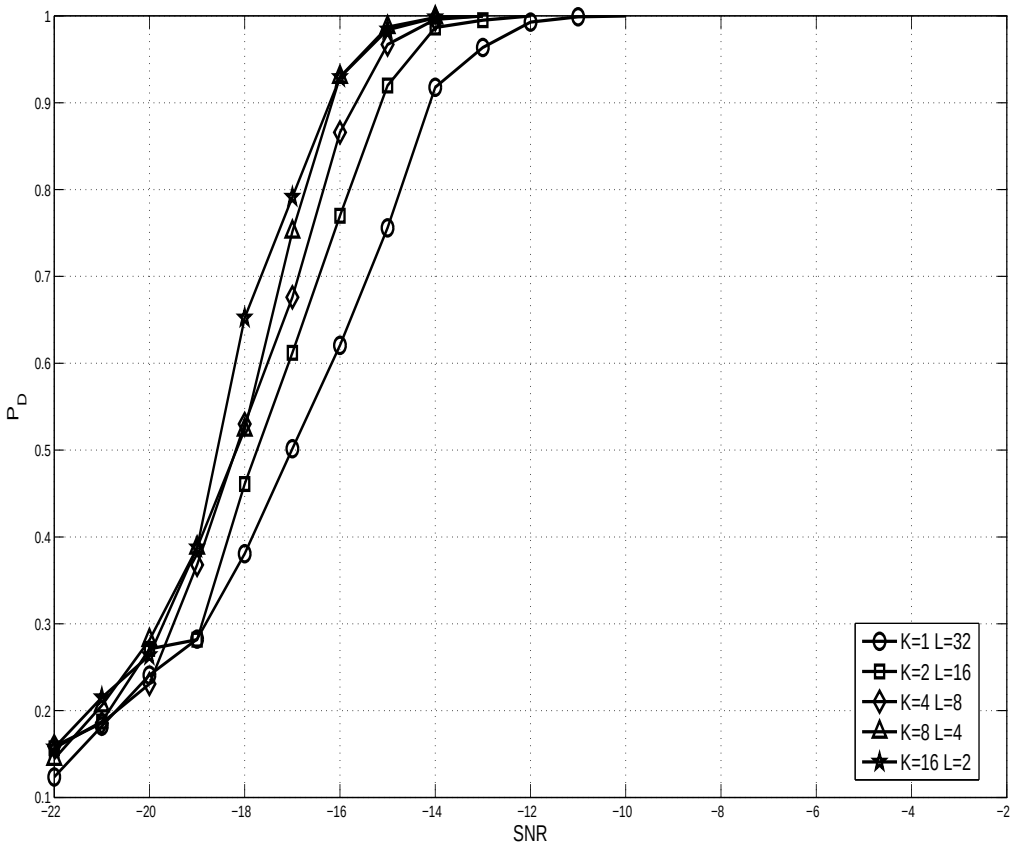

Figure 3.7: Performance using the C2-LMS algorithm and the energy detector for different configurations of the same computational complexity ($K \times L = 16$)

.

algorithm is tested. The cyclostationary detector is used to detect the conjugate cyclic autocorrelation peak at $2f_c$. The performances of the proposed spectrum sensing structure in conjunction with a cyclostationary detector under different situations are plotted in Figure 3.9. It is observed that the detector performance does not degrade due to noise uncertainty, as expected. It is also observed that an increase in the number of samples, as well as the detector complexity lead to an improvement in the detector performance. The gains in dB for different configurations of the space-time FRESH filter over a simple cyclostationary detector at a detection rate of 0.95 are listed in Table 3.3.

3.7.6 Discussion and summary of results

An increase in both the FRESH filter lengths and the number of antennas is observed to cause an improvement in the detector performance. However, as discussed previously, the relative gain offered by more number of antennas is more than that offered by larger filter lengths. The slight degradation in performance of the system based on the C2-LMS in comparison to the spectrum sensor based on the modified ACS algorithm may be attributed to the misadjustment caused due to incorporation of the stochastic gradient in the weight update algorithm instead of the deterministic gradient. Comparing Tables 3.2 and 3.3, we observe that employing FRESH filters with a cyclostationary detector results in gains similar to those obtained by employing FRESH filters along with energy detectors.

It may be noted here, that the modified ACS algorithm reduces to the standard ACS algorithm for a single delay tap ($L = 1$) and in this case the method becomes similar to the one used in [35]. Similarly, for a single-antenna ($K = 1$) the C2-LMS algorithm reduces to the standard LMS algorithm and the resultant method is identical to the one used in [105].

3.8 Conclusion

The performance enhancement achieved using the Space-Time FRESH filtering structure with regard to spectrum sensing in cognitive radios is studied in this chapter. A novel blind Space-Time FRESH filtering structure has been proposed for the purpose of enhancing a primary cyclostationary signal embedded in noise. It has been shown that this structure may be used in conjunction with the energy detector to improve its detection performance. The ACS algorithm for cyclostationary beamforming is modified in order to adapt the proposed structure, following which a method to sense the spectrum based on the proposed structure is proposed. Keeping in view the high computational complexity of the modified ACS algorithm, a low complexity stochastic gradient algorithm is derived and its application to spectrum sensing is studied.

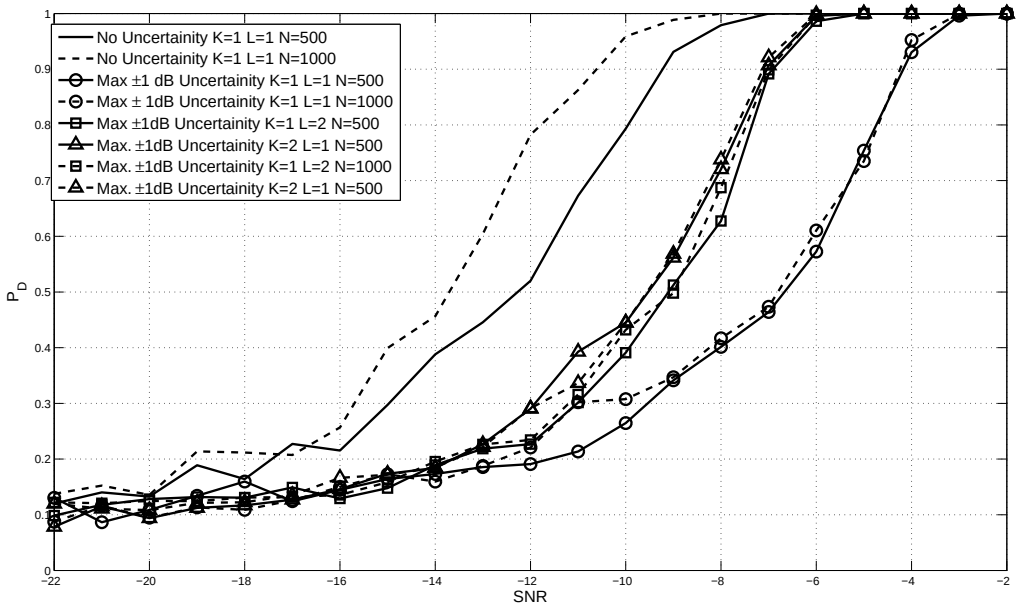

Figure 3.8: Performance using the C2-LMS algorithm and the energy detector for different configurations under noise uncertainity

.

Table 3.3: Gains (in Decibel) offered by the proposed algorithm at $N = 500$

	L=1	2	4	8	16	32
K=1	0	0.9	2.49	3.722	4.58	5.16
2	1.69	3.02	3.96	5.21	5.95	6.54
4	3.22	4.43	5.54	6.52	7.43	8.72
8	4.66	5.61	6.85	7.68	8.5	8.82
16	5.87	6.81	7.85	8.73	9.52	9.67

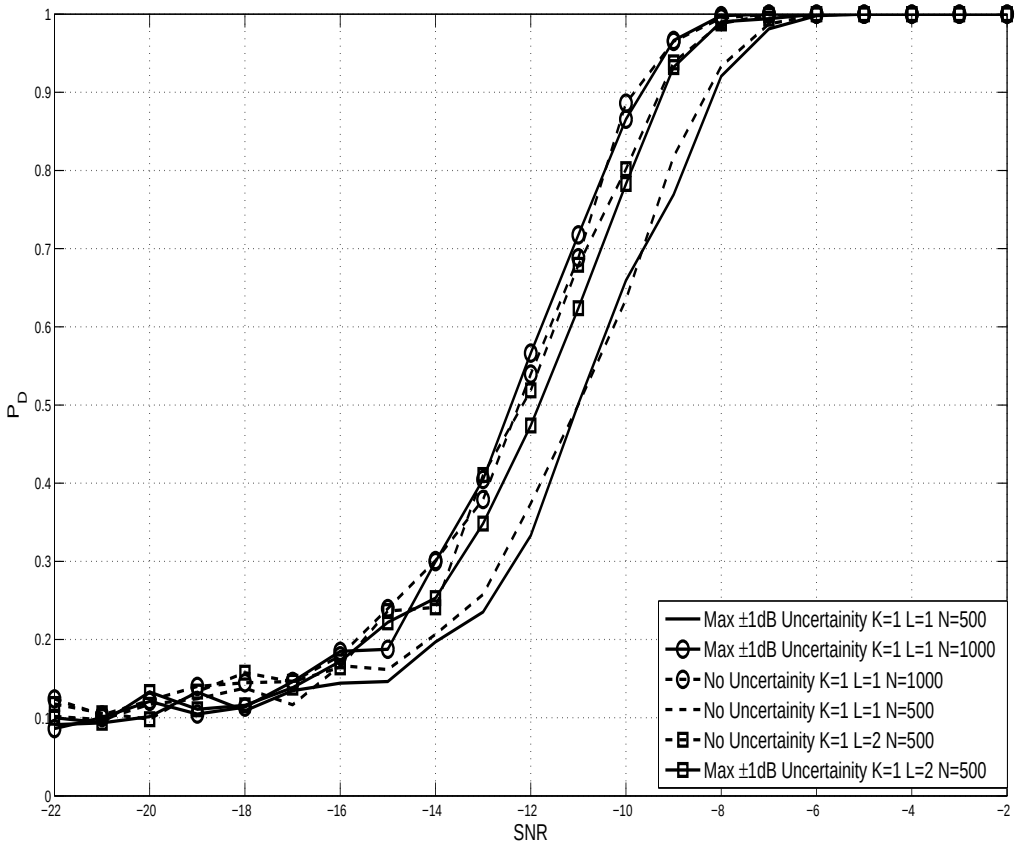

Figure 3.9: Performance using the C2-LMS algorithm and the cyclostationary detector for different filter configurations under noise uncertainity.

Chapter 4

Performance Analysis of FRESH filter based Spectrum Sensing

In the previous chapter, it was demonstrated via simulation that sapce-time FRESH filtering of the sampled signal prior to detection results in gains of as much as 10 dB over standard single-antenna energy detector. In this chapter, the single-antenna based spectrum sensor is studied in more detail. Here, performance results are derived for a single-user single-antenna FRESH filter-based system. The performance enhancements in the cases of both the energy detector as well as the cyclostationarity detector are considered. Following this, the performance of FRESH filter based spectrum sensors in the presence of noise uncertainty is also evaluated. It is shown that FRESH filtering the received signal prior to detection improves the performance of the spectrum sensors in all these cases.

The signal, sensing and filtering models are introduced in Section 4.1. The performance of the energy detector based on FRESH filtering is derived and verified using simulation results in Section 4.2. The cyclostationary detector for a FRESH filter-based spectrum sensor along with its performance is studied in 4.3. The performances of these detectors, viz. FRESH filter-based energy detector and FRESH filter-based cyclostationary detector under noise uncertainty, are studied in Section 4.4. The conclusions constitute Section 4.5.

4.1 The Signal, Filtering and Sensing Models

4.1.1 The Signal and Filtering Model

The primary signal $s[n]$ is assumed to be zero mean complex Gaussian with a variance σ_s^2. It is assumed, as discussed in Chapter 2, that $s[n]$ exhibits cyclostationarity at cyclic frequencies $\alpha_1, \alpha_2, \ldots, \alpha_{M_1} \in \mathcal{A}$ and conjugate cyclostationarity at $\beta_1, \beta_2, \ldots, \beta_{M_2} \in \mathcal{B}$ and, therefore, may be expressed as

$$s[n] = \sum_{\alpha \in \mathcal{A}} \sum_{l=0}^{L_\alpha - 1} a_\alpha[l] s^\alpha[n-l] + \sum_{\beta \in \mathcal{B}} \sum_{l=0}^{L_\beta - 1} a_\beta[l] s^{*\beta}[n-l] + \zeta[n] \tag{4.1}$$

where $\zeta[n]$ is the innovation component and $s^\alpha[n]$ and $s^{*\beta}[n]$ are respectively the frequency shifted and the conjugate frequency shifted versions of the signal $s[n]$ defined as

$$s^\alpha[n] = s[n] e^{-j2\pi\alpha n} \tag{4.2}$$

$$s^{*\beta}[n] = s^*[n] e^{-j2\pi\beta n} \tag{4.3}$$

The cyclic autocorrelation function at cyclic frequency α and lag τ, defined earlier may be written as

$$R_{ss}^\alpha[\tau] = E\left[s^\alpha[n] s^*[n-\tau]\right], \tag{4.4}$$

and the conjugate cyclic autocorrelation function as

$$R_{ss^*}^{\beta *}[\tau] = E\left[s^{*\beta}[n] s^*[n-\tau]\right], \tag{4.5}$$

It was observed in the previous chapter that the optimal filter for a cyclostationary signal may be represented as a FRESH filter. It was also shown that the problem of optimal FRESH filtering for a signal $x[n]$ exhibiting cyclostationarity at M_1 number of cyclic frequencies ($\alpha \in \mathcal{A}$) and conjugate cyclostationarity at M_2 number of cyclic frequencies ($\beta \in \mathcal{B}$) may be considered as the problem of finding the optimal weight vector $\mathbf{w}_o$ such that the mean square value of the error signal, defined as

$$\begin{aligned} e[n] &= x[n] - \mathbf{w}_o^H \mathbf{u}[n] \\ &= x[n] - v[n], \end{aligned} \tag{4.6}$$

is minimized.
Here $\mathbf{u}[n]$ is the filter input vector, defined as

$$\begin{aligned} \mathbf{u}[n] &= \left[\mathbf{x}^{\alpha_1 T}[n] \ldots \mathbf{x}^{\alpha_{M_1} T}[n] \mathbf{x}^{*\beta_1 T}[n] \ldots \mathbf{x}^{*\beta_{M_2} T}[n]\right]^T \\ \mathbf{x}^\alpha &= \left[x^\alpha[n], \ldots, x^\alpha[n - L_\alpha + 1]\right]^T \\ \mathbf{x}^{*\beta} &= \left[x^{*\beta}[n], \ldots, x^{*\beta}[n - L_\beta + 1]\right]^T, \end{aligned} \tag{4.7}$$

and L_α is the filter length corresponding to the frequency shift α. Here, for the sake of simplicity, the length of the FIR filters attached to each of the M ($M = M_1 + M_2$) number of FRESH branches is assumed to be fixed to L. The overall length of the regression vector $\mathbf{u}[n]$, therefore, becomes ML.

It was observed in the previous chapter that the optimal FRESH filter weights may be determined adaptively without the need for a reference signal, thus resulting in a Blind Adaptive FRESH (BA-FRESH) filter, as shown in Figure 4.1. Here, this structure is assumed to be adapted using either the FRESH-LMS or the FRESH-RLS algorithms. These adaptation algorithms are described in Algorithms 1 and 2, respectively [61,105]. In Algorithm 1, μ_L is the adaptation step size while μ_R is the forgetting factor in Algorithm 2 [61].

4.1.2 The Sensing Model

It is assumed that the spectrum sensor collects N samples of the signal $x[n]$ from the environment. This signal, under the two hypotheses, may be written as

$$x[n] = \begin{cases} \nu[n] & \mathcal{H}_0 \\ s[n] + \nu[n] & \mathcal{H}_1 \end{cases} \tag{4.8}$$

where $\nu[n]$ is the wide sense stationary, zero mean complex Gaussian noise having zero mean and a variance σ_ν^2, $s[n]$ is the primary user signal, the null Hypothesis $\mathcal{H}_0$ corresponds to the absence of a primary signal and the alternate hypothesis $\mathcal{H}_1$ to its presence.

It has been proposed in the previous chapter to use these samples to adapt the filter weights to obtain the weight vector $\mathbf{w}[N]$. The samples used to adapt the filter are stored and then passed through the adapted filter to obtain the signal $y[n]$ such that

$$y[n] = \mathbf{w}^H[N]\mathbf{u}[n] \tag{4.9}$$

where $\mathbf{w}[N]$ is the adapted filter weight vector. The filtered signal $y[n]$ is then used to detect the presence of a primary signal. For this purpose, $y[n]$ may be fed to an energy detector or a cyclostationary detector, as described in the previous chapter. The detection statistics and the performances of these detectors in the case of AWGN channel are detailed in the following sections.

4.2 Performance of the Energy Detector

The noise component $\nu[n]$ of the signal $x[n]$ does not exhibit cyclostationarity and therefore, will not be enhanced due to FRESH filtering. On the other hand, the cyclostationary component of the received signal, if present, will be enhanced by FRESH filtering. The

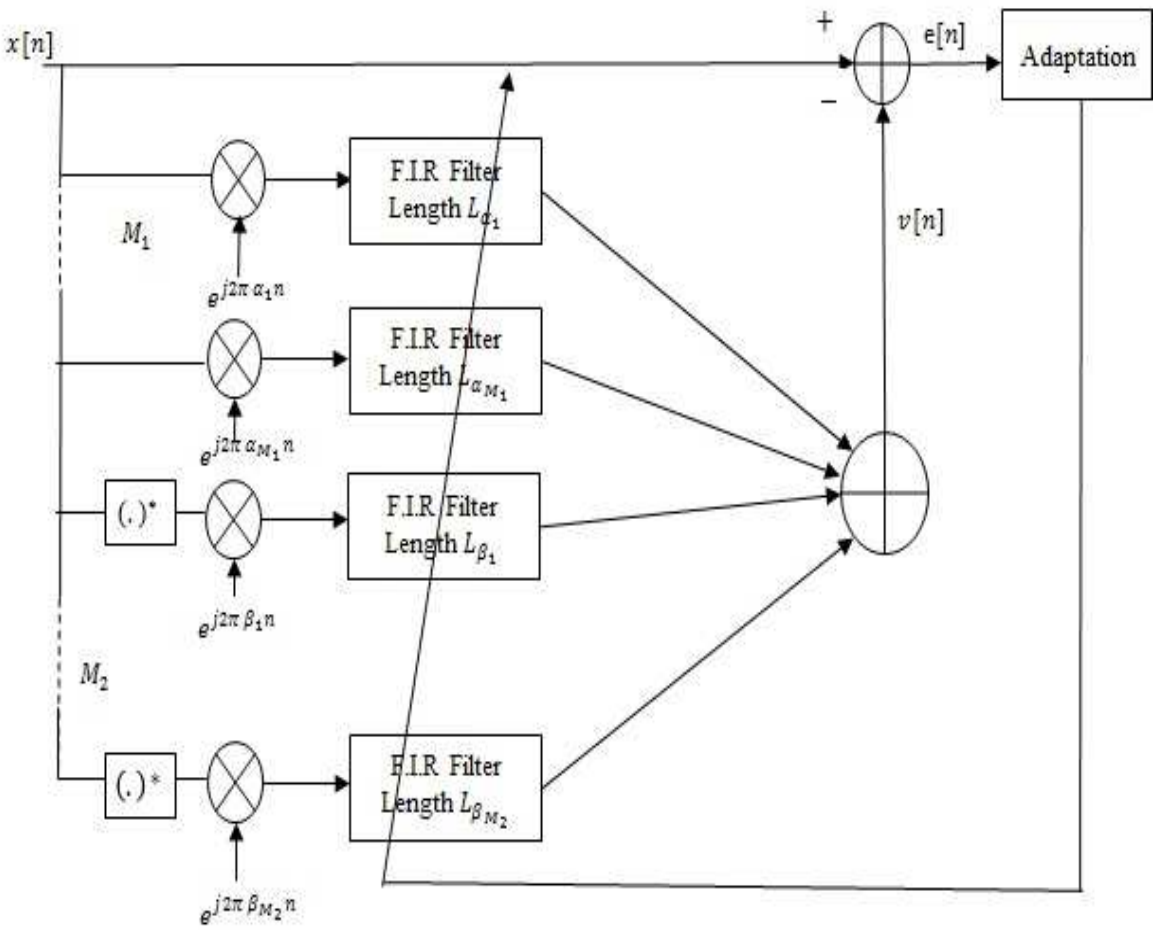

Figure 4.1: Blind Adaptive FRESH filter structure, as proposed in [145]

Algorithm 1 The FRESH-LMS algorithm

Initialize the weight vector $\mathbf{w}[0] = \mathbf{0}$
For the nth sample, calculate $e[n] = x[n] - \mathbf{w}^H[n]\mathbf{u}[n]$
Update $\mathbf{w}[n+1] = \mathbf{w}[n] + \frac{\mu_L}{\|\mathbf{u}[n]\|^2}\mathbf{u}[n]e^*[n]$

Algorithm 2 The FRESH-RLS algorithm

Initialize the weight vector $\mathbf{w}[0] = \mathbf{0}$ and $\mathbf{P}[0] = \delta^{-1}\mathbf{I}$
For the nth sample, calculate :
$e[n] = x[n] - \mathbf{w}^H[n-1]\mathbf{u}[n]$
$\boldsymbol{\pi}[n] = \mathbf{P}[n-1]\mathbf{u}[n]$
$\mathbf{k}[n] = \frac{\boldsymbol{\pi}[n]}{\mu_R + \mathbf{u}^H[n]\boldsymbol{\pi}[n]}$
Update
$\mathbf{w}[n+1] = \mathbf{w}[n] + \mathbf{k}[n]e^*[n]$
$\mathbf{P}[n] = \mu_R^{-1}\mathbf{P}[n-1] - \mu_R^{-1}\mathbf{k}[n]\mathbf{u}^H[n]\mathbf{P}[n-1]$

simplest strategy for the detection of this enhanced component is to compare the finite-time energy of the filtered signal against the noise floor. The test statistic in this case, therefore, becomes

$$\begin{aligned} T_E &= \tfrac{1}{N}\textstyle\sum_{n=0}^{N-1}|y[n]|^2 \\ &= \tfrac{1}{N}\textstyle\sum_{n=0}^{N-1}\mathbf{w}^H[N]\mathbf{u}[n]\mathbf{u}^H[n]\mathbf{w}[N] \end{aligned} \tag{4.10}$$

It may be observed that both $\mathbf{u}[n]$ and $\mathbf{w}[N]$ are random vectors. Consequently, for a large number of samples, the test statistic T_E may be assumed to have a normal probability density function (pdf) [122]. In order to determine the performance of this detector, the mean and variance of the test statistics under the two hypotheses are required.

Taking expectation on both sides of (4.10)

$$E[T_E] = \frac{1}{N}\sum_{n=0}^{N-1} E\left[\mathbf{w}^H[N]\mathbf{u}[n]\mathbf{u}^H[n]\mathbf{w}[N]\right] \tag{4.11}$$

Assuming that the adapted weights and the regression vectors are independent [61] we have,

$$\begin{aligned} E[T_E] &= \tfrac{1}{N}\textstyle\sum_{n=0}^{N-1} E\left[\mathbf{w}^H[N]E\left[\mathbf{u}[n]\mathbf{u}^H[n]\right]\mathbf{w}[N]\right] \\ &= \tfrac{1}{N}\textstyle\sum_{n=0}^{N-1} E\left[\mathbf{w}^H[N]\mathbb{R}_{uu}\mathbf{w}[N]\right] \\ &= E\left[\mathbf{w}^H[N]\mathbb{R}_{uu}\mathbf{w}[N]\right] \end{aligned} \tag{4.12}$$

where $\mathbb{R}_{uu} = E\left[\mathbf{u}[n]\mathbf{u}^H[n]\right]$ is the covariance matrix of the regression vector $\mathbf{u}[n]$. Under the null hypothesis $\mathcal{H}_0$

$$\mathbb{R}_{uu} = \sigma_\nu^2\mathbb{I}. \tag{4.13}$$

where, $\mathbb{I}$ is the ML dimensional identity matrix and the weight vector $\mathbf{w}[N]$ is normalized such that $\|\mathbf{w}[N]\|_2^2 = 1$

Therefore,

$$E[T_E|\mathcal{H}_0] = E\left[\|\mathbf{w}[N]\|_2^2\sigma_\nu^2\right] = \sigma_\nu^2. \tag{4.14}$$

On the other hand under the alternate hypothesis $\mathcal{H}_1$, where the primary signal is present, $x[n] = s[n] + \nu[n]$ and consequently,

$$\mathbb{R}_{uu} = \mathbb{R}_{ss} + \sigma_\nu^2\mathbb{I} \tag{4.15}$$

where,

$$\begin{aligned}\mathbb{R}_{ss} &= E\left[\begin{bmatrix}\mathbf{s}^{\alpha_1}[n]\\ \vdots \\ \mathbf{s}^{\alpha_{M_1}}[n]\\ \mathbf{s}^{*\beta_1}[n]\\ \vdots \\ \mathbf{s}^{*\beta_{M_2}}[n]\end{bmatrix}[\mathbf{s}^{\alpha_1 H}[n]\dots\mathbf{s}^{\alpha_{M_1} H}[n]\mathbf{s}^{*\beta_1 H}[n]\dots\mathbf{s}^{*\beta_{M_2} H}[n]]\right] \\ &= \begin{bmatrix}\mathbf{R}_{ss}^{0}[0] & \mathbf{R}_{ss}^{\alpha_1-\alpha_2}[0] & \dots & \mathbf{R}_{ss}^{\alpha_1+\beta_{M_2}}[0]\\ \vdots & \vdots & \ddots & \vdots \\ \mathbf{R}_{ss}^{-\beta_{M_2}-\alpha_1}[0] & \mathbf{R}_{ss}^{-\beta_{M_2}-\alpha_2}[0] & \dots & \mathbf{R}_{ss}^{0}[0]\end{bmatrix}\end{aligned} \tag{4.16}$$

here $\mathbf{R}_{ss}^{\alpha_i-\alpha_k}[\tau]$ is the cyclic autocorrelation matrix of the primary signal at cyclic frequency $\alpha_i - \alpha_k$ and lag τ.

$$\mathbf{R}_{ss}^{\alpha_i-\alpha_k}[\tau] = E[\mathbf{s}^{\alpha_i}[n]\mathbf{s}^{\alpha_k H}[n-\tau]] \tag{4.17}$$

This matrix will be non-zero only if $s[n]$ exhibits cyclostationarity at $\alpha_i - \alpha_k$. The weight vector $\mathbf{w}[N]$ may be decomposed as $\mathbf{w}[N] = \mathbf{w}_o + \tilde{\mathbf{w}}[N]$, with $\mathbf{w}_o$ being the optimal weight vector and $\tilde{\mathbf{w}}[N] = \mathbf{w}_o - \mathbf{w}[N]$ the weight error vector.

Defining

$$\mathbf{Q}[N] = E[\tilde{\mathbf{w}}[N]\tilde{\mathbf{w}}^H[N]], \tag{4.18}$$

the mean of the test statistic under the alternative hypothesis may be written as [61]

$$E[T_E|\mathcal{H}_1] = \sigma_\nu^2 + \mathbf{w}_o^H\mathbb{R}_{ss}\mathbf{w}_o + tr(\mathbf{Q}[N]\mathbb{R}_{ss}) \tag{4.19}$$

It may be observed that the weight error vector consists of two terms. An exponentially decaying term due to the weight error and a fixed term, proportional to the step size. Therefore, for a sufficiently large N and sufficiently small adaptation step size, the last term in the above expression due to the weight error vector will be negligibly small [61] in comparison to the first term and may be ignored. Therefore,

$$E[T_E|\mathcal{H}_1] \approx \sigma_\nu^2 + \mathbf{w}_o^H\mathbb{R}_{ss}\mathbf{w}_o \tag{4.20}$$

It may be observed that the optimal weight vector is defined as

$$\mathbf{w}_o^H = \mathbb{R}_{ss}^{-1}\mathfrak{r}_{ss}[0] \tag{4.21}$$

where

$$\mathfrak{r}_{ss}[0] = [\mathbf{r}_{ss}^{\alpha_1}, \dots, \mathbf{r}_{ss}^{\beta_{M_2}}]^T \tag{4.22}$$

and

$$\mathbf{r}_{ss}^{\alpha}[0] = [R_{ss}^{\alpha_1}[0], \ldots, \mathbf{r}_{ss}^{\alpha}[L-1]]^T \tag{4.23}$$

Therefore,

$$E[T_E|\mathcal{H}_1] \approx \sigma_\nu^2 + \mathfrak{r}_{ss}^H \mathbb{R}_{ss}^{-1} \mathfrak{r}_{ss} \tag{4.24}$$

The second moment of the test statistic, required to determine its variance, may be calculated as,

$$\begin{aligned} E[|T_E|^2] &= E\left[\tfrac{1}{N}\left(\textstyle\sum_{n=0}^{N-1}|y[n]|^2\right)^2\right] \\ &= E\left[\tfrac{1}{N^2}\textstyle\sum_{n=0}^{N-1}\sum_{m=0}^{N-1}\mathbf{w}^H[N]\mathbf{u}[m]\mathbf{u}^H[m]\mathbf{w}[N]\mathbf{w}^H[N]\mathbf{u}[n]\mathbf{u}^H[n]\mathbf{w}[N]\right] \\ &= E\left[\tfrac{1}{N^2}\textstyle\sum_{m=0}^{N-1}\sum_{n=0}^{N-1}\sum_{i=1}^{ML}\sum_{k=1}^{ML}\sum_{p=1}^{ML}\sum_{q=1}^{ML} w_i^* w_k w_p w_q^* u_i[m]u_k^*[m]u_p^*[n]u_q[n]\right] \\ &= \tfrac{1}{N^2}\textstyle\sum_{m=0}^{N-1}\sum_{n=0}^{N-1}\sum_{i=1}^{ML}\sum_{k=1}^{ML}\sum_{p=1}^{ML}\sum_{q=1}^{ML} E[w_i^* w_k w_p w_q^*]E[u_i[m]u_k^*[m]u_p^*[n]u_q[n]] \end{aligned} \tag{4.25}$$

where w_i represents the ith element of the weight vector $\mathbf{w}[N]$ and $u_i[n]$ represents the ith element of the regression vector $\mathbf{u}[n]$. Invoking the Isserlis' Theorem [97], the term $E[u_i[m]u_k^*[m]u_p^*[n]u_q[n]]$ may be written as

$$\begin{aligned} E[u_i[m]u_k^*[m]u_p^*[n]u_q[n]] &= E[u_i[m]u_k^*[m]]E[u_p^*[n]u_q[n]] + E[u_i[m]u_q[n]]E[u_k^*[m]u_p^*[n]] \\ &\quad + E[u_i[m]u_p^*[n]]E[u_k^*[m]u_q[n]] \end{aligned} \tag{4.26}$$

In the absence of the primary signal, this term reduces to

$$E[u_i[m]u_k^*[m]u_p^*[n]u_q[n]|\mathcal{H}_0] = \sigma_\nu^4\left(\delta[i-k]\delta[p-q] + \delta[(m-n)-(i-p)]\delta[(m-n)-(k-q)]\right) \tag{4.27}$$

where $\delta[.]$ represents the Kronecker Delta function. Substituting (4.27) in (4.25) and using $\|\mathbf{w}[N]\| = 1$, we have,

$$E[|T_E|^2|\mathcal{H}_0] = \sigma_\nu^4 + \frac{\sigma_\nu^4}{N}\left(\sum_p\left(\sum_{i=1}^{ML} E[w_i^* w_{i-p}]\right)^2\right) \tag{4.28}$$

The first term in this expression corresponds to $(E[T_E|\mathcal{H}_0])^2$ and the second term is the variance of the test statistic. That is,

$$var(T_E|\mathcal{H}_0) = \frac{\sigma_{E_0}^2}{N} = \frac{\sigma_\nu^4}{N}\left(\sum_p\left(\sum_{i=1}^{ML} E[w_i^* w_{i-p}]\right)^2\right) \tag{4.29}$$

Here, the term $\sigma_{E_0}^2$ is introduced for notational convenience. The optimal weight vector, under the null hypothesis, is the null vector. Therefore, the variance of the test statistic under the null hypothesis is entirely a function of the weight error vector. It may be seen

that the term within the brackets corresponds to the sum of the elements of the weight error covariance matrix. Therefore, it is not possible to determine a closed form expression for this term.

However, it may be observed that this term will be minimized when the individual weight error terms are independent of each other, resulting in a diagonal weight error covariance matrix. Also, it may be shown that this term will be maximized when all the entries in the weight error covariance matrix are equal. Based on these, the variance of the test statistic may be observed to be bounded as

$$\sigma_\nu^4 \leq \sigma_{E_0}^2 \leq ML\sigma_\nu^4 \tag{4.30}$$

In the presence of a primary user signal, the simplification of (4.25) and subsequent subtraction of the term corresponding to the square of the mean of the test statistic yields

$$\begin{aligned} var(T_E|\mathcal{H}_1) &= \tfrac{\sigma^4}{N}\textstyle\sum_p \Bigg(\Big(\sum_{i=1}^{ML} E[w_i w_{i-p}^*] \Big)^2 \\ &\quad +2\gamma_i \textstyle\sum_{i=1}^{ML}\sum_{j=1}^{ML}\sum_{k=1}^{ML} E[w_i w_j^* w_k^* w_{k-p}]\rho_{ss}[p-(i-j)] \Big) \\ &\quad +\gamma_i^2 \tfrac{\sigma_\nu^4}{N^2} \textstyle\sum_{m=0}^{N-1}\sum_{n=0}^{N-1}\sum_{i=1}^{ML}\sum_{j=1}^{ML}\sum_{k=1}^{ML}\sum_{l=1}^{ML} E[w_i w_j^* w_k^* w_l] \\ &\quad (\rho_{ss}((n-m)-(i-j))\rho_{ss}((n-m)-(k-l)) \\ &\quad \rho_{ss}((n-m)-(i-l))\rho_{ss}((n-m)-(k-j))) \end{aligned} \tag{4.31}$$

where γ_i denotes the SNR at the input of the FRESH filter defined as $\gamma_i = \frac{\sigma_s^2}{\sigma_\nu^2}$. It may be observed that the last term may be ignored under low SNR conditions and the above expression may be approximated as

$$\begin{aligned} var(T_E|\mathcal{H}_1) &= \tfrac{\sigma^4}{N}\textstyle\sum_p \Bigg(\Big(\sum_{i=1}^{ML} E[w_i w_{i-p}^*] \Big)^2 \\ &\quad +2\gamma_i \textstyle\sum_{i=1}^{ML}\sum_{j=1}^{ML}\sum_{k=1}^{ML} E[w_i w_j^* w_k^* w_{k-p}]\rho_{ss}[p-(i-j)] \Big) \end{aligned} \tag{4.32}$$

This function again becomes analytically indeterminable due to its dependence on the weight correlation matrices. However, in this case, due the weight error being negligible in comparison to the optimal weights, we can discard the expectation operation. Also, this expression will be maximized when the correlation coefficient is uniformly 1 and all the weights are equal so as to maximize the individual cross terms. The variance of the test statistic under the alternate hypothesis may then be bounded as

$$var(T_E|\mathcal{H}_1) \leq \frac{\sigma_\nu^2}{N}\sum_p \left(\left(\sum_{i=1}^{ML} \frac{1}{ML} \right)^2 + 2\gamma_i \sum_{i=1}^{ML}\sum_{j=1}^{ML}\sum_{k=1}^{ML} \left(\frac{1}{ML} \right)^2 \right) \tag{4.33}$$

This may be simplified to

$$var(T_E|\mathcal{H}_1) = \frac{\sigma_{E_1}^2}{N} \leq \frac{\sigma_\nu^4}{N} ML(1+2\gamma_i ML) \tag{4.34}$$

Consequently, the distribution of the test statistic under the two hypotheses may be written as

$$T_E \sim \begin{cases} \mathcal{N}\left(\sigma_\nu^2, \frac{\sigma_{E_0}^2}{N}\right) & \mathcal{H}_0 \\ \mathcal{N}\left(\sigma_\nu^2 + \mathbf{w}_o^H \mathbb{R}_{ss} \mathbf{w}_o, \frac{\sigma_{E_1}^2}{N}\right) & \mathcal{H}_1 \end{cases} \tag{4.35}$$

The probability of false alarm for a threshold λ is

$$P_{fa} = Q\left(\frac{\sqrt{N}(\lambda - \sigma_\nu^2)}{\sigma_{E_0}}\right) \tag{4.36}$$

where $Q(.)$ is the Marcum-Q function [69]. Accordingly, the detection threshold for a constant false alarm rate (CFAR) detector takes the form

$$\lambda = \frac{\sigma_{E_0} Q^{-1}(P_{fa})}{\sqrt{N}} + \sigma_\nu^2 \tag{4.37}$$

Probability of detection for a fixed threshold, is

$$P_d = Q\left(\sqrt{N}\frac{\lambda - (\sigma_\nu^2 + \mathbf{w}_o^H \mathbb{R}_{ss} \mathbf{w}_o)}{\sigma_{T_1}}\right) \tag{4.38}$$

Substituting (4.37) into (4.38) and simplifying we get,

$$P_d = Q\left(\frac{Q^{-1}(P_{fa}) - \sqrt{N}\frac{\mathbf{w}_o^H \mathbb{R}_{ss} \mathbf{w}_o}{\sigma_{E_0}}}{\frac{\sigma_{E_1}}{\sigma_{E_0}}}\right) \tag{4.39}$$

Defining the output SNR of the FRESH filter as

$$\begin{aligned} \gamma_o &= \frac{\mathbf{w}_o^H \mathbb{R}_{ss} \mathbf{w}_o}{\sigma_{E_0}} \\ &= \gamma_i \frac{\mathbf{w}_o^H \mathbb{R}_{ss} \mathbf{w}_o}{\sigma_s^2} \frac{\sigma_s^2}{\sigma_{E_0}^2} \end{aligned} \tag{4.40}$$

The term $\frac{\mathbf{w}_o^H \mathbb{R}_{ss} \mathbf{w}_o}{\sigma_s^2}$ may be defined as the FRESH filter gain for the primary signal.

The detection performance is expected to improve with the FRESH filter length as long as the term $\frac{\mathbf{w}_o^H \mathbb{R}_{ss} \mathbf{w}_o \sigma_\nu^2}{\sigma_s^2 \sigma_{E_0}^2}$ is greater than unity. In this term, both the numerator and the denominator are non-decreasing functions of the number of FRESH filter branches (M) and lengths (L). This expression may be solved to find the optimal values of M and L. Also, (4.39) may be solved to find the number of samples (N) required to obtain a given detection rate (P_d) for a pre-defined false alarm rate (P_{fa}) as

$$N = \left(\frac{Q^{-1}(P_{fa}) - \frac{\sigma_{E_0}}{\sigma_{E_1}} Q^{-1}(P_d)}{\gamma_o}\right)^2 \tag{4.41}$$

It may be observed that the number of samples required varies as the inverse square of the output SNR which in turn depends on the FRESH filter configuration. Therefore, the sensing time for a FRESH filter-based spectrum sensing system also depends on the FRESH filter configuration. It is observed in the simulation results that appropriate FRESH filter configurations may reduce the sensing time by more than one order of magnitude.

4.2.1 Evaluation of Variances

It is observed that variances of the test statistic under both the hypotheses depend on the filter and the primary user structure and cannot be determined in a closed form. However, bounds on their values along with simulation experiments may be used to determine empirical approximates. For the purpose of these simulation experiments, the primary user signal is considered to be BPSK modulated with a data rate (f_b) 10 kilo bits per second, a carrier frequency (f_c) 100 kHz. The spectrum sensor is assumed to take samples at 1 MHz. It is known that a BPSK signal exhibits conjugate cyclostationarity at $2f_c$ [50]. Therefore, the FRESH filter consists of a single conjugate frequency ($M = M_2 = 1$) shift branch at 200 kHz. The length of the FRESH filter attached to this branch is varied and takes values between 1 and 32.

In all the experiments, the FRESH filter is first adapted using the sensed signal. These samples are saved and passed through the adapted filter to generate a filtered signal which is then used to generate the test statistic. The test statistics are generated for different noise variances and different numbers of samples. These trials are repeated using both the FRESH-LMS and the FRESH-RLS algorithms to ensure that the obtained test statistics are independent of the algorithm used for adaptation. Ten thousand independent test statistics are generated for each combination of noise variance and FRESH filter length under both the hypotheses. It is verified in all the experiments that the variance of the test statistic in all the aforementioned cases is simply inversely proportional to the number of samples being used, and follows the bounds determined earlier. The variances of the test statistic for different filter lengths, at an SNR of -10 dB are listed in Table 4.1.

It may be observed that the variance of the test statistic under the null hypothesis stays close to the lower bound, but cannot be approximated by it. It may also be observed that it is not possible to derive a tighter bound due to the dependence of this term on the weight error covariance matrix. Therefore, the test statistic variance under the null hypothesis has to be determined empirically. It may be observed that in the absence of a primary user signal, the weight error vector will depend only on the filter configuration. Consequently, the variance of the test statistic under the null hypothesis will also be a function of the filter configuration and is given by

$$var(T_E|\mathcal{H}_0) = \frac{\sigma_\nu^4}{N}\left(1 + g_0(M, L)\right)^2 = \frac{\sigma_{E_0}^2}{N} \tag{4.42}$$

where $g_0(M, L)$ is an empirically determinable function of M and L. In the present case, as $M = 1$ this function may be reduced to $g_0(L)$. From the simulation results, it is observed that the term $g_0(L)$ in (4.42) may be plotted against the filter length (L) as shown by the black dots in Figure 4.2. These points are obtained by averaging the experimentally determined value of $g_0(L)$ over different noise variances, with different number of samples and for both the adaptation algorithms described in the previous section. It is observed from the plot that the function $g_0(L)$ is an increasing function of the filter length L and may be approximated as

$$g_0(L) = c_1 \ln(1 + c_2(L - 1)) \tag{4.43}$$

The parameters c_1 and c_2 are determined using MATLAB curve fitting toolbox and $c_1 = .07857$, and $c_2 = 8.89$. The fit using these values in (4.43) is shown in Figure 4.2 by the solid line.

Alternatively, the cross correlation coefficient of the weight vector may safely be assumed to be inversely proportional to the lag parameter factor, p. That is,

$$E[w_i^* w_{i-p}] \propto \frac{1}{p} \tag{4.44}$$

We may therefore write the summation term as

$$\left(\sum_{i=1}^{ML} E[w_i^* w_{i-p}] \right)^2 = g_1(p) \tag{4.45}$$

with $g_1(.)$ as a decreasing function of the argument. Taking $g_1(p) = p^{-c_2}$, for simplicity we may write the test statistic variance under the null hypothesis as

$$\frac{\sigma_{E_0}^2}{N} = \frac{\sigma_\nu^4}{N} \sum_{p=1}^{ML} p^{-c_3} \tag{4.46}$$

Yet again, in the absence of any knowledge about the correlation structure of the weight error vector, the term c_3 has to be determined empirically. The value of this parameter was found out to be $c_3 = 1.6$. Figure 4.3 plots the predicted and experimental values of the null hypothesis variance of the test statistics against the FRESH filter length.

Figure 4.4 compares the variance of the test statistic evaluated using simulation under the hypothesis $\mathcal{H}_1$ against the derived upper bound at different SNRs. It is observed that for SNRs below -5 dB, the simulated test statistic variance closely follows the upper bound and, therefore, may be approximated as

$$\sigma_{E_1}^2 \approx \sigma_\nu^4 ML(1 + 2\gamma_i ML) \tag{4.47}$$

Hence, it may be concluded that the variance of the test statistic lies close to the lower

Table 4.1: Test statistic variance under the null hypothesis compared against the bounds

Filter Length	1	2	4	8	16	32
Lower Bound	0.100	0.100	0.100	0.100	0.100	0.100
Simulated Value	0.100	0.130	0.159	0.180	0.194	0.204
Upper Bound	0.100	0.200	0.400	0.800	1.600	3.200

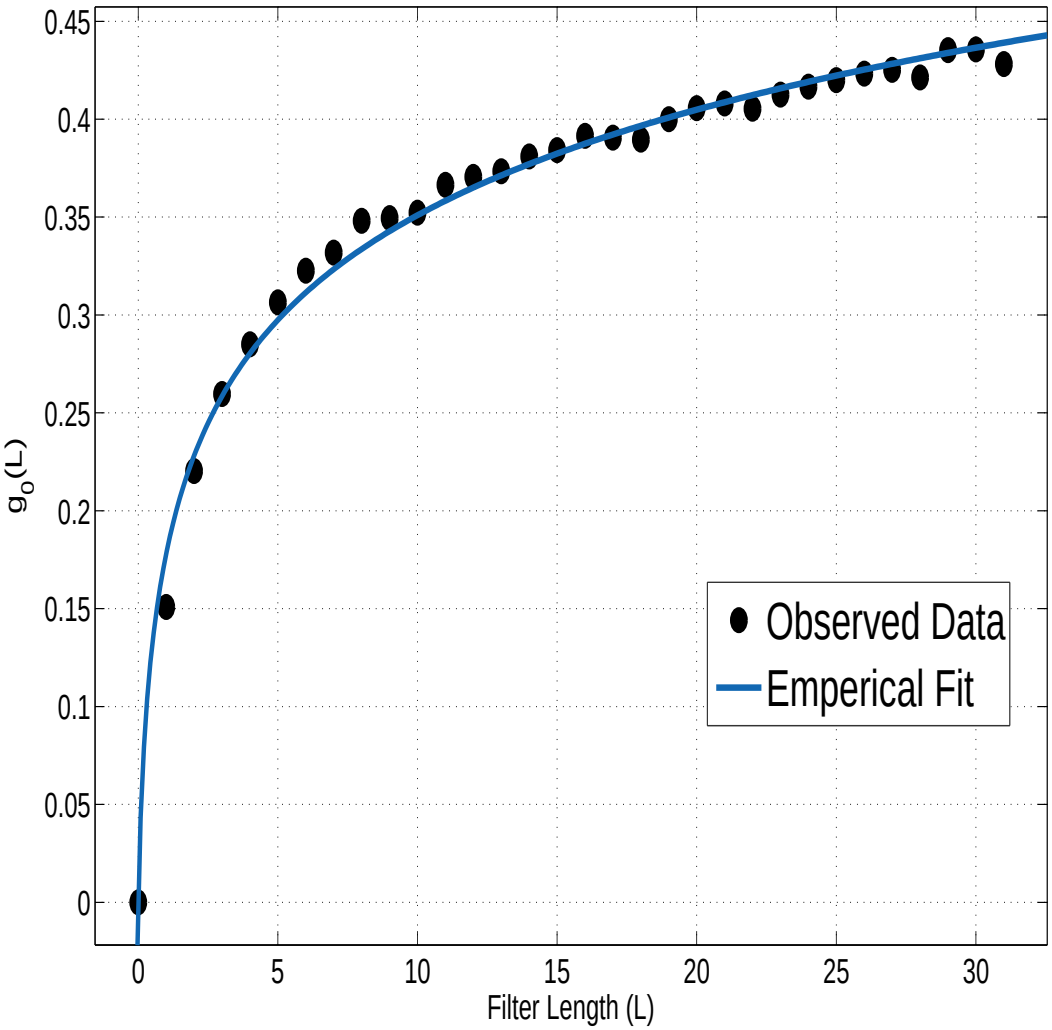

Figure 4.2: Empirical determination of the energy detector standard deviation in the absence of a primary signal for different filter lengths

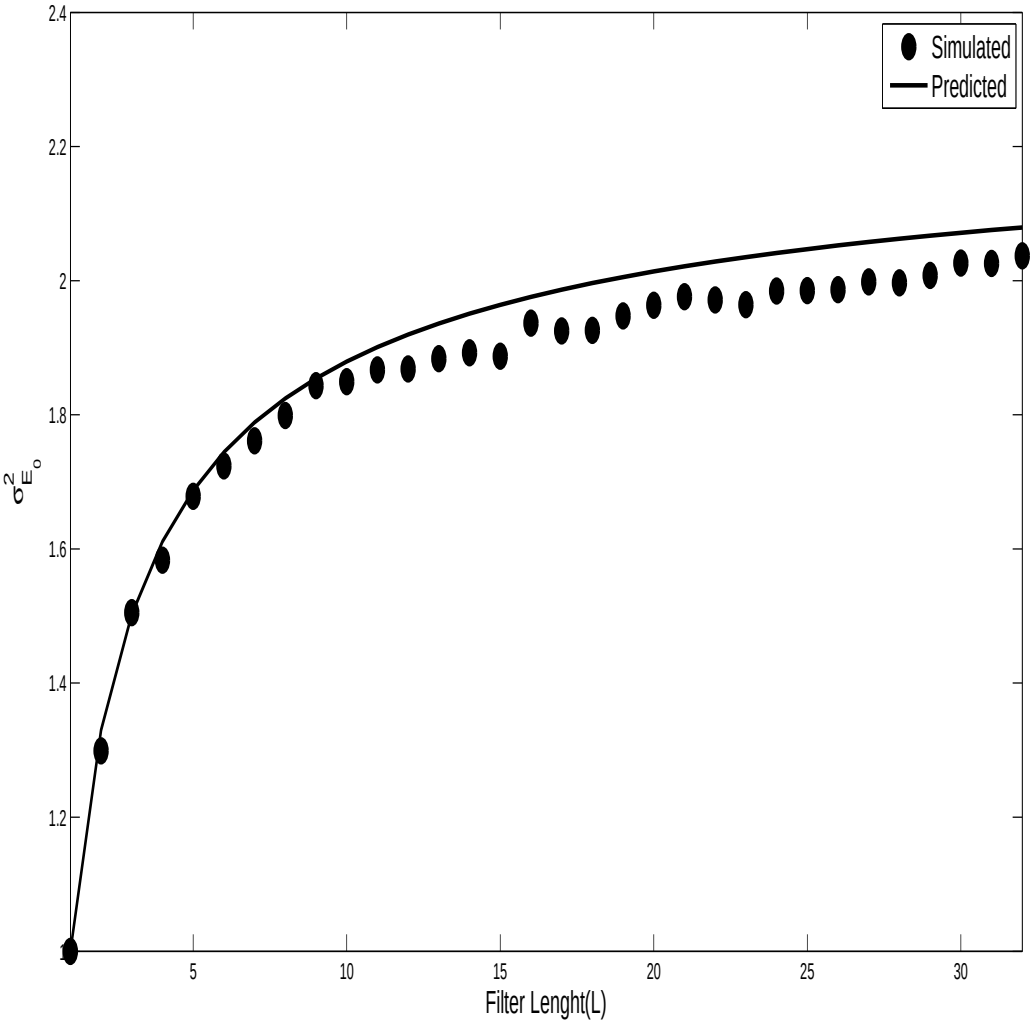

Figure 4.3: Empirical determination of the energy detector standard deviation in the absence of a primary signal for different filter lengths

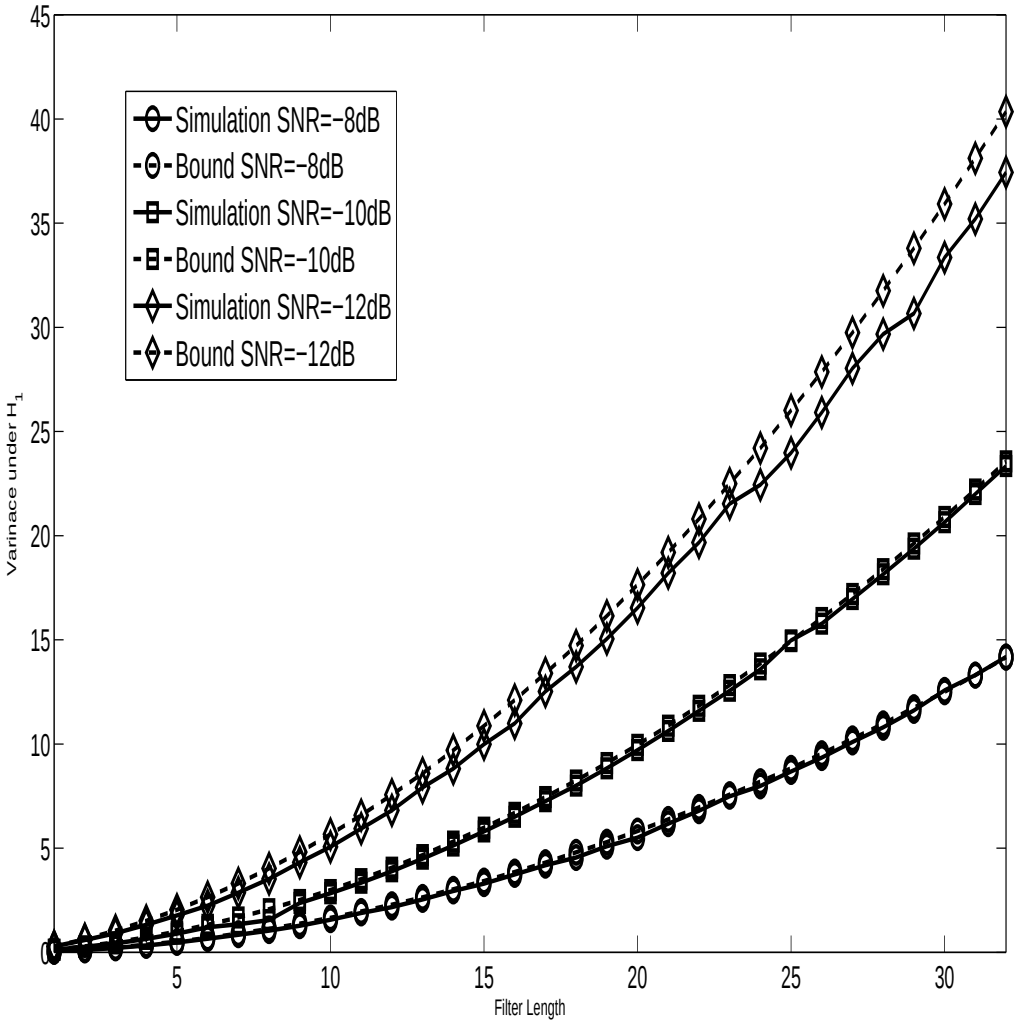

Figure 4.4: Test statistic variance for different SNRs under the alternate hypothesis

bound under the null hypothesis but has to be determined empirically. It may be noted that this variance is independent of the primary user signal structure. Therefore, this may be calculated offline for a given FRESH filter configuration. Also, either of the two empirical estimates may be used to determine this. However, the test statistic variance under the alternate hypothesis can be closely approximated by the derived upper bound in equation (4.34).

4.2.2 Performance Evaluation

Here, simulation results using randomly generated signals for the theory developed above, are presented. For this purpose, the primary user signal and the FRESH filtering system are assumed to be same as those used for the determination of empirical parameters. In all these experiments, the primary user variance is fixed at unity and the variance of the additive noise is varied to achieve different SNRs as per the requirement of the experiment. The system performance is evaluated in terms of the detection rate for input SNRs varying from -20 dB to 0 dB for 500 samples, and in terms of the number of samples required to achieve a successful detection performance at an input SNR of -14 dB. The false alarm rate in all these experiments is fixed at 1%. For theoretical evaluation, the test statistic variance under the null hypothesis is approximated using (4.42). This is used to calculate the threshold for a given false alarm rate as derived in equation (4.36). The variance of the test statistic under the alternate hypothesis is approximated as in (4.47). The detection threshold, and the two variances are then used to determine the detection performance by the use of (4.38). For simulation based evaluation, 1000 independent trials in the absence of a primary user signal are conducted to fix the detection threshold corresponding to a false alarm rate of 1%. Following this, 2000 independent trials, with the presence of a primary user signal controlled by a random variable, are conducted to determine the detection performance.

Figure 4.5 illustrates the performance of the FRESH filter-based spectrum sensor followed by an energy detector for different filter lengths. This experiment considers weights adapted using both the LMS and the RLS algorithms. It is observed that the FRESH-RLS algorithm-based system performs marginally better than the FRESH-LMS-based system at the cost of increased computational complexity. It may also be observed that increasing the FRESH filter length from 1 to 32 results in a gain of nearly 6 dB for a successful detection rate of 90%. In the figure, the no enhancement case refers to a FRESH filter length of 1 which essentially is the standard energy detector.

It was observed during the experiments that the number of samples required for the FRESH filter weights to converge is much larger than the number of samples being used for detection. Consequently, the predicted results differ significantly from the simulation results. This is because the predicted results assume the filter weights to be optimal. To alleviate this discrepancy, the knowledge about the optimal FRESH filter weights was

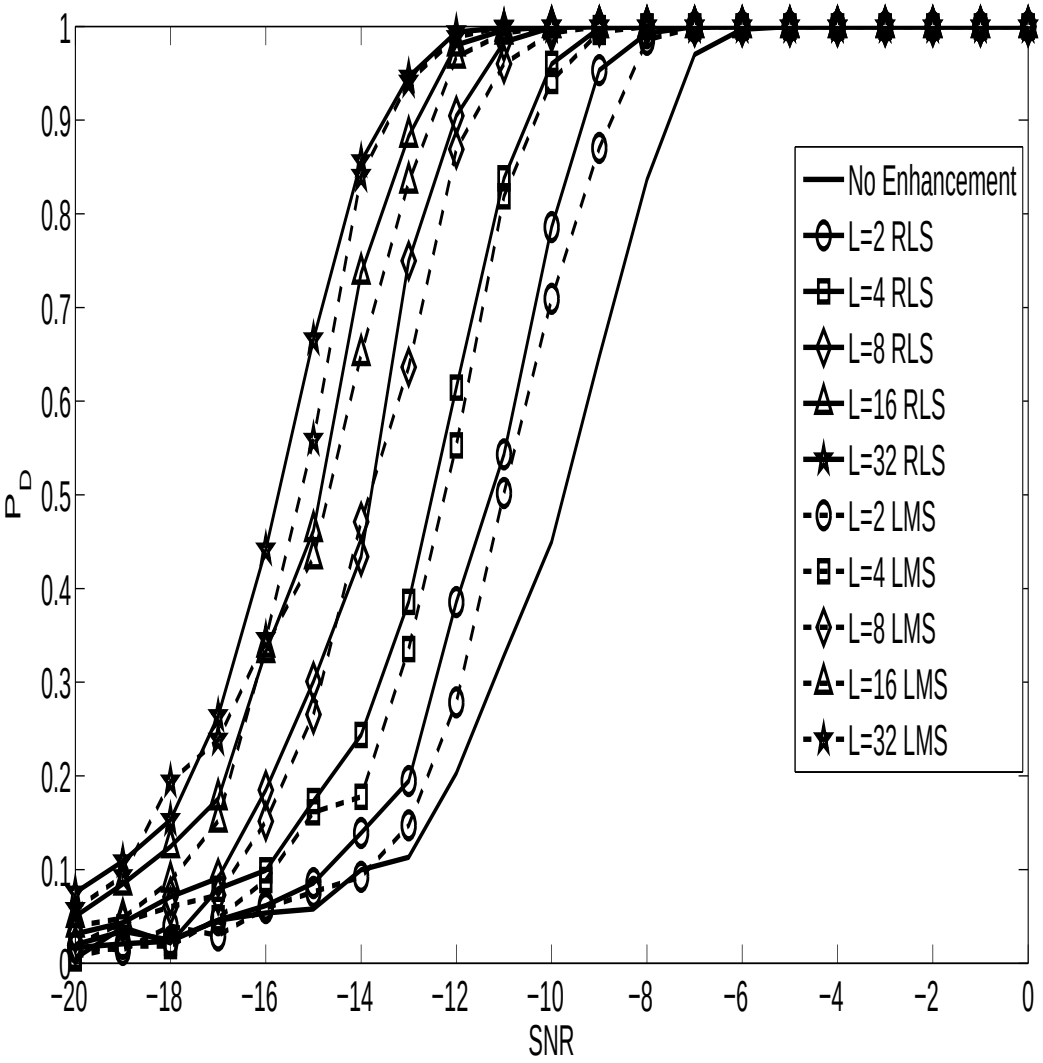

Figure 4.5: Performance of a FRESH filter based energy detector for different filter lengths and adaptation algorithms

assumed at the spectrum sensor and the signal samples were passed through a FRESH filter having optimal weights. The optimal filter weights are determined by first allowing the FRESH filters to converge by using a large number of samples for adaptation and then averaging these weights over 2000 independent realizations.

Figure 4.6 compares the predicted detection rate at different SNRs with the detection rate achieved using optimal and adapted (using the RLS algorithm) filter weights for different filter lengths. It may be observed that the plots for the cases where the optimal weights are known closely follow the behavior of the system predicted by (4.38) and (4.36). It may also be observed that if the correlation structure of the primary signal, and hence the optimal FRESH filter weights, are known then gain of 6 dB is achieved by increasing the filter length from 1 to 8.

In Figure 4.7 the number of samples required to achieve 90% detection rate and 10 % false alarm rate obtained using (4.41) is compared against the number of samples required to achieve this performance for the following cases: weights adapted using the LMS algorithm, weights adapted using the RLS algorithm, and optimal weights known to the system. It is seen that the required number of samples drops by more than two orders of magnitude when the FRESH filter weights are known at the spectrum sensor. Also, in case the FRESH filter weights are not known apriori, then an increase in the FRESH filter length from 1 to 32 may reduce the number of required samples by more than one order of magnitude.

The energy detector for a FRESH filtered signal is simple, but suffers from the same problems as encountered in the standard energy detector [122]. It is shown in Section 4.4 that the phenomenon of SNR walls occurs in an energy detector-based spectrum sensor because of an uncertainty in the mean of the test statistics under both the hypotheses. In order to avoid the phenomenon of SNR walls due to noise uncertainty, the mean of the test statistic under both the hypotheses should be independent of the ambient noise variance. It is, therefore, desired to develop an alternative detector such that its test statistics are independent of the ambient noise variance. It is shown in the next section that a cyclostationarity detector may be designed to achieve these requirements.

4.3 The Cyclostationarity Detector

The finite-time cyclic autocorrelation function of the filtered signal $y[n]$ at a cyclic frequency η and lag τ for N samples is defined as

$$\hat{R}^{\eta}_{yy}[N,\tau] = \frac{1}{N-\tau}\sum_{n=\tau}^{N-1} y[n]y^{*}[n-\tau]e^{-j2\pi\eta n} \tag{4.48}$$

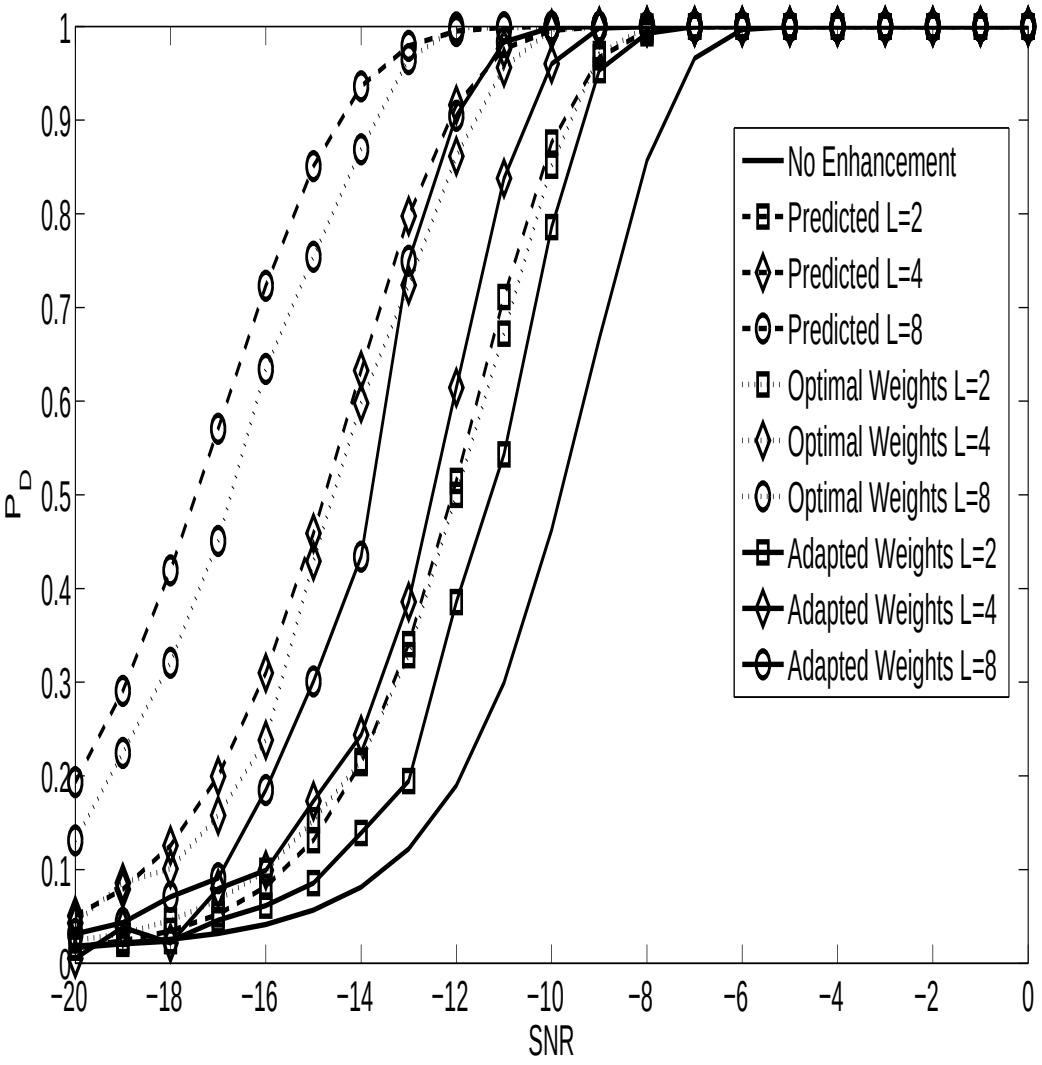

Figure 4.6: Comparison of predicted and actual performances of a FRESH filter based energy detector for different filter lengths

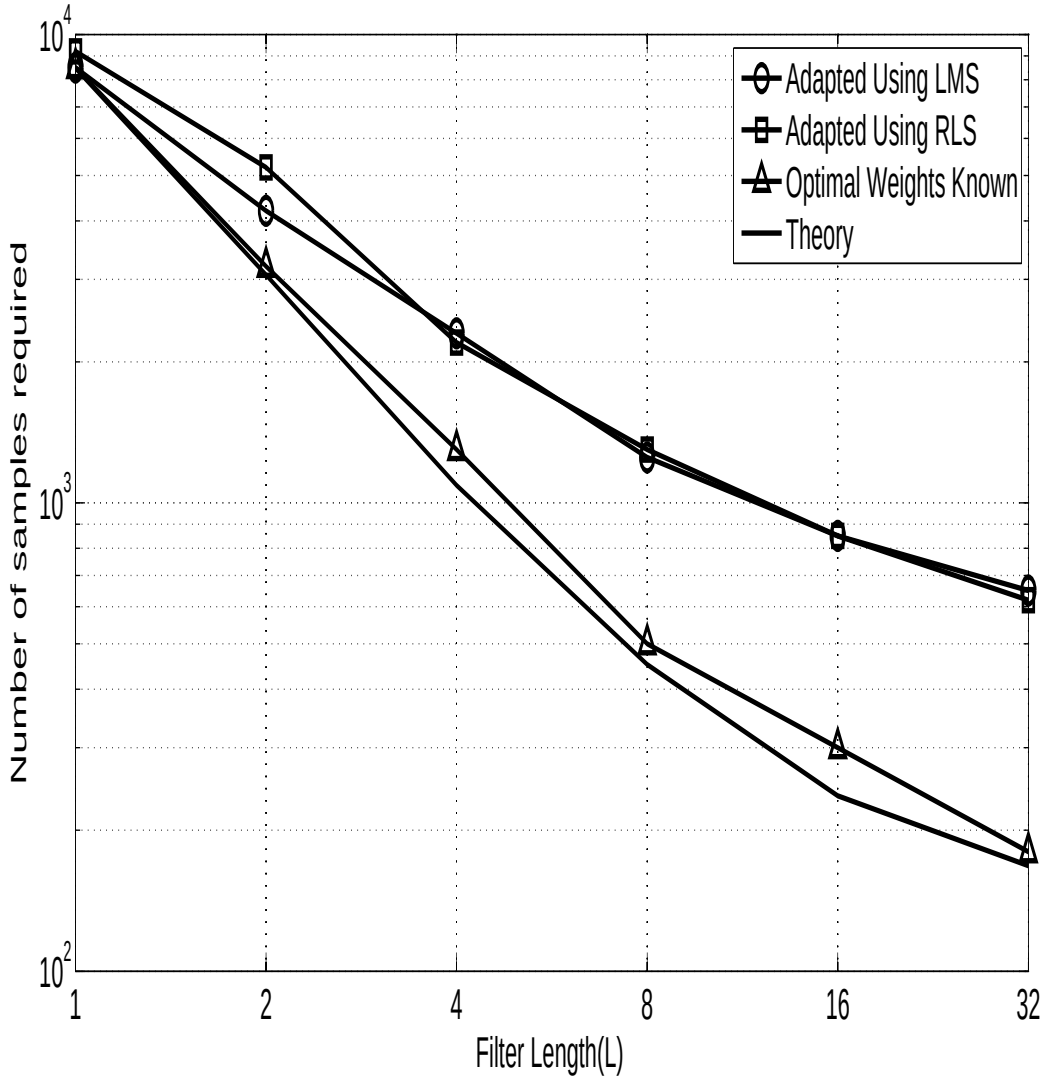

Figure 4.7: Number of samples required to achieve a 90% detection rate in an energy detector based spectrum sensor

Similarly, the finite-time conjugate cyclic autocorrelation function at cyclic frequency η and lag τ may be defined as

$$\hat{R}^{\eta}_{yy^*}[N,\tau] = \frac{1}{N-\tau}\sum_{n=\tau}^{N-1} y[n]y[n-\tau]e^{-j2\pi\eta n} \tag{4.49}$$

Depending on the cyclostationary properties of the signal, either of these may be used as a test statistic. In this section, only the cyclic autocorrelation function is considered. Similar steps may be followed to determine the behavior of the conjugate cyclic autocorrelation function as a test statistic

Using the definition of $y[n]$, (4.48) may also be written as

$$\hat{R}^{\eta}_{yy}[\tau] = \frac{1}{N-\tau}\sum_{n=\tau}^{N-1} \mathbf{w}^H[N]\mathbf{u}[n]\mathbf{u}^H[n-\tau]\mathbf{w}[N]e^{-j2\pi\eta n} \tag{4.50}$$

Again, this may be assumed to have a Gaussian pdf under both the hypotheses. The characteristics of this distribution may be obtained in a manner similar to that of the energy detector. Taking the expectation of (4.48) and considering the independence of the weight ($\mathbf{w}[N]$) and the regression ($\mathbf{u}[n]$) vectors, we have

$$E\left[\hat{R}^{\eta}_{yy}[N,\tau]\right] = \frac{1}{N-\tau}\sum_{n=\tau}^{N-1} E\left[\mathbf{w}^H[N]E\left[\mathbf{u}[n]\mathbf{u}^H[n-\tau]e^{-j2\pi\eta n}\right]\mathbf{w}[N]\right] \tag{4.51}$$

It may be shown via simple manipulation that

$$E[x^{\alpha_p}[n]x^{\alpha_q *}[n-\tau]e^{-j2\pi\eta n}] = R^{\alpha_p-\alpha_q+\eta}_{xx}[n-\tau] \tag{4.52}$$

Note that $x^{\alpha *}[n]$ is different from $x^{*\alpha}[n]$, where the former is the conjugate of a frequency shifted version of $x[n]$, while the latter is the conjugate frequency shifted version of $x[n]$ such that $x^{\alpha *}[n] = x^{*-\alpha}[n]$. Consequently, the cyclic autocorrelation matrix at cyclic frequency $\alpha_p - \alpha_q + \eta$ and lag τ may be written as

$$\mathbf{R}^{\alpha_p-\alpha_q+\eta}_{xx}[\tau] = E[\mathbf{x}^{\alpha_p}[n]\mathbf{x}^{\alpha_q H}[n-\tau]e^{-j2\pi\eta n}] \tag{4.53}$$

In view of this, the block cyclic correlation matrix of the regression vector $\mathbb{R}^{\eta}_{uu}[\tau]$ at cyclic frequency η and lag τ may be defined as

$$\begin{aligned}\mathbb{R}^{\eta}_{uu}[\tau] &= E\left[\mathbf{u}[n]\mathbf{u}^H[n-\tau]e^{-j2\pi\eta n}\right] \\ &= \begin{bmatrix} \mathbf{R}^{\eta}_{xx}[\tau] & \dots & \mathbf{R}^{\alpha_1+\beta_{M_2}+\eta}_{xx}[\tau] \\ \vdots & \ddots & \vdots \\ \mathbf{R}^{-\beta_{M_2}-\alpha_1+\eta}_{ss}[\tau] & \dots & \mathbf{R}^{\eta}_{ss}[\tau] \end{bmatrix}\end{aligned} \tag{4.54}$$

Therefore,

$$E\left[\hat{R}_{yy}^{\eta}[\tau]\right] = E\left[\mathbf{w}^H[N]\mathbb{R}_{uu}^{\eta}[\tau]\mathbf{w}[N]\right] \tag{4.55}$$

If there exist $\alpha_p, \alpha_q \in \{\mathcal{A} \cup -\mathcal{B}\}$, such that $\eta = \alpha_p - \alpha_q$, then $\mathbf{R}_{xx}^{\eta+\alpha_p-\alpha_q}[\tau] = \mathbf{R}_{xx}[\tau]$. In this case for, $\tau < L$, the matrix $\mathbf{R}_{xx}[\tau]$ will contain the term $R_{xx}[0]$. This will result in the mean of the test statistic being dependent on the ambient noise variance which in turn will deteriorate the detector performance when the value of the ambient noise variance is uncertain. Hence, the choice of $\mathcal{A}, \mathcal{B}$ and η becomes important. Now, in the absence of the primary signal and due to the whiteness and stationarity of the noise, $\mathbb{R}_{\nu\nu}^{\eta}[\tau] = \mathbb{O}$, with $\mathbb{O}$ being a null matrix having the same dimensions as $\mathbb{R}_{\nu\nu}^{\eta}[\tau]$. Therefore,

$$E\left[\hat{R}_{yy}^{\eta}[N,\tau]|\mathcal{H}_0\right] = 0 \tag{4.56}$$

whereas, under the alternate hypothesis $\mathcal{H}_1$, this becomes

$$E\left[\hat{R}_{yy}^{\eta}[N,\tau]|\mathcal{H}_1\right] = \mathbf{w}_o^H\mathbb{R}_{ss}^{\eta}\mathbf{w}_o + tr(\mathbb{R}_{ss}^{\eta}[\tau]\mathbf{Q}[N]) \tag{4.57}$$

where $\mathbf{Q}[N]$ is as defined in (4.18). It may be noted that the matrix $\mathbb{R}_{ss}^{\eta}[\tau]$ is not Hermitian and hence the term $\mathbf{w}_o^H\mathbb{R}_{ss}^{\eta}[\tau]\mathbf{w}_o$ will in general be complex-valued and may be written in the form

$$\mathbf{w}_o^H\mathbb{R}_{ss}^{\eta}[\tau]\mathbf{w}_o = \xi e^{j\phi} \tag{4.58}$$

similar to the finite-time energy. The variance of $\hat{R}_{yy}^{\eta}[N,\tau]$, under the two hypotheses, may be expressed as

$$\frac{\sigma_\nu^4}{N-\tau} \leq var\left(\hat{R}_{yy}^{\eta}[N,\tau]|\mathcal{H}_0\right) = \frac{\sigma_{C_0}^2}{N-\tau} \leq ML\frac{\sigma_\nu^4}{N-\tau} \tag{4.59}$$

$$var\left(\hat{R}_{yy}^{\eta}[N,\tau]|\mathcal{H}_1\right) = \frac{\sigma_{C_1}^2}{N-\tau} \leq \frac{\sigma_\nu^4}{N-\tau}ML(1+2\gamma_i ML) \tag{4.60}$$

The distribution of $\hat{R}_{yy}^{\eta}[N,\tau]$ under the two hypotheses may therefore, be written as

$$\hat{R}_{yy}^{\eta}[N,\tau] \sim \begin{cases} \mathcal{N}_c\left(0, \frac{\sigma_{C_0}^2}{N-\tau}\right) & \mathcal{H}_0 \\ \mathcal{N}_c\left(\xi e^{j\phi}, \frac{\sigma_{C_1}^2}{N-\tau}\right) & \mathcal{H}_1 \end{cases} \tag{4.61}$$

The phase ϕ in the term $\xi e^{j\phi}$ depends on the correlation structure of the primary user signal. If ϕ is known, then $\Re\{\hat{R}_{yy}^{\eta}[N,\tau]e^{-j\phi}\}$ will have a real positive mean which may be used as a test statistic for the detection of a primary signal, as follows

$$\Re\{\hat{R}_{yy}^{\eta}[N,\tau]e^{-j\phi}\} \sim \begin{cases} \mathcal{N}\left(0, \frac{\sigma_{C_0}^2}{2(N-\tau)}\right) & \mathcal{H}_0 \\ \mathcal{N}\left(\xi, \frac{\sigma_{C_1}^2}{2(N-\tau)}\right) & \mathcal{H}_1 \end{cases} \tag{4.62}$$

For a detection threshold λ, the probabilities of detection and false alarm may, respectively, be expressed as

$$P_d = Q\left(\frac{\sqrt{2(N-\tau)}(\lambda-\xi)}{\sigma_{C_1}}\right) \tag{4.63}$$

$$P_{fa} = Q\left(\frac{\sqrt{2(N-\tau)}\lambda}{\sigma_{C_0}}\right) \tag{4.64}$$

The threshold for a constant false alarm rate therefore is derived as

$$\lambda = \frac{\sigma_{C_0} Q^{-1}(P_{fa})}{\sqrt{2(N-\tau)}} \tag{4.65}$$

Based on this, the number of samples required to obtain a desired detection rate is obtained as

$$N = \tau + \frac{1}{2}\left(\frac{\sigma_{C_0} Q^{-1}(P_{fa}) - \sigma_{C_1} Q^{-1}(P_d)}{\xi}\right)^2 \tag{4.66}$$

However, in the absence of the knowledge of ϕ, the absolute value of the finite-time cyclic autocorrelation function may be used as the test statistic which will be distributed as

$$|\hat{R}^{\eta}_{yy}[N,\tau]| \sim \begin{cases} Rice\left(0, \frac{\sigma_{C_0}}{\sqrt{N-\tau}}\right) & \mathcal{H}_0 \\ Rice\left(\xi, \frac{\sigma_{C_1}}{\sqrt{N-\tau}}\right) & \mathcal{H}_1 \end{cases} \tag{4.67}$$

The false alarm rate for a given detection threshold λ for this test statistic will be

$$P_{fa} = e^{-\frac{(N-\tau)\lambda^2}{\sigma^2_{C_0}}} \tag{4.68}$$

This may be used to determine the threshold to achieve a given false alarm rate. However, a closed form expression is not available for its cumulative distribution function. The performance of this detector must therefore be determined via simulation. The robustness of this detector to uncertainty in noise variance is shown in the next section.

4.3.1 Evaluation of Variances

Similar to the treatment in case of energy detector discussed in the previous section , the primary user signal here is considered to be BPSK modulated with a data rate (f_b) 10 kilobits per second, a carrier frequency (f_c) 100 kHz, and sampled at 1 MHz. The FRESH filter structure is also assumed to be similar to the one used for energy detector. Here, the conjugate cyclic autocorrelation function at twice the carrier frequency is used for detection. It is assumed that the phase of the resultant cyclic autocorrelation function is known. Following this, the test statistic $\Re\{\hat{R}^{\eta}_{yy^*}e^{j\phi}\}$ is calculated under both the hypotheses, for different filter lengths and different noise variances. Similar to the energy detector, 10000 independent test statistics are generated for each possible case. Using these, the parameters

for the distribution of $\Re\{\hat{R}^{\eta}_{yy^*}e^{j\phi}\}$ are determined via curve fitting. The variance of the test statistics across all the cases is again found to be inversely proportional to the number of samples used.

It is again found that the variance under the null hypothesis needs to be determined empirically, whereas that under the alternate hypothesis may be approximated by the upper bound. It is observed from the shape of the plot that both the approximations of the test statistic variance developed for the energy detector will be applicable here. Considering the logarithmic approximation, the constants c_1 and c_2 are found out to be $c_1 = 0.1754$ and $c_2 = 0.901$.

Taking the functional form of the variance of the cyclostationarity detector similar to series summation described in the previous section, the factor c_3 is found out to be approximately 1.55.

4.3.2 Performance Evaluation

The experimental setup is similar to the one used in case of energy detector. Here, the variances of the test statistics under the two hypotheses may be determined as described in the previous section. Following this, equation (4.64) and is used to determine the detection threshold for a false alarm rate of 1% and (4.63) is used to determine probability of detection. In simulation-based experiments, 1000 independent trials, with the primary signal absent, are used to determine the detection thresholds and 2000 independent trials being used for the determination of the detection performance. The number of samples to evaluate the detection performance is again fixed at 500.

Figure 4.9 compares the predicted detection performance obtained in (4.63) with the simulation results for different filter lengths at different SNRs when the phase of the primary user cyclic autocorrelation function and the optimal filter weights are known. It is again observed that the simulation results closely follow the predicted behaviour. Moreover, in this case as well, a gain of more than 8 dB is achieved by increasing the FRESH filter length from 1 to 16.

The effect of the knowledge of the phase of the cyclic autocorrelation function of the primary signal component in the filtered signal is studied in Figure 4.10. The figure plots the performances under different cases for an 8-tap FRESH filter-based spectrum sensor. It is seen that with the optimal weights being known, the performance of the spectrum sensor is marginally improved due to the knowledge of the phase of the cyclic autocorrelation function. However, there is no visible effect of this knowledge when adapted weights are used.

The number of samples required to achieve a 90% detection rate for different cases is plotted in Figure 4.11. It is observed that, similar to an energy detector, the number of samples the spectrum sensor reduces by approximately two orders of magnitude as the filter

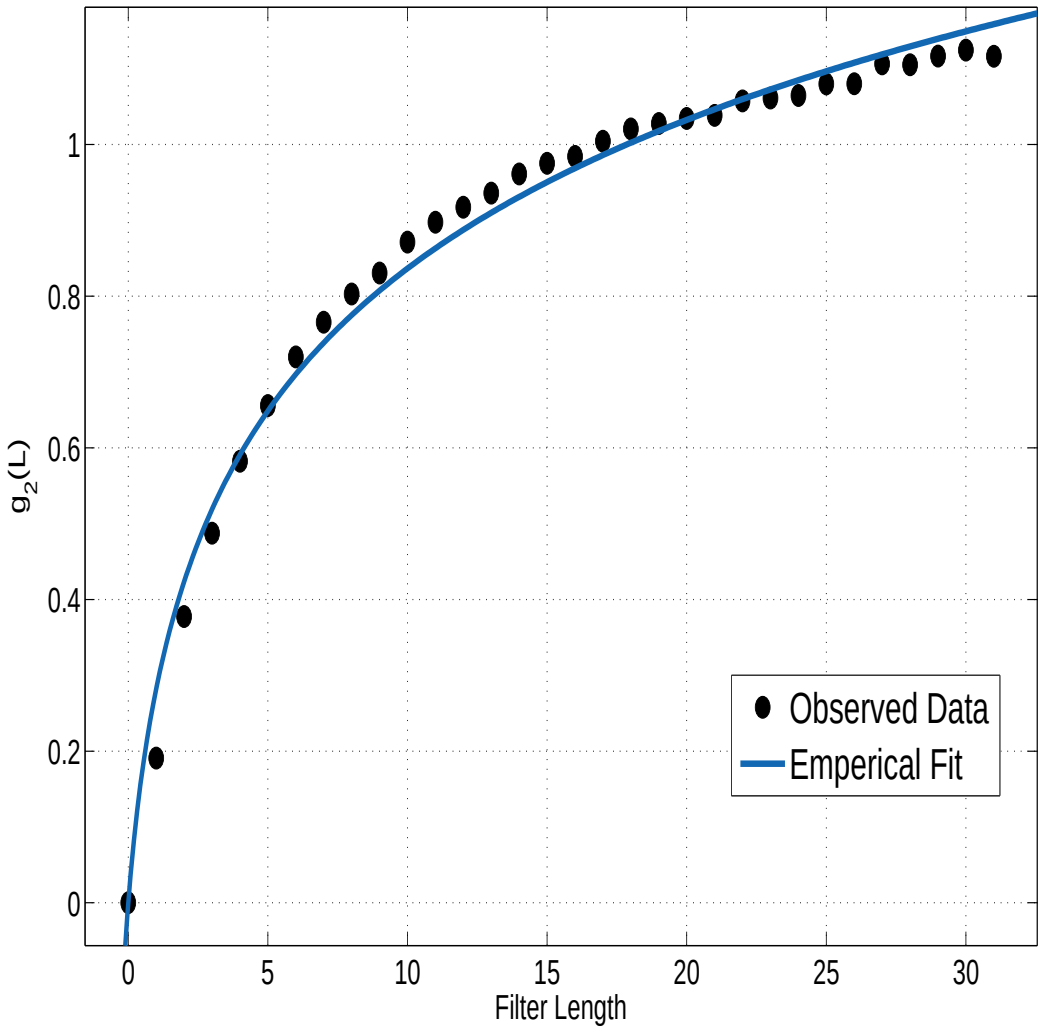

Figure 4.8: Empirical determination of the standard deviation of the test statistic for the cyclostationary detector in the absence of a primary signal for different filter lengths

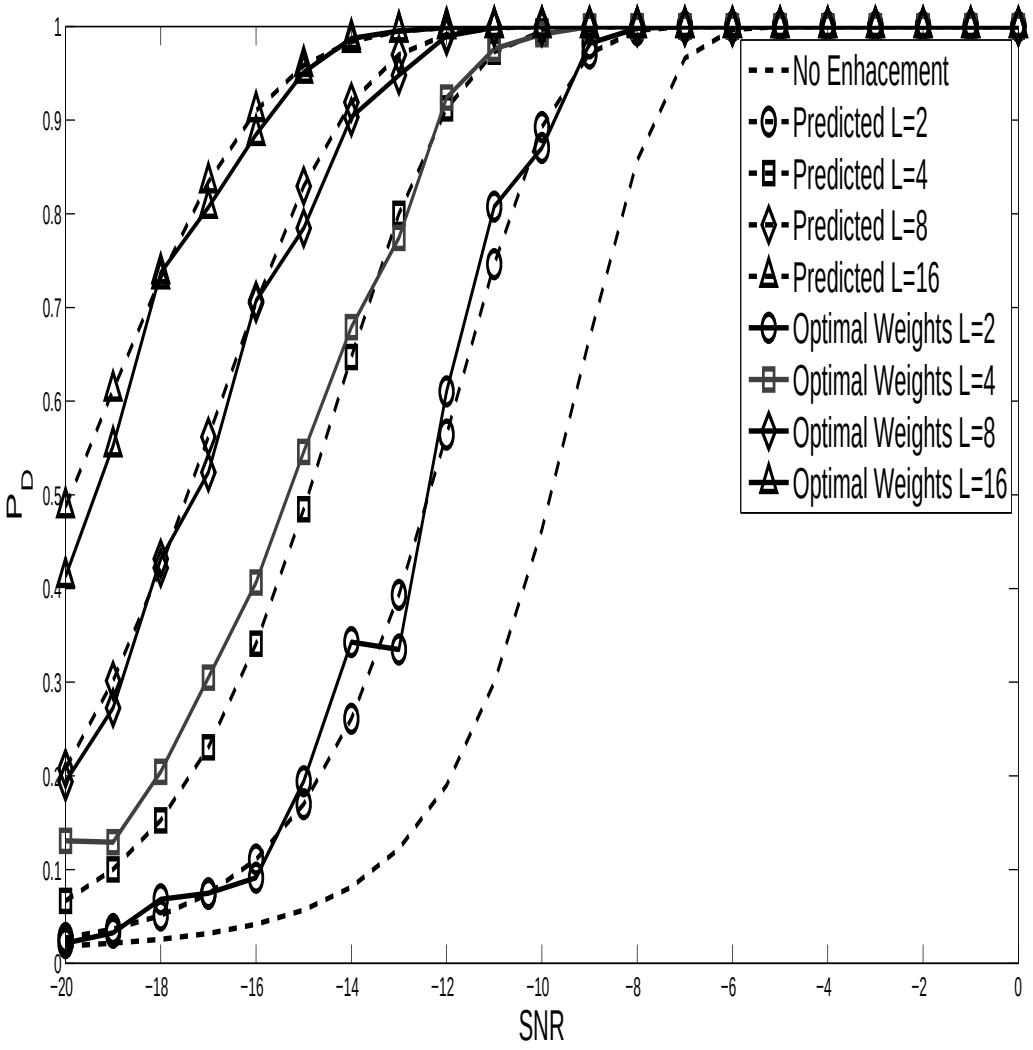

Figure 4.9: Comparison of predicted and actual performances of a FRESH filter based cyclostationary detector for different filter lengths

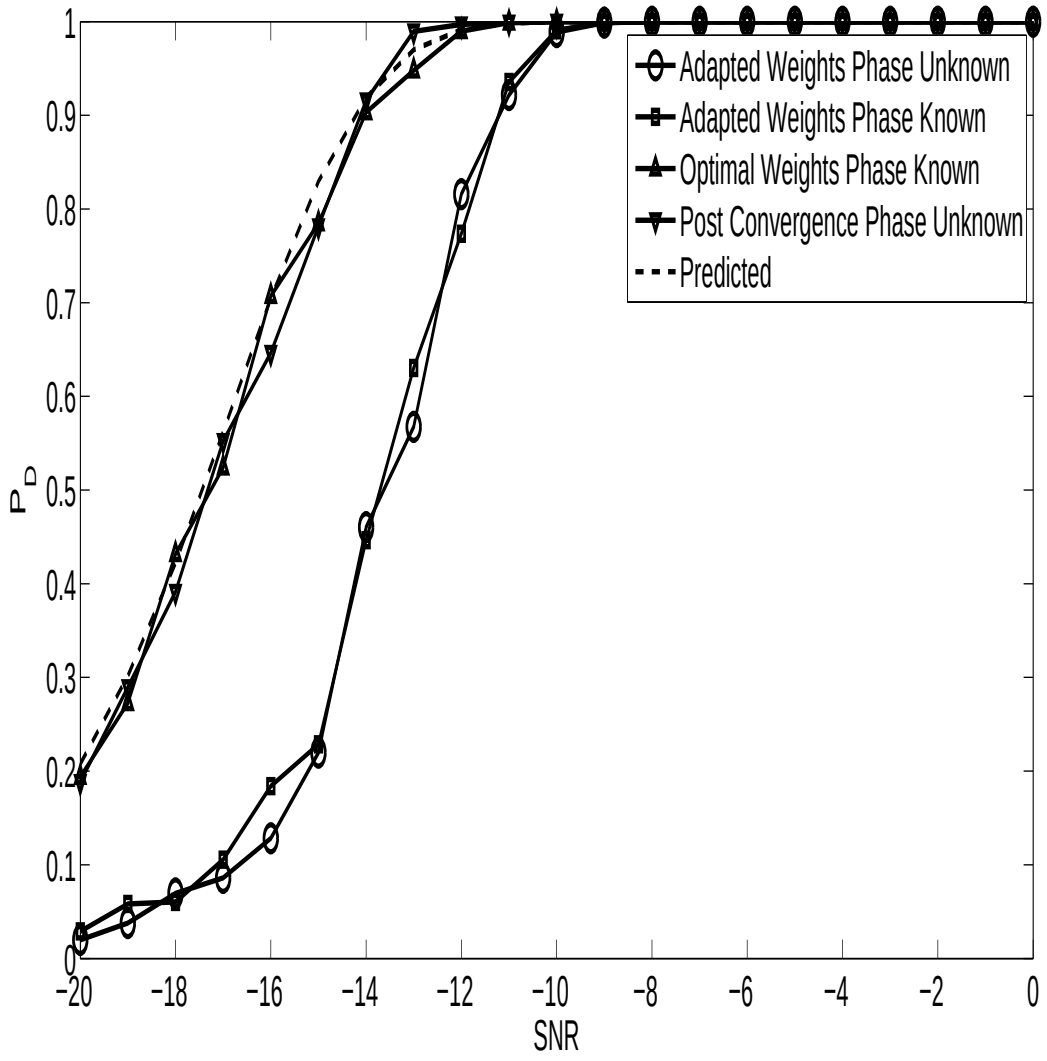

Figure 4.10: Comparison of performances of an 8 tap FRESH filter based cyclostationary detector under different cases

length is increased from 1 to 32, when the knowledge of optimal FRESH filter weights is available at. On the other hand, if these weights are adapted, then the number of samples required for a FRESH filter length of 32 is less than one-tenth of those required without any enhancement.

4.4 Performance in the Presence of Impairments

4.4.1 Noise Uncertainty

It may be noted that the statistical properties of both the test statistics discussed earlier depend on the ambient noise variance and the values of these parameters become uncertain when there is some uncertainty in the noise variance. This uncertainty in parameters will, therefore, have a direct impact on the detection performance of the spectrum sensor. Consider now that the known noise variance σ_ν^2 is an estimate of the true noise variance σ_0^2. If the noise component of the average input SNR has an uncertainty of ρ_{dB} dB then the noise variance estimate may be said to have an uncertainty by a factor $\rho > 1$. The noise variance estimate (σ_ν^2) may be thought of as uniformly distributed in the interval $\left[\frac{1}{\rho}\sigma_0^2, \rho\sigma_0^2\right]$ [122], where σ_0^2 is the true ambient noise variance.

Considering the worst case scenario, i.e. $\sigma_\nu^2 = \rho\sigma_0^2$ in the absence of a primary signal and $\sigma_\nu^2 = \frac{1}{\rho}\sigma_0^2$ when it is present the statistics of an energy detector may be written as

$$T_E \sim \begin{cases} \mathcal{N}\left(\rho\sigma_0^2, \frac{\rho^2\sigma_0^4(1+g_0(M,L))^2}{N}\right) & \mathcal{H}_0 \\ \mathcal{N}\left(\frac{\sigma_0^2}{\rho} + \mathbf{w}_o^H\mathbb{R}_{ss}\mathbf{w}_o, \frac{\sigma_0^4 ML(1+2\gamma_i ML)}{\rho^2 N}\right) & \mathcal{H}_1 \end{cases} \tag{4.69}$$

From these, the number of samples required to achieve a given detection performance may be obtained as

$$N = \left(\frac{\left(\frac{(ML(1+2\gamma_i ML))^{1/2}}{\rho}Q^{-1}(P_D) - Q^{-1}(P_{fa})(\rho(1+g_0(M,L)))\right)}{\left(\rho - \frac{1}{\rho} - \frac{\mathbf{w}_o^H\mathbb{R}_{ss}\mathbf{w}_o}{\sigma_0^2}\right)}\right)^2 \tag{4.70}$$

The number of samples N tends to infinity as the term $\frac{\mathbf{w}_o^H\mathbb{R}_{ss}\mathbf{w}_o}{\sigma_0^2}$ tends to $\left(\rho - \frac{1}{\rho}\right)$. Therefore, the phenomenon of SNR walls, for energy detector as described in [122], also exists in this case. As reported in [122], the phenomenon of SNR walls occurs in a standard energy detector if $\gamma_i \to \left(\rho - \frac{1}{\rho}\right)$. However, if the FRESH filter gain, as defined in Section 4.2, is greater than unity, then the FRESH filter-based spectrum sensor will work for input SNRs smaller than $\left(\rho - \frac{1}{\rho}\right)$. In other words, it may be stated that the use of FRESH filters lowers the SNR wall.

Similarly, the statistics of a cyclostationary detector with the phase ϕ known, may be

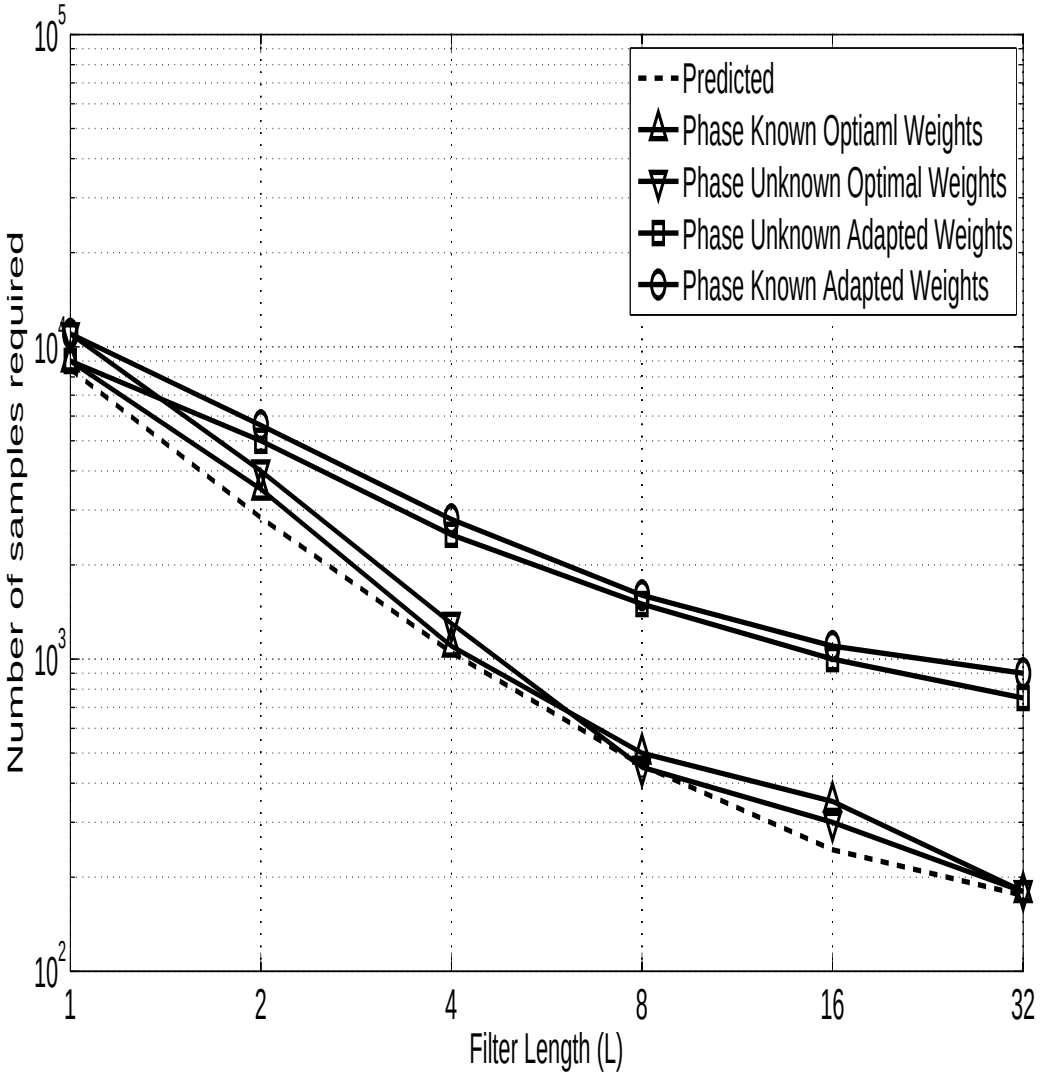

Figure 4.11: Number of samples required to achieve a 90% detection rate in a cyclostationary detector based spectrum sensor

written as

$$\Re\{\hat{R}_{yy}^{\eta}[N,\tau]e^{-j\phi}\} \sim \begin{cases} \mathcal{N}\left(0, \frac{\rho^2\sigma_0^4(1+g_2(M,L))^2}{2(N-\tau)}\right) & \mathcal{H}_0 \\ \mathcal{N}\left(\mathbf{w}_o^H\mathbb{R}_{ss}^{\alpha}[\tau]\mathbf{w}_o, \frac{\sigma_0^4 ML(1+2\gamma_i ML)}{\rho^2(N-\tau)}\right) & \mathcal{H}_1 \end{cases} \tag{4.71}$$

The number of samples required to achieve a desired detection performance, hence, takes the form

$$N = \tau + \frac{1}{2}\left(\frac{\sigma_0^2(1+g_2(M,L)) - \frac{\sigma_0^2(ML(1+2\gamma_i ML))^{1/2}}{\rho}Q^{-1}(P_D)}{\xi}\right)^2 \tag{4.72}$$

It may be seen that, in this case also the number of samples required to achieve a desired performance will increase but will not tend to infinity as in the case of an energy detector.

The performance comparison of a cyclostationary detector and an energy detector for different number of samples and filter lengths under noise uncertainty is shown in Figure 4.13. It may be observed that in the presence of noise uncertainty, an increase in the number of samples improves the performance of a cyclostationary detector, whereas the performance of the energy detector is largely unaffected. However, an increase in the filter length still improves the detection performance of the energy detector.

4.4.2 Simulation Based Performance Evaluation

The performance of FRESH filter-based spectrum sensors in the presence of noise uncertainty is presented in Figs. 4.12 and 4.13. In Figure 4.12, the solid lines plot the number of samples required to achieve a detection rate of 90% under ±1 dB noise uncertainty for different filter lengths. The dotted lines depict the values of input SNRs, as predicted by (4.70), at which an SNR wall exists for the given filter lengths. It is observed that increasing the FRESH filter length from 1 to 32 lowers the SNR wall by approximately 14dB, thereby making the energy detector more robust to noise uncertainty.

4.5 Conclusion

The performance enhancement achievable in spectrum sensors by the use of FRESH filtering is studied in this chapter. It is shown quasi analytically that the use of a FRESH filter improves the detection performance of both the energy detector and the cyclostationary detector. It is also shown that the increase in filter length, in general, improves the detection performance of the spectrum sensor. It has been shown that in the presence of the knowledge of the primary user correlation structure, the number of samples required to achieve a given detection performance may be reduced by around 99%. It is also shown that if the exact correlation structure is not known in practice, then the required number of samples may still be reduced by one order of magnitude. This results in smaller sensing

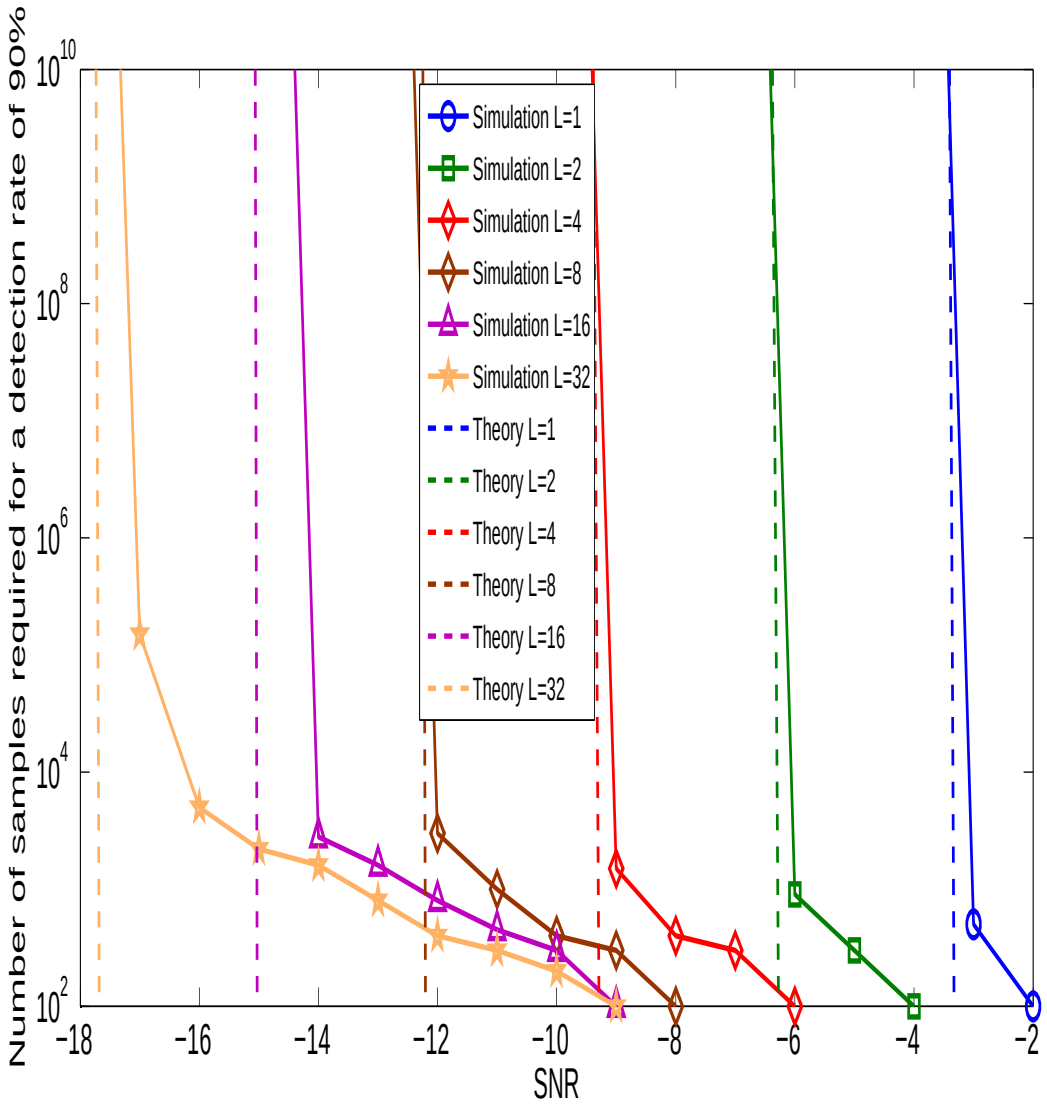

Figure 4.12: Number of samples required to achieve a 90% detection rate in an energy detector under noise uncertainity

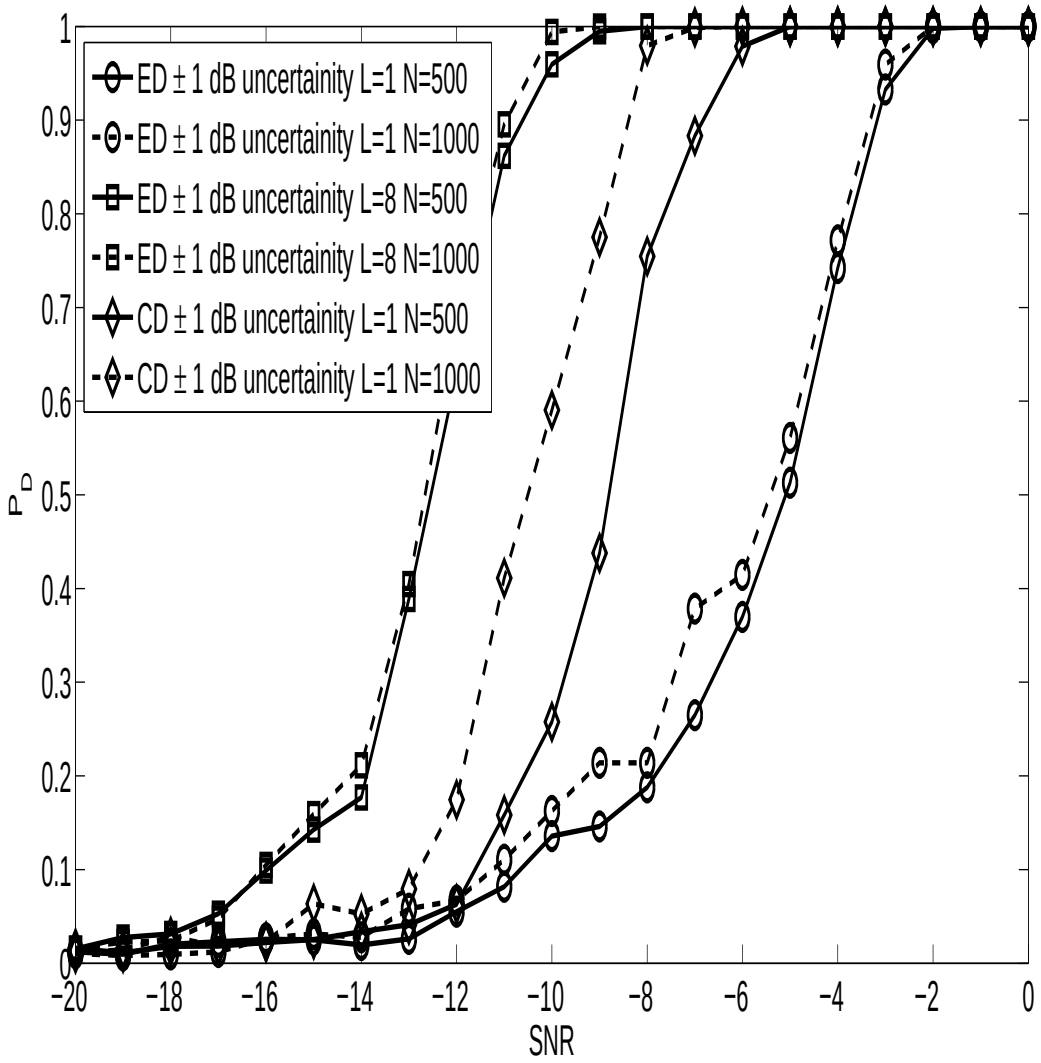

Figure 4.13: Performance of the energy detector and the cyclostationary detector in the presence of ±1 dB noise uncertainty

times thereby increasing the secondary user throughput. Here, empirical and simulation results are derived only for BPSK signals; this can be extended to other modulation classes as well.

Apart from this, the performance of the FRESH filter-based spectrum sensor under impairments has been studied. It has been found that the use of FRESH filtering may lower the SNR wall arising due to noise uncertainty by as much as 14 dB.

Chapter 5

Collaborative FRESH filter based Spectrum Sensing

It was shown in the previous chapters that enhancing the received signal using FRESH filters, prior to the detection step, results in improved performance for both the energy detector as well the cyclostationary detector in single as well as multi-antenna systems. This was shown for single-user systems in AWGN channels. However, as discussed earlier, single-user systems are susceptible to performance degradation due to fading, shadowing and the hidden terminal problem [9]. Accordingly, it has been proposed earlier that multiple secondary users should collaborate to counter these effects [10, 32, 53]. Based on this idea, it is proposed in this chapter [1] to extend the framework of FRESH filter-based spectrum sensing from a single-user to multiple collaborating users. The FRESH filter or the Space-Time FRESH filter may be used here to boost the performance of each individual user, hence improving the overall detection performance of the system.

It is assumed in this chapter that all the secondary users collaborate to sense the presence of the same primary user signal. Therefore, the optimal FRESH filter weights for different users must either be same or be correlated. Recent works in statistical signal processing [1,17,107] show that the convergence rate of multiple adaptive filters estimating the same set of weights may be improved by the use of joint adaptation. The joint adaptation techniques may therefore be employed to improve the performance of collaborative FRESH filter-based spectrum sensors as well.

The contribution of this chapter is twofold. First, FRESH filter-based spectrum sensing is extended to a collaborative system and the effect of increase in filter length is studied. Here, each user is assumed to adapt its filter weights individually. Following this, algorithms for joint adaptation of filter weights at different nodes are considered and it is proposed to use these to jointly adapt the filter weights at different nodes. Using simulation techniques, it is demonstrated that joint adaptation may lead to a better sensing performance as

[1] The work related to centralized cooperation has been published in the proceedings of the 2015 National Conference on Communications(NCC-2015) under the title " Cooperative Spectrum Sensing for Cognitive Radios using Jointly Adaptive FRESH Filters"

compared to localized adaptation.

The need for collaborative spectrum sensing along with the motivation to use FRESH filters in such a setting is given in Section 5.1. The signal model under the flat fading and the dispersive fading cases is detailed in Section 5.2. The spectrum sensing models for the cooperative, the distributed and the general multi-antenna multi-user cases are presented in Section 5.3. The FRESH filter adaptation algorithms for the flat fading channels are developed in Section 5.4 and those for the dispersive fading channels are developed in Section 5.5. The simulation results are presented in Section 5.6. Finally, the conclusions are drawn in Section 5.7.

5.1 Background and Motivation

Ghasemi and Sousa in [53] showed that for log-normal shadowing the performance of a single energy detector deteriorates considerably. It has been argued that the situation worsens if the channel between the cognitive terminal and the primary transmitter is going through a deep fade during the time of sensing. In this case, it is virtually impossible for the cognitive user to detect the presence of a primary user. As a solution to this problem, the authors propose cooperation among different secondary users.

It is proposed in [53] to use multiple sensing (energy detecting) nodes reporting to a fusion center to decide on the presence of a primary user. The nodes sense the spectrum locally and send their individual decisions to the fusion center over a control channel. The fusion center after receiving these decisions declares a primary signal to be present if even a single sensing node reports so.

This is the simplest method for cooperative spectrum sensing and other methods may be developed by varying one or more of its design parameters. The parameters for collaboration among multiple sensing users, in general, may be listed as follows.

- **Test Statistics at individual secondary users :** The scheme discussed earlier uses the energy detector at different nodes to sense the spectrum. Due to its simplicity, the energy detector has been the most popular choice for cooperative spectrum sensing [55]. However, other test statistics have also been used with encouraging results [82, 114].

- **Information shared by the cooperating users :** The example discussed previously uses transmission of the binary decisions taken by the sensing nodes. It is reported in [83] that significant performance improvement results if two-bit quantized statistics are transmitted instead of one-bit decisions. It has been shown that higher performance enhancement may be achieved by increasing the number of quantizations bits. These systems perform still better if the collaborating users transmit their test

statistics. It may be noted that this improvement in the system performance comes at the cost of control channel bandwidth.

The effect of reporting channel errors on soft and hard combination schemes is studied in [26]. In this pape,r a cooperative detection scheme with a fusion center is considered. It is assumed that the one-bit hard decisions as well as quantized soft decisions are sent to the fusion center over a channel that may cause reporting errors. The effects of an improper reporting channel are interpreted in terms of its bit error probability (BEP). A combination rule for soft decisions under erroneous channels is then derived where the K out of N rule is used for hard decisions. It is shown that soft-decision-based cooperation always outperforms hard-decision-based cooperation. It is further shown that if the BEP of the reporting channel is more than a certain fixed limit, then the required detection and false alarm rates can never be achieved. This effect is similar to the effect of noise uncertainty and is termed as a BEP wall. It is then shown that soft-decision schemes are more robust to BEP walls as compared to hard-decision-based schemes.

- **Combination Rules** While the aforementioned simple OR rule-based detection improves the protection to the primary user, it also increases the probability of false alarm resulting in reduced throughput. Consequently other combination rules such as AND and K out of N may as well be applied [10]. For nodes transmitting soft decisions techniques such as equal gain combining and maximal ratio combining may be used for decision fusion.

- **Existence of a fusion center** The example discussed previously involved the use of a fusion center to globally decide the presence or absence of a primary signal. This is susceptible to node failure and also requires a high communication overhead. It is also possible that sensing nodes far from the fusion center may not be synchronized to stay silent during the sensing periods. Therefore, it is important to develop distributed cooperation schemes for spectrum sensing. Another method here might be to use a hierarchical structure in the form of clusters [9] so that the nodes within each cluster report to the respective cluster heads which in turn report to the fusion center.

  Peer-to-peer cooperation for spectrum sensing was first considered in [42] using distributed detection theory. The classification framework is based on time-frequency analysis and the short-time power spectrum is used as a feature. Here multiple devices cooperate to sense the spectrum and classify the overlapping air interfaces. The proposed algorithm employed to distinguish between Bluetooth and 802.11 WLAN serves as an example for the same.

Any combination of these parameters may be used to design a collaboration scheme. However, it must be noted that any collaborative sensing scheme must take care of the following requirements

Firstly, similar to all dynamic access systems, all cooperative sensing schemes must ensure minimal interference to the primary user transmission while maximizing the throughput of the secondary users. Secondly, the power and computational constraints of sensing nodes must be considered and it should be seen that the sensing time is minimized so as to maximize the overall throughput of the system.Thirdly, it must be noted that the cognitive users communicate with each other over a control channel. The characteristics of the control channel i.e. the bandwidth and BER of this should also be considered while designing a cooperative sensing scheme.

It should be noted that while the problem of spectrum sensing is a detection problem, the problem of FRESH filtering is essentially an optimal weight estimation problem. During the past few years, similar to distributed detection approaches discussed above and also in the first chapter, much activity has been reported in distributed estimation techniques as well. Therefore, distributed adaptation algorithms may be used to improve the convergence performance of the FRESH filters in the collaborating users. A brief review of distributed adaptation techniques is presented in the sequel.

The problem of distributed linear estimation is introduced in [77]. In this paper, it is assumed that each node is able to derive local estimates and share them with its pre-defined neighbors. The objective here is to arrive at an estimate of the parameters of interest which would have otherwise resulted from each node having information possessed by every other node in the network. For this purpose, a distributed estimation problem is formulated and a distributed version of the LMS algorithm is proposed to solve it.

A cooperative strategy for adaptation is studied in [78]. In the proposed peer-to-peer diffusion adaptation protocol, one-hop neighbors are allowed to communicate with each other for each iteration. The communication involves exchange of the local node estimates. These local estimates are then fused to improve the estimation accuracy. The fusion operation ensures that the estimates at each node are functions of the observations across the entire network. This paper also studies the reliability of different nodes in terms of the data supplied by them.

More variations of the diffusion LMS algorithm are proposed in [17]. These are shown to outperform the previously proposed techniques both analytically as well as via simulations. It is shown that the algorithm discussed in [78] is a special case of the algorithms discussed here. A global formulation of the estimation problem, resulting in the global-LMS algorithm is also proposed here. The performance of the global-LMS algorithm acts as a baseline for assessing the performance of other distributed adaptation algorithms.

The diffusion strategies discussed above are extended to Kalman filtering in [18]. Here, the problems of Kalman filtering, fixed lag smoothing and fixed point smoothing for distributed networks are studied. Different diffusion algorithms are proposed for each of these problems. Here again, each individual node shares its state estimate with its immediate neighbors. The mean and mean-square performance of the resulting algorithm is derived.

As an example, this algorithm is applied to the estimation and tracking of a projectile.

Distributed detection based on estimation techniques is studied in [19]. Here, the adapted weight vector is correlated with the optimal weight vector and the correlation coefficient is used as a test statistic. A sequential version of this test statistic is also proposed. The resulting detection algorithms are inherently adaptive and can track changes in the active hypothesis. This technique allows each node to have its own decision on the presence of a primary user signal. It is important to note that in this case a consensus on the presence of the signal of interest is not reached among the sensing nodes.

In [71], in addition to sharing information with its neighbouring nodes, each node is allowed to filter and process past estimates so as to improve the overall estimation accuracy. The resulting adaptation algorithms consist of three stages viz. adaptation, spatial processing and temporal processing. Each node is provided with a local memory for the purpose of temporal processing. It is shown that temporal processing may be used to counter the effects of noise over communication channels. In [150], the mean-square performance of different diffusion LMS strategies is analyzed. It is shown that diffusion strategies result in a lower excess-mean-square-error in comparison to centralized solutions.

In [107] it is assumed that a subset of nodes, known as bridge nodes, arrives at a consensus regarding the filter weights. It is assumed that each sensor node is connected to at-least one bridge sensor via a single hop communication link. Here, the nodes communicate with each other after each adaptation step and update the connected bridge nodes about the local estimates. The bridge nodes on receiving these estimates arrive at a consensus regarding the weights and start the next adaptation step. It is important to note that while consensus-based techniques try to make the nodes agree on a single value, diffusion adaptation does not require the convergence to a single value. Therefore, while consensus is necessary in deciding on the presence of a primary user, diffusion adaptation techniques may be used to estimate the filter weights at each node [129].

Consequently, in this chapter, we propose to adapt the filter weights at different nodes by using diffusion adaptation while the decision is taken only after the cooperating nodes reach a consensus regarding the presence of a primary user signal.

5.2 The Primary Signal and Channel Models

Consider a primary user signal $s(t)$ exhibiting cyclostationarity at cyclic frequencies $\alpha_1, \alpha_2, \ldots \alpha_{M_1} \in \mathcal{A}$ and conjugate cyclostationarity at $\beta_1, \beta_2, \ldots \beta_{M_2} \in \mathcal{B}$. This signal, due to its spectral coherence [48, 50], may be expressed in the form

$$\begin{aligned} s(t) &= \sum_{\alpha\in\mathcal{A}} \int_0^{V_\alpha} a_\alpha(v) s^\alpha(t-v)dv \\ &\quad + \sum_{\beta\in\mathcal{B}} \int_0^{V_\beta} a_\beta(v) s^{*\beta}(t-v)dv + \zeta(t) \end{aligned} \tag{5.1}$$

where $\zeta(t)$ is the innovation process, $s^{\alpha}(t) = s(t)e^{-j2\pi\alpha t}$ and $s^{*\beta}(t) = s^{*}(t)e^{-j2\pi\beta t}$ are, respectively, the frequency shifted and the conjugate frequency shifted versions of the signal $s(t)$ with $a_{\alpha}(t)$ and $a_{\beta}(t)$ as their respective weighting functions. This signal, after passing through a multipath channel, is sensed by K sensing nodes, each equipped with a single antenna. Consequently, for the signal $x_k(t)$ received at the kth secondary user, the hypothesis test may be written as

$$x_k(t) = \begin{cases} \nu_k(t) & \mathcal{H}_0 \\ \varphi_k(t) * s(t) + \nu_k(t) & \mathcal{H}_1 \end{cases} \tag{5.2}$$

where $\nu_k(t)$ is the additive noise with zero mean and variance σ_{ν}^2 at the kth sensing node and $\varphi_k(t)$ is the impulse response of the channel between the primary user and the kth secondary user. It may be assumed that the sensing nodes are placed sufficiently apart so that there exists no correlation between the impulse responses of different channels. If the kth sensing node samples the channel at a frequency F_s, then the following two cases may arise.

Case 1 : The delay spread, of all the channels is smaller than the inter-sample interval $T_s = \frac{1}{F_s}$. In this case, the discrete-time equivalent channel will be memoryless and the received signal sample under the alternate hypothesis will take the form

$$x_k[n] = \varphi_k s[n] + \nu_k[n] \tag{5.3}$$

Substituting (5.1) in (5.3), we obtain

$$\begin{aligned} x_k[n] \;=\; & \varphi_k \Big(\textstyle\sum_{\alpha\in\mathcal{A}} \sum_{l=0}^{P_{\alpha}-1} a_{\alpha}[l] s^{\alpha}[n-l] \\ & + \textstyle\sum_{\beta\in\mathcal{B}} \sum_{l=0}^{P_{\beta}-1} a_{\beta}[l] s^{*\beta}[n-l] + \zeta[n] \Big) + \nu_k[n] \end{aligned} \tag{5.4}$$

where the noise $\nu_k[n]$ may be assumed to be wide sense stationary. It follows that

$$\begin{aligned} x_k[n] \;=\; & \textstyle\sum_{\alpha\in\mathcal{A}} \sum_{l=0}^{P_{\alpha}-1} a_{\alpha}[l] x_k^{\alpha}[n-l] \\ & + \textstyle\sum_{\beta\in\mathcal{B}} \sum_{l=0}^{P_{\beta}-1} a_{\beta}[l] x_k^{*\beta}[n-l] + \zeta[n] + \nu_k[n] \end{aligned} \tag{5.5}$$

The regression coefficients $a_{\alpha}[n]$ are same for all the sensing users. The signals received at different antennas may, therefore, be viewed as different realizations of the same spectrally correlated process. The optimal weights for these may hence be estimated at the same time. This is discussed in more detail in the next section.

Case 2 : The delay spread of some or all of the channels is greater than the inter-sample interval. In this case, the received samples of the signal under the alternate hypothesis will take the form

$$x_k[n] = \sum_{\tau=0}^{T-1} \varphi_k[\tau] s[n-\tau] + \nu_k[n] \tag{5.6}$$

where $\varphi_k[\tau]$ is the discrete-time equivalent of the channel between the primary user and the kth spectrum sensor, and T is the delay spread of the discrete-time equivalent of the channel. Consequently,

$$\begin{aligned} x_k[n] &= \sum_{\tau=0}^{T} \varphi_k[\tau] \Big(\sum_{\alpha\in\mathcal{A}} \sum_{l=0}^{P_\alpha-1} a_\alpha[l] s^\alpha[n-l] \\ &\quad + \sum_{\beta\in\mathcal{B}} \sum_{l=0}^{P_\beta-1} a_\beta[l] s^{*\beta}[n] + \zeta[n] \Big) + \nu_k[n] \\ &= \sum_{\alpha\in\mathcal{A}} \sum_{l=0}^{P_\alpha-1} b_{\alpha,k}[l] x^\alpha[n-l] \\ &\quad + \sum_{\beta\in\mathcal{B}} \sum_{l=0}^{P_\beta-1} b_{\beta,k}[l] x^{*\beta}[n] + \xi_k[n] + \nu_k[n] \end{aligned} \tag{5.7}$$

where $\xi_k[n]$ is the innovation component of the signal sampled at the kth spectrum sensor. Therefore, the optimal weights of the FRESH filters at different sensing nodes will be different. However, the signals received at different nodes will still be correlated and may be estimated jointly.

5.3 Spectrum Sensing Models

This chapter considers three different setups, viz. the Centralized model, the Distributed model and the Hierarchical model, as illustrated in Figure 5.1. The Centralized detection model assumes the existence of a fusion center and also assumes that all the cooperating users forward all their sensed data to the fusion center. The distributed detection model does not assume a fusion center and assumes that all the nodes are capable of sensing the spectrum as well as processing the sensed data. It is assumed that these nodes form a fully connected graph. The hierarchical model assumes the existence of two different forms of nodes in the network, viz. the sensing and the processing nodes. The sensing nodes simply sense the spectrum and forward it to the associated processing nodes and are incapable of processing the sensed data. The processing nodes on the other hand, being incapable of sensing the spectrum themselves, can only process the data forwarded by the sensing nodes.

5.3.1 Centralized Detection

In this model, a total of K sensing nodes, each equipped with a single antenna followed by a FRESH filter consisting of M frequency shifts (M_1 non-conjugate frequency shifts and M_2 conjugate frequency shifts, $M = M_1 + M_2$) and length L are assumed. It is also assumed that all the sensing nodes report to a single processing node or a fusion center via an unrestricted communication link. It is further assumed that each secondary user collects N samples of the sensed signal. These samples are used for adaptation of the FRESH filters as well as for sensing. Let, the regression vector at the kth user be defined as

$$\mathbf{u}_k[n] = [\mathbf{u}_{k1}[n], \ldots, \mathbf{u}_{kM}[n]]^T \tag{5.8}$$

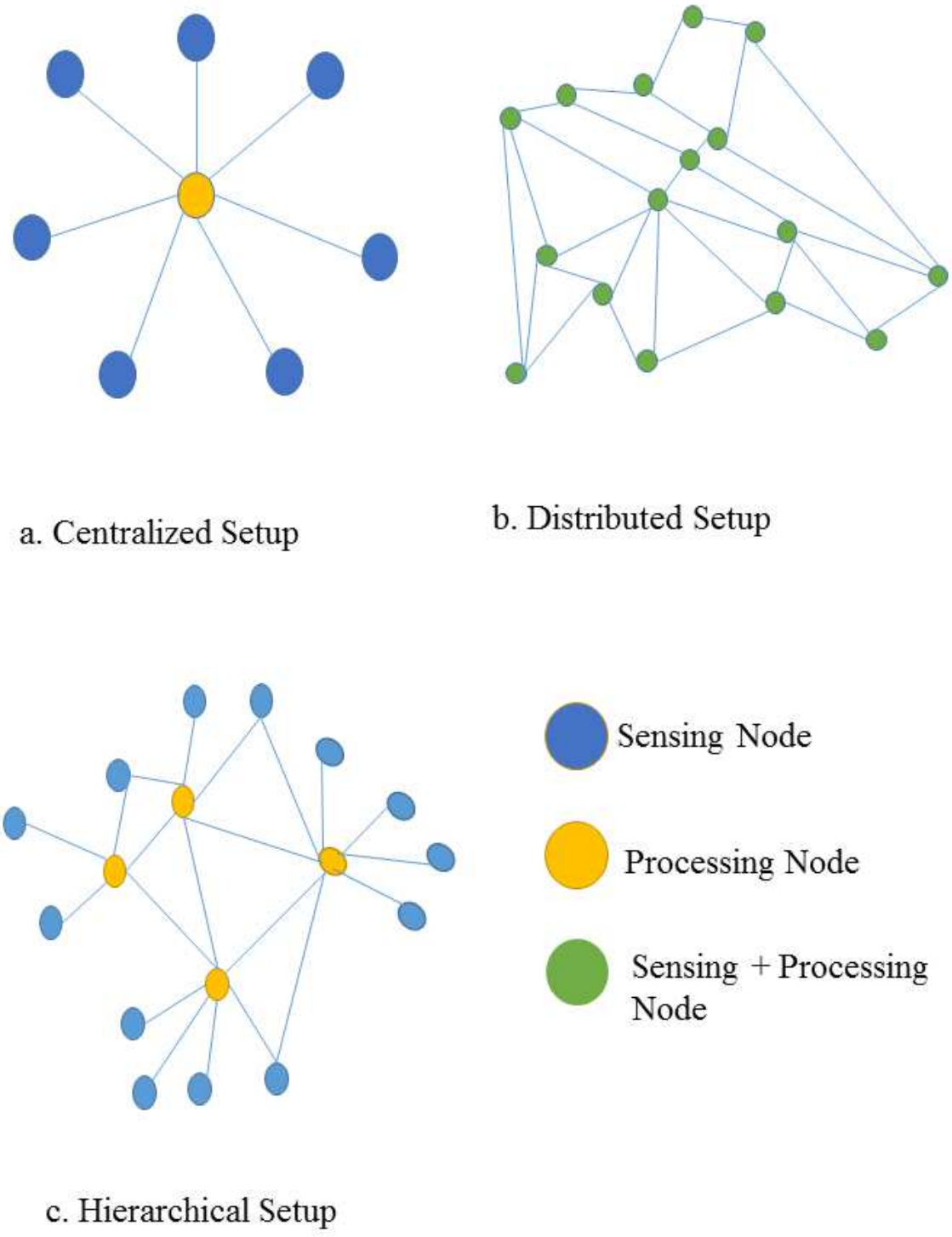

Figure 5.1: Different models for Collaborative Spectrum Sensing

where

$$\begin{aligned} \mathbf{u}_{km}[n] &= [u_{km}[n], \ldots, u_{km}[n-L+1]]^T \\ u_{km}[n] &= x_k^{(*)\alpha_m}[n] \end{aligned} \tag{5.9}$$

Here, $\mathbf{u}_{km}[n]$ denotes the vector containing the input to the mth FRESH branch of the kth user, and $u_{km}[n]$ is the optionally conjugated and frequency shifted version (for the mth FRESH branch) of the signal received by the kth user at the nth instant. Considering $x_k[n]$ as the reference signal for the kth user, the weight vector $\mathbf{w}_k$ may be determined so that the mean square error defined by the following equation is minimized [145].

$$J_k(\mathbf{w}_k) = E\left[\left|x_k[n] - \mathbf{w}_k^H \mathbf{u}_k[n]\right|^2\right] \tag{5.10}$$

The optimal weights may also be determined adaptively using the method described in [61]. Let the final weights after adaptation at the kth user be given as $\mathbf{w}_k[N]$. Then the filtered signal $y_k[n]$ at the kth user is given as

$$y_k[n] = \mathbf{w}_k^H[N]\mathbf{u}_k[n] \tag{5.11}$$

and distributed as

$$y_k[n] \sim \begin{cases} \mathcal{N}_c(0, \sigma_\nu^2 \|\mathbf{w}_k[N]\|^2) & \mathcal{H}_0 \\ \\ \mathcal{N}_c(0, (\|\boldsymbol{\varphi}_k\|^2)\, \mathbf{w}_k[N]^H \mathbf{R}_k \mathbf{w}_k[N] + \sigma_\nu^2 \|\mathbf{w}_k[N]\|^2) & \mathcal{H}_1 \end{cases} \tag{5.12}$$

where $\boldsymbol{\varphi}_k$ is the tap vector (scalar for a flat fading channel) of the channel between the primary user and the kth secondary user and $\mathbf{R}_k$ is defined as

$$\mathbf{R}_k = E[\mathbf{u}_k[n]\mathbf{u}_k^H[n]] \tag{5.13}$$

If the energy of the filtered signal is used as the test statistic then the test statistic at the kth user will take the form

$$z_k = \sum_{n=0}^{N-1} |y_k[n]|^2 \tag{5.14}$$

and will be distributed as

$$z_k \sim \begin{cases} \mathcal{N}(\sigma_\nu^2, \frac{\sigma_{z_0}^2}{N}) & \mathcal{H}_0 \\ \mathcal{N}(\mu_{z_1}(\boldsymbol{\varphi}_k), \frac{\sigma_{z_1}^2}{N}(\boldsymbol{\varphi}_k)) & \mathcal{H}_1 \end{cases} \tag{5.15}$$

where

$$\mu_{z_1}(\boldsymbol{\varphi}_k) = \|\boldsymbol{\varphi}_k\|^2 \mathbf{w}_k^H[N]\mathbf{R}_k\mathbf{w}_k[N] + \sigma_\nu^2 \tag{5.16}$$

σ_{z_0} and σ_{z_1} are functions of the adapted filter weights as discussed in the previous chapter

It is assumed that the collaborating users report their statistics to the fusion center.

The fusion center in the absence of the knowledge of the individual channel coefficients averages them such that

$$T = \frac{1}{K}\sum_{k=1}^{K} z_k, \tag{5.17}$$

Normalizing the adapted weights to a unit norm $\|\mathbf{w}[N]\| = 1$, the distribution of T under the two hypotheses may be derived as

$$T \sim \begin{cases} \mathcal{N}(\sigma_\nu^2, \frac{\sigma_{T_0}^2}{N}) & \mathcal{H}_0 \\ \mathcal{N}(\mu_{T_1}(\boldsymbol{\varphi}), \frac{\sigma_{T_1}^2}{N}(\boldsymbol{\varphi})) & \mathcal{H}_1 \end{cases} \tag{5.18}$$

where

$$\sigma_{T_0}^2 = \frac{\sigma_{z_0}^2}{K} \tag{5.19}$$

$$\mu_{T_1}(\boldsymbol{\varphi}_k) = \frac{\sum_{k=1}^{K}\|\boldsymbol{\varphi}_k\|^2 \mathbf{w}_k^H[N]\mathbf{R}_k\mathbf{w}_k[N]}{K} + \sigma_\nu^2 \tag{5.20}$$

$$\sigma_{T_1}^2 = \frac{\sum_{k=1}^{K}\sigma_{z_1}^2(\boldsymbol{\varphi}_k)}{K^2} \tag{5.21}$$

and $\boldsymbol{\varphi}$ is the joint channel vector for all the users, defined as

$$\boldsymbol{\varphi} = [\boldsymbol{\varphi}_1^T, \boldsymbol{\varphi}_2^T, \ldots, \boldsymbol{\varphi}_K^T]^T \tag{5.22}$$

It may also be observed that the mean and variance of the test statistic under the alternate hypothesis are dependent on $\boldsymbol{\varphi}$. Therefore, for a given channel vector $\boldsymbol{\varphi}$ and detection threshold λ, the test statistic distributions, as described in, (5.18) may be used to derive the probabilities of detection and false alarm as

$$P_d|\boldsymbol{\varphi} = Q\left(\frac{\lambda - \mu_{T_1}(\boldsymbol{\varphi})}{\sigma_{T_1}(\boldsymbol{\varphi})}\right) \tag{5.23}$$

$$P_{fa} = Q\left(\frac{\lambda - \sigma_\nu}{\sigma_{T_0}}\right) \tag{5.24}$$

5.3.2 Distributed Detection

This model considers K FRESH filter-equipped single-antenna nodes. Each node is assumed to be connected to its immediate neighbors via a single hop link. Let the nodes lying in the neighborhood of the kth node be contained in the index set $\mathcal{I}_k$. It is also assumed that these nodes form a fully connected network, i.e. there exists a finite-hop path between any two nodes and the connected nodes can share information among themselves. This information may be the observed data as well as the test statistic. In the absence of a fusion center, the nodes must form a consensus among themselves regarding the presence of a primary signal.

It is assumed that each collaborating node collects N samples of the sensed signal which are to be used for adaptation as well as for sensing. The adapted weight vector $\mathbf{w}_k[N]$ at the kth node is used to generate the filtered signal $y_k[n]$, defined as

$$y_k[n] = \mathbf{w}_k^H[N]\mathbf{u}_k[n] \tag{5.25}$$

where

$$\mathbf{u}_k[n] = [\mathbf{u}_{k1}[n], \ldots, \mathbf{u}_{kM}[n]]^T \tag{5.26}$$

Each node uses the local finite time energy of the filtered signal as the local test statistic calculated at the kth user as

$$z_k[0] = \sum_n |y_k[n]|^2 \tag{5.27}$$

and may be shown to be distributed as

$$z_k[0] \sim \begin{cases} \mathcal{N}(\sigma_\nu^2, \frac{\sigma_{z_0}^2}{N}) & \mathcal{H}_0 \\ \mathcal{N}(\mu_{z_1}(\boldsymbol{\varphi}_k), \frac{\sigma_{z_1}^2(\boldsymbol{\varphi}_k)}{N}) & \mathcal{H}_1 \end{cases} \tag{5.28}$$

where

$$\mu_{z_1}(\boldsymbol{\varphi}_k) = \|\boldsymbol{\varphi}_k\|^2 \mathbf{w}_k^H[N]\mathbf{R}_k\mathbf{w}_k[N] + \sigma_\nu^2 \tag{5.29}$$

σ_{z_0} and σ_{z_1} are also empirical functions of the adapted weights. After each node calculates its initial local test statistic defined here as $z_k[0]$, it tries to reach a consensus with the neighboring nodes [75]. In the qth consensus iteration, the test statistic at the kth node is updated as

$$z_k[q] = \sum_{i \in \mathcal{I}_k} c_{ik} z_i[q-1] \tag{5.30}$$

where c_{ik} is the weight assigned to the observation of the ith node by the kth node. If the nodes i and k are not directly connected then $c_{ik} = 0$ otherwise $0 < c_{ik} \leq 1$. Also, for $\mathbf{c}_k = [c_{1k}, c_{2k}, \ldots, c_{Kk}]^T$, $\mathbf{1}^T\mathbf{c}_k = 1$ that is the sum of the elements of $\mathbf{c}_k$ is unity. Here $\mathbf{1}$ is the the K dimensional all one vector such that $\mathbf{1} = [1, 1, \ldots, 1]^T$

Defining

$$\mathbf{z}[q] = [z_1, z_2, \ldots, z_K]^T \tag{5.31}$$

and

$$\mathbf{C} = [\mathbf{c}_1, \mathbf{c}_2, \ldots, \mathbf{c}_K] \tag{5.32}$$

the qth consensus step may be written as

$$\mathbf{z}[q] = \mathbf{C}\mathbf{z}[q-1] \tag{5.33}$$

and, therefore, for a total of Q consensus steps

$$\mathbf{z}[Q] = \mathbf{C}^Q \mathbf{z}[0] \tag{5.34}$$

Decomposing $\mathbf{C}$ as

$$\mathbf{C} = \mathbf{P}\mathbf{D}\mathbf{P}^{-1} \tag{5.35}$$

$\mathbf{z}[Q]$ may be written as

$$\mathbf{z}[Q] = \mathbf{P}\mathbf{D}^Q\mathbf{P}^{-1}\mathbf{z}[0] \tag{5.36}$$

It may be observed that the matrix $\mathbf{C}$ is a Markov matrix with all the eigenvalues lying between zero and one [117]. If $\mathbf{C}$ is fully connected then only one eigenvalue will be equal to 1 and all others will have smaller values. Therefore, for a sufficiently large Q it may be shown that D^Q converges to a rank one matrix such that [117],

$$D^Q = \begin{bmatrix} 1 & 0 & \dots & 0 \\ 0 & 0 & \dots & 0 \\ \vdots & \vdots & \ddots & \vdots \\ 0 & 0 & \dots & 0 \end{bmatrix} \tag{5.37}$$

and

$$\mathbf{z}[Q] = \mathbf{p}_1(\mathbf{P}^{-1})_1\mathbf{z}[0] \tag{5.38}$$

where $(\mathbf{P}^{-1})_1$ is the first row of $\mathbf{P}^{-1}$ and $\mathbf{p}_1$ is the dominant eigenvector of $\mathbf{C}$. It is observed that $\mathbf{C}^T\mathbf{1} = \mathbf{1}$, and therefore $\mathbf{1}$ is the dominant eigenvector of $\mathbf{C}$. Hence, all the elements of $\mathbf{p_1}$ are equal. This results in all the elements of $\mathbf{z}[Q]$ being equal. Therefore, for all k and a large enough Q,

$$z_k[Q] = \tilde{\mathbf{c}}^T\mathbf{z}[0] \tag{5.39}$$

where

$$\tilde{\mathbf{c}} = \frac{1}{K}(\mathbf{P}^{-1})_1. \tag{5.40}$$

The final weight vector $\tilde{\mathbf{c}}$ will, therefore, depend on the structure of $\mathbf{C}$. On the other hand the speed of convergence will depend on the second largest eigenvalue of $\mathbf{C}$.

The final test statistic on all the nodes may therefore be written as

$$Z = \sum_{k=1}^{K} \tilde{c}_k z_k[0] \tag{5.41}$$

which is distributed as

$$Z \sim \begin{cases} \mathcal{N}(\sigma_\nu^2, \frac{\sigma_{Z_0}^2}{N}) & \mathcal{H}_0 \\ \mathcal{N}(\mu_{Z_1}(\boldsymbol{\varphi}), \frac{\sigma_{Z_1}^2(\boldsymbol{\varphi})}{N}) & \mathcal{H}_1 \end{cases} \tag{5.42}$$

where $\boldsymbol{\varphi}$ is the joint channel vector defined previously,

$$\sigma_{Z_0}^2 = \sigma_{z_0}^2 \sum_{k=1}^{K} \tilde{c}_k^2 \tag{5.43}$$

such that $\frac{1}{K} \leq \sum_{k=1}^{K} \tilde{c}_k^2 \leq 1$ and

$$\mu_{Z_1}(\boldsymbol{\varphi}_k) = \sum_{k=1}^{K} \tilde{c}_k \|\boldsymbol{\varphi}_k\|^2 \mathbf{w}_k^H[N] \mathbf{R}_k \mathbf{w}_k[N] + \sigma_\nu^2 \tag{5.44}$$

$$\sigma_{Z_1}^2 = \sum_{k=1}^{K} \tilde{c}_k^2 \sigma_{z_1}^2(\boldsymbol{\varphi}_k) \tag{5.45}$$

In this case, for a given channel vector $\boldsymbol{\varphi}$ and detection threshold λ, the probabilities of detection and false alarm may be derived as

$$P_d|\boldsymbol{\varphi} = Q\left(\frac{\lambda - \mu_{Z_1}(\boldsymbol{\varphi})}{\sigma_{Z_1}(\boldsymbol{\varphi})}\right) \tag{5.46}$$

$$P_{fa} = Q\left(\frac{\lambda - \sigma_\nu^2}{\sigma_{Z_0}}\right) \tag{5.47}$$

It may be observed that the probabilities of detection and false alarm depend on the structure of the network matrix.

5.3.3 The Generalized Hierarchical Model

Under this model, the network is assumed to consist of two types of nodes, viz. the sensing and the processing nodes. As discussed before, the sensing nodes are devoid of any signal processing any capabilities and hence simply forward the collected samples to the connected processing node(s). On the other hand, the processing nodes cannot sense the spectrum by themselves but can only process the data supplied to them by the sensing nodes. In a centralized detection scheme, the cooperating users may be thought of as sensing nodes and the fusion center as the processing node. Similarly, in a purely distributed case, each sensing node may be considered as attached to a processing node.

Let, the secondary user network in this case consist of K_S sensing and K_P processing nodes. It is assumed that each sensing node is connected to at least one processing node and vice versa. Multiple processing nodes, whenever present, are assumed to share the test statistics among themselves. It is also assumed that the processing nodes form a fully connected graph.

Let the indices of the sensing nodes connected to the pth processing node be contained in the index set $\mathcal{I}_p$ and those of the connected processing nodes be contained in the index set $\mathcal{P}_p$. It is again assumed that each sensing node collects N samples and forwards these

to each of its connected processing nodes. The attached processing nodes use these samples to adapt the associated filter weights and calculate the local test statistics. The finite time energy $\mathcal{E}_{kp}$, defined for the kth sensing node at the pth processing node, may be written as

$$\mathcal{E}_{kp} = \frac{1}{N}\sum_{n=0}^{N-1}|y_{kp}[n]|^2 \tag{5.48}$$

where y_{kp} is the signal sensed by the kth sensing node, filtered by the pth processing node given as

$$y_{kp}[n] = \mathbf{w}_{kp}^H[N]\mathbf{u}_{kp}[n] \tag{5.49}$$

where $\mathbf{w}_{kp}^H[N]$ and $\mathbf{u}_{kp}[n]$ are, respectively, the adapted weight vector and the regression vector for the kth sensing node at the pth processing node. $\mathcal{E}_{kp}$ may be shown to be distributed as

$$\mathcal{E}_{kp} \sim \begin{cases} \mathcal{N}(\sigma_\nu^2, \frac{\sigma_{\mathcal{E}_0}^2}{N}) & \mathcal{H}_0 \\ \mathcal{N}(\mu_{\mathcal{E}_1}(\boldsymbol{\varphi}_k), \frac{\sigma_{\mathcal{E}_1}^2(\boldsymbol{\varphi}_k)}{N}) & \mathcal{H}_1 \end{cases} \tag{5.50}$$

where

$$\mu_{\mathcal{E}_1}(\boldsymbol{\varphi}_k) = \|\boldsymbol{\varphi}_k\|^2\mathbf{w}_k^H[N]\mathbf{R}_k\mathbf{w}_k[N] + \sigma_\nu^2 \tag{5.51}$$

with $\sigma_{\mathcal{E}_0}$ and $\sigma_{\mathcal{E}_1}$ again being empirical functions of the adapted weights.

The initial test statistic at the pth processing node is then calculated as

$$z_p[0] = \frac{1}{|\mathcal{I}_p|}\sum_{k\in\mathcal{I}_p}\mathcal{E}_{kp} \tag{5.52}$$

Based on this and the results derived earlier, the distribution of $z_p[0]$ under the two hypotheses takes the form

$$z_p[0] \sim \begin{cases} \mathcal{N}(\sigma_\nu^2, \frac{\sigma_{z_0,p}^2}{N}) & \mathcal{H}_0 \\ \mathcal{N}(\mu_{z_1,p}(\boldsymbol{\varphi}_p), \frac{\sigma_{\mathcal{E}_1}^2(\boldsymbol{\varphi}_p)}{N}) & \mathcal{H}_1 \end{cases} \tag{5.53}$$

where $\boldsymbol{\varphi}_p$ is the joint channel vector for the sensing nodes reporting to the given processing node,

$$\sigma_{z_0,p}^2 = \frac{\sigma_{z_0}^2}{|\mathcal{I}_p|} \tag{5.54}$$

$$\mu_{z_1,p}(\boldsymbol{\varphi}_p) = \frac{\sum_{k\in\mathcal{I}_p}\|\boldsymbol{\varphi}_k\|^2\mathbf{w}_{k,p}^H[N]\mathbf{R}_{k,p}\mathbf{w}_{k,p}[N]}{|\mathcal{I}_p|} + \sigma_\nu^2 \tag{5.55}$$

and

$$\sigma_{z_1,p}^2 = \frac{\sum_{k\in\mathcal{I}_p}\sigma_{z_1,k}^2}{|\mathcal{I}_p|^2} \tag{5.56}$$

Following this, the different processing nodes arrive at a consensus among themselves such

that the final test statistic at each node is given as

$$Z = \sum_{p=1}^{K_P} \tilde{c}_p z_p[0] \tag{5.57}$$

where $\tilde{c}_p$ is the weight of the pth cognitive user in the consensus mechanism described in the previous subsection. Therefore, Z is distributed as

$$Z \sim \begin{cases} \mathcal{N}(\sigma_\nu^2, \frac{\sigma_{Z_0}^2}{N}) & \mathcal{H}_0 \\ \mathcal{N}(\mu_{Z_1}(\boldsymbol{\varphi}), \frac{\sigma_{Z_1}^2}{N}(\boldsymbol{\varphi})) & \mathcal{H}_1 \end{cases} \tag{5.58}$$

where $\boldsymbol{\varphi}$ is the joint channel vector and

$$\sigma_{Z_0}^2 = \sum_{p=1}^{K_P} \sigma_{z_0,p}^2 \tilde{c}_p^2 \tag{5.59}$$

$$\mu_{Z_1}(\boldsymbol{\varphi}) = \sum_{p=1}^{K_P} \tilde{c}_p \frac{\sum_{k\in\mathcal{I}_p} \|\boldsymbol{\varphi}_k\|^2 \mathbf{w}_{k,p}^H[N] \mathbf{R}_{k,p} \mathbf{w}_{k,p}[N]}{|\mathcal{I}_p|} + \sigma_\nu^2 \tag{5.60}$$

$$\sigma_{T_0}^2 = \sum_{p=1}^{K_P} \tilde{c}_p^2 \sigma_{z_1}^2(\boldsymbol{\varphi}_p) \tag{5.61}$$

Therefore, for a given channel vector $\boldsymbol{\varphi}$ and detection threshold λ, the probabilities of detection and false alarm may be obtained as

$$P_d|\boldsymbol{\varphi} = Q\left(\frac{\lambda - \mu_{Z_1}(\boldsymbol{\varphi})}{\sigma_{Z_1}(\boldsymbol{\varphi})}\right) \tag{5.62}$$

$$P_{fa} = Q\left(\frac{\lambda - \sigma_\nu^2}{\sigma_{Z_0}}\right) \tag{5.63}$$

It may be noted that the performance depends on the structure of $\mathbf{C}$ and needs to be determined using simulation techniques. It may also be noted that the performance of these structures depends on the adapted FRESH filter weights. The adaptation error in the LMS algorithm is a function of the instantaneous SNR of the training signal [61] and, hence, the filter weights of the users experiencing a deep fade may be misadjusted. Consequently, it is desired to have cooperation for the weight adaptation stage to improve the overall detection performance. The adaptation algorithms for the three cooperation strategies discussed in this section are detailed in the following two sections.

5.4 Adaptation Algorithms for Flat Fading

5.4.1 Centralized Adaptation

For this structure, the optimal weight vector $\mathbf{w}_k$ at the kth user may be determined by minimizing the cost function $J_k(\mathbf{w}_k)$, defined as

$$J_k(\mathbf{w}_k) = E\left[\left|x_k[n] - \mathbf{w}_k^H \mathbf{u_k}[n]\right|^2\right] \tag{5.64}$$

From (5.5) it may be observed that as the primary signal exhibits cyclostationarity and the additive noise does not, the optimal $\mathbf{w}_k$ is independent of k. Therefore, the problem may equivalently be stated as minimizing

$$J(\mathbf{w}) = E\left[\left|\sum_{k=1}^{K}(x_k[n] - \mathbf{w}^H \mathbf{u}_k[n])\right|^2\right] \tag{5.65}$$

This is similar to the global cost function for filter weight adaptation, as presented in [17]. The solutions developed in [17] may, therefore, be extended to joint FRESH filter adaptation case. In a centralized detection scheme, this may be done in the following two ways

1. All the secondary users forward their sensed data to the fusion center which globally adapts the filter weights.

2. Each node adapts its own filter weights and after each adaptation step exchanges information with the fusion center so as to arrive at a consensus on the weight values.

Following the first approach, the Global-LMS algorithm, as presented in [17], may be modified as follows

1. Initialize $\mathbf{w}[0] = \mathbf{0}$

2. For the nth iteration, update $\mathbf{w}[n]$ as

$$\mathbf{w}[n+1] = \mathbf{w}[n] + \mu \sum_{k=1}^{K} \frac{1}{\|\mathbf{u}_k[n]\|^2} \mathbf{u}_k[n](x_k[n] - \mathbf{w}^H[n]\mathbf{u}_k[n])^* \tag{5.66}$$

where, μ is the adaptation step size. It may be noted that the data from all the nodes, though normalized by the norm squared of the instantaneous regression vector, are given equal weights. This is due to the absence of knowledge about the channel coefficients at different nodes. However, if the fading coefficients of the different secondary users are known to the fusion center, then the data from the secondary users with greater fading coefficient may be allotted more weight to improve the adaptation performance.

The case where different secondary users average their weights after each step may be considered similar to the ATC (Adapt Then Combine)-LMS algorithm derived in [17]. This may be described as

1. Initialize the weight vector at each secondary user as $\mathbf{w}_k[0] = \mathbf{0}$ and the global weight vector as $\boldsymbol{\psi}[0] = \mathbf{0}$.

2. For the nth iteration, update $\mathbf{w}[n]$ at each secondary user as

$$\mathbf{w}_k[n+1] = \boldsymbol{\psi}[n] + \mu \frac{1}{\|\mathbf{u}_k[n]\|^2} \mathbf{u}_k[n](x_k[n] - \boldsymbol{\psi}^H[n]\mathbf{u}_k[n])^* \tag{5.67}$$

3. Update $\boldsymbol{\psi}[n+1]$ as

$$\boldsymbol{\psi}[n+1] = \frac{1}{K} \sum_{k=1}^{K} \mathbf{w}_k[n+1] \tag{5.68}$$

Under this setting, the regression coefficient vector of each secondary user is assigned equal weight due to the lack of knowledge about the channel coefficients. These weights, however, may be modified if the instantaneous fading coefficients at different users are known.

In the global LMS-based solution, all the computation may be performed at the fusion center. However this requires storage capability at the fusion center. In this case, as each node needs to send a sample at every sampling instant, there are K transmissions per sampling instant and a total of (KN) transmissions for N samples. The fusion center, in this case, needs to perform (KML) complex multiplications per received sample. Therefore, the total number of complex multiplications required is $(NKML)$.

On the other hand, the ATC-Diffusion LMS-based model does not require any storage capability at the fusion center. Instead, each secondary user adapts its (ML) weights and transmits them to the fusion center. Consequently, there are $(2KML)$ transmissions per sampling instant and a total of $(2NKML)$ transmissions. Here, every individual sensing node separately requires (ML) complex multiplications per sampling instant and therefore, (NML) complex multiplications are required at each secondary user.

Also, as in the case of the Global LMS-based scheme, the data sensed by all the nodes are available at the fusion center. Therefore, the sensing nodes need not transmit their statistics separately. However, in the ATC-Diffusion LMS-based scheme, an additional K transmissions will be required to report the statistics to the fusion center.

5.4.2 Distributed Adaptation

In this case, it is not possible to use global adaptation due to the absence of a fusion center. Here, each node communicates only with its immediate neighbors. Therefore, if the data generating model at different nodes is same, then each node may utilize the data sensed by

its neighbors to adapt its local weight vector. The local cost function J_k may be defined as

$$J_k(\mathbf{w}_k) = E\left[\left|\sum_{i\in\mathcal{I}_k} c_{ik}(x_i[n] - \mathbf{w}_k\mathbf{u}_i[n])\right|^2\right] \tag{5.69}$$

where c_{ik} is the weight assigned to the observation of the ith user as assigned by the kth user. This is similar to the local cost function defined in [17]. Different strategies are proposed in [17] for the solution of this problem and it has been shown that the ATC-LMS algorithm results in the best convergence performance. Consequently, we use this algorithm as described below for joint adaptation of the FRESH filters at different sensing nodes.

1. Initialize the weight vector $\mathbf{w}_k$, and the intermediate weight vector $\boldsymbol{\psi}_k$ at each secondary user as $\mathbf{w}_k[0] = \mathbf{0}$ and $\boldsymbol{\psi}_k = \mathbf{0}$

2. For the nth iteration update $\boldsymbol{\psi}_k[n]$ at each secondary user as

$$\boldsymbol{\psi}_k[n+1] = \mathbf{w}_p[n] + \mu\sum_{i\in\mathcal{I}_k} c_{ik}\frac{1}{\|\mathbf{u}_i[n]\|^2}\mathbf{u}_i[n](x_i[n] - \mathbf{w}_k^H[n]\mathbf{u}_i[n])^* \tag{5.70}$$

3. Update $\mathbf{w}_k[n+1]$ as

$$\mathbf{w}_k[n+1] = \sum_{i\in\mathcal{I}_k} c_{ik}\boldsymbol{\psi}_i[n+1] \tag{5.71}$$

The weights may depend on the knowledge of the channel, in the absence of which the connectivity of the nodes may be used to decide their values. It is shown in [17] that assigning a higher weight to more connected nodes results in a better convergence performance.

As for the communication and computational complexity of this setup, it may be observed that for each adaptation step, each node needs to transmit its data as well as its adapted filter weights. That is, a total of $(K(1+ML))$ transmissions are required per sampling instant. However, if the combination step, that is Step 3 of the above algorithm, is ignored then only K transmissions per step are needed. Also, a total of $(K(3+ML)\sum_k |\mathcal{I}_k|)$ complex multiplications are required for the above algorithm while $(K(2+ML)\sum_k |\mathcal{I}_k|)$ complex multiplications are required if the combination step of the adaptation algorithm is ignored.

5.4.3 The General Hierarchical Case

In this case, it is assumed that a processing node receives data only from the sensing nodes connected to it. However, the connected processing nodes may be used for achieving a consensus on weights. Therefore, the optimal weight vector at the pth processing node

may be obtained by minimizing the function J_p defined as

$$J_p(\mathbf{w_p}) = E\left[\left|\sum_{i\in\mathcal{I}_p} c_{ip}(x_i[n] - \mathbf{w}_p\mathbf{u}_i[n])\right|^2\right] \tag{5.72}$$

Using the neighboring nodes for consensus on weights, the ATC algorithm described earlier, may be modified as

1. Initialize the weight vector $\mathbf{w}_p$, and the intermediate weight vector $\boldsymbol{\psi}_p$ at each secondary user as $\mathbf{w}_p[0] = \mathbf{0}$ and $\boldsymbol{\psi}_p = \mathbf{0}$

2. For the nth iteration, update $\psi_p[n]$ at each processing node as

$$\boldsymbol{\psi}_p[n+1] = \mathbf{w}_p[n] + \mu\sum_{i\in\mathcal{I}_p} c_{ip}\frac{1}{\|\mathbf{u}_i[n]\|^2}\mathbf{u}_i[n](x_i[n] - \mathbf{w}_p^H[n]\mathbf{u}_i[n])^* \tag{5.73}$$

3. Update $\mathbf{w}_p[n+1]$ as

$$\mathbf{w}_p[n+1] = \sum_{i\in\mathcal{P}_p} a_{ip}\boldsymbol{\psi}_i[n+1] \tag{5.74}$$

In this algorithm, a_{ip} and c_{jp} are, respectively, the weights assigned by the pth processing node to the data reported by the ith processing node and the jth sensing node.

For this algorithm, a total of $(K+PML)$ transmissions are required per adaptation step. At the same time, there will be a total of $(ML\sum_p|\mathcal{I}_p| + \sum_p|\mathcal{P}_p|)$ complex multiplications per adaptation step. In case the processing nodes do not combine their adapted weights, then there will be a total of K transmissions and $(ML\sum_p|\mathcal{I}_p|)$ complex multiplications per adaptation step.

5.5 Adaptation Algorithms for Dispersive Fading

5.5.1 Centralized Adaptation

It is observed that if the inter-sample interval is smaller than the channel delay spread then the cyclic regression coefficients of the signal received at different secondary users will be different. Hence, it may not be possible for the secondary user to estimate them via either of the algorithms described in the previous section. However, the samples received at different secondary users are still correlated, and in case all the samples are available at the fusion center, the weights for the signals received at different secondary users may be adapted jointly. Defining the vectors $\mathbf{x}[n]$ and $\mathbf{u}[n]$ as

$$\begin{aligned}\mathbf{x}[n] &= [x_1[n], x_2[n], \ldots, x_K[n]]^T \\ \mathbf{u}[n] &= \left[\mathbf{u}_1^T[n], \mathbf{u}_2^T[n], \ldots, \mathbf{u}_K^T[n]\right]^T\end{aligned} \tag{5.75}$$

Weight vectors $\mathbf{w}$ and $\mathbf{h}$ minimizing the following cost function may be determined in a manner similar to Space-Time FRESH filtering discussed in the third chapter

$$J(\mathbf{w}, \mathbf{h}) = E\left[\left|\mathbf{h}^H\mathbf{x}[n] - \mathbf{w}^H\mathbf{u}[n]\right|^2\right] \tag{5.76}$$

As a solution to this problem, the C2-LMS algorithm derived in the third chapter may be modified as follows.

1. Initialize $\mathbf{w}[0] = \mathbf{0}$ and $\mathbf{h}[0] = g\mathbf{i}[k]$ where $\mathbf{i}[k]$ is the kth column of the identity matrix and g is an arbitrary constant.

2. For the nth iteration, update $\mathbf{w}$ and $\mathbf{h}$ as

$$\mathbf{w}[n+1] = \mathbf{w}[n] + \mu_w\mathbf{u}[n]e^*[n] \tag{5.77}$$

and

$$\mathbf{h}[n+1] = k[n]\mathbf{h}[n] - \mu_h\mathbf{x}[n]e^*[n] \tag{5.78}$$

where

$$e[n] = y[n] - v[n] \tag{5.79}$$

It may be noted that

$$v[n] = \mathbf{w}^H[n]\mathbf{u}[n] \tag{5.80}$$

$$y[n] = \mathbf{h}^H[n]\mathbf{x}[n] \tag{5.81}$$

and

$$\mu_h = \frac{\mu}{\left\|\mathbf{x}[n]\right\|_2^2}, \quad \mu_w = \frac{\mu}{\left\|\mathbf{u}[n]\right\|_2^2} \tag{5.82}$$

$$b[n] = \mu_h\Re\{y^*[n]e[n]\} \tag{5.83}$$

$$c[n] = \mu_h^2\left\|\mathbf{x}[n]\right\|_2^2\left|e[n]\right|^2 - g^2 \tag{5.84}$$

$$k[n] = b[n] + \sqrt{(b[n])^2 - c[n]} \tag{5.85}$$

The symbol $\Re$ denotes the real part of a complex number and the step size μ is normalized w.r.t the inputs $\mathbf{x}[n]$ and $\mathbf{u}[n]$ so as to accommodate large variations in their values.

This algorithm also requires the transmission of all the sensed samples to the fusion center and, therefore, requires a total of (KN) transmissions. A total of $(2K + KLM + 2)$ multiplications are required per iteration step, thereby resulting in a requirement of $(N(2K + KLM + 2))$ multiplications at the fusion center.

5.5.2 Distributed Adaptation

In a distributed setting, each node may treat the inputs from the connected nodes as if they are coming from different antennas connected to it. Therefore, input or the reference vector in this case may be written in the form

$$\underline{\mathbf{x}}_k[n] = [x_i[n]]_{i\in\mathcal{I}_k} \tag{5.86}$$

i.e. $\underline{\mathbf{x}}_k[n]$ is a concatenation of all the inputs arriving at the kth node. Note that the index set $\mathcal{I}_k$ contains the indices of the nodes connected to the kth node. Similarly, the regression vector at the kth node may be written as

$$\underline{\mathbf{u}}_k[n] = [\mathbf{u}_i[\,n]]_{i\in\mathcal{I}_k} \tag{5.87}$$

The optimal weight vectors at the kth node, $\mathbf{h}_k$ and $\mathbf{w}_k$ will minimize the objective function defined as

$$J_k(\mathbf{w}_k, \mathbf{h}_k) = E\left[\left|\mathbf{h}_k^H \underline{\mathbf{x}}_k[n] - \mathbf{w}_k^H \underline{\mathbf{u}}_k[n]\right|^2\right] \tag{5.88}$$

Therefore, the C2-LMS algorithm may be used at each node to adapt the weight vectors $\mathbf{h}$ and $\mathbf{w}$. In this case again, K transmissions and $ML\sum_k|\mathcal{I}_k|$ complex multiplications are required per adaptation step.

5.5.3 The General Hierarchical Case

Here, each processing node may treat each sensing node connected to it as a different antenna and construct the regression vector and reference vectors as

$$\underline{\mathbf{u}}_p[n] = [\mathbf{u}_i[\,n]]_{i\in\mathcal{I}_p} \tag{5.89}$$

and

$$\underline{\mathbf{x}}_p[n] = [x_i[n]]_{i\in\mathcal{I}_p} \tag{5.90}$$

The C2-LMS algorithm for finding the weights $\mathbf{w}_p$ and $\mathbf{h}_p$ minimizing the cost function J_p defined at the pth user as

$$J_p(\mathbf{w}_p, \mathbf{h}_p) = E\left[\left|\mathbf{h}_p^H \underline{\mathbf{x}}_p[n] - \mathbf{w}_p^H \underline{\mathbf{u}}_p[n]\right|^2\right] \tag{5.91}$$

subject to

$$\|\mathbf{h}\| = g \tag{5.92}$$

A total of K transmissions and $(ML\sum_p|\mathcal{I}_p|)$ complex multiplications are required per adaptation step.

5.6 Simulation Results

This section presents simulation results obtained with randomly generated signals. It is assumed that each user in the secondary network samples the environment at a rate of 1 MHz. It is further assumed that the FRESH filter attached to each of these users has a similar structure with a single conjugate frequency shift branch at $2f_c$. The primary signal is assumed to be BPSK modulated with a carrier frequency $f_c = 100$ kHz. The average power of the primary signal is fixed at unity while the variance of the additive noise is varied to achieve different values of the average input SNR. The fading coefficients are assumed to be Rayleigh distributed and a 4-tap channel is assumed for the dispersive case. In all the experiments, 500 samples are used to adapt the FRESH filter. The samples used to adapt the filters are stored and then passed through the adapted filters to obtain a filtered signal. This filtered signal is then subjected to energy detection to test for the presence of a primary signal.

The performance of the spectrum sensor is evaluated in terms of the probability of detection with different SNRs for a fixed false alarm rate of 1%. 1000 independent trials in the absence of a primary signal are conducted to determine the detection thresholds. Following this, the detection performance is tested using 2000 independent trials.

5.6.1 Centralized Detection

Figure 5.2 plots the performance of the proposed cooperative spectrum sensing scheme for 16 cooperating users with different filter lengths. The system is adapted using the Global-LMS algorithm. The 'no enhancement' case represents a single-tap FRESH filter (L=1) which is equivalent to a standard energy detector. A gain of nearly 5 dB is observed as the FRESH filter length is increased from 1 to 32 for a successful detection rate of 90%.

The performances of the three adaptation algorithms with different filter configurations are compared in Figure 5.3. It is observed that the systems based on ATC-LMS and Global-LMS behave almost identically offering a gain of more than 2 dB over the Local-LMS-based system, for a successful detection rate of 90%.

The gains achieved by different adaptation algorithms for a successful detection rate of 90% with different filter configurations are summarized in Table 5.1. Trends similar to the ones seen in Figure 5.3 are observed for different filter lengths.

The performance improvement by increasing the number of cooperating users for a fixed filter length (L=8) is shown in Figure 5.4. It is seen that increasing the number of cooperating users from 1 to 16 leads to performance improvement of nearly 8 dB.

Figure 5.5 depicts the performance of the proposed system in case of 8 cooperating users in a dispersive fading environment. It is again observed that increasing the FRESH filter length from 1 to 32 results in gains more than 4 dB for a successful detection rate of 90%.

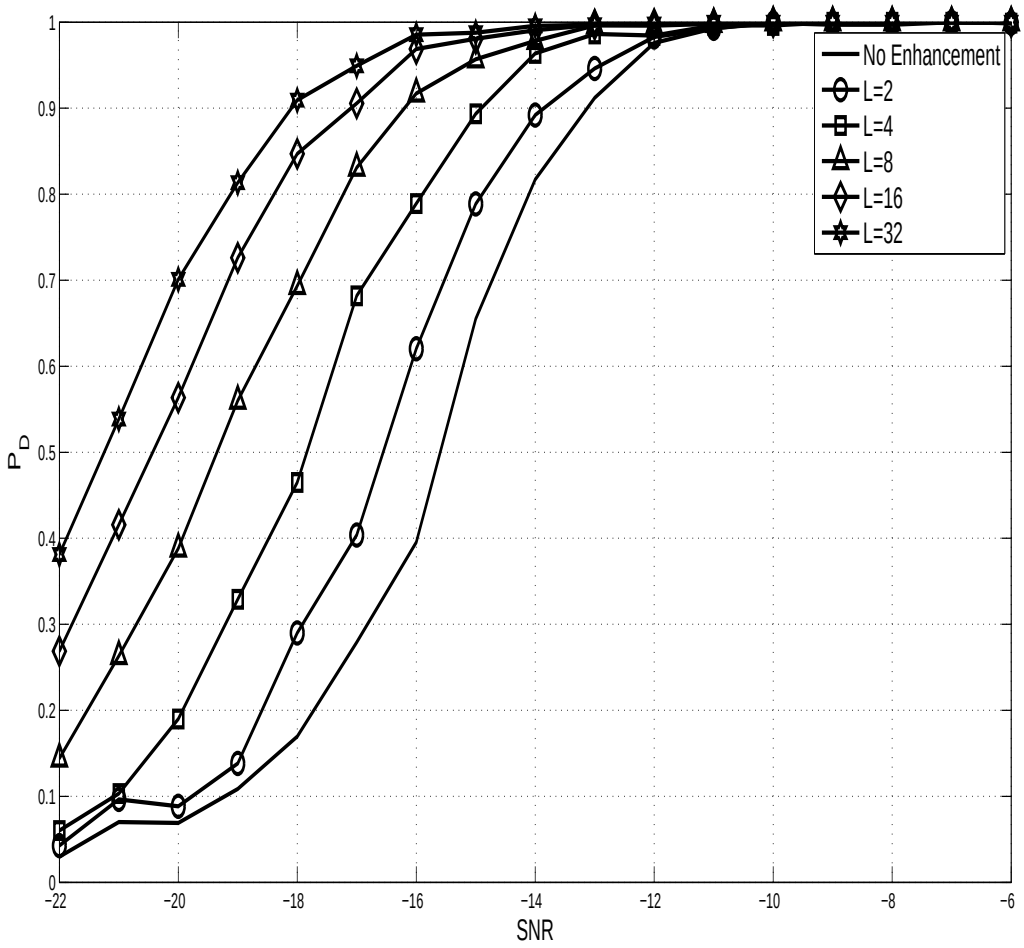

Figure 5.2: Performance using the Global LMS algorithm and the energy detector for 16 users and different filter lengths

.

Table 5.1: Gains (in Decibel) offered by the different algorithms for $N = 500$ and $K = 16$ for a flat fading channel

Filter Length	1	2	4	8	16	32
Local LMS	0	0.16	1	1.85	2.4	2.81
Diffusion LMS	0	0.67	1.83	3.13	4.14	5
Global LMS	0	0.85	1.95	3.2	4	5

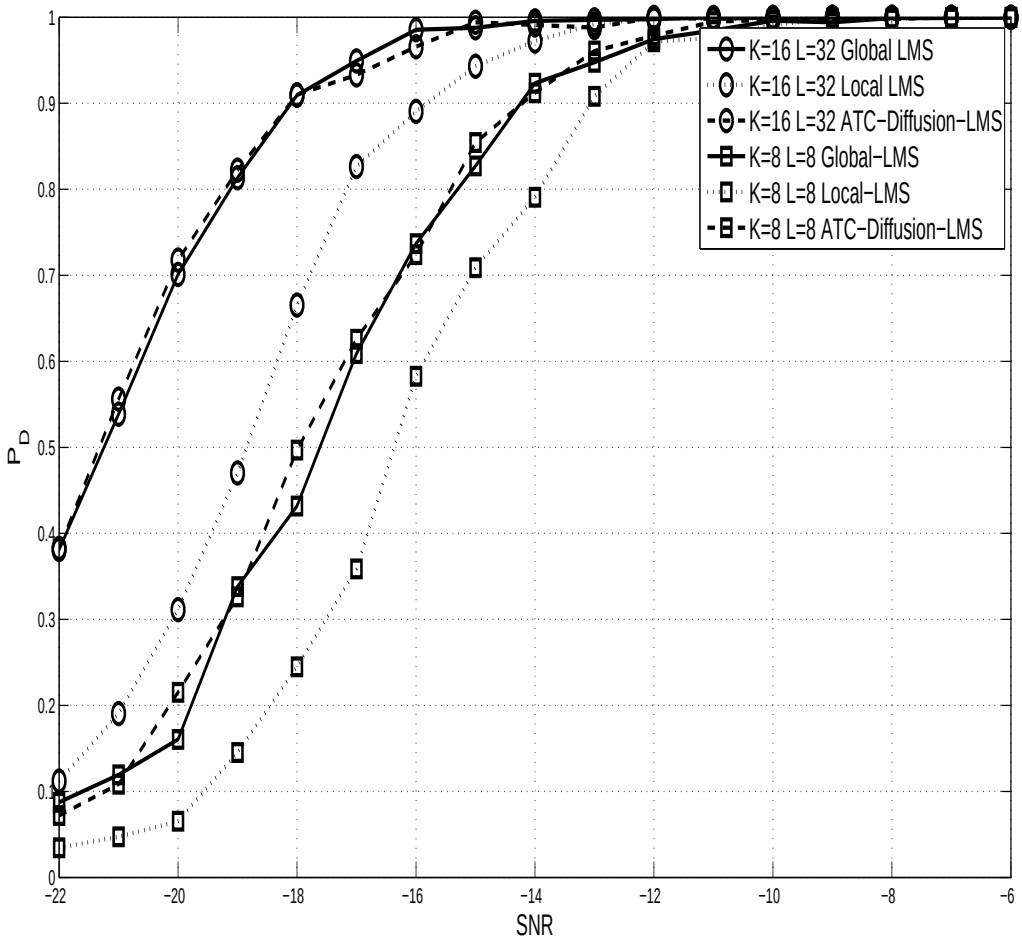

Figure 5.3: Comparison of the different adaptation algorithms for different user/filter configurations

Figure 5.6 illustrates the performance comparison for different adaptation algorithms in a dispersive multipath channel. In this case, for a successful detection rate of 90%, joint adaptation leads to gain of nearly 1 dB over the conventional adaptation methods. Similar trends are observed in Table 5.2 which summarizes the gains achieved by two algorithms with different filter lengths in a 16-user system.

It is demonstrated that an increase in the FRESH filter length causes the detector performance to improve, regardless of the adaptation algorithm. However, joint adaptation of the FRESH filters at different secondary users leads to better gains as compared to their independent adaptations. This improved performance comes at the cost of communication requirements within the secondary user network. It is also seen that both the Global-LMS and the ATC-LMS algorithms offer similar gains. However, in the present case, the ATC-LMS algorithm has greater communication requirements. Hence, the Global-LMS algorithm should be preferred over the ATC-Diffusion-LMS algorithm.

5.6.2 Distributed Detection

The performance of a fully distributed sensing system for 16 users and different filter lengths in a flat fading case is shown in Fig 5.7. The increase in filter length is again shown to improve the detection performance by nearly 6 dB.

The effect of the choice of adaptation algorithm on the system performance for a fully distributed system under flat fading is illustrated in Figure 5.8. Similar to the centralized case, it is observed that the ATC-LMS algorithm improves the detection performance by as much as 1 dB in comparison to the local LMS algorithm.

Fig 5.9 illustrates the effect of the number of consensus steps on the performance of a fully distributed system comprising of 8 users each equipped with a a FRESH filter of length 8 adapted using the ATC-LMS algorithm. It is observed that in general, a K-user system arrives at a consensus in $\log_2 K$ consensus steps.

The performance of the C2-LMS algorithm-based system under dispersive fading for an 8 user system with different filter lengths is plotted in Figure 5.10. Performance enhancement of nearly 4 dB may be observed as a result of increasing the filter length from 1 to 32.

5.6.3 The Hierarchical Case

The effect of the choice of adaptation algorithms on a collaborative sensing system consisting of 16 sensing and 8 processing nodes for a FRESH filter length of 16 in a flat fading channel is illustrated in Figure 5.11. It may be observed that the detection performance for the ATC-LMS algorithm with inter processing node cooperation outperforms both local LMS as well as ATC-LMS without node cooperation. Therefore, it may be inferred that an increase in the communication cost results in an improved detection performance. The effect of increasing the FRESH filter length in a flat fading case the same number of nodes

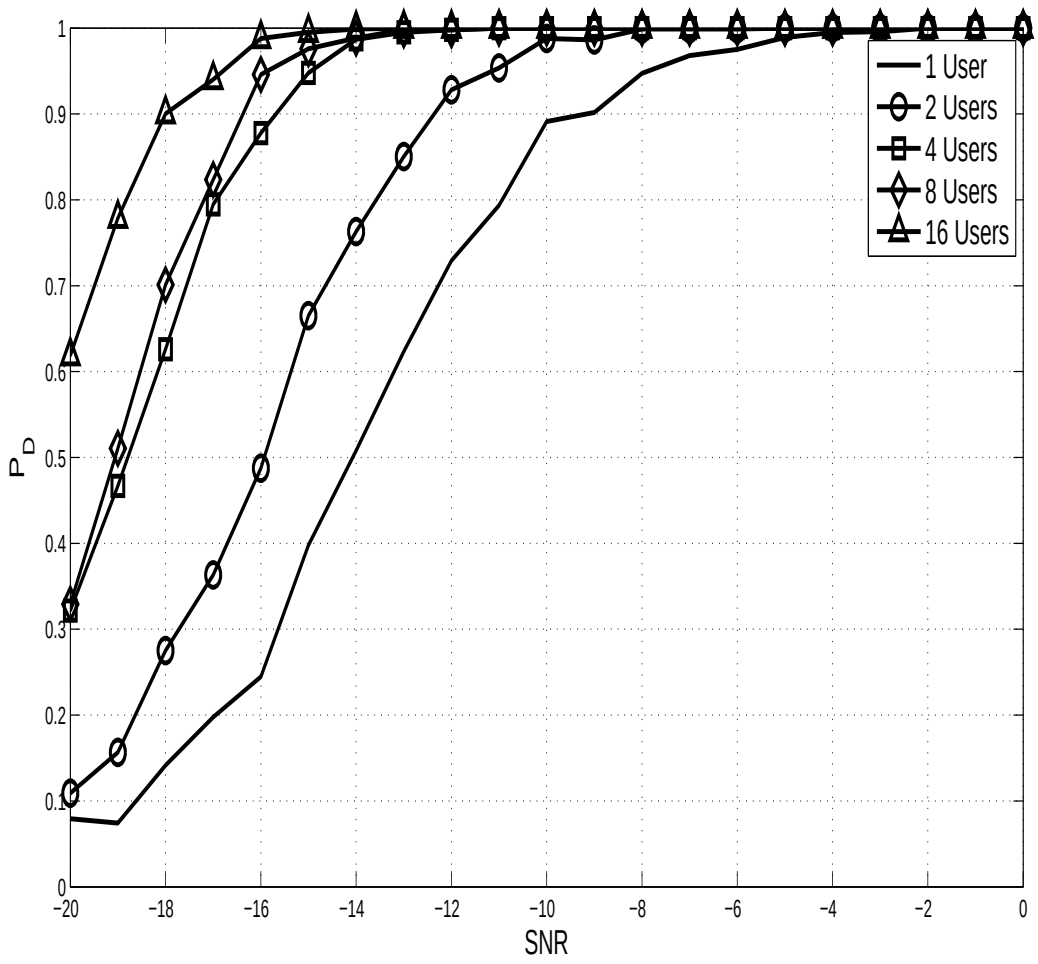

Figure 5.4: Performance using the C2LMS algorithm and the energy detector for a FRESH filter length of 8 and different number of users in a dispersive channel

Table 5.2: Gains (in Decibel) offered by the different algorithms for $N = 500$ and $K = 16$ for a dispersive Channel

Filter Length	1	2	4	8	16	32
Local LMS	0	0.1	0.835	1.817	2.76	3.32
C2LMS	0	0.98	2.32	2.97	3.54	4.07

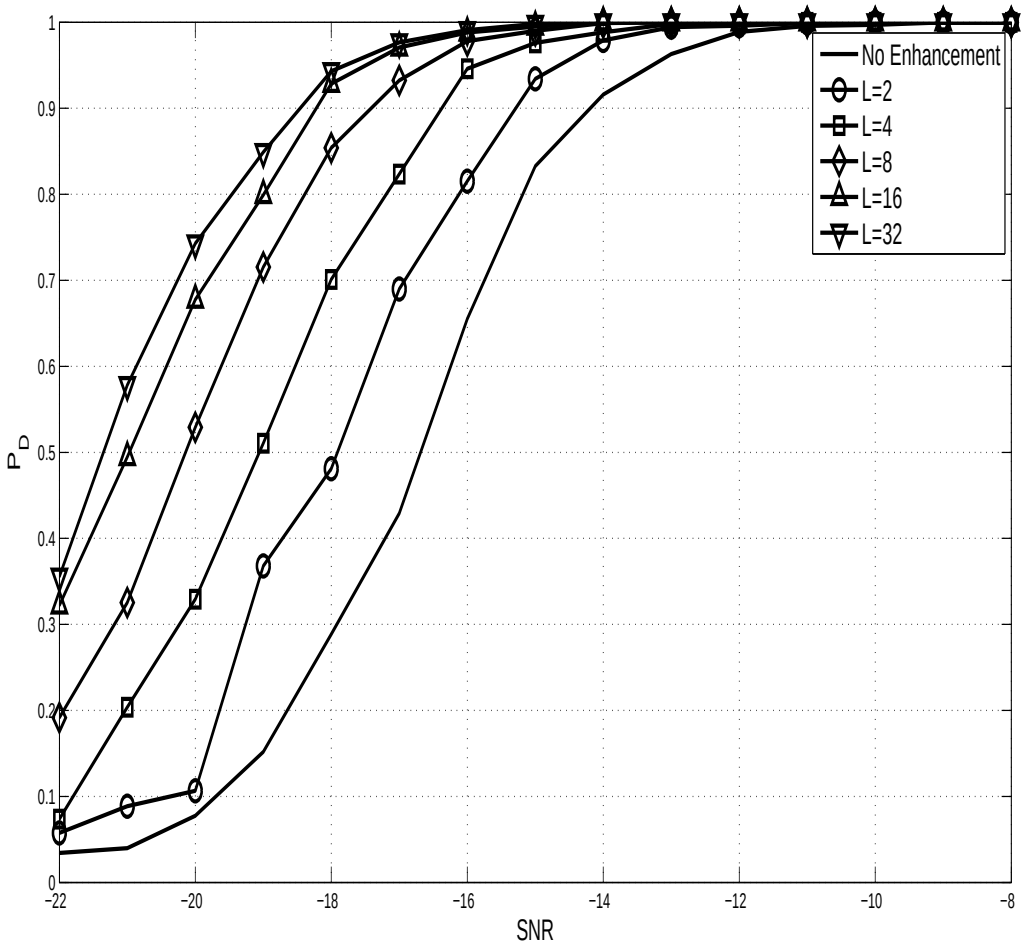

Figure 5.5: Performance using the C2LMS algorithm and the energy detector for 8 users and different filter lengths in a dispersive channel

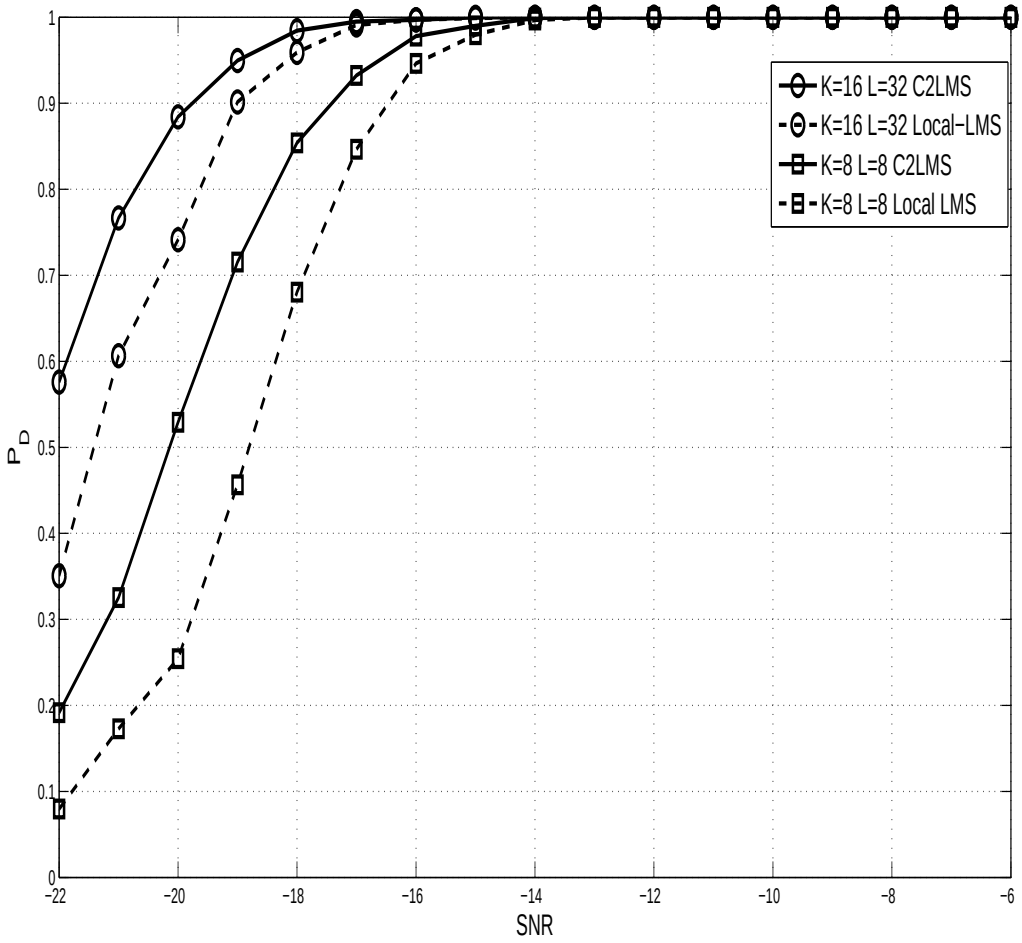

Figure 5.6: Comparison of different adaptation algorithms for different user/filter configurations in a dispersive channel

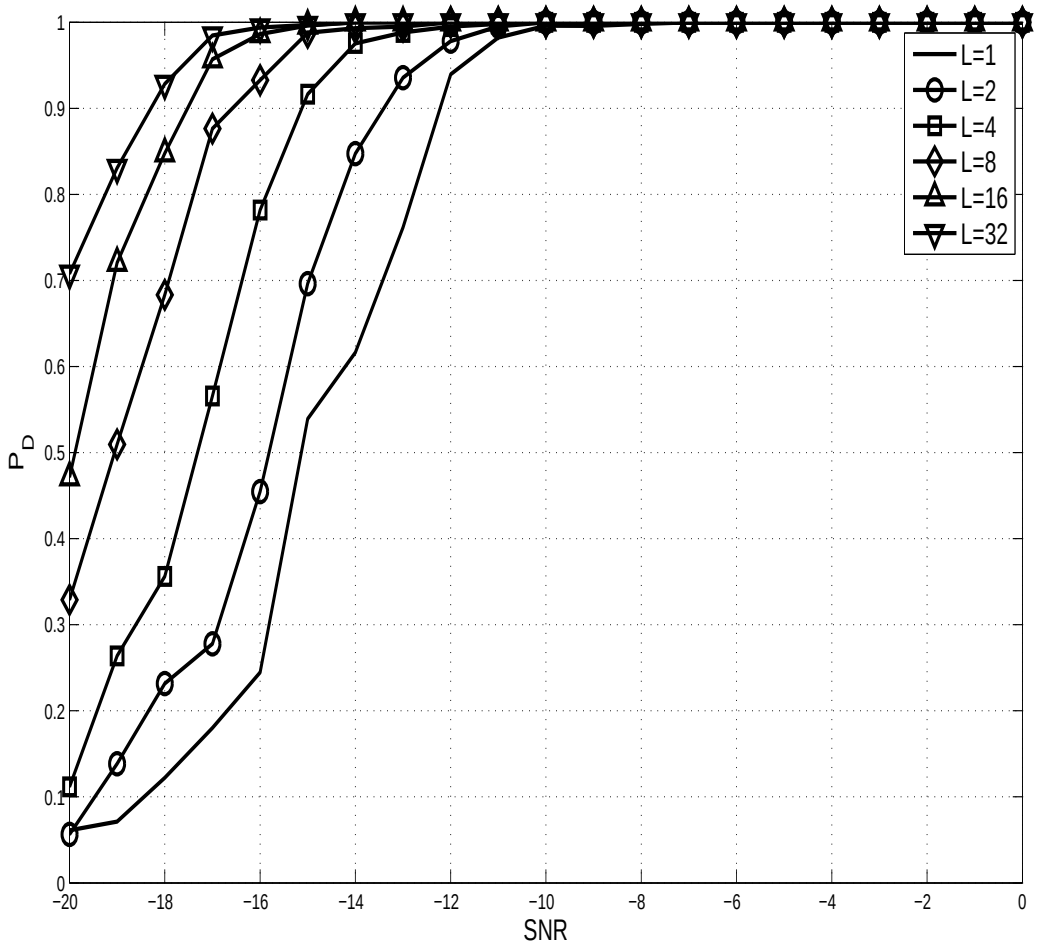

Figure 5.7: Performance of a 16 antenna fully distributed system for different filter lengths adapted using the ATC-LMS algorithm

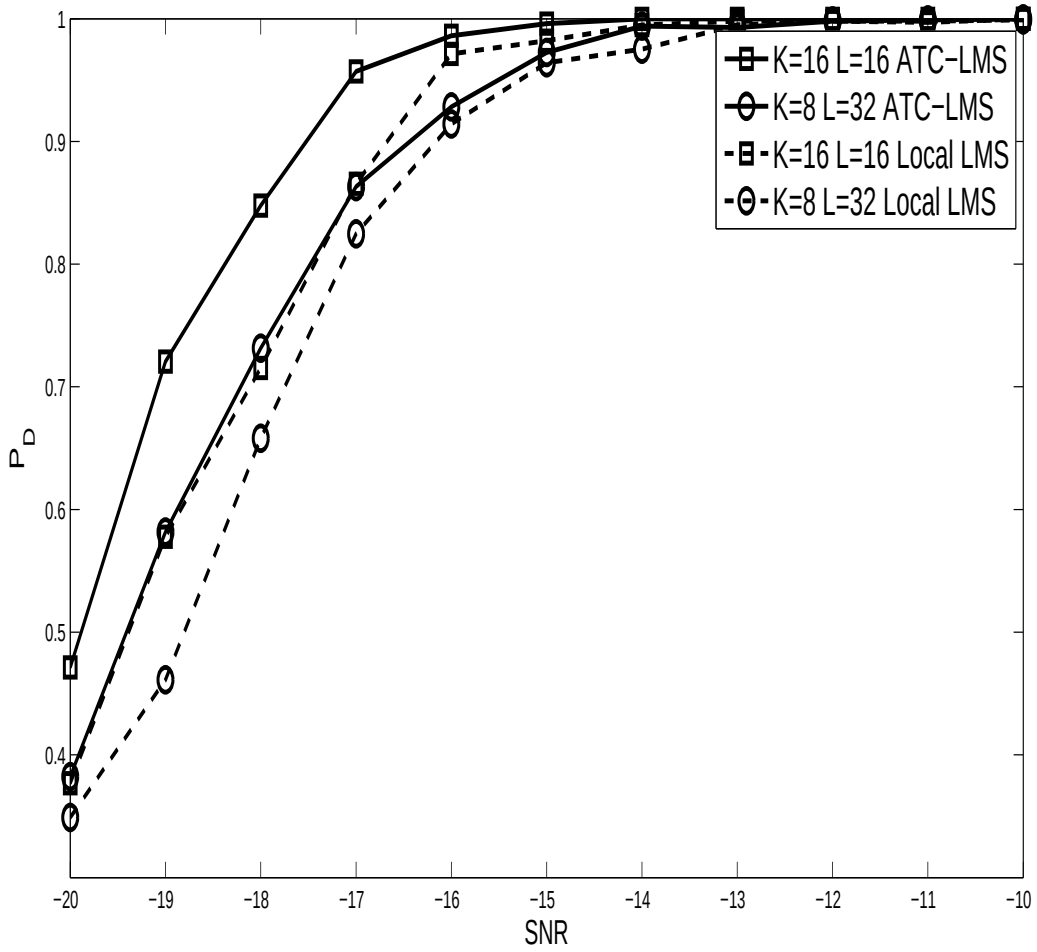

Figure 5.8: The effect of the choice of adaptation algorithm on a fully distributed system

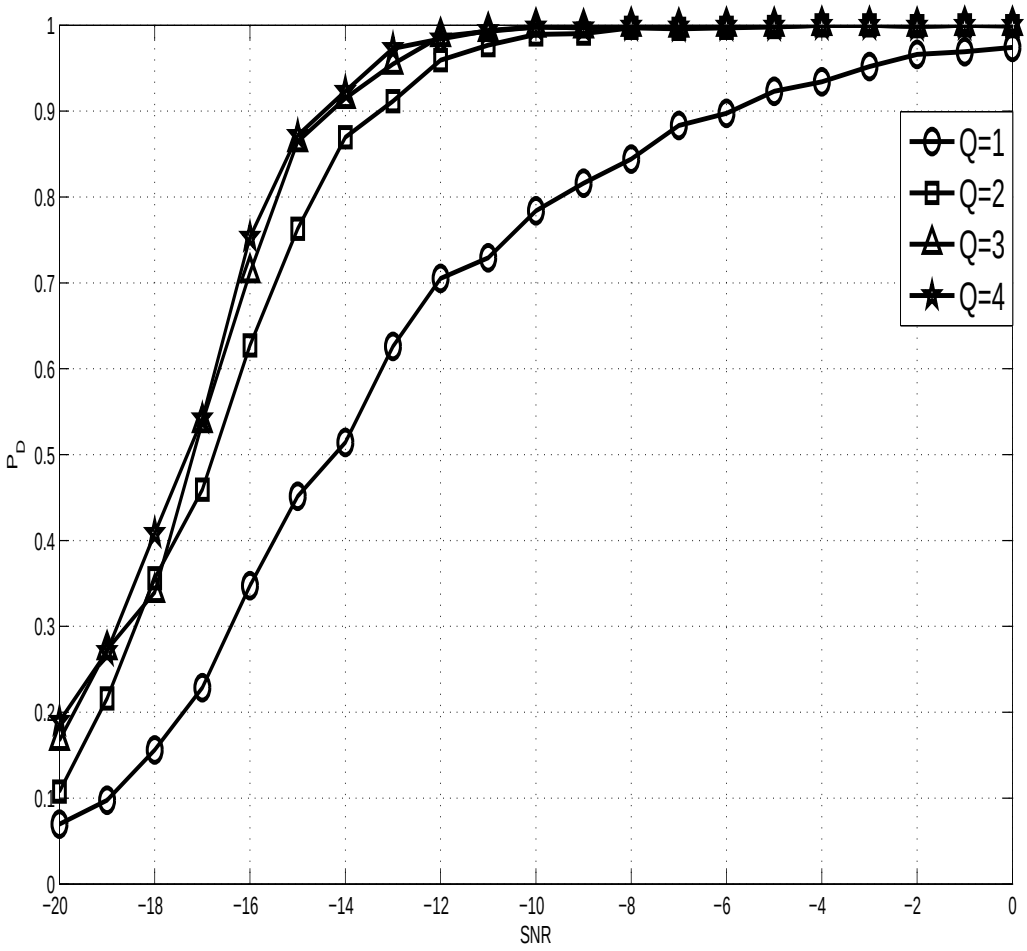

Figure 5.9: The effect of the number of consensus steps on the performance of a fully distributed system

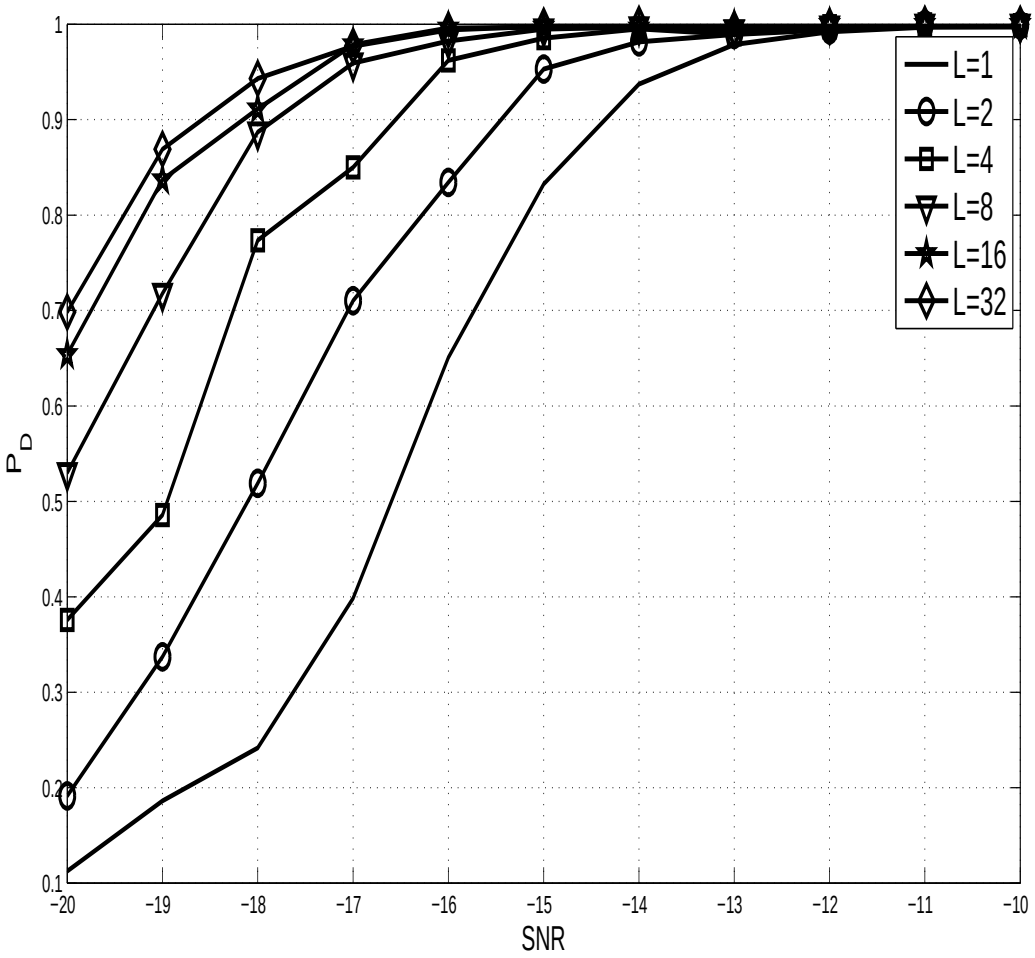

Figure 5.10: Performance of the distributed sensing setup for an 8 user system for different filter lengths under dispersive fading

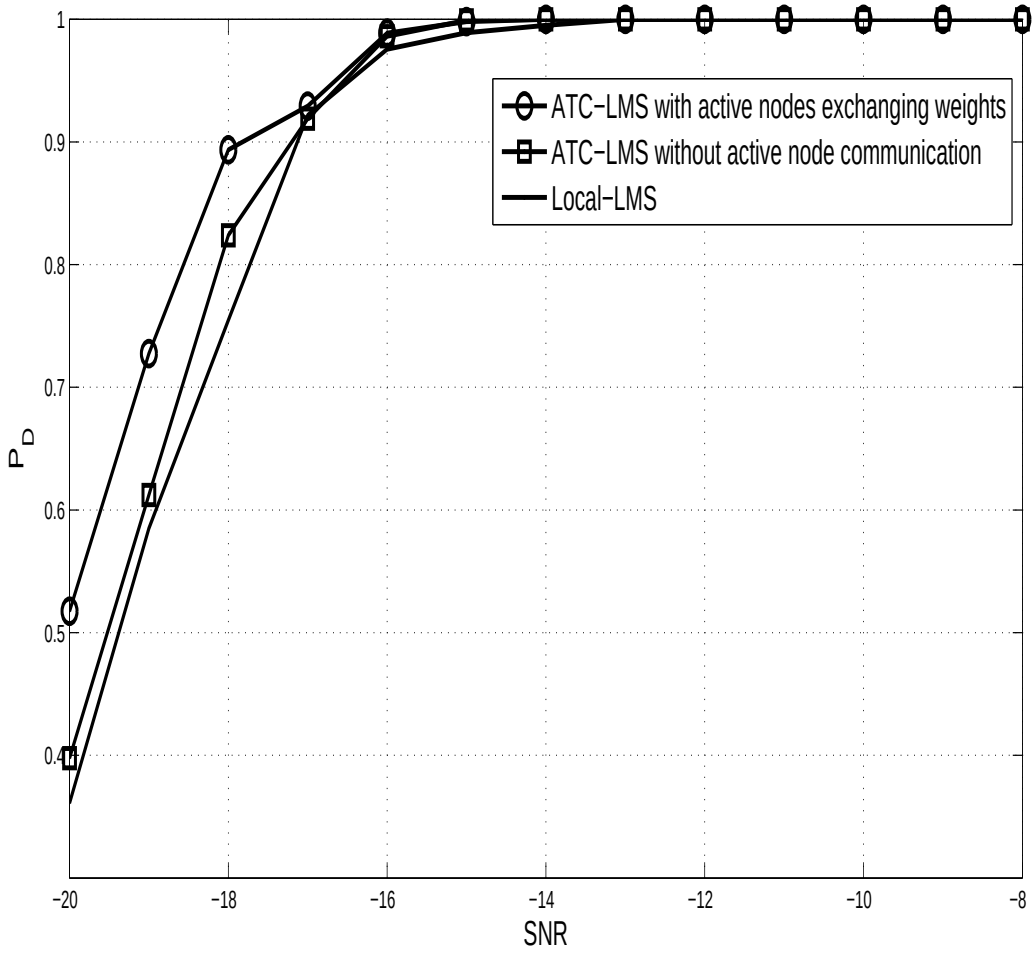

Figure 5.11: Comparison of performance of different adaptation algorithms for 16 sensing and 8 processing nodes for a FRESH filter length of 16

.

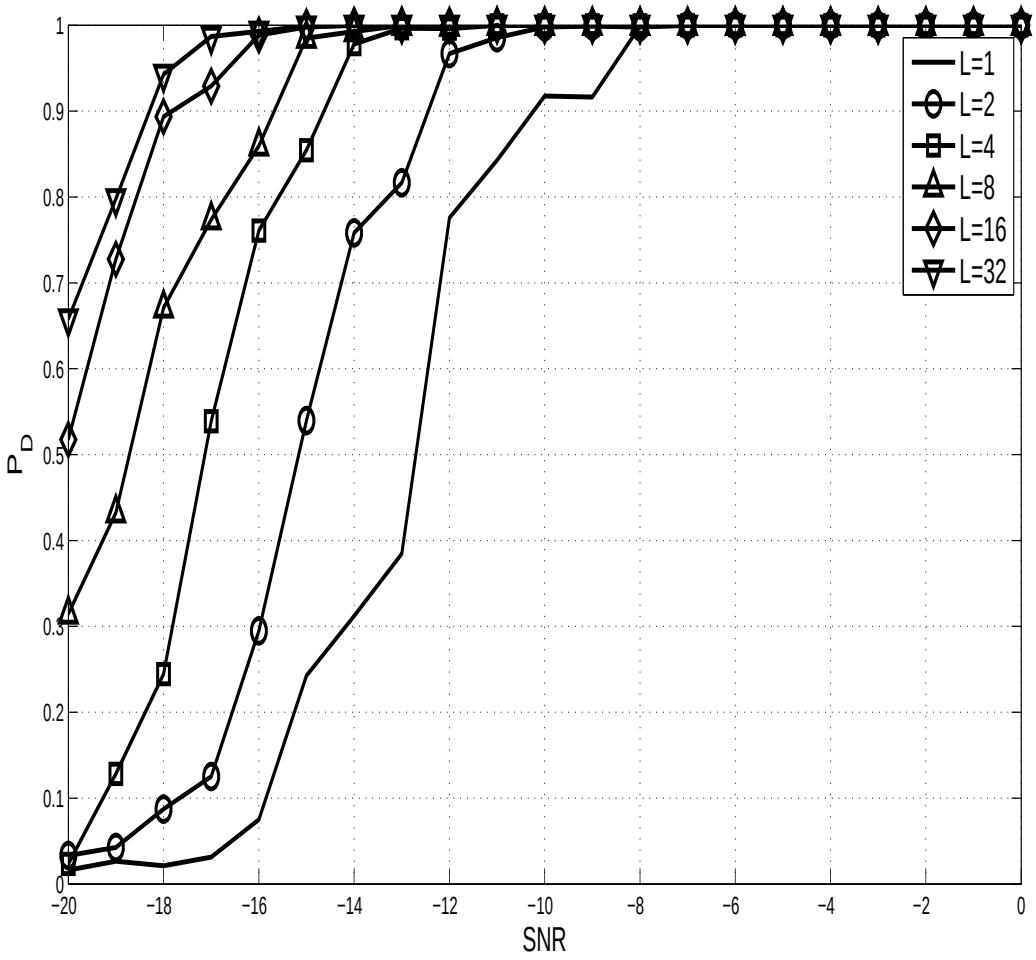

Figure 5.12: Comparison of performance of different filter lengths for 16 sensing and 8 processing nodes adapted using the ATC-LMS algorithm

.

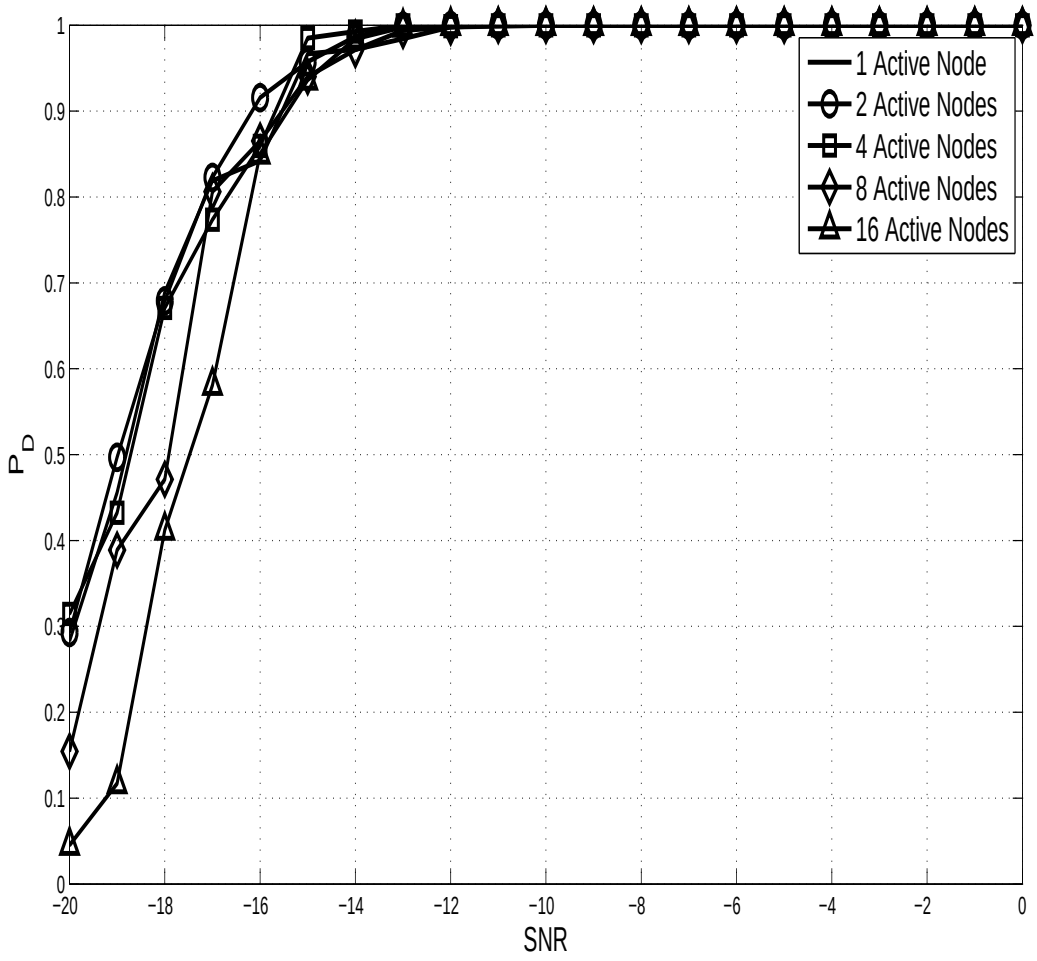

Figure 5.13: Comparison of performance for different number of processing nodes for 16 sensing nodes for a FRESH filter of length 8

is shown in Figure 5.12. Yet again a gain of more than 8 dB for a successful detection rate of 90% is observed here.

The effect of increasing the number of processing nodes for a 16 sensing node network with a FRESH filter of length 8 is shown in Figure 5.13. A slight performance degradation at the lower SNRs is observed as the system moves from purely centralized to purely distributed. This may also be viewed as a comparison of the three approaches for spectrum sensing. Here, the single active node case is equivalent to the purely centralized setup and the 16 active node case is similar to the purely distributed setup.

5.7 Conclusions

The performance enhancement achieved using FRESH filters in a multiple secondary users case, as well as the performance enhancement introduced due to joint adaptation of these filters, are studied in this chapter. It is shown that the optimal FRESH filter weights for a spectrum sensor depend on the channel conditions and the inter sample interval at the spectrum sensor. Based on this fact, different algorithms to adapt the FRESH filters present at different secondary users have been proposed. This is considered for three different cooperation scenarios viz. centralized, distributed and hierarchical.

Simulation results show that the performance of FRESH filter-based collaborative sensing algorithms depend on the filter length, structure of the sensing network as well as the adaptation algorithm being employed. It is further shown that in the case of a flat fading channel joint adaptation offers significant gains at the cost of a higher communication requirement. Similar results are observed for a dispersive channel although the gains in this case are not as significant as those in the flat fading case.

Chapter 6

Cyclosatationary Spectrum Sensing for OFDM Signals in the Presence of Cyclic Frequency Offset

In this chapter, a detector for the cyclostationarity induced due to correlation in pilot tones of OFDM signals is proposed[1]. This detector uses the cyclic autocorrelation function of the received signal at different cyclic frequencies and lags as features and it is shown that the detector performance improves with an increase in the number of features being used.

As noted in the previous chapters, the performance of this detector depends on the correct knowledge of the cyclic frequency of the primary signal. The performance of this detector in the presence of a cyclic frequency offset is derived and hence seen to degrade considerably under the effects of CFO and must be compensated for. As an alternative to the method proposed in [103], it is proposed to estimate the correct cyclic frequency from the received samples. The Crammer-Rao bound on the variance of the true cyclic frequency estimator is derived and it is found that the variance of the cyclic frequency estimate is directly proportional to the magnitude of the CFO. As a consequence, recursive algorithms to estimate the true cyclic frequency of the primary signal are developed.

A brief review of the state of the art in the spectrum sensing techniques for OFDM signals is given in Section 6.1. The detector for cyclostationary features introduced due to correlated pilots has been derived along with its performance in Section 6.2. The effect of CFO on the detector performance is derived and the necessity for CFO estimation are explained in Section 6.3. Section 6.4 contains the Cramer-Rao bound on the performance of a CFO estimator. Using this bound, Section 6.5 proposes a recursive CFO estimation algorithm based on gradient ascent while Section 6.6 proposes a higher complexity CFO estimation algorithm based on the greedy search approach. Simulation results are presented

[1]A part of this work has been published in International Conference on Signal Processing and Communications (SPCOM 2014) as "Cyclostationary Spectrum Sensing for OFDM Signals in the Presence of Cyclic Frequency Offset" and the complete work has been communicated to IEEE Transactions on Vehicular Technology

in Section 6.7 following which the conclusions are drawn in Section 6.8.

6.1 Background and Motivation

Most of the methods developed for OFDM signal sensing are based on the detection characteristics introduced due to one or more of its inherent features, such as the cyclic prefix or the pilot tones. These characteristics include temporal and spectral correlation within an OFDM symbol. It is shown in [133] that OFDM signals lose their cyclostationarity properties due to the subcarrier orthogonality. It is also shown in this paper, that the cyclic prefix reintroduces cyclostationarity in an OFDM signal because of the periodicity introduced due to symbol repetition.

In [25], the authors proposed to use the autocorrelation properties introduced due to the cyclic prefix as features. It is observed that the cyclic prefix inserted in an OFDM symbol in order to avoid multipath effects introduces temporal correlation in the symbol, and may be used to distinguish it from white noise. It is shown that the log likelihood ratio test reduces to a function of the length of the cyclic prefix. Also the detection performance of this detector is shown to be directly proportional to the cyclic prefix length. This method is then extended to a collaborative scheme and its performance is tested under various fading channels. Further, a sequential detection scheme based on the proposed test statistic is developed and its performance is evaluated and compared against the fixed sample size scheme.

Another method that exploits the correlation introduced due to the cyclic prefix in an OFDM system was given by Axell and Larsson in [8]. The authors in this case developed optimal and sub optimal detectors for an OFDM system containing cyclic prefixes of known lengths. The first case is when the signal and noise variances are known to the cognitive user. In this case the optimal likelihood ratio test is a function of the length of the cyclic prefix and reduces to the energy detector when the cyclic prefix is absent. In case the signal and noise variances are unknown at the secondary user terminal, the authors also proposed a GLRT based test for the presence of the primary signal. This test uses the fact that the presence of a cyclic prefix causes the primary signal to have a time varying autocorrelation function and hence becomes non=stationary. The test statistic in this case is based on the variation of the autocorrelation function at a fixed lag with time.

It is shown in [13] that the performance of the standard cyclic prefix based sensing algorithms may degrade in a rich multipath fading environment. As a remedy to this a constrained GLRT-based sensing algorithm is proposed to detect the primary user signal under such environments. It is further shown that Cyclic Prefix Correlation-based detector is a special case of the proposed constrained GLRT detector. Following this, a GLRT-based detection algorithm is developed for unsynchronized OFDM signals.

A coexistence scheme between OFDM-based WiMAX and ultra-wideband (UWB) sys-

tems is studied in [123]. The proposed method exploits cyclostationarity introduced due to the cyclic prefix. Since a cyclostationary signal has a nonzero cyclic autocorrelation function only at certain fixed values of the cyclic frequencies, the test statistic is the ratio of the absolute value of the cyclic ACF of the received signal at a known cyclic frequency to its value at an arbitrary cyclic frequency. The presence of a primary signal will result in a high value of this test statistic whereas in its absence this ratio will be close to unity.

It is observed in [105] that the cyclostationarity induced due to cyclic prefix is weak and performs much worse in comparison to an energy detector except at very low signal to noise ratios. Alternatively, it is proposed to allow excess bandwidth while designing the OFDM symbol in the frequency domain. Raised cosine pulse shaping is used for this purpose. However, this too does not improve the detection performance much.

Pilots are inserted in OFDM symbols for various purposes such as synchronization and channel estimation. However, the pilots being repeated across different OFDM symbols, these may be correlated to each other, and introduce certain correlation properties in the primary user signal which may be used to detect its presence. The use of pilot tones for detection of an OFDM symbol was first proposed in [27]. It is assumed that the locations and values of the pilot tones remain unchanged across different OFDM symbols and, therefore, the pilot components of these symbols will also remain constant. As a result, different OFDM symbols are correlated. The empirical symbol correlation may be used as a test statistic. The performance of this technique is tested for the DTV-B standard and is compared against various cyclic prefix-based methods.

Pilot induced temporal correlation has also been exploited in [144]. This paper considers OFDM signals using both continuous as well as scattered pilots. A likelihood ratio test based on the statistical properties of the finite time autocorrelation function is derived. Practical approximations of different parameters required for this test are then proposed and a GLRT like method is developed. It is also shown that the autocorrelation function may as well be used to estimate the Carrier Frequency Offset in the concerned system.

It is observed in [138] that correlated pilots may result in spectral correlation among OFDM symbols and, therefore, a primary signal using OFDM for modulation will exhibit cyclostationarity.In this paper the cyclic spectral density of the received signal is used as a feature. The test statistic is obtained as the empirical correlation between the short time Fourier transform of the received signal. This method requires symbol level synchronisation between the primary and the secondary users. It is shown that the loss of synchronization results in performance degradation. Following this, the performance of this detector is studied under various impairments, viz. Carrier Frequency Offset, I/Q imbalance, Phase Noise and Sampling Clock Frequency Offset. Methods to compensate for the performance loss caused due to these impairments are also described in detail.

It is observed that the received signal amplitude varies drastically in the presence of fading and shadowing. The variation in amplitudes will also affect the strength of the

cyclic autocorrelation peaks which will reduce the reliability of the detector. A method to circumvent this problem is given in [80]. The authors here proposed the use of the cyclic autocorrelation of the sign function of the complex envelop received signal. The sign function for a complex number z is defined as

$$sign(z) = \frac{z}{|z|}$$

It is shown in [80] that the cyclostationary properties of the signal are preserved if the sign function is used instead of the actual values. This fact is used to derive the cyclostationary features of the sign function of a received signal. It has been shown that tests similar to the ones used to detect the presence of cyclostationary signals may be applied here to detect the presence of the signal. The loss of information due to the signal amplitudes is compensated for by the use of larger number of samples. Sequential and cooperative techniques using this scheme have also been proposed in [80]. It is observed in [130] that the angle of the sign cyclic autocorrelation function is uniformly distributed in the absence of a primary signal. This property was used by the authors in [130] to develop a test for the presence of the primary OFDM signal.

Artificially induced cyclostationarity to assist OFDM signal detection are proposed in [120]. The proposed method involves artificially correlating different subcarriers of the transmitted signal so as to introduce a spectral coherence in the signal. This may be done at one or more frequency differences as per the requirement for features. It is seen that if multiple cyclic frequencies are introduced then the effect of frequency selective fading upon the detector performance can be overcome. An optimal detector for detecting induced cyclostationary signatures has been developed in [105].

Induced cyclostationarity-based methods for OFDM signal detection have also been considered in [115]. It is argued in this paper that the cyclostationary signatures should not affect the capacity of the system. Consequently, methods that introduce cyclostationary signatures in the symbol while trying to maximize its capacity are derived. It is proposed in this paper to use the higher order statistics of the recieved signal to detect the presence of these signatures. However, the methods based on induced cyclostationarity require changing the primary user signal structure and, therefore, may only be used for detecting secondary user signals.

In this chapter, we use the correlated pilot induced cyclostationarity to develop a detector for OFDM signals. The finite time cyclic autocorrelation function at different lags is used as a test statistic. The performance of this detector is also studied under cyclic frequency offset. It is found that the effects caused due to CFO agree with those reported in [103]. However, the technique proposed in [103] causes a loss in the number of features being used for detection, thereby compromising the detection performance. Therefore, as an alternative, it is proposed in this chapter to first estimate the true cyclic frequency of

received signal and then use it to detect the presence of the primary signal.

We develop a recursive greedy search algorithm to find the optimal cyclic frequency maximizing the SCORE objective function as proposed in [73]. The performance of this algorithm is studied via simulation and it is found that the proposed algorithm can compensate for the effects of CFO. A gradient ascent algorithm for Cyclic Frequency estimation is proposed in [73]. The convergence properties of this algorithm are studied and it is shown using simulation results that this algorithm can compensate for the effects of CFO.

6.2 Signal Model and The Proposed Detector

6.2.1 The Primary User Signal Model

Let the primary user OFDM signal consist of N_d data subcarriers. Out of these, let N_p be uniformly spaced pilot subcarriers whose locations are given by the elements of the index set Π. Let, the OFDM symbol use a cyclic prefix of length N_c resulting in a total OFDM symbol length $N_s = N_c + N_d$. If the symbol being sent over the mth subcarrier of the kth OFDM symbol is given as $\tilde{s}_k[m]$ then, as in [138], the following two conditions are assumed to be true. First, the magnitudes and phases of the pilots remain constant over all OFDM symbols, i.e. for $m \in \Pi$,

$$\tilde{s}_k[m] = p[m] = \sqrt{\mathcal{E}_s} e^{j\theta_m} \quad \forall k \tag{6.1}$$

where $\mathcal{E}_s$ is the average subcarrier energy of the OFDM symbol and θ_m is the phase associated with the mth subcarrier. Secondly, it is assumed that correlation exists between the pilot values which is purely a function of the difference in pilot locations, i.e. for $m, l \in \Pi$

$$E\left[p[m]p^*[l]\right] = \mathcal{E}_s e^{j\theta_{m-l}} \tag{6.2}$$

The primary signal transmitted at the nth instant of time may be written in the form

$$s[n] = \sum_k s_k[n - KN_s](u[n - KN_s] - u[n - (k+1)N_s + 1]) \tag{6.3}$$

where $s_k[n]$ is the nth sample of the kth OFDM symbol, defined as

$$s_k[n] = \begin{cases} \frac{1}{\sqrt{N_d}} \sum_{m=1}^{N_d} s_k[m] e^{\frac{j2\pi mn}{N_d}} & 0 \le n \le N_s - 1 \\ 0 & \text{otherwise} \end{cases} \tag{6.4}$$

For $0 \leq n < N_s$ this may be re written as

$$\begin{aligned} s_k[n] &= \frac{1}{\sqrt{N_d}} \sum_{m=1}^{N_d} \tilde{s}_k[m] e^{\frac{j2\pi mn}{N_d}} \\ &= \frac{1}{\sqrt{N_d}} \sum_{m\in\Pi} \tilde{s}_k[m] e^{\frac{j2\pi mn}{N_d}} + \frac{1}{\sqrt{N_d}} \sum_{m\notin\Pi} \tilde{s}_k[m] e^{\frac{j2\pi mn}{N_d}} \\ &= \frac{1}{\sqrt{N_d}} \sum_{m\in\Pi} p[m] e^{\frac{j2\pi mn}{N_d}} + \frac{1}{\sqrt{N_d}} \sum_{m\notin\Pi} \tilde{s}_k[m] e^{\frac{j2\pi mn}{N_d}} \\ &= s_k^{(p)}[n] + s_k^{(d)}[n] \end{aligned} \tag{6.5}$$

The pilot locations and values remain unchanged over different OFDM symbols. Therefore, we have

$$s^{(p)}[n] = s^{(p)}[n + kN] \tag{6.6}$$

6.2.2 The Spectrum Sensing Model

The task of the spectrum sensor is to decide the presence of a primary signal based on the received samples. It is assumed that the sensing receiver knows the transmitting signal parameters and the received signal is down-converted to baseband while maintaining the sampling rate of the primary user. Thus, the received signal $x[n]$ under the two hypotheses may be written as

$$x[n] = \begin{cases} \nu[n] & \mathcal{H}_0 \\ s[n] + \nu[n] & \mathcal{H}_1 \end{cases} \tag{6.7}$$

where $\nu[n]$ is the zero mean complex Gaussian noise having a variance σ_ν^2, $\mathcal{H}_0$ is the null hypothesis corresponding to the absence of a primary signal and $\mathcal{H}_1$ is the alternate hypothesis corresponding to its presence.

Let $\hat{R}_{xx}^{\alpha}[N, \tau]$ be the time-averaged frequency-shifted lag product at lag τ and frequency shift α, defined for N received samples as

$$\hat{R}_{xx}^{\alpha}[N, \tau] = \frac{1}{N-\tau} \sum_{n=\tau}^{N-1} \xi_{xx}^{\alpha}[n, \tau] \tag{6.8}$$

where

$$\xi_{xx}^{\alpha}[n, \tau] = x[n] x^*[n - \tau] e^{-2\pi\alpha n} \tag{6.9}$$

is the frequency shifted lag product of $x[n]$. The signals $s[n]$ and $\nu[n]$ may both be assumed to be independent of each other. Also, the individual samples of both $s[n]$ and $\nu[n]$ may be assumed as identically distributed Gaussian. Therefore, the samples of $x[n]$ and, hence, $\xi_{xx}^{\alpha}[n - \tau]$ may be assumed to be identically distributed. Further, as $\hat{R}_{xx}^{\alpha}[N, \tau]$ is a sum of a large number of random variables, it may be assumed to have a complex Gaussian pdf under both the hypotheses.

Now,

$$\begin{aligned} E\left[\hat{R}_{xx}^{\alpha}[N, \tau]\right] &= \frac{1}{N-\tau} \sum_{n=\tau}^{N-1} E\left[\xi_{xx}^{\alpha}[n, \tau]\right] \\ &= E\left[\xi_{xx}^{\alpha}[n, \tau]\right] \end{aligned} \tag{6.10}$$

In the absence of the primary user signal, we have

$$\xi_{xx}^{\alpha}[\tau]\,|\mathcal{H}_0 = \nu[n]\nu^*[n-\tau]e^{-j2\pi\alpha n} \tag{6.11}$$

Since the noise is assumed to be zero mean wide sense stationary i.i.d.,

$$E\left[\xi_{xx}^{\alpha}[\tau]\,|\mathcal{H}_0\right] = \sigma_\nu^2\delta(\alpha)\delta[\tau] \tag{6.12}$$

where $\delta(.)$ represents the Dirac Delta function and $\delta[.]$ represents the Kronekar Delta function

In case the primary user signal is present then, we get

$$\xi_{xx}^{\alpha}[\tau]\,|\mathcal{H}_1 \;=\; (s^{(p)}[n]+s^{(d)}[n]+\nu[n])(s^{(p)*}[n-\tau]+s^{(d)*}[n-\tau]+\nu^*[n-\tau])e^{-j2\pi\alpha n} \tag{6.13}$$

Since $s^{(d)}[n]$, $s^{(p)}[n]$ and $\nu[n]$ are zero mean and independent of each other [144],we have

$$\begin{aligned} E\left[\xi_{xx}^{\alpha}[\tau]\,|\mathcal{H}_1\right] \;=\; & E\left[s^{(d)}[n]s^{*(d)}[n-\tau]e^{-j2\pi\alpha n}\right] + E\left[s^{(p)}[n]s^{*(p)}[n-\tau]e^{-j2\pi\alpha n}\right] \\ & + E\left[\nu[n]\nu^*[n-\tau]e^{-j2\pi\alpha n}\right] \end{aligned} \tag{6.14}$$

It may be shown that

$$E\left[s^{(p)}[n]s^{*(p)}[n-\tau]e^{-j2\pi\alpha n}\right] = \begin{cases} \frac{N_p}{N_d}\mathcal{E}_s e^{j\theta_\alpha} & \alpha = \frac{m-l}{N_d}, m,l\in\Pi, \tau = kN \\ 0 & \text{otherwise} \end{cases} \tag{6.15}$$

$$E\left[s^{(d)}[n]s^{*(d)}[n-\tau]e^{-j2\pi\alpha n}\right] = \begin{cases} \frac{N_c}{N_s}\mathcal{E}_s & \alpha = 0, \tau = \pm N_d \\ \mathcal{E}_s & \alpha = 0, \tau = 0 \\ 0 & \text{otherwise} \end{cases} \tag{6.16}$$

It may also be shown that for $\alpha \neq 0$

$$var\left(\hat{R}_{xx}^{\alpha}[\tau]\,|\mathcal{H}_0\right) = \frac{1}{N-\tau}\sigma_\nu^4 \tag{6.17}$$

$$var\left(\hat{R}_{xx}^{\alpha}[\tau]|\mathcal{H}_1,\right) = \frac{1}{N-\tau}\left(\mathcal{E}_s+\sigma_\nu^2\right)^2 \tag{6.18}$$

Therefore, the distributions of $\hat{R}_{xx}^{\alpha}[N,\tau]$ for $\alpha = m\frac{1}{N_d}, m\in\{1,2,\ldots,N_p\}$ and $\tau = kN_s, k\in\left\{1,2,\ldots,\left\lfloor\frac{N}{N_s}\right\rfloor\right\}$ under the two hypotheses are

$$\hat{R}_{xx}^{\alpha}[N,\tau] \sim \begin{cases} \mathcal{N}_c\left(0,\frac{\sigma_\nu^4}{N-\tau}\right) & \mathcal{H}_0 \\ \mathcal{N}_c\left(\frac{N_p}{N_d}\mathcal{E}_s e^{j\theta_\alpha},\frac{\left(\mathcal{E}_s+\sigma_\nu^2\right)^2}{N-\tau}\right) & \mathcal{H}_1 \end{cases} \tag{6.19}$$

It may also be noted here that in addition to the correlated pilots, the cyclic prefix will also cause $x[n]$ to exhibit cyclostationarity. However, as discussed previously these cyclostationary features are weak and are dependent on the length of the cyclic prefix, which is a function of the channel conditions. Therefore, we consider only the effects of pilot induced cyclostationarity. Now, $\hat{R}^{\alpha}_{xx}[N,\tau]$ may be assumed to be independent for different values of α and τ. Hence, the values of the time averaged frequency shifted lag product, also known as the finite time cyclic autocorrelation function [50], at different values of α and τ may be used to detect the presence of the primary user. Thus, the performance of the detector depends on the correct knowledge of the noise variance σ^2_ν, the primary signal energy at the spectrum sensor $\mathcal{E}_s$, and the phase θ_α. However, while the knowledge of σ^2_ν and θ_α at the spectrum sensor may be assumed, the exact knowledge of $\mathcal{E}_s$ may not be available at the spectrum senor. Nevertheless, as shown subsequently, detectors without the knowledge of these parameters may still be designed but at the cost of detection performance. For a cyclic frequency α the feature vector $\mathbf{r}_\alpha$ may be defined as

$$\mathbf{r}_\alpha = [\Re\{\hat{R}^{\alpha}_{xx}[N,N_s]e^{-j\theta_\alpha}\},\Re\{\hat{R}^{\alpha}_{xx}[N,2N_s]e^{-j\theta_\alpha}\},\ldots,\Re\{\hat{R}^{\alpha}_{xx}[N,PN_s]e^{-j\theta_\alpha}\}]^T \tag{6.20}$$

where P is the total number of lags being used as features and $\Re\{.\}$ denotes the real part of a complex number. Since the variances of different elements of $\mathbf{r}_\alpha$ are different, maximal ratio combining is preferred to obtain their optimal combination [100]. The vector $\mathbf{w} = [\sqrt{(N-N_s)},\sqrt{(N-2N_s)},\ldots,\sqrt{(N-PN_s)}]^T$, is defined as the weight vector to combine the cyclostationary features at different lags. These weights are chosen such that the weight assigned to a feature in the final test statistic is inversely proportional to its variance [100, 144]. Consequently, the test statistic detecting the presence of a signal exhibiting cyclostationarity at a cyclic frequency α may be written as

$$Z_\alpha = \mathbf{w}^T\mathbf{r}_\alpha = \sum_{k=1}^{P}\sqrt{(N-kN_s)}\Re\{\hat{R}^{\alpha}_{xx}[N,kN_s]e^{-j\theta_\alpha}\} \tag{6.21}$$

It may be observed that if the primary user signal exhibits cyclostationarity at more than one cyclic frequencies then Z_α for different cyclic frequencies are i.i.d. Gaussian. Let, a total of A cyclic frequencies may be used for signal detection and $\mathcal{A}$ be the set of the possible cyclic frequencies such that $|\mathcal{A}| = A$. Using all $\alpha \in \mathcal{A}$, the test statistic becomes

$$Z = \sum_{\alpha\in\mathcal{A}} Z_\alpha = \sum_{\alpha\in\mathcal{A}}\sum_{k=1}^{P}\sqrt{(N-kN_s)}\Re\{\hat{R}^{\alpha}_{xx}[N,kN_s]e^{-j\theta_\alpha}\} \tag{6.22}$$

From this, it becomes evident that

$$Z \sim \begin{cases} \mathcal{N}_s\left(0,\frac{AP\sigma^4_\nu}{2}\right) & \mathcal{H}_0 \\ \mathcal{N}_s\left(A\frac{N_p}{N_d}\mathcal{E}_s\sum_{k=1}^{P}\sqrt{(N-kN_s)},\frac{AP(\mathcal{E}_s+\sigma^2_\nu)^2}{2}\right) & \mathcal{H}_1 \end{cases} \tag{6.23}$$

If the above is used as a test statistic then the probabilities of false alarm and successful detection for a given threshold λ are given as

$$P_{fa} = Q\left(\frac{\lambda}{\sigma_\nu^2\sqrt{\frac{AP}{2}}}\right) \tag{6.24}$$

$$P_d(\lambda) = Q\left(\frac{\lambda - A\frac{N_p}{N_d}\mathcal{E}_s\sum_{k=1}^{P}\sqrt{(N-kN_s)}}{(\mathcal{E}_s+\sigma_\nu^2)\sqrt{\frac{AP}{2}}}\right) \tag{6.25}$$

It may be observed that the correct knowledge of $\mathcal{E}_s$ is essential for this detector. It is, however ,possible to design a constant false alarm rate (CFAR) detector even in the absence of this knowledge. If σ_ν^2 is unknown at the spectrum sensor then it may be approximated as [144]

$$\hat{\sigma}_\nu^2 = \frac{1}{N}\sum_{n=0}^{N-1}|y[n]|^2 \tag{6.26}$$

In case θ_α is not known at the spectrum sensor, then the feature vector may alternatively be given as $\mathbf{r}_\alpha = [\hat{R}_{xx}^\alpha[N,N_s],\hat{R}_{xx}^\alpha[N,2N_s],\ldots,\hat{R}_{xx}^\alpha[N,KN_s]\}]^T$ and the test statistic may be defined as

$$Z = \left|\sum_\alpha \mathbf{w}^H\mathbf{r}_\alpha\right| = \left|\sum_{\alpha\in\mathcal{A}}\sum_{k=1}^{P}\sqrt{(N-kN_s)}\hat{R}_{xx}^\alpha[N,kN_s]\right| \tag{6.27}$$

Consequently,

$$Z \sim \begin{cases} Rice\left(0,\sigma_\nu^2\sqrt{\frac{AP}{2}}\right) & \mathcal{H}_0 \\ Rice\left(A\frac{N_p}{N_d}\mathcal{E}_s\sum_{k=1}^{P}\sqrt{(N-kN_s)},(\mathcal{E}_s+\sigma_\nu^2)\sqrt{\frac{AP}{2}}\right) & \mathcal{H}_1 \end{cases} \tag{6.28}$$

where $Rice(p,q)$ represents a Rician distribution with a shifting factor p and a scaling factor q [94]. Therefore, in this case, the probability of false alarm for a given threshold λ will take the form

$$P_{fa}(\lambda) = e^{\frac{-\lambda^2}{AP\sigma_\nu^4}} \tag{6.29}$$

Alternatively, the detection threshold may be determined via simulation using the Neyman-Pearson criterion.

6.3 Effects of Cyclic Frequency Offset on a Cyclostationarity Detector

For a cyclostationary signal $x[n]$, the finite time approximation of the cyclic autocorrelation function, may be written as [72, 73, 103]

$$\begin{aligned}\hat{R}^{\alpha}_{xx}[N,\tau] &= \tfrac{1}{N-\tau}\sum_{n=\tau}^{N-1} x[n]x^*[n-\tau]e^{-j2\pi\alpha n} \\ &= \tfrac{1}{N-\tau}\sum_{n=-\infty}^{\infty} x[n]x^*[n-\tau]e^{-j2\pi\alpha n}\left(u[n-\tau]-u[n-N+1]\right) \\ &= \tfrac{1}{N-\tau}\sum_{n=-\infty}^{\infty} x[n]x^*[n-\tau]e^{-j2\pi\alpha n} * \sum_{n=-\infty}^{\infty}\left(u[n-\tau]-u[n-N+1]e^{-j2\pi\alpha n}\right) \\ &= R^{\alpha}_{xx}[\tau] * \left(e^{-j\pi\alpha(N-\tau-1)}\tfrac{sin(\pi(N-\tau)\alpha)}{(N-\tau)sin(\pi\alpha)}\right).\end{aligned} \tag{6.30}$$

where $R^{\alpha}_{xx}[\tau]$ is the true value of the cyclic autocorrelation function and $*$ denotes convolution over cyclic frequency. If the signal $x[n]$ exhibits cyclostationarity at certain discrete cyclic frequencies whose values are contained in the set Γ, then the cyclic autocorrelation function may be written as

$$R^{\alpha}_{xx}[\tau] = \sum_{\gamma\in\Gamma} R^{\gamma}_{xx}[\tau]\delta(\alpha-\gamma) \tag{6.31}$$

Substituting (6.31) in (6.30), we have

$$\hat{R}^{\alpha}_{xx}[N,\tau] = \sum_{\gamma\in\Gamma} R^{\gamma}_{xx}[\tau]\left(e^{j\pi(\alpha-\gamma)(N-\tau-1)}\frac{\sin(\pi(N-\tau)(\alpha-\gamma))}{(N-\tau)\sin(\pi(\alpha-\gamma))}\right) \tag{6.32}$$

Now, for $\alpha_m \in \Gamma$, if the cyclic frequency known at the receiver is $\alpha = \alpha_m + \Delta$, where Δ is the CFO introduced due to one or more reasons as described earlier, (6.32) may be re-written as

$$\begin{aligned}\hat{R}^{\alpha}_{xx}[N,\tau] &= R^{\alpha_m}_{xx}[\tau]\left(e^{j\pi(\Delta)(N-\tau-1)}\tfrac{\sin(\pi(N-\tau)(\Delta))}{(N-\tau)\sin(\pi(\Delta))}\right) \\ &\quad + \textstyle\sum_{\gamma\in\Gamma,\gamma\neq\alpha_m} R^{\gamma}_{xx}[\tau]\left(e^{j\pi(\alpha-\gamma)(N-\tau-1)}\tfrac{\sin(\pi(N-\tau)(\alpha-\gamma))}{(N-\tau)\sin(\pi(\alpha-\gamma))}\right)\end{aligned} \tag{6.33}$$

For small Δ, the second term in (6.33) may be ignored leading to

$$\begin{aligned}\hat{R}^{\alpha}_{xx}[N,\tau] &\approx R^{\alpha_m}_{xx}[\tau]\left(e^{j\pi(\Delta)(N-\tau-1)}\tfrac{\sin(\pi(N-\tau)(\Delta))}{(N-\tau)\sin(\pi(\Delta))}\right) \\ &= R^{\alpha_m}_{xx}[\tau]g(\Delta,N-\tau)\end{aligned} \tag{6.34}$$

where

$$g(\Delta,N-\tau) = e^{j\pi(\Delta)(N-\tau-1)}\frac{\sin(\pi(N-\tau)(\Delta))}{(N-\tau)\sin(\pi(\Delta))} \tag{6.35}$$

It may be observed that, for a fixed Δ, the value of $g(\Delta, N)$ decreases with an increasing N, weakening the features and consequently degrading the detector performance. To avoid this behavior of the detector, Rebeiz et. al. in [103] proposed to divide the received

samples into Q non overlapping blocks each of length L $(QL < N)$, followed by calculating the finite time approximation of the cyclic autocorrelation function for each of these blocks, and finally averaging these estimates. The feature $\check{R}^{\alpha}_{ss}[Q, L, \tau]$ used for detection is thus defined as

$$\check{R}^{\alpha}_{xx}[Q, L, \tau] \;=\; \tfrac{1}{Q}\sum_{i=0}^{Q-1}\tfrac{1}{L-\tau}\sum_{iL+\tau}^{i+1} x[n]x^{*}[n-\tau]e^{j2\pi\alpha((n))_L} \tag{6.36}$$

where $((.))_L$ is the modulo L operator. In this case, a trade-off is required between the values of the block length (L) and the number of blocks (Q). It is proposed in [103] to arrive at an optimal combination of L and Q using convex optimization. However, it may be observed that $\tau \leq L$ and, hence, it is not possible to use the values of the cyclic autocorrelation function at lags greater than the block length as features, thereby limiting the detector performance. This is significant in cases such as the detector proposed in the previous section where the features exist only for large values of τ. This necessitates to look for alternative methods that avoid the effects of CFO while keeping the number of usable features unaltered. Accordingly, it is proposed that the CFO be first estimated from the available data and then compensated for. Approaches towards improving the performance of adaptive cyclostationary structures by compensating for the CFO have earlier been reported in [72, 73, 135]. However, to the best of our knowledge, no bounds on the performance of a CFO estimator have been reported in the literature so far. Motivated by this, the next section derives the Cramer Rao lower bound on the performance of a CFO estimator.

6.4 Cramer-Rao Bound for the CFO Estimator

Assume that N samples of a cyclostationary signal $s[n]$ corrupted by additive noise $\nu[n]$ are received by the spectrum sensor. If $s[n]$ exhibits cyclostationarity at a cyclic frequency α_m with the value of the cyclic autocorrelation function being $R^{\alpha_m}_{ss} = \eta e^{j\phi}$ then for a CFO Δ, the finite time approximate of the cyclic autocorrelation function at a cyclic frequency α and lag τ will be

$$\hat{R}^{\alpha}_{xx}[N, \tau] = \eta e^{j\phi} g(\Delta, N-\tau) + \zeta[N-\tau] \tag{6.37}$$

where $\zeta[N-\tau]$ is the error introduced due to finite averaging and $\zeta[N-\tau] \sim \mathcal{N}_c(0, \sigma^2_{\zeta,N-\tau})$ and $\sigma^2_{\zeta,N-\tau} \approx \frac{\sigma^4_{\nu}}{N-\tau}$ for low SNRs. Based on this, the probability density function (pdf) of $\hat{R}^{\alpha}_{xx}[N, \tau]$ may be obtained as

$$p\left(\hat{R}^{\alpha}_{xx}[N, \tau]|\eta, \phi, \Delta\right) = \frac{1}{\pi\sigma_{\zeta,N-\tau}} e^{-\left(\frac{\hat{R}^{\alpha}_{xx}[N,\tau]-\eta e^{j\phi}g(\Delta,N-\tau)}{\sigma_{\zeta,N-\tau}}\right)^2} \tag{6.38}$$

Defining

$$\mathbf{r} = \left[\Re\left\{\hat{R}^{\alpha}_{xx}[N, N_s]e^{-j\phi}\right\}, \Re\left\{\hat{R}^{\alpha}_{xx}[N, 2N_s]e^{-j\phi}\right\}, \ldots, \Re\left\{\hat{R}^{\alpha}_{xx}[N, PN_s]e^{-j\phi}\right\}\right]^T \quad (6.39)$$

the pdf of $\mathbf{r}$ may then be obtained as

$$p\left(\mathbf{r}|\eta\phi\Delta\right) = \prod_{k=1}^{P} \frac{1}{\sqrt{\pi}\sigma_{\zeta,N-kN_s}} e^{-\left(\frac{\hat{R}^{\alpha}_{xx}[N,\tau]-\eta e^{j\phi}g(\Delta,N-kN_s)}{\sigma_{\zeta,N-kN_s}}\right)^2} \quad (6.40)$$

Defining,

$$l(\mathbf{r}|\Delta) = \log\left(p\left(\mathbf{r}|\eta,\phi,\Delta\right)\right) \quad (6.41)$$

and substituting (6.40), we get

$$l\left(\mathbf{r}|\Delta\right) = \sum_{k=1}^{P} \log\left(\pi\sigma^2_{\zeta,N-kN_s}\right) - \sum_{k=1}^{P}\left(\frac{\hat{R}^{\alpha}_{xx}[N,\tau]-\eta e^{j\phi}g(\Delta,N-kN_s)}{\sigma_{\zeta,N-kN_s}}\right)^2 \quad (6.42)$$

Defining $f_{x_i}\left(x_1, x_2, \ldots, x_n\right)$ as the partial derivative of the function $f\left(x_1, x_2, \ldots, x_n\right)$, with respect to x_i, we may write the partial derivative of $l(r|\Delta)$ with respect to Δ as

$$l_{\Delta}\left(\mathbf{r}|\Delta\right) = 2\Re\left\{\sum_{k=1}^{P} \frac{\eta e^{j\phi}g_{\Delta}(\Delta,N-kN_s)\left(\hat{R}^{\alpha}_{xx}[N,\tau]-\eta e^{j\phi}g(\Delta,N-kN_s)\right)}{\sigma^2_{\zeta,N-kN_s}}\right\} \quad (6.43)$$

Since $E\left[l_{\Delta}\left(\mathbf{r}|\Delta\right)\right] = 0$, therefore, the Cramer-Rao bound on the variance of the estimation error of Δ exists [68].

Therefore, the variance of any arbitrary estimator $\hat{\Delta}$ of Δ must satisfy the following inequality.

$$var\left(\hat{\Delta}\right) \geq \frac{1}{I(\Delta)} \quad (6.44)$$

where $I(\Delta)$ is the Fisher information about Δ contained in $\mathbf{r}$, defined as $I(\Delta) = -E[l_{\Delta\Delta}\left(\mathbf{r}|\Delta\right)]$. where

$$\begin{aligned} l_{\Delta\Delta}\left(\mathbf{r}|\Delta\right) &= 2\Re\left\{\sum_{k=1}^{P} \frac{\eta e^{j\phi}g_{\Delta\Delta}(\Delta,N-kN_s)\left(\hat{R}^{\alpha}_{xx}[N,kN_s]-\eta e^{j\phi}g(\Delta,N-kN_s)\right)}{\sigma^2_{\zeta,N-kN_s}}\right\} \\ &\quad -2\Re\left\{\sum_{k=1}^{P} \frac{\eta^2|g_{\Delta}(\Delta,N-kN_s)|^2}{\sigma^2_{\zeta,N-kN_s}}\right\} \end{aligned} \quad (6.45)$$

As

$$E\left[\hat{R}^{\alpha}_{xx}[N,\tau]-\eta e^{j\phi}g(\Delta,N-kN_s)\right] = 0 \quad (6.46)$$

we have

$$E\left[l_{\Delta\Delta}\left(\mathbf{r}|\Delta\right)\right] = E\left[2\Re\left\{\sum_{k=1}^{P} \frac{\eta^2\left|g_{\Delta}(\Delta,N-kN_s)\right|^2}{\sigma^2_{\zeta,N-kN_s}}\right\}\right] \quad (6.47)$$

Now

$$|g_{\Delta}(\Delta, N-kN_s)|^2 = \frac{\pi^2}{sin^2(\pi\Delta)}\left[1-\frac{2sin(\pi\Delta(N-kN_s))[cot(\pi\Delta)cos((N-kN_s)\pi\Delta)+sin((N-kN_s)\pi\Delta)]}{N-kN_s} + \frac{sin^2((N-kN_s)\pi\Delta)csc^2(\pi\Delta)]}{(N-kN_s)^2}\right] \tag{6.48}$$

For $N-kN_s >> 1$ we have

$$|g_{\Delta}(\Delta, N-kN_s)|^2 \approx \frac{\pi^2}{sin^2(\pi\Delta)} \tag{6.49}$$

Substituting this in the definition of $I(\Delta)$ and simplifying

$$I(\Delta) = \frac{P\eta^2\pi^2}{\sigma_{\nu}^2 sin^2(\pi\Delta)}\left[N-\frac{(P+1)N_s}{2}\right] \tag{6.50}$$

Further substituting (6.50) into (6.44), the Cramer-Rao bound on the variance of an estimate $\hat{\Delta}$ of Δ may be written as

$$var(\hat{\Delta}) \geq \frac{\sigma_{\nu}^4 sin^2(\pi\Delta)}{2\eta^2\pi^2 P\left[N-\frac{(P+1)N_s}{2}\right]} \tag{6.51}$$

It is assumed for the purpose of this derivation that both η and ϕ are known. However, if these parameters are unknown then the estimator variance will naturally be greater than the case where they are known. This implies that (6.51) provides the lower bound on the CFO estimator variance for all cases.

It is observed that there exists no function $h(\mathbf{r})$ such that the following equation can be satisfied

$$\frac{dl(\mathbf{r}|\Delta)}{d\Delta} = I(\Delta)(h(\mathbf{r})-\Delta) \tag{6.52}$$

This implies that the minimum variance unbiased estimator cannot be found directly by the use of (6.52) [68]. Therefore, it becomes necessary to devise some alternative estimators for Δ.

It may also be observed from (6.51) that the minimum variance of $\hat{\Delta}$ depends on Δ and that Δ should be minimized in order to minimize the variance of $\hat{\Delta}$. It is evident that $\alpha = \alpha_m + \Delta$ where α_m is a fixed bias. Therefore (6.51) also gives the Cramer-Rao bound for an estimator of the true cyclic frequency of the signal of interest.

If the true cyclic frequency α of the SOI is estimated recursively, then ideally the magnitude of Δ should decrease with each successive estimation, thereby reducing the variance of the estimator. Consequently, it is desired to have a recursive estimate of α. The following sections propose two methods which attempt to obtain a recursive estimate of the actual value of the cyclic frequency of the signal of interest from the given samples.

6.5 The Gradient Ascent Algorithm

It may be seen that the primary signal component of each element r_k of $\mathbf{r}$ is individually maximized when $\alpha = \alpha_m$ and therefore, a linear combination of the same will also be maximized for $\alpha = \alpha_m$. Now, the function $|g(\Delta, N)|$ is concave within the window $\left[\frac{-1}{N}, \frac{1}{N}\right]$ and hence may be maximized by moving along the gradient. Since each element of $\mathbf{r}$ corresponds to $g(\Delta, N)$ with a different N, all of which are maximized at the same point. Maximizing a linear combination of different elements of $\mathbf{r}$ is equivalent to maximizing the individual $g(\Delta, N)$ for each N. Further if the weights of the different components of $\mathbf{r}$ are assigned in inverse proportion to their variances, then the linear combination of the elements of $\mathbf{r}$ to be maximized is $\mathbf{w}^H\mathbf{r}$. Now, $\mathbf{r}$ can be both real as well as complex, depending on the knowledge of the phase of the cyclic autocorrelation function. Accordingly, maximization of the objective function $J = |\mathbf{w}^H\mathbf{r}|^2$ is considered here.

The objective function may be rewritten as

$$J = \mathbf{r}^H\mathbf{W}\mathbf{r} \tag{6.53}$$

where $\mathbf{W} = \mathbf{w}\mathbf{w}^H$. Differentiating it w.r.t. α, we get,

$$\nabla_\alpha J = \nabla_\alpha \mathbf{r}^H\mathbf{W}\mathbf{r} + \mathbf{r}^H\mathbf{W}\nabla_\alpha\mathbf{r} = 2\Re\left\{\nabla_\alpha\mathbf{r}^H\mathbf{W}\mathbf{r}\right\} \tag{6.54}$$

Considering the more general case where ϕ is not known, we have

$$r_k = \frac{1}{N - kN_s}\sum_{n=kN}^{n=N-1} x[n]x^*[n - KN_s]e^{-j2\pi\alpha n} \tag{6.55}$$

and

$$b_k = \nabla_\alpha r_k = \frac{1}{N - kN_s}\sum_{n=kN}^{n=N-1} x[n]x^*[n - KN_s]e^{-j2\pi\alpha n}(-j2\pi n) \tag{6.56}$$

If it is assumed that there is only a small change in $\hat{\alpha}$, the estimate of α, from one iteration to another, then both r_k and b_k can be computed recursively. These may then be used to update $\hat{\alpha}$, which may again be used to update r_k and b_k. Consequently, the recursive estimation procedure for α based on gradient ascent may be summarized as follows.

1. **Initialize**

   - The number of samples to be used for the initial estimate as B,
   - The cyclic frequency estimate $\hat{\alpha}[B] = \alpha_0$ as the apriori known value of the cyclic frequency,
   - The initial length of feature and the gradient vectors $P = \left\lfloor \frac{B}{N_s} \right\rfloor$.
     Based on this, for $1 \leq k \leq P$ initialize the following

- $r_k[B] = \frac{1}{B-kN}\sum_{n=kN}^{n=B} x[n]x^*[n-KN_s]e^{-j2\pi\hat{\alpha}[B]n}$
- $b_k[B] = \frac{1}{B-kN}\sum_{n=kN}^{n=B} x[n]x^*[n-KN_s]e^{-j2\pi\hat{\alpha}[B]n}(-j2\pi n)$
- $w_k[B] = B - kN_s$

2. For the nth step, $B < n < N$, update

   - $P = \left\lfloor \frac{B}{N_s} \right\rfloor$
     Then for $1 \leq k \leq P$ update
   - $r_k[n] = \frac{n-kN_s-1}{n-kN_s} r_k[n-1] + \frac{1}{n-kN_s} x[n]x^*[n-kN_s]e^{-j2\pi\hat{\alpha}[n]n}$
   - $b_k[n] = \frac{n-kN_s-1}{n-kN_s} b_k[n-1] + \frac{1}{n-kN_s} x[n]x^*[n-kN_s]e^{-j2\pi\hat{\alpha}[n]n}(-j2\pi n)$
   - $w_k = n - kN_s$

3. Based on this, update

$$\hat{\alpha}[n+1] = \hat{\alpha}[n] + 2\mu[n]\Re\{\mathbf{b}^H\mathbf{W}\mathbf{r}\} \tag{6.57}$$

   where

$$\mu[n] = \frac{\mu}{\|\mathbf{b}[n]\|^2}$$

   and μ is the step size for adaptation, normalized at each step w.r.t. the instantaneous norm squared value of the gradient. At low SNRs, the contribution of noise to the instantaneous estimates of both the cyclic autocorrelation function as well as gradient will be quite large and the amplitudes of both will depend mainly on the noise power. This will result in larger steps at lower SNRs which may lead to erroneous adaptations. Therefore, in order to avoid such a possibility, the step size is normalized w.r.t. the norm square of the instantaneous gradient.

   It is observed that each step requires P^2 complex multiplications. If the value of P is fixed or capped to a maximum then the overall computational complexity of the adaptive algorithm for N samples may be expressed as $\mathcal{O}(NP^2)$.

6.6 The Greedy Approach

An alternative approach to find $\hat{\alpha}$ that maximizes the test statistic is to search for it from among all the available cyclic frequencies. As the search for the optimal $\hat{\alpha}$ is being constrained within the main lobe of $g(\Delta, N)$, the size of the search window is inversely proportional to the number of samples being used. Hence, it is preferred to use a smaller number of samples during the search operation so as to keep the optimum $\hat{\alpha}$ within the search window. However, on the other hand, the error introduced due to averaging over a smaller number of samples will be large, thereby reducing the reliability of the estimate.

Keeping this in view, an iterative procedure that starts with a large search window but gradually shrinks in size may be a good compromise. It may be a good option here to use a greedy approach which selects $\hat{\alpha}$ that maximizes the value of the objective function within a given search window and then builds the new search window centred around the previous best. Here, if the value of ϕ is known, then the optimal $\hat{\alpha}$ for a given window will satisfy

$$\hat{\alpha_o} = \arg\max_{\hat{\alpha}} \left\{ \Re \left\{ \sum_{k=1}^{P} (N - kN_s)(\hat{R}_{xx}^{\hat{\alpha}}[N, N_s] e^{-j\phi}) \right\} \right\} \tag{6.58}$$

In case ϕ is not known, then the optimal $\hat{\alpha}$ satisfies

$$\hat{\alpha_o} = \arg\max_{\hat{\alpha}} \left\{ \left| \sum_{k=1}^{P} (N - kN_s)(\hat{R}_{xx}^{\hat{\alpha}}[N, N_s]) \right| \right\} \tag{6.59}$$

Based on this and following an approach similar to [73], the greedy approach to find the optimum value of $\hat{\alpha}$ may be described as follows.

1. Divide the N number of received samples into smaller blocks of length L_B each.
2. **Initialize**
   - The number of sample blocks B to be considered for the initial estimate of $\hat{\alpha}$ so that the initial length of the sample block becomes $Q_B = BL_B$.
   - The initial estimate of the cyclic frequency, $\beta_B = \alpha$
   - The iteration counter $q = B$
3. For $B \leq q \leq \left\lfloor \frac{N}{L_B} \right\rfloor$
   - **Define**
     - The number of lags to be considered for the estimate $P_q = \left\lfloor \frac{Q_q}{N_s} \right\rfloor$
     - The normalized width of the cyclic frequency search window $W_Q = \frac{1}{Q_q}$
   - Split the search window from $\beta_q - W_q$ to $\beta_q + W_q$ into S search points,
   - For each point γ_{qp} around β_q, calculate $\hat{R}_{xx}^{\gamma_{qp}}[qL_B, kN_s]$ for $1 \leq k \leq P_q$.
   - Based on the information available about ϕ, set β_{q+1} as the cyclic frequency that maximizes (6.58) or (6.59).
4. Assign $Q_{q+1} = Q_q + L_B$ and $q = q + 1$

The cyclic frequency to be used for sensing is taken to be the one obtained in the final step of iterations. It may be observed that the calculation of the cyclic autocorrelation function for the qth block with a given lag kN_s requires qL_B complex multiplications and therefore, the search in each window requires qLP complex multiplications. As there are a

total of q_{max} blocks, the total number of multiplications will be summation over q from 1 to q_{max}. Thus, with $B = 1$ the entire greedy search operation will require $q_{max}(q_{max}+1)LP = (q_{max}^2 + q_{max})LP$ complex multiplications, where $q_{max} = \left\lfloor \frac{N}{L_B} \right\rfloor$. Consequently, the overall order of complexity of the proposed algorithm for a fixed P turns out to be $\mathcal{O}(PN^2)$.

6.6.1 Performance of the CFO estimators

The performance of the cyclostationary detector is based directly on the strength of the cyclostationary features being detected which depends on the residual CFO. It may be observed from the nature of $g(\Delta, N)$ that the spectrum sensing operation will fail if the absolute value of the residual CFO lies above a certain threshold, beyond which the strength of the cyclic autocorrelation function becomes negligible. The 3 dB point in the function $g(\Delta, N)$ may be considered as one such threshold. Therefore, the performance metric for any CFO may be formulated as a hit/miss function, with the residual CFO lying within the 3 dB window of $g(\Delta, N)$ counted as a hit, and that outside it as a miss. The performance of the CFO estimator may, therefore, be determined in terms of the probability of hit that is the probability of the residual CFO lying within the 3 dB window of $g(\Delta, N)$ for a given number of samples, or the probability of miss which is the probability of the residual CFO lying outside the said window.

Another important factor to consider here is the computational complexity of the CFO estimation algorithm. Ideally, it is desired that the computational complexity of the spectrum sensing algorithm should be linear in the number of samples being used as well as the number of features being employed for detection. However, it is seen that the addition of a CFO estimator to the spectrum sensor results in an additional computational complexity for the spectrum sensor. In case the greedy search approach is followed, the order of complexity of the CFO estimator is $\mathcal{O}(N^2)$ for N samples. On the other hand, in case the gradient ascent approach, the order of complexity of the CFO estimator is $\mathcal{O}(N)$. It will be shown in the following section that this reduced complexity comes at the cost of CFO estimation performance.

6.7 Simulation Results

In this section, simulation results using randomly generated signals are presented. The primary user OFDM signal is assumed to be consisting of 2048 data subcarriers out of which 256 are pilots subcarriers. A cyclic prefix of length 256 is added to the signal, making the total length of the OFDM symbol equal to 2304. The signal is assumed to be sampled at 9 MHz and the sampling duration, unless specified, is assumed to be 5 ms, resulting in a total of 45000 samples being used. For the purpose of these experiments, the primary user signal variance is kept constant at unity and the variance of the additive noise

is varied to achieve SNRs in the range −20 dB to 0 dB. Also, it is assumed that the phase of the cyclic autocorrelation function is known at the spectrum sensor. For the experiments involving CFO estimators, the cyclic autocorrelation function at a single cyclic frequency and all the possible lags is considered. It is assumed that the known cyclic frequency is offset by 1% from its true value. The performance of a spectrum sensing algorithm is evaluated in terms of the probability of successful detection at different input SNRs. Unless specified, the detection thresholds are set to give a constant false alarm rate of 1%. Here, 2000 independent trials are conducted to determine the detection performance of the algorithm and 1000 trials are conducted to determine its CFO estimation performance.

6.7.1 Performance of the proposed detector without any CFO

Figure 6.1 illustrates the performance of the proposed detector in the absence of any CFO for different number of lags and cyclic frequencies. It is observed that the simulation results agree with that expected as per the theory derived in equations (6.24) and (6.25) . Also, it is observed that the derived performance improves considerably as the number of features being used is increased. A gain of nearly 5 dB for a successful detection probability of 90% is observed as the number of features being used is increased from 1 to 19 for a single cyclic frequency. It is also observed that increasing the number of cyclic frequencies from 1 to 2 results in an additional gain of 1.5dB. This implies that, if for a given number of cyclic frequencies, the number of temporal features are limited then the detector performance will suffer.

6.7.2 Performance of the gradient ascent algorithm in the presence of CFO

Figures 6.2 and 6.3 depict the performance of the gradient ascent algorithm at different SNRs with different step sizes. The number of samples for the initial estimates (B_s) in these experiments was fixed at 10000. Figure 6.2 shows the plots for the probability of the estimated cyclic frequency lying outside the 3 dB point of the main lobe of the sinc function window around the true cyclic frequency for different SNRs. Figure 6.3 plots the probability of detection for the given signal after the CFO is estimated. In both the cases discussed above, the initial CFO is assumed to be 1% of the true cyclic frequency.

It is observed that the performance of the gradient ascent-based CFO estimation algorithm is dependent on the step size. Smaller step size means that the system is more likely to ascend the correct gradient. It also results in slower convergence thereby limiting the performance of the estimator as well as the detector. It may be observed from Figure 6.2 that a small step size results in a greater probability of miss, thereby indicating that the number of samples required by the algorithm for convergence to the true cyclic frequency is larger than the available number of samples. On the other hand, larger step size results

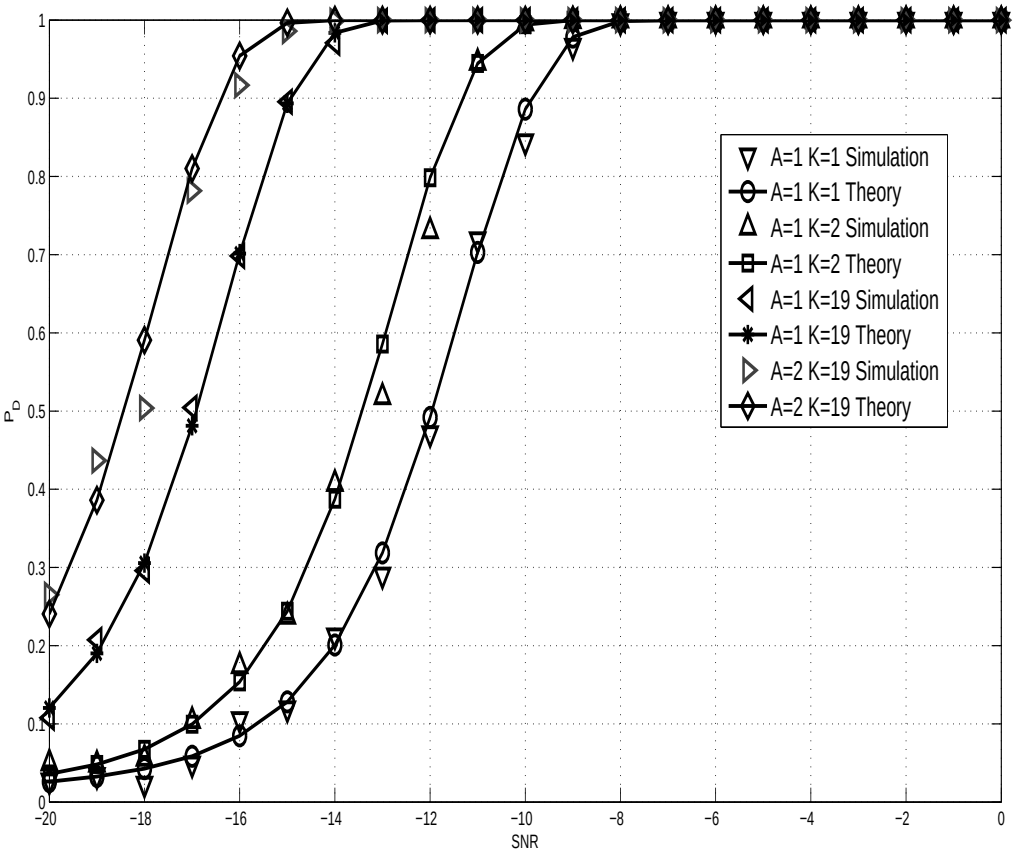

Figure 6.1: Performance of the proposed detector for different number of features in the absence of any CFO

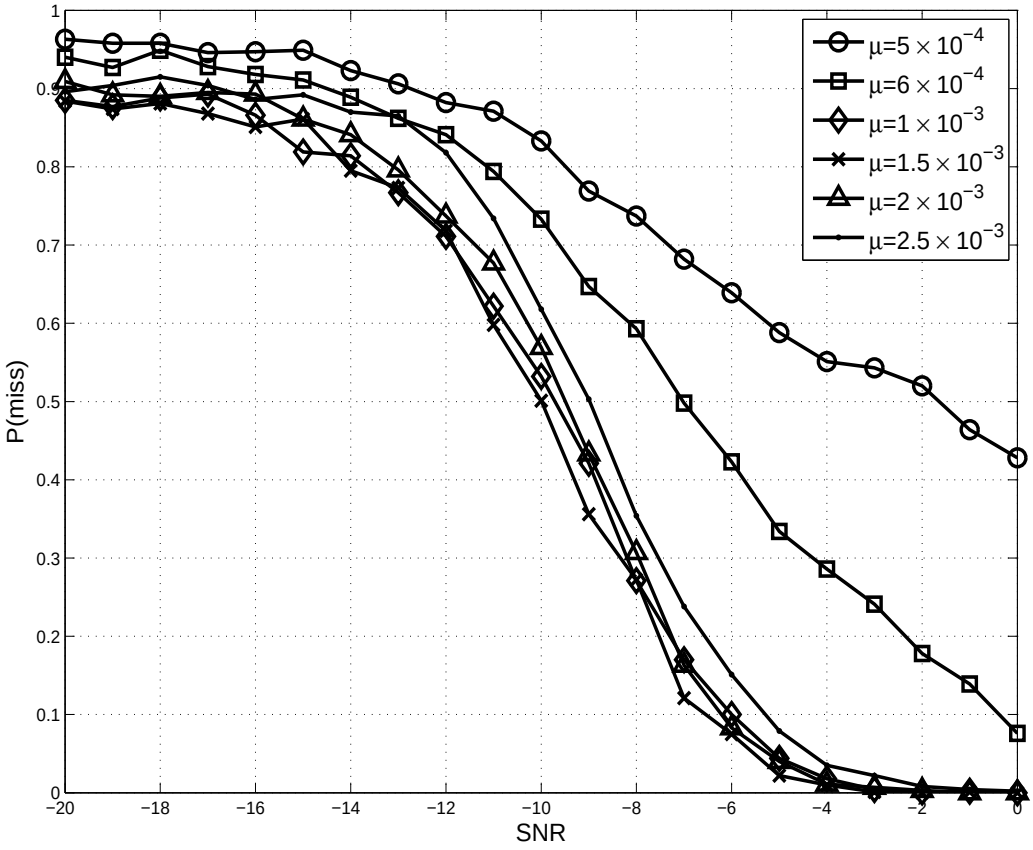

Figure 6.2: CFO estimation performance of the gradient ascent algorithm for different step sizes at different SNRs

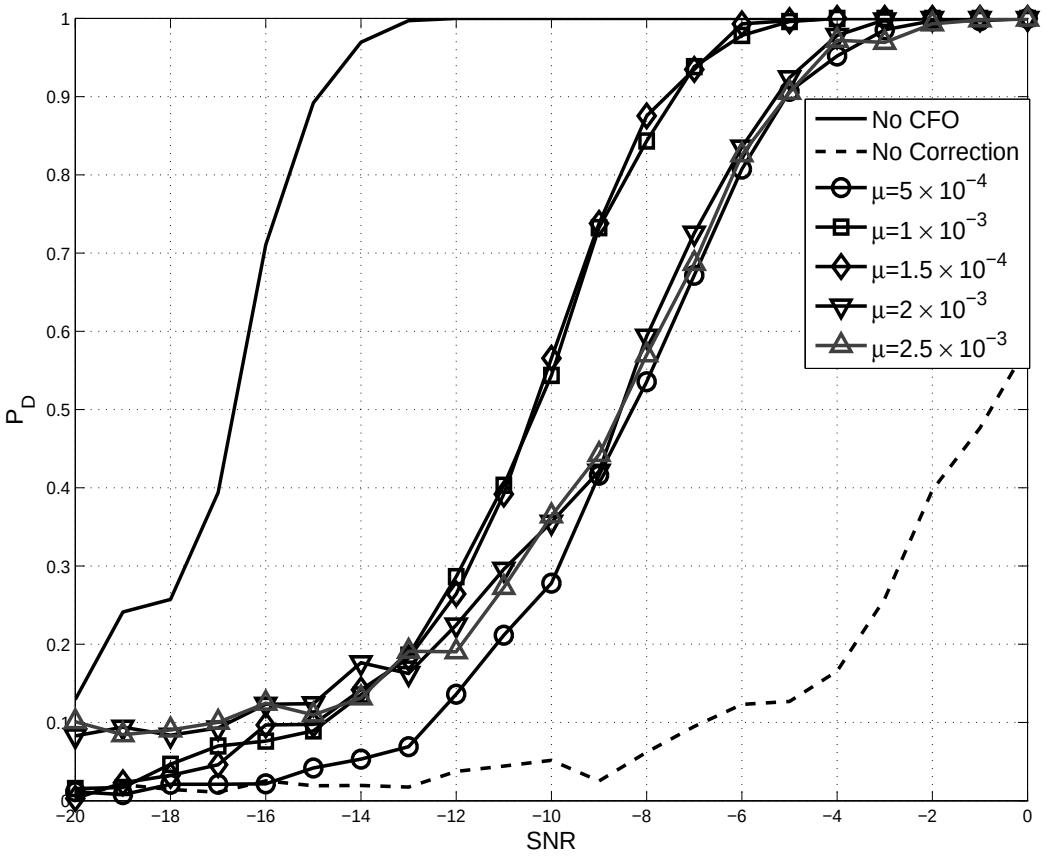

Figure 6.3: Detection performance of the gradient ascent algorithm for different step sizes at different SNRs

in faster convergence of the algorithm but yields a larger residual CFO, again limiting the detector performance. In the present case, it is found via simulation that a step size in the range $(1 - 1.5) \times 10^{-3}$ is a good choice for the given number of samples. The performance loss due to CFO in this case is nearly 7 dB. It may be noted here that smaller step sizes will work better for larger number of samples and vice versa.

6.7.3 Performance of the greedy search algorithm in the presence of CFO

In this set of experiments, the variation in the performance of a spectrum sensor with a CFO estimator based on greedy search algorithm for different signal to noise ratios and block sizes is studied. The number of blocks (B) for the initial estimate is given $B = \left\lfloor \frac{10000}{L_B} \right\rfloor$ for a block size L_B . Figure 6.4 shows the probability of the estimated cyclic frequency lying outside the 3 dB point of the main lobe of the sinc function window cantered around the true cyclic frequency for different SNRs. Figure 6.5 shows the plots for the probability of detection after the CFO is estimated in an AWGN channel. It may be seen that reducing the size of the search block from $\frac{3N_s}{2}$ to $\frac{N_s}{2}$ results in gains of upto 4 dB. However, this improvement in the performance comes at the cost of additional computational complexity.

Figure 6.6 plots the detection performance of the spectrum sensor using a greedy search based CFO estimator when the phase of the cyclic autocorrelation function is unknown in different cases. The detection threshold in this case is determined via simulation. 1000 independent trials in the absence of a primary signal are conducted so as to determine the detection threshold for a fixed false alarm rate of 1%. It is observed that the performance in the case of no-CFO is slightly degraded in comparison to the case where the phase is known. It is observed that smaller block sizes tend to improve the detection performance by as much as 2 dB for a successful detection rate of 90%. This, however, still shows a loss of more than 2 dB in comparison to the no-CFO case.

Figure 6.7 shows the complimentary ROCs of spectrum sensor with a greedy search-based CFO estimator at an SNR of -10 dB. Yet again, it is observed that smaller block sizes result in better detection performances at the spectrum sensor.

6.7.4 Comparison with the existing method

Figure 6.8 compares the performance of different CFO compensation schemes at different SNRs. It is found that the algorithm proposed in [103] performs best for a block size $\frac{N_s}{2}$ and hence those results may be used as benchmarks for comparison with other methods. It is observed that for a successful detection rate of 90%, the gradient ascent-based approach provides a gain of nearly 1 dB while the greedy search approach results in a gain of nearly 6 dB in comparison to the method proposed in [103].

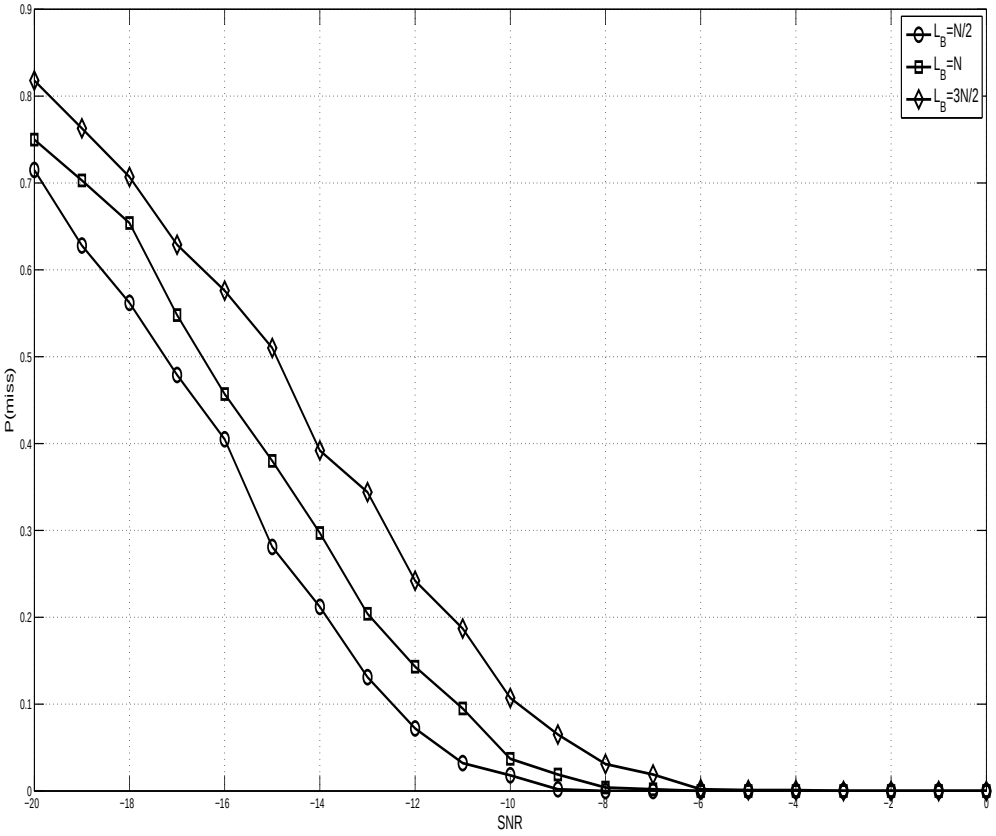

Figure 6.4: CFO estimation performance of the greedy search algorithm for different block sizes at different SNRs

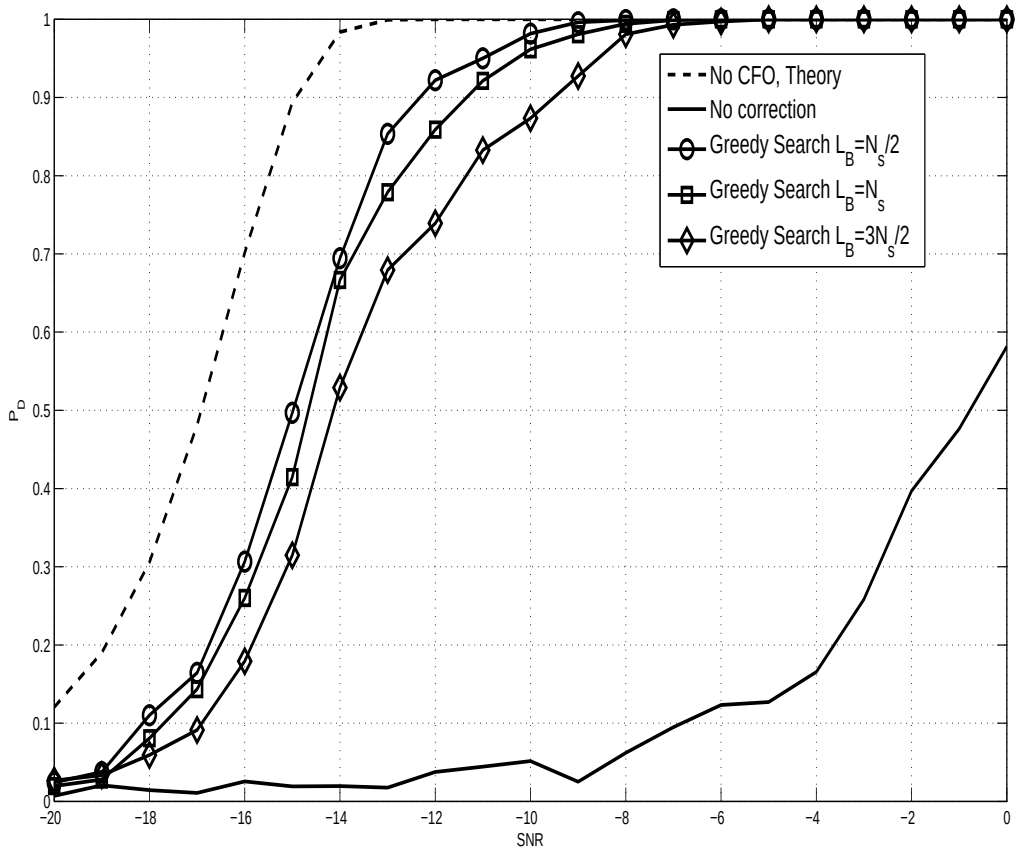

Figure 6.5: Detection performance of the greedy search algorithm for different block sizes at different SNRs

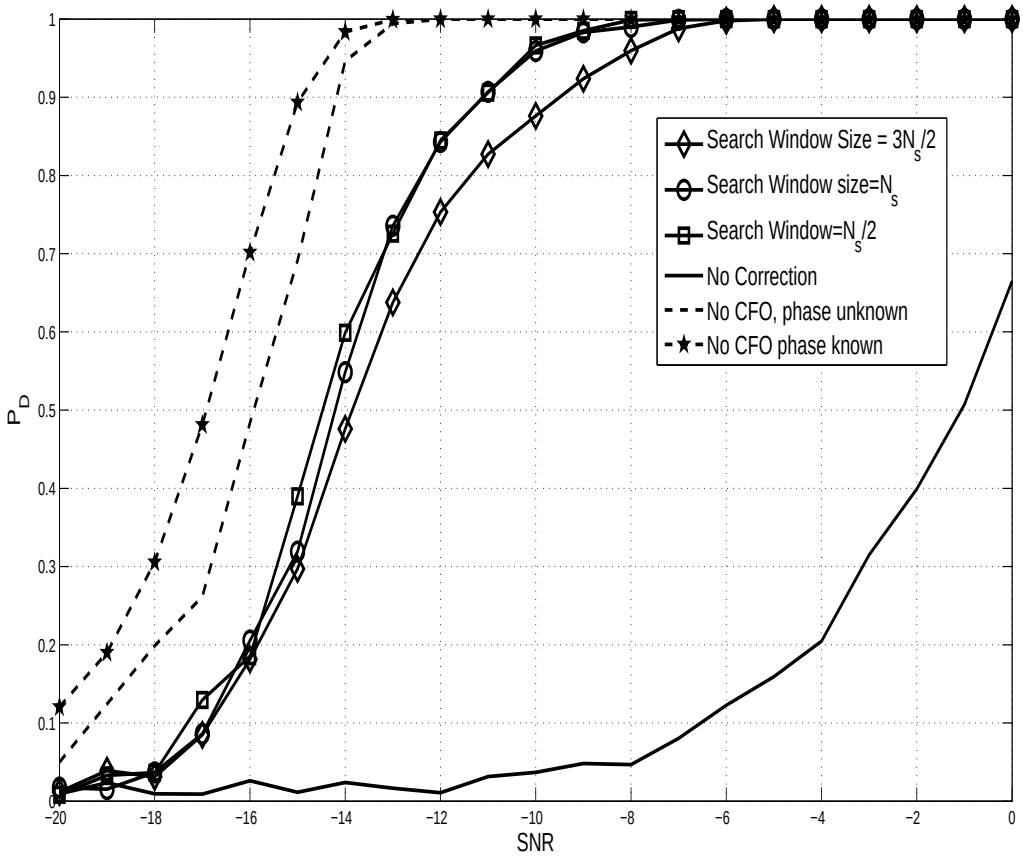

Figure 6.6: Detection performance of the greedy search algorithm for different block sizes at different SNRs when the phase of the cyclic autocorrelation function is unknown

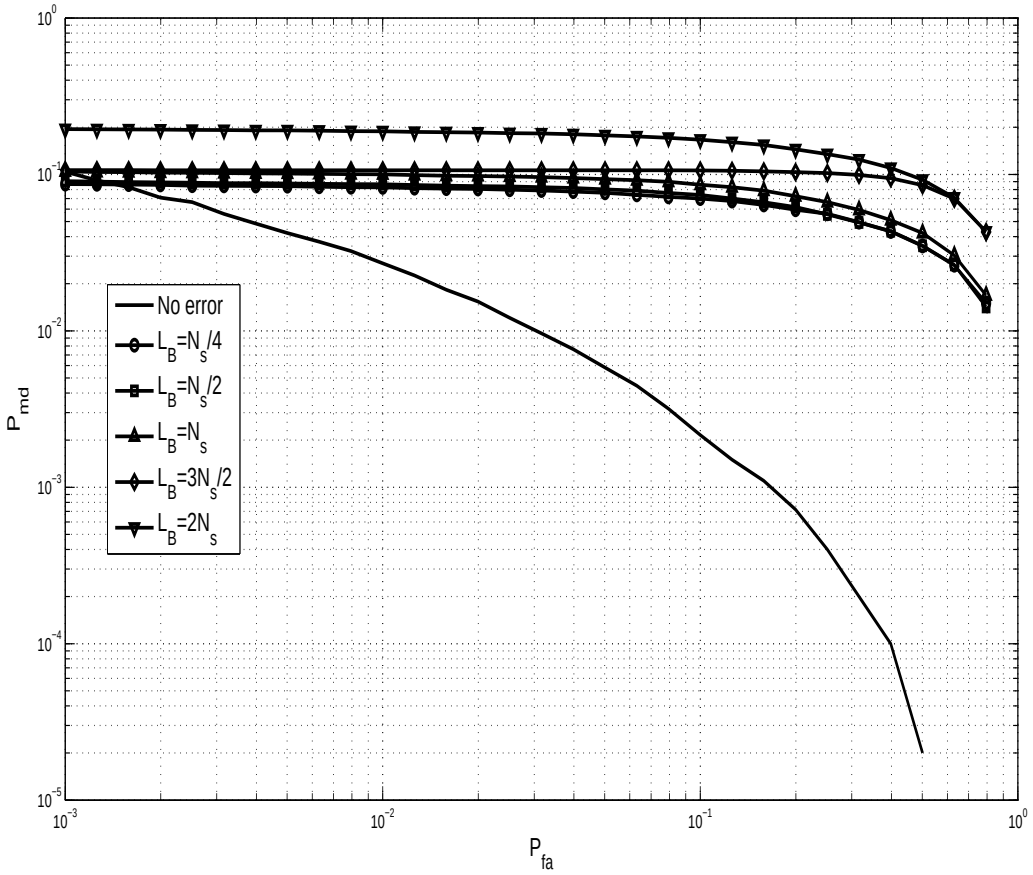

Figure 6.7: Complimentary ROCs of spectrum sensor with a greedy search-based CFO estimator at an SNR of -10 dB for different block sizes

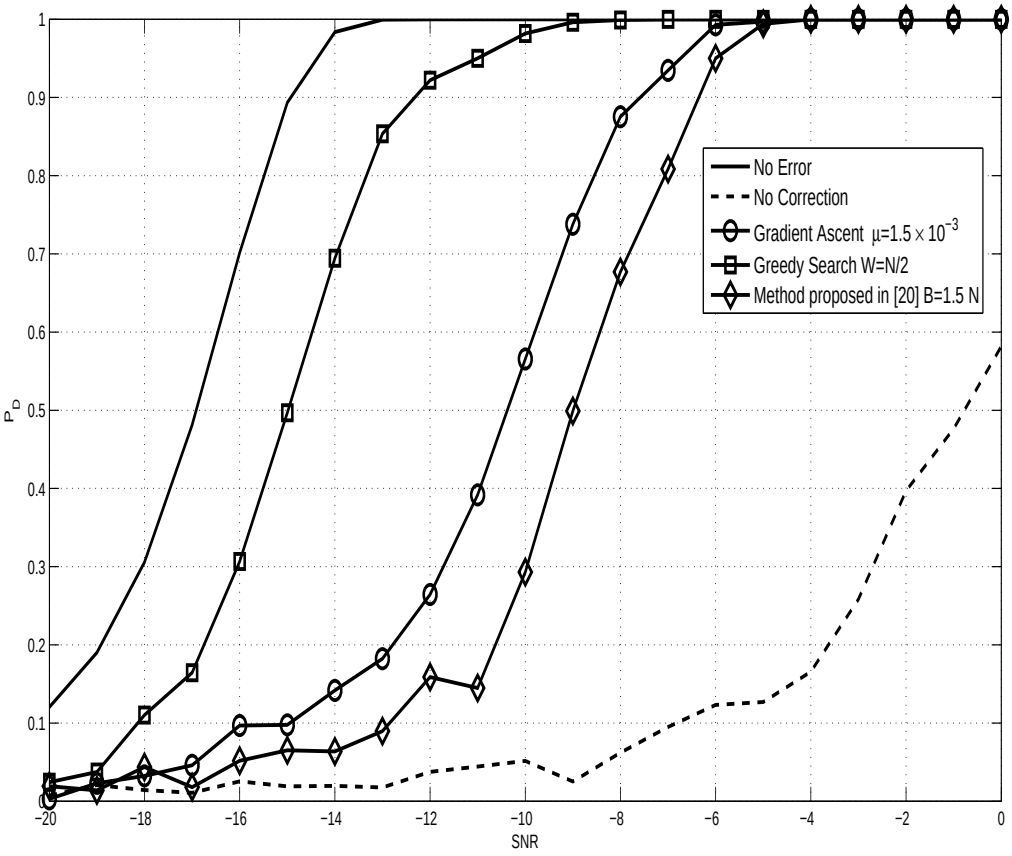

Figure 6.8: Detection performance of different CFO compensation schemes at different SNRs

In Figure 6.9, the performances of different CFO compensation methods are plotted against different values of the CFO. It is observed that the gradient ascent algorithm provides good performance for smaller values of the CFO but its performance degrades as the CFO increases. It is also observed that the greedy search algorithm outperforms other methods by a large margin but at the cost of increased computational complexity.

6.7.5 Performance under Fading Channels

In the case of a fading channel, the received signal under the two hypotheses will be given as

$$x[n] = \begin{cases} \nu[n] & \mathcal{H}_0 \\ \varphi[n] * s[n] + \nu[n] & \mathcal{H}_1 \end{cases} \tag{6.60}$$

where $\varphi[n]$ is the channel impulse response. This may be represented as a scaler φ for a flat fading channel and a vector $\boldsymbol{\varphi}$, with a length equal to the channel length in the case of a frequency selective channel. In view of this, the distribution of the test statistics under the two hypotheses for a fading channel will take the form [50, 144]

$$Z \sim \begin{cases} \mathcal{N}_s\left(0, \frac{AP\sigma_\nu^4}{2}\right) & \mathcal{H}_0 \\ \mathcal{N}_s\left(\|\boldsymbol{\varphi}\|^2 A \frac{N_p}{N_d} \mathcal{E}_s \sum_{k=1}^{P} (N - kN_s), \frac{AP(\|\boldsymbol{\varphi}\|^2 \mathcal{E}_s + \sigma_\nu^4)^2}{2}\right) & \mathcal{H}_1 \end{cases} \tag{6.61}$$

Consequently, the expression for the probability of false alarm remains unchanged as given by (6.24), but the probability of detection, conditioned on φ becomes

$$P_d(\lambda|\boldsymbol{\varphi}) = Q\left(\frac{\lambda - A\frac{N_p}{N_d}\|\boldsymbol{\varphi}\|^2 \mathcal{E}_s \sum_{k=1}^{P} \sqrt{(N - kN_s)}}{(\|\boldsymbol{\varphi}\|^2 \mathcal{E}_s + \sigma_\nu^4)\sqrt{\frac{AP}{2}}}\right) \tag{6.62}$$

The overall probability of detection for a fading channel may be obtained by averaging the above over $\boldsymbol{\varphi}$. This may not be possible analytically and numerical integration may be required, as in [33]. However, detection thresholds for a constant false alarm rate may be obtained by using (6.24). In this case, the thresholds are determined to keep the false alarm rate fixed at 1%. These thresholds may then be used to determine the corresponding detection rates via simulation. For the purpose of these simulations, the primary signal component in the received signal, when present, is convolved with a channel vector having Rayleigh distributed elements with an exponentially decaying power profile. Following this, the cyclic autocorrelation function of the received signal is calculated for different lags. These are then combined to form the test statistics to be compared against a detection threshold determined by (6.24). Further, 2000 independent trials are conducted to determine the detection performance. This is done both in the absence and the presence of a 1% CFO. When present, the CFO is corrected by the greedy search algorithm for different block sizes. The performance of the spectrum sensor using a greedy search-based

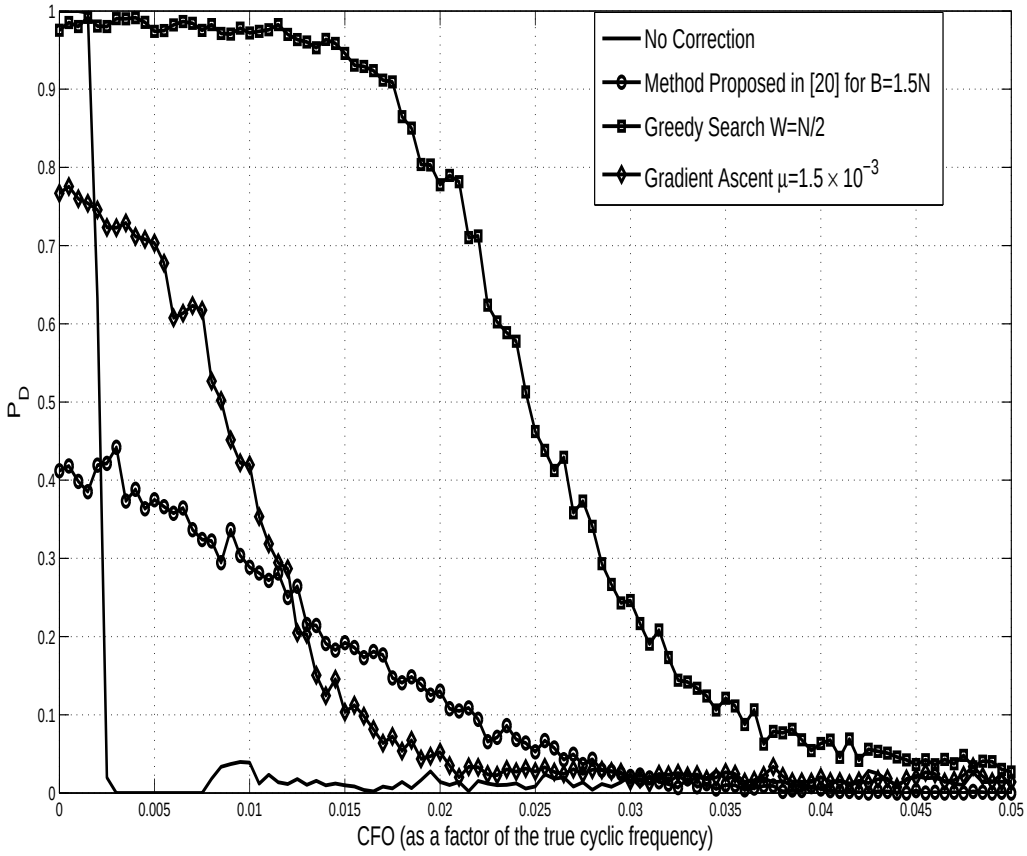

Figure 6.9: Detection performance performance of different CFO compensation algorithms at $-10dB$ for different values of the CFO

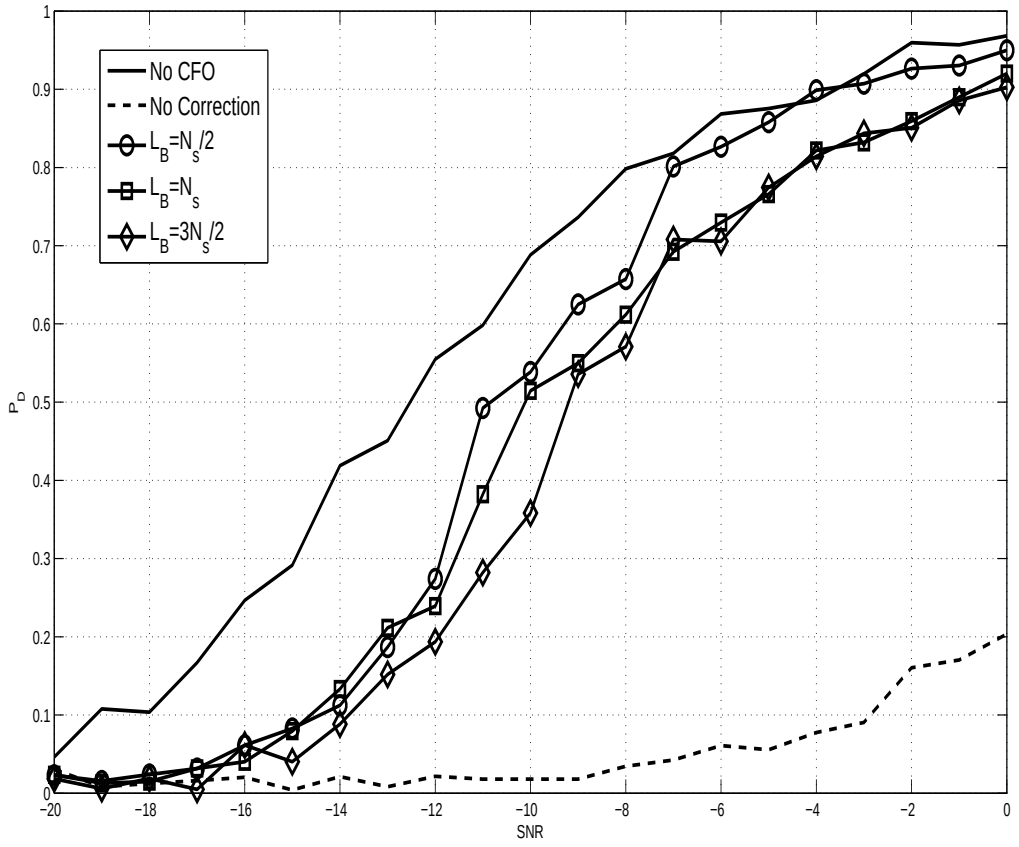

Figure 6.10: Detection performance of the greedy search algorithm for different block sizes at different SNRs for a flat fading channel

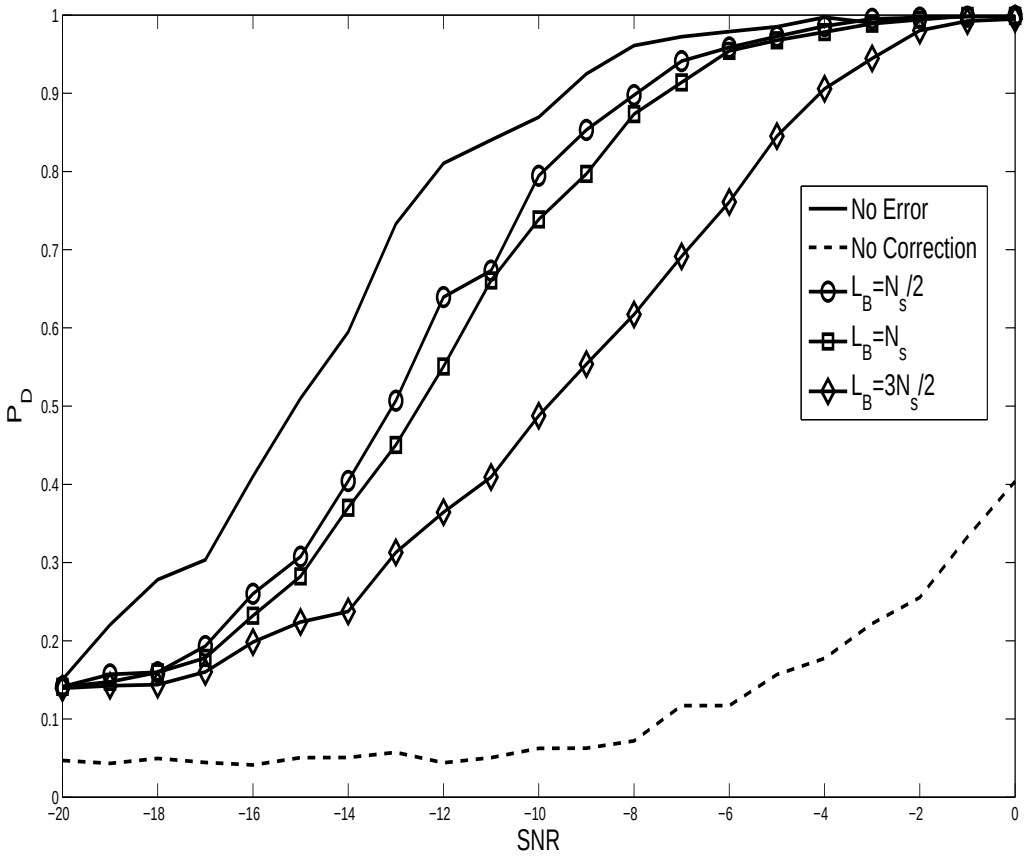

Figure 6.11: Detection performance of the greedy search algorithm for different block sizes at different SNRs for a frequency selective fading channel

CFO estimation for different block sizes under flat fading is compared against the no-CFO case and the no-correction case as shown in Figure 6.10. It may again be observed that for a detection rate of 90%, reducing the search block size from $\frac{3N_s}{2}$ to $\frac{N_s}{2}$ results in gains of as much as 4 dB. The perofrmance of a greedy search system under a 128 tap frequency selective fading channel is shown in Figure 6.11. It may again be observed that reducing the search block size from $\frac{3N_s}{2}$ to $\frac{N_s}{2}$ improves the detection performance by 4 dB.

6.8 Conclusion

This chapter considers the problem of sensing OFDM signals using correlated pilots. It is observed that the inter-pilot correlation causes the OFDM signal to exhibit cyclostationarity which may be used to detect its presence. A feature detector for detecting cyclostationarity at multiple cyclic frequencies and temporal lags is proposed and its performance is derived in case of an AWGN channel. Following this, the effect of any deviation from the known value of the cyclic frequency on the system performance is evaluated. It is observed that for large number of samples, even for a small offset in the cyclic frequency, it may cause severe degradation in the detector performance. The method for compensating the effects of the CFO, as proposed in [103] is studied and is found to be inadequate in case of the proposed detector, where the features to be detected are placed far apart.

Alternatively, it is proposed to estimate and then compensate for the effects of CFO, thereby enabling the use of all possible features. The Cramer-Rao bound on the performance of the CFO estimator is derived and it is observed that the variance of the CFO estimator depends on the actual value of the CFO. As a result, it is proposed to estimate the CFO recursively. Following this, two iterative algorithms are proposed for the purpose. The first is the less complex gradient ascent-based algorithm which works only for small values of CFO. The second approach is based on greedy search which works for larger offsets in the cyclic frequency as well, but at the cost of increased computational complexity. These methods are compared with the algorithm in [103] and it is observed that the greedy search algorithm provides an advantage of more than 6 dB over the method proposed therein but at the cost of computational complexity.

Chapter 7

FRESH Filter based spectrum sensing in the presence of Cyclic Frequency Offset

FRESH filter-based spectrum sensors considered so far assume accurate knowledge of the cyclic frequencies of the signal. This cyclic frequency is used to provide an appropriate frequency shift to the sensed signal so as to adapt the FRESH filter weights. However, as discussed in the previous chapter, the knowledge of the cyclic frequency at the spectrum sensor may be flawed and may lead to incorrect adaptation of the filter weights. Similar to the detection stage, an offset in the cyclic frequency at the adaptation stage may nullify the gains offered by FRESH filtering.

In the previous chapter, the effects of CFO on cyclostationarity-based spectrum sensing were discussed. It was observed that even a small error in the cyclic frequency of the primary signal leads to significant loss in the performance of the system in question. It was also observed that the received samples may be used to estimate the true cyclic frequency. In the previous chapter, two algorithms viz. the gradient ascent algorithm and the greedy search algorithm, were proposed for this purpose.

In this chapter, we study the effects of CFO on the adaptation stage of a FRESH filter-based spectrum sensor. The effects of CFO on the adaptation stage of a FRESH filter-based spectrum sensor are derived for both the energy detector and the cyclostationary detector. In order to compensate for these effects, it is proposed to determine the true cyclic frequency of the cyclostationary component in the received signal prior to the filter adaptation stage. Here, the greedy search algorithm developed in the previous chapter is modified to suit the purpose.

The system and sensing model is introduced and the performances of the energy and the cyclostationarity detector are presented in Section 7.1. The effects of CFO in the adaptation stage for both the detectors are derived in Section 7.2. The compensation mechanism for CFO along with the modified greedy algorithm is presented in Section 7.3. The simulation

results using this algorithm are presented in Section 7.4 and the conclusions are presented in Section 7.5.

7.1 The Signal and Sensing Models

Consider a primary user signal $s[n]$ exhibiting cyclostationarity or conjugate cyclostationarity at a cyclic frequency α. A single-user, single-antenna spectrum sensor is used to decide on the presence of this signal in the presence of AWGN noise $\nu[n]$ with a variance σ_ν^2. The sensed signal $x[n]$ under the two hypotheses may be written as

$$x[n] \sim \begin{cases} \nu[n] & \mathcal{H}_0 \\ s[n] + \nu[n] & \mathcal{H}_1 \end{cases} \tag{7.1}$$

The spectrum sensor is assumed to be equipped with a FRESH filter consisting of a single L-tap frequency shift branch for introducing a frequency shift α. It is assumed that the spectrum sensor works in two stages; the adaptation stage and the sensing stage. During the adaptation stage, the spectrum sensor collects N_A samples in the presence of a primary user signal and uses these to adapt the weight vector $\mathbf{w}[n]$.

Following this, during each sensing stage, the spectrum sensor collects N samples of $x[n]$ and passes these through the adapted filter so as to generate the filtered signal $y[n]$ defined as,

$$y[n] = \mathbf{w}^H[N_A]\mathbf{u}[n] \tag{7.2}$$

where

$$\mathbf{u}[n] = [x^\alpha[n], x^\alpha[n-1], \ldots, x^\alpha[n-L+1]]^T \tag{7.3}$$

and

$$x^\alpha[n] = x[n]e^{-j2\pi\alpha n}. \tag{7.4}$$

The filtered signal $y[n]$ is then subjected to either energy detection or to cyclostationary detection to detect the presence of a primary signal component within it.

For energy detection, the finite time energy of the filtered signal, defined as follows, is used as the test statistic.

$$T_E = \sum_{n=0}^{N-1} |y[n]|^2 \tag{7.5}$$

The distribution of this test statistic under the two hypotheses may be written as [122]

$$T_E \sim \begin{cases} \mathcal{N}\left(\sigma_\nu^2, \frac{\sigma_{E_0}^2}{N}\right) & \mathcal{H}_0 \\ \mathcal{N}\left(\sigma_\nu^2 + \mathbf{w}_o^H \mathbf{R}_{ss} \mathbf{w}_o, \frac{\sigma_{E_1}^2}{N}\right) & \mathcal{H}_1 \end{cases} \tag{7.6}$$

where $\mathbf{w}_o$ is the optimal weight vector, $\mathbf{R}_{ss}$ is the correlation matrix of $s[n]$, and $\sigma_{E_0}^2$ and

$\sigma^2_{E_1}$, are the variances of the test statistic under the two hypotheses, that are empirically determinable functions. The related detection and false alarm rates are derived as

$$P_d = Q\left(\sqrt{N}\frac{\lambda - (\sigma_\nu^2 + \mathbf{w}_o^H \mathbf{R}_{ss}\mathbf{w}_o)}{\sigma_{T_1}}\right) \tag{7.7}$$

$$P_{fa} = Q\left(\frac{\sqrt{N}(\lambda - \sigma_\nu^2)}{\sigma_{E_0}}\right) \tag{7.8}$$

The finite time cyclic autocorrelation function of $y[n]$ at a cyclic frequency η and lag τ is defined as

$$\hat{R}^\eta_{yy} = \sum_{n=0}^{N-1} y[n]y^*[n-\tau]e^{-j2\pi\eta n} \tag{7.9}$$

This is distributed as [31]

$$\hat{R}^\eta_{yy}[N,\tau] \sim \begin{cases} \mathcal{N}_c\left(0, \frac{\sigma^2_{C_0}}{N-\tau}\right) & \mathcal{H}_0 \\ \mathcal{N}_c\left(\xi e^{j\phi}, \frac{\sigma^2_{C_1}}{N-\tau}\right) & \mathcal{H}_1 \end{cases} \tag{7.10}$$

where $\xi e^{j\phi} = \mathbf{w}_o^H \mathbf{R}^\alpha_{ss}\mathbf{w}_o$ is a complex number, and $\sigma^2_{C_0}$ and $\sigma^2_{C_1}$ are empirically determinable functions. The cyclic autocorrelation matrix of $s[n]$, $\mathbf{R}^\alpha_{ss}$ being non-Hermitian results in $\hat{R}^\eta_{yy}[N,\tau]$ to be complex-valued. It may be observed that based on the knowledge of the phase ϕ, either $\Re\{\hat{R}^\eta_{yy}[N,\tau]e^{-j\phi}\}$ or $|\hat{R}^\eta_{yy}[N,\tau]|$ may be used as a test statistic. In this chapter, no prior knowledge about the phase ϕ is assumed and the absolute value of the finite time cyclic autocorrelation function is used as a test statistic. This is shown to be distributed as

$$|\hat{R}^\eta_{yy}[N,\tau]| \sim \begin{cases} Rice\left(0, \frac{\sigma_{C_0}}{\sqrt{N-\tau}}\right) & \mathcal{H}_0 \\ Rice\left(\xi, \frac{\sigma_{C_1}}{\sqrt{N-\tau}}\right) & \mathcal{H}_1 \end{cases} \tag{7.11}$$

The false alarm rate for a given detection threshold λ is then derived as

$$P_{fa} = e^{-\frac{(N-\tau)\lambda^2}{\sigma^2_{C_0}}} \tag{7.12}$$

It has been shown that the cyclostationary detector unlike the energy detector, is robust to uncertainty in noise variance [105,122]. However, as shown in the following section, both these methods are prone to CFO during the adaptation stage.

7.2 Effect of CFO on the adaptation Stage

To explain the effect of CFO on the adaptation stage, assume that the cyclic frequency known at the spectrum sensor α is different from the true cyclic frequency α_0 of the signal

of interest $s[n]$ by a random offset Δ such that $\alpha = \alpha_0 + \Delta$.

It may be observed that the noise component, $\nu[n]$ is wide sense stationary. Therefore the optimal weight vector under the null hypothesis is always the null vector. Hence, the behavior of the test statistics under the null hypothesis, regardless of the presence of CFO, remains same as described in the previous section.

Under the alternate hypothesis, $\mathcal{H}_1$,as neither the primary signal nor the noise component exhibit cyclostationarity at α, both the cyclic autocorrelation vector and the optimal weight vector $\mathbf{w}_o$ are null vectors. In view of this, the adapted weight vector $\mathbf{w}[N_A]$ should also converge to a null vector. However, due to the adaptive nature of the weights, there will be a finite random error present in the converged weight vector [61]. It may be noted that the accumulated error vector is the sum of a large number of terms and hence, it may be assumed to be Gaussian distributed. Constraining $\|\mathbf{w}[N_A]\| = 1$, the weight vector $\mathbf{w}[N_A]$ may be assumed to be distributed as

$$\mathbf{w}[N_A] \sim \mathcal{N}_c\left(0, \mathbf{Q}[N_A]\right) \tag{7.13}$$

where $tr(\mathbf{Q}[N_A]) = 1$

For an energy detector, the mean of the test statistic under $\mathcal{H}_1$ will be given as

$$E[T_E] = \sigma_\nu^2 + E[\mathbf{w}^H[N_A]\mathbf{R}_{ss}\mathbf{w}[\mathbf{N_A}]] \tag{7.14}$$

It may be noted that the matrix $\mathbf{R}_{ss}$ is positive definite and therefore, second term will be a positive real number. Also, $\mathbf{R}_{ss}$ being Hermitian, it may be written in the form $\mathbf{R}_{ss} = \mathbf{PDP}^H$, with $\mathbf{P}$ being the eigenvector matrix of $\mathbf{R}_{ss}$ and $\mathbf{D}$ being a diagonal matrix containing its eigenvalues. Therefore,

$$E[\mathbf{w}^H[N_A]\mathbf{R}_{ss}\mathbf{w}[N_A]] = E\left[\sum_{l=1}^{L} d_l |\bar{w}_l[N_A]|^2\right] \tag{7.15}$$

where d_l is the lth eigenvalue of $\mathbf{R}_{ss}$ and $\bar{w}_l$ is the lth element of $\bar{\mathbf{w}}[N_A]$ such that $\bar{\mathbf{w}}[N_A] = \mathbf{P}^H\mathbf{w}[N_A]$. This summation depends on the behavior of the filter weights. Therefore, both the mean and the variance of the test statistics under the alternative hypothesis are functions of the adaptive filter weights. Due to the adaptive nature of the filter weights, it is not possible to write the overall detection performance in closed form. The performance of this detector must, therefore, be determined experimentally.

For a cyclostationarity detector the mean of the finite-time cyclic autocorrelation function under the alternative hypothesis will be given as

$$E\left[\hat{R}_{yy}^{\eta}[\tau]\right] = E\left[\mathbf{w}^H[N_A]\mathbf{R}_{ss}^{\eta}[\tau]\mathbf{w}[N_A]\right] \tag{7.16}$$

Here, the matrix $\mathbf{R}_{ss}$ is not Hermitian and $\mathbf{w}[N_A]$ is random. Therefore, the entire term

inside the expectation will have a random phase. It is, therefore, not possible to use the knowledge of the phase as a part of the test statistic. Consequently, the absolute value of the finite time cyclic autocorrelation function should be used as a test statistic.

7.3 Compensation of the CFO effect

It was observed in the previous chapter that the received signal samples may be used to determine the true cyclic frequency of the cyclostationary component of the signal of interest. It is therefore proposed to estimate the cyclic frequency of the primary component in the signal prior to filter adaptation. The overall spectrum sensing system may be given as illustrated in Figure 7.1.

In the adaptation stage, which in this case is offline, the collected samples are used to recursively determine the true cyclic frequency and related FRESH filter weights. During the online sensing stage, the adapted cyclic frequency and filter weights are used to sense the presence of the primary user signal.

It has been assumed that the primary signal $s[n]$ is present during the adaptation stage. Therefore, for a FRESH filter of length L, it may safely be assumed that the cyclic autocorrelation function $R_{xx}^{\alpha_0}[\tau]$ of the received signal $x[n]$, at the true cyclic frequency α_0 is non-zero, at least for $0 \leq \tau \leq L-1$.

It was shown earlier that the finite time cyclic autocorrelation function of $x[n]$ at a cyclic frequency $\alpha = \alpha_0 + \Delta$ and lag τ may be written as

$$\begin{aligned} \hat{R}_{xx}^{\alpha}[N_A, \tau] &\approx R_{xx}^{\alpha_0}[\tau] \left(e^{j\pi(\Delta)(N_A-\tau-1)} \frac{\sin(\pi(N_A-\tau)(\Delta))}{(N_A-\tau)\sin(\pi(\Delta))} \right) \\ &= R_{xx}^{\alpha_0}[\tau] g(\Delta, N_A-\tau) \end{aligned} \tag{7.17}$$

where

$$g(\Delta, N_A-\tau) = e^{j\pi(\Delta)(N_A-\tau-1)} \frac{\sin(\pi(N_A-\tau)(\Delta))}{(N_A-\tau)\sin(\pi(\Delta))} \tag{7.18}$$

The optimal estimate of the true cyclic frequency $\hat{\alpha}_o$ will, therefore, satisfy

$$\hat{\alpha_o} = \arg\max_{\hat{\alpha}} \left\{ \sum_{\tau=0}^{L-1} \left| \sqrt{N_A-\tau} (\hat{R}_{xx}^{\hat{\alpha}}[N_A, \tau]) \right| \right\} \tag{7.19}$$

Based on this, the greedy search algorithm to obtain $\hat{\alpha_o}$ may be written as

1. Divide the N_A received samples into smaller blocks of length L_B each.
2. **Initialize**
   - The number of sample blocks B to be considered for the initial estimate of $\hat{\alpha}$ so that the initial length of the sample block becomes $Q_B = BL_B$.
   - The initial estimate of the cyclic frequency, $\beta_B = \alpha$

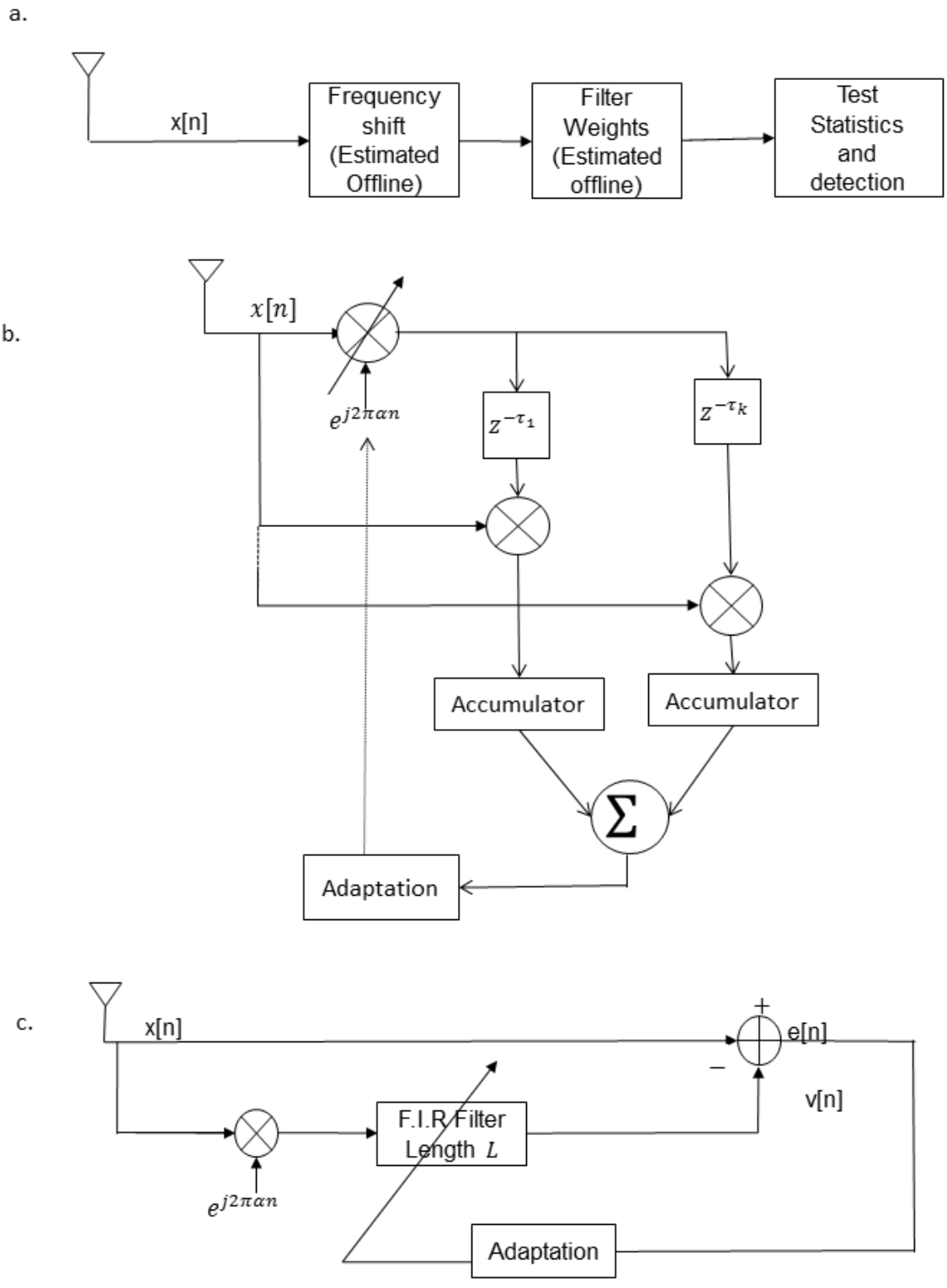

Figure 7.1: (a) Block Schematic of the proposed sensing scheme (b) The CFO estimation stage (c) Weight Adaptation Stage

- The iteration counter $q = B$

3. For $B \leq q \leq \left\lfloor \frac{N_A}{L_B} \right\rfloor$
   - Define the normalized width of the cyclic frequency search window $W_Q = \frac{1}{Q_q}$
   - Split the search window from $\beta_q - W_q$ to $\beta_q + W_q$ into P search points,
   - For each point γ_{qp} around β_q, calculate $\hat{R}_{yy}^{\gamma_{qp}}[qL_B, \tau]$ for $0 \leq \tau \leq L$.
   - Set β_{q+1} as the cyclic frequency that maximizes equation (7.19).
4. Assign $Q_{q+1} = Q_q + L_B$ and $q = q + 1$

The cyclic frequency obtained after the final iteration may be used to adapt the filter weights. The adaptation stage may therefore be assumed to consist of two sub-stages where the received samples are first used to estimate the true value of the cyclic frequency and are then used to adapt the filter weights.

7.4 Simulation Results

In these experiments, the primary user signal is assumed to be BPSK modulated with a data rate (f_b) 10 kilo bits per second and a carrier frequency (f_c) 100 kHz. It is assumed that the spectrum sensor samples at 1 MHz. The FRESH filter is assumed to consist of a single varible length conjugate frequency shift branch at 200 kHz. In all these experiments the primary user variance is fixed at unity and the variance of the additive noise is varied to achieve different SNRs as per the requirement of the experiment. The system performance is evaluated in terms of the detection rate for input SNRs varying from -20 dB to 0 dB. The number of samples being used for adaptation (N_A) is assumed to be 2000 while the number of samples being used for detection (N) is 500. The false alarm rate for all these experiments is fixed at 1%. In each case, 2000 independent trials are conducted to determine the detector performance.

7.4.1 The Effects of CFO

The performance of the energy detector for different FRESH filter lengths with 1% CFO of the true cyclic frequency is shown in Figure 7.2. It may be observed that the detection performance is severely degraded due to the presence of CFO. Still, it is observed that an increase in the filter length improves the detection performance. However, the gain at a detection rate of 90% due to a length-32 FRESH filter reduces to less than 1 dB as compared to 6 dB as shown in the fourth chapter.

The performance of the cyclostationary detector in the presence of CFO is inspected in Figure 7.3. Here again it is observed that an increase in the FRESH filter length improves

the detection performance. However, in this case, the performance of the length-16 filter with CFO is still 7 dB worse as compared to a length-1 filter with no CFO.

7.4.2 The Performance of the Greedy Search Algorithm

The probability of a miss, that is the probability of the estimated cyclic frequency lying outside the 3dB point of the main lobe of the resulting sinc function window is plotted in Figure 7.4 for different filter lengths. In this case, the search block size L_B is fixed at 200. It may be observed that the performance improves with an increase in the FRESH filter length that is the number of feature points included in the objective function described by equation (7.19). It may also be observed that increasing the number of feature points from 4 to 32 improves the performance of the algorithm by nearly 3dB.

Figure 7.5 plots the probability of miss at different SNRs for a FRESH filter length of 8 for different sized search blocks. The initial CFO in this case is taken to be 0.5% of the true cyclic frequency. The probability of miss increases marginally as the size of the search block is increased. This is consistent with the observations in the previous chapter.

The performance of an energy detector following a FRESH filter, whose true cyclic frequency is determined using the greedy search algorithm at different SNRs and filter lengths, is plotted in Figure 7.6. It may be observed that the use of greedy-search-based algorithm for cyclic frequency estimation reduces the loss due to CFO by more than 5 dB.

The performance of a cyclostationary detector following a FRESH filter whose true cyclic frequency is determined using the greedy search algorithm at different SNRs and filter lengths is plotted in Fig 7.7. Here, the performance loss due to CFO may be recovered by as much as 14 dB for all filter lengths.

The performance of a cyclostationary detector following a FRESH filter of length 8, whose true cyclic frequency is determined using the greedy search algorithm at an SNR of -12, dB is plotted against the CFO for different search block sizes in Fig 7.8. It is observed that an appropriate choice of the search block size, L_B, compensates the effects of CFO as large as 3% of the true cyclic frequency.

7.5 Conclusions

The effect of CFO (Cyclic Frequency Offset) on the performance of a FRESH filter-based spectrum sensor is analyzed in this chapter. It is shown that the performance of both the energy detector and the cyclostationary detector is severely degraded by the presence of a CFO during the adaptation stage. However, it is observed in the simulation results that an increase in the FRESH filter length still improves the detection performance.

As a solution, it is proposed to use the collected samples to estimate the true value of the cyclic frequency and then use this estimate for the adaptation of FRESH filter weights.

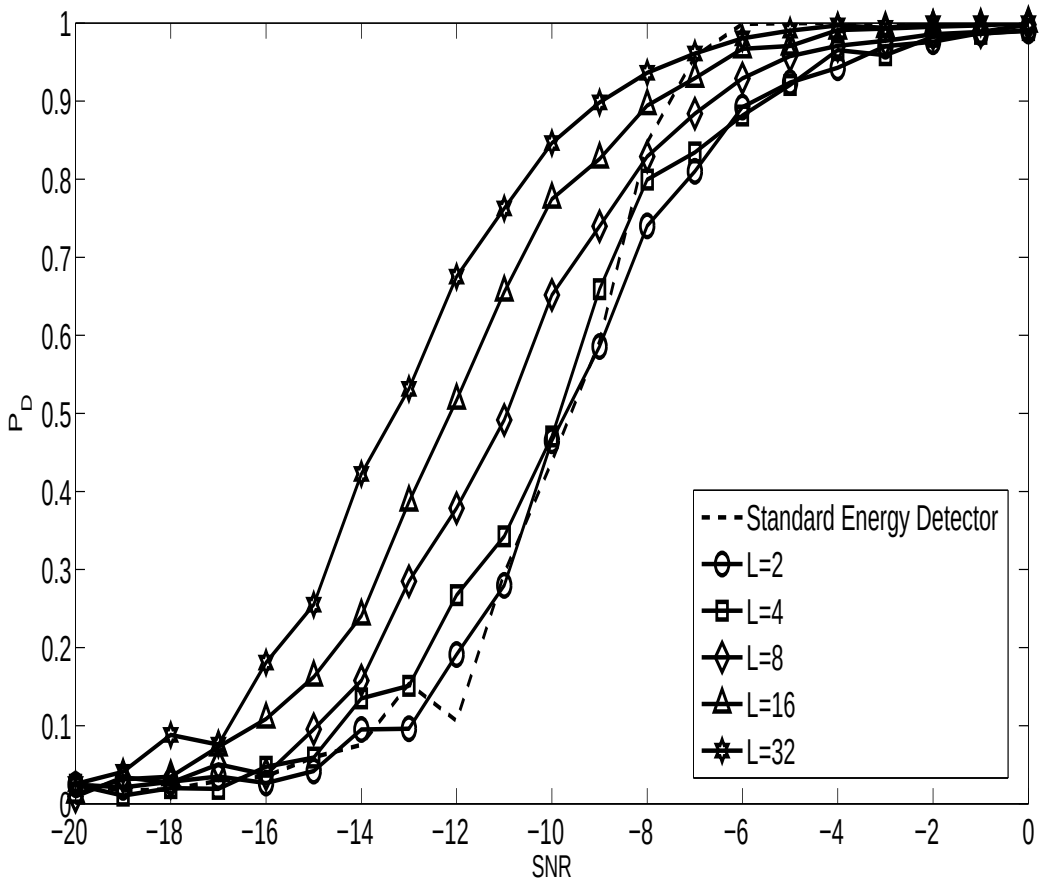

Figure 7.2: Performance of the energy detector in the presence of 1% CFO for different FRESH filter lengths

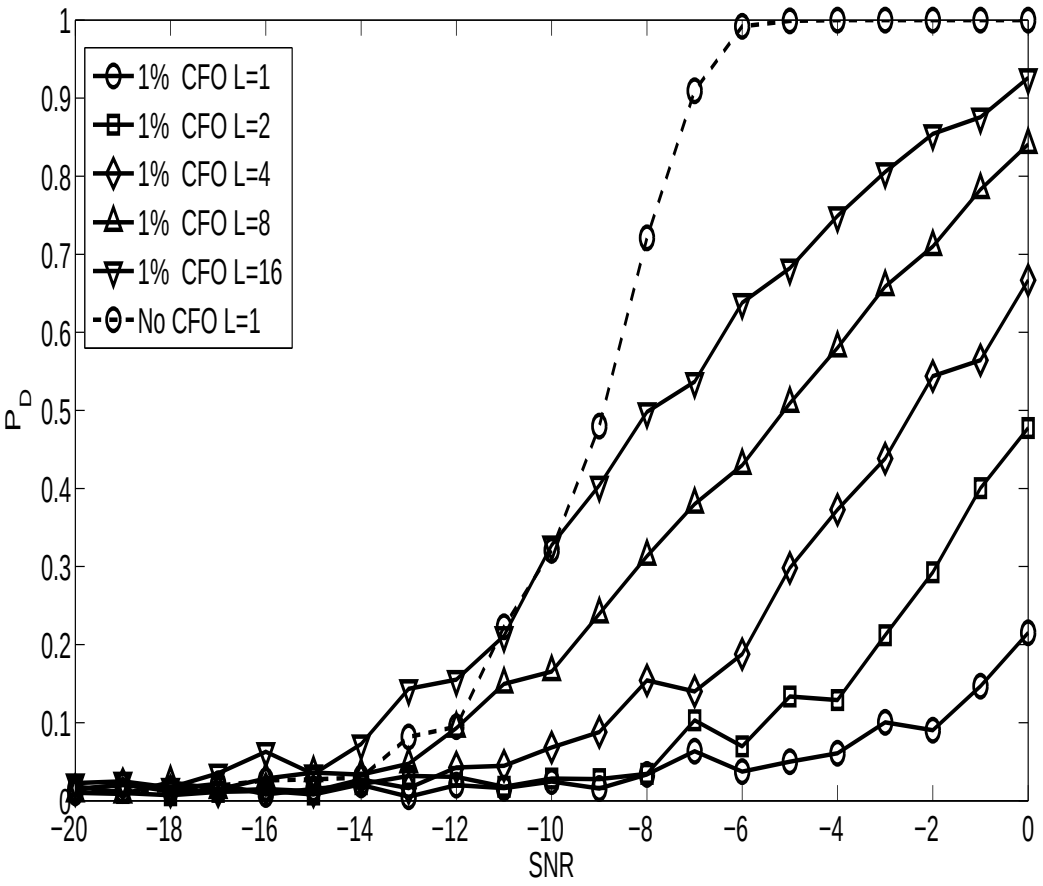

Figure 7.3: Performance of the energy detector in the presence of 1% CFO for different FRESH filter lengths

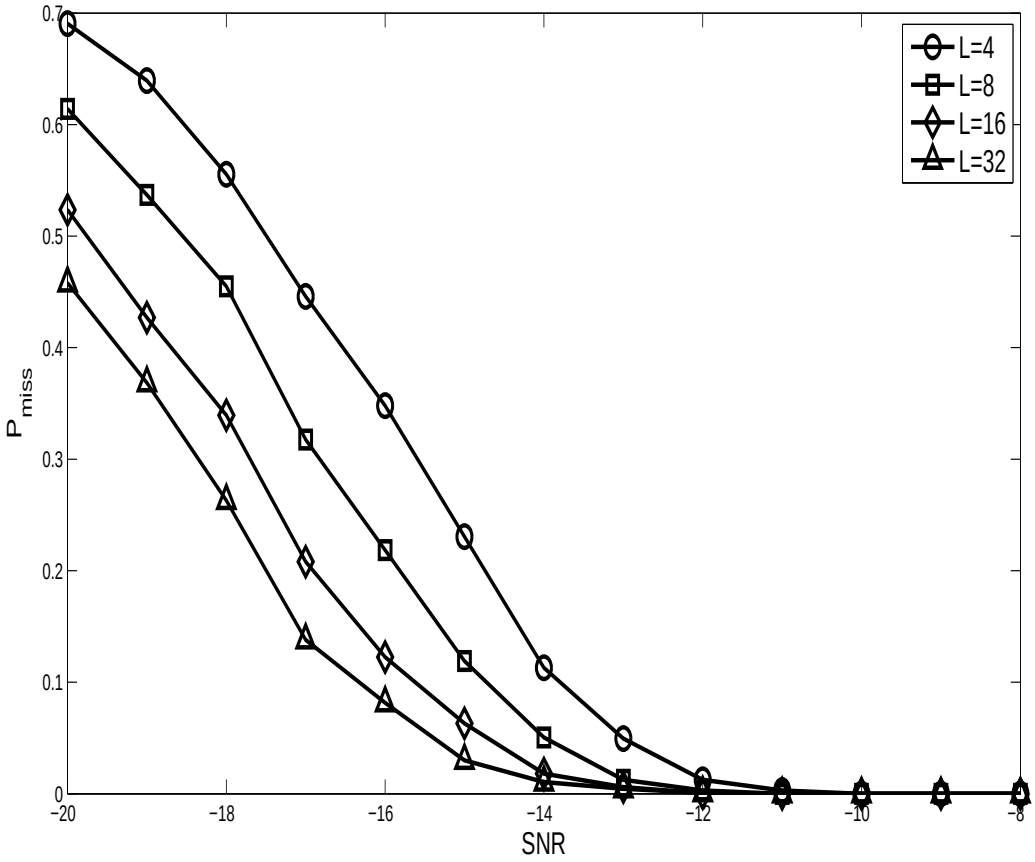

Figure 7.4: Performance of the greedy algorithm for a block size $L_B = 200$ for different FRESH filter lengths in the presence of 0.5% error in the cyclic frequency

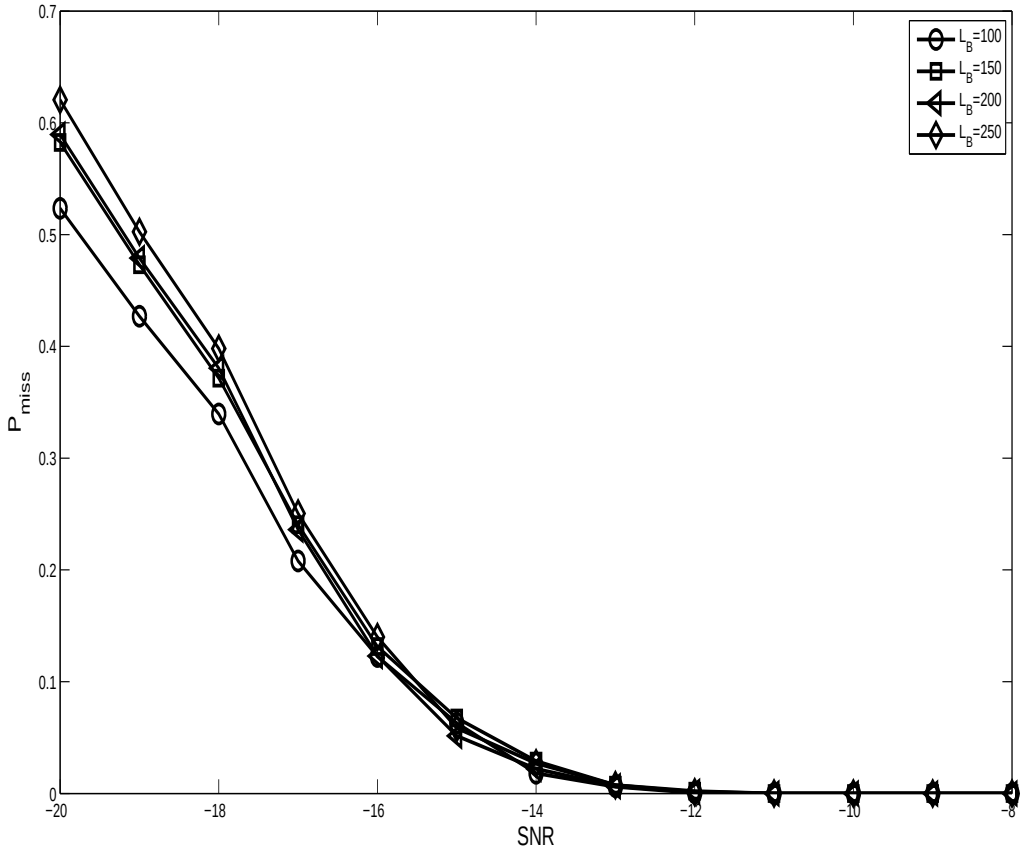

Figure 7.5: Performance of the greedy algorithm for a different block sizes for a FRESH filter length 8 in the presence of 0.5% error in the cyclic frequency

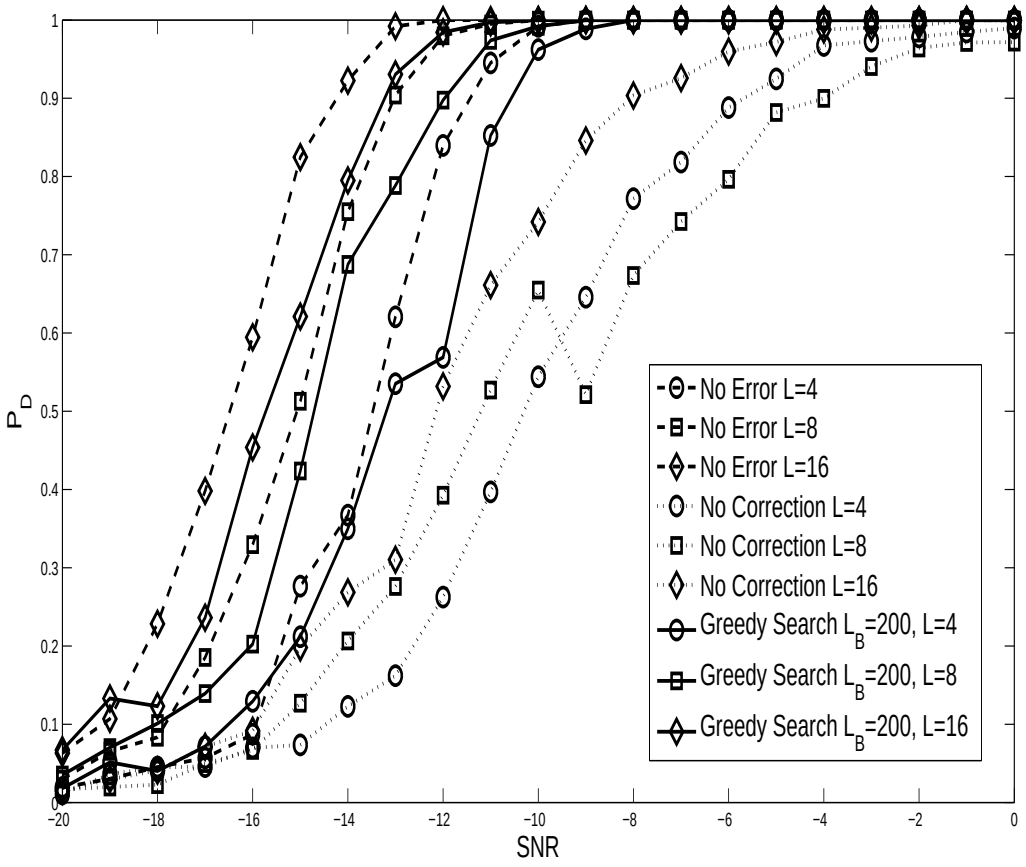

Figure 7.6: Performance of the energy detector with the greedy algorithm for a block size 200 for different FRESH filter lengths in the presence of 1% error in the cyclic frequency

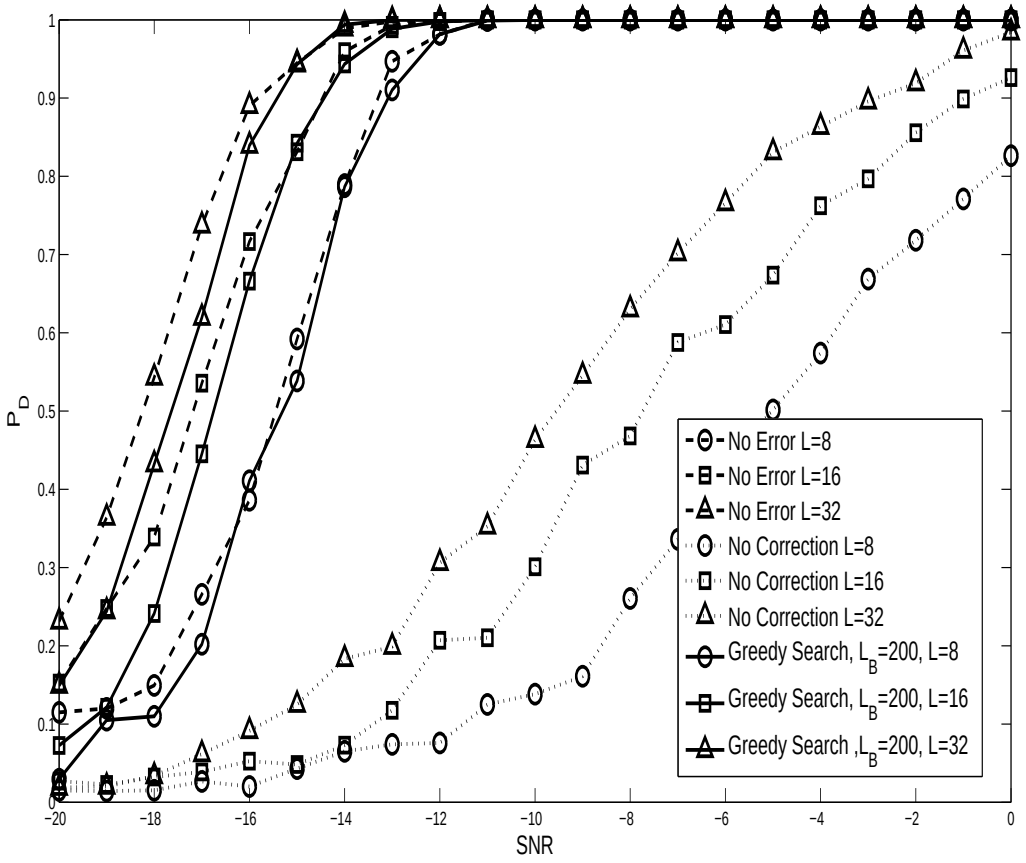

Figure 7.7: Performance of the cyclostationary detector with the greedy algorithm for a block size 200 for different FRESH filter lengths in the presence of 1% error in the cyclic frequency

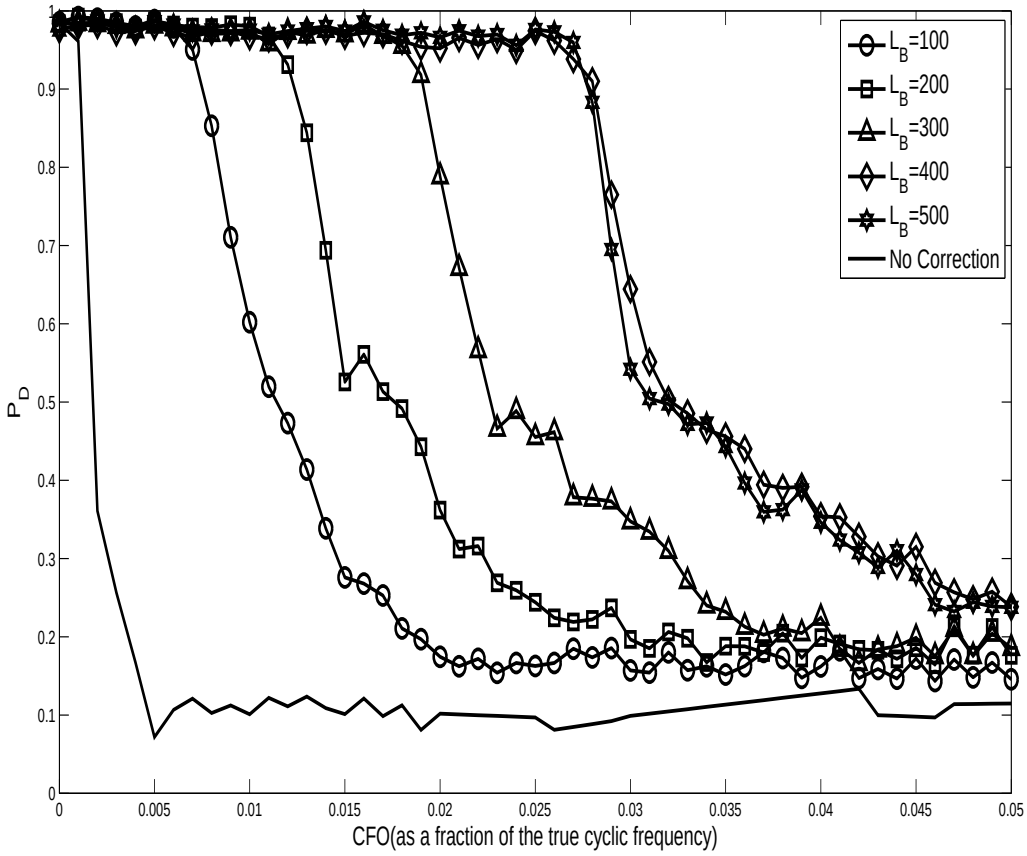

Figure 7.8: Performance of the cyclostationary detector with the greedy algorithm for a block size 200 for a FRESH filter length 8 at -12 dB for different values of the cyclic frequency offset

For this purpose, the greedy search algorithm developed in the previous chapter is modified to fit the present case. The performance of the proposed algorithm in conjunction with FRESH filter-based spectrum sensing is studied by using simulation experiments. It is observed in these experiments that the proposed method may reduce the loss by as much as 5 dB for an energy detector and 14 dB for a cyclostationary detector.

Chapter 8

Conclusions

In this thesis, we have studied the problems of FRESH filter-based spectrum sensing of cylcostationary signals, and the detection of cyclostationary signals in the presence of a Cyclic Frequency Offset. Adaptive techniques for both these problems have been developed. In the following sections, we list the key conclusions drawn in this thesis and identify some open problems for future research in this area.

8.1 Conclusions

In the third chapter, it is proposed to combine the ideas of FRESH filtering [105] and SCORE beam-forming [35] for the purpose of sensing cyclostationary signals. A Space-Time FRESH filtering structure is proposed to exploit the spatial, temporal and spectral redundancy in the primary user signal. The ACS algorithm proposed in [35] for adapting cyclostationarity based beam forming arrays is modified to adapt the proposed structure. It is found that the modified ACS algorithm, with a computational complexity of $\mathcal{O}(N(KLM)^2)$ for an N-antenna M-branch L-tap filter, acts as a bottleneck in the proposed sensing scheme.

In order to reduce the computational complexity, the correlation maximization problem of the ACS algorithm is remodeled as a constrained Mean Squared Error (MSE) minimization problem. The constraints are placed so as to avoid a trivial solution of the MMSE problem. A stochastic gradient based C2-LMS algorithm with a linear complexity is developed as an adaptive solution to this problem. It is shown that the performance of the sensing algorithm depends on the adapted filter weights and should be determined via simulation.

It is observed that an increase in the number of filter taps as well as an increase in the number of taps results in an improved detection performance. It is also observed that a suitable Space-Time FRESH filtering configuration may lead to gains of as much as 10 dB in the detection performance for both the energy detector and the cyclostationary detector. If the computational complexity of the structure is fixed then it is observed that using more

antennas leads to better gains as compared to the use of a larger number of filter taps. A 16-antenna length-2 configuration is observed to perform 2 dB better than a single-antenna system with a FRESH filter of length 32. Further, it is observed that increasing the FRESH filter length in a 2 antenna configuration reduces the probability of missed detection for a given false alarm rate by more than one order of magnitude. It is also shown via simulations that the effects of noise uncertainty in an energy detector may be mitigated to some extent by the use of a Space-Time FRESH filters.

A model for the performance of a single-antenna single-user FRESH filter-based spectrum sensor is developed in the fourth chapter. Here, the effect of FRESH filtering prior to detection is studied on both the energy detector as well as the cyclostationarity detector. It is observed that for normalized filter weights, the mean of the finite time energy under the null hypothesis equals the noise variance. Under the alternative hypothesis, the mean of the test statistic is observed to depend on the adapted filter weights and hence the primary user signal correlation structure. The variance of the test statistic under both the hypotheses is found to be analytically intractable, and therefore bounds on its value under both the hypotheses are derived. It is shown that the test statistic variance under the null hypothesis depends purely on the filter structure. Similarly, the variance of the signal under the alternative hypothesis is found to be an empirical function of the input SNR and the filter structure. Using the distributions of the test statistics under the two hypotheses, the expressions for the probabilities of detection and false alarm are derived. These expressions are then used to derive the number of samples required to achieve given detection and false alarm rates.

Randomly generated signals are used to determine the empirical parameters via curve fitting. The derived results are then verified by the use of simulation experiments. It is observed that the number of samples required for convergence of filter weights is much greater than the number of samples being used for detection and hence filter adaptation. Therefore, the spectrum sensing scheme behaves differently for optimal and adapted filter weights. For example, increasing the FRESH filter length from 1 to 8 leads to a gain of nearly 4 dB for adapted filter weights and more than 6 dB for optimal filter weights. It is also observed that in case of the filter weights being unknown, the detection performance also depends on the adaptation algorithm being used. It is observed that FRESH filters based on the RLS algorithm perform marginally better than the systems based on the LMS algorithms. Further, the number of samples required to achieve a given detection performance for a fixed false alarm rate are determined via simulation. It is observed that using optimal filter weights reduces the number of samples required to achieve a 90% probability of detection for 1% false alarm rate by as much as two orders, of magnitude as predicted by the derived results. In the absence of this knowledge the number of samples required to achieve these detection and false alarm rates reduces by more than one order of magnitude. For a cyclostationarity detector, it is observed that the finite time cyclic

autocorrelation function is a complex number. Therefore, the test statistic is decided based on the knowledge of its phase. Similar to the energy detector it is found that the mean of the test statistic under the alternative hypothesis depends on the correlation structure of the primary user signal. The variances under the two hypotheses are empirically determinable functions.

The derived performances are again verified for randomly generated signals. It is observed that the knowledge of the phase of the cyclic autocorrelation function does not affect the performance much, whereas the knowledge of the optimal filter weights again has a significant impact on the detection performance. In the case of an eight-tap FRESH filter, the knowledge of predicted weights is observed to give an advantage of more than 2 dB over the adapted weights. Increasing the length of the FRESH filter from 1 to 16 improves the detection performance by as much as 8 dB when the optimal filter weights are known. Analogous to the energy detector, the number of samples required for a cyclostationary detector to achieve 90% successful detection rate for a false alarm rate of 1% is reduced by two orders of magnitude when the filter weights are known and by one order of magnitude when they are adapted. The performance of the energy detector under noise uncertainty is then derived and it is found that FRESH filtering helps in lowering the SNR walls. It is observed that a length 32 FRESH filter may lower the SNR walls by as much as 14 dB.

Collaboration schemes for FRESH filter based spectrum sensing are considered in the fifth chapter. All the three collaboration models, i.e. centralized, distributed, and hierarchical, are considered. It is first shown that in case multiple secondary users are sensing signals from a single primary user, then,based on the sensing time and the channel delay spread, the optimal FRESH filter weights at each secondary user can be either same or correlated. Following this, the statistics of the energy detector, derived in the previous chapter are extended to the three collaborative settings. For the centralized setting, the existence of a fusion center having unrestricted access to all the sensed data is assumed. No fusion center is assumed for purely distributed collaboration. However in this case it is assumed that the collaborating nodes can communicate among themselves to arrive at a consensus on the presence of a primary user signal. It is shown that for the sensing nodes forming a fully connected graph, the system eventually converges to a consensus. Under the hierarchical model, the system is assumed to consist of two types of nodes, the sensing and the processing nodes. Each sensing node is assumed to be connected to one or more processing nodes and vice versa. The sensing nodes simply forward their sensed data to the processing nodes. The processing nodes then use these data to calculate the test statistics and collaborate among themselves to reach a consensus on the final decision.

If the channel delay spread at all the sensing nodes is less than the inter-sample interval, then the optimal filter weights at these nodes will also be the same. Therefore, joint adaptation algorithms may be used to estimate these. Hence, the global-LMS algorithm developed in [17] is used for adaptation in the centralized case whereas the ATC-LMS [17]

algorithm is used for adaptation in purely distributed and hierarchical cases. In case the delay spread of all the channels is not less than the inter-sample interval, then the optimal weights for different FRESH filters will still be correlated though unequal. The C2-LMS algorithm developed in the third chapter is, therefore, modified so as to handle this case.

For a centralized setting, it is observed that increasing the FRESH filter length from 1 to 32 in a 16-user setting results in a gain of 3 dB for local LMS-based adaptation. Here, joint adaptation using the global-LMS algorithm leads to an additional gain of 2 dB while the use of C2-LMS algorithm under dispersive fading results in an additional gain of 1 dB. In a purely distributed setting, increasing the filter length from 1 to 32 results in a gain of 4 dB with local adaptation and an additional 1 dB with joint adaptation for both the flat fading and dispersive fading cases. It is also shown that an N-node network arrives at a consensus in a maximum of $\log_2(N)$ steps. It is observed that the detection performance falls by nearly 1 dB as the system moves from a purely centralized setting to a purely distributed setting.

The sixth chapter addresses the problem of cyclic frequency offset in the sensing stage of a cyclostationarity-based detector. In this chapter, the problem of sensing an OFDM signal with correlated pilots is studied. It is shown that correlated pilots in an OFDM signal lead to spectral coherence in the signal of interest. It is then shown that this cyclostationarity may be detected by the use of the finite-time cyclic autocorrelation function as a test statistic. Following this, it is argued that the detection performance can be improved by combining the cyclic autocorrelation function at different frequencies and lags. For 45000 samples and a false alarm rate of 1%, it is observed that increasing the number of temporal features from 1 to 19 improves the detection performance by 5 dB. At the same time, using two cyclic frequencies, instead of one, further improves this performance by more than 1 dB.

Following this, it is shown that a cyclic frequency offset causes the detector performance to deteriorate as the number of samples being used for detection increases. Based on this, it is proposed to use the collected samples to estimate the true cyclic frequency of the sensed signal. The Crammer-Rao bound for the true cyclic frequency estimator is derived and it is found that the variance of the estimator depends on the magnitude of CFO. Therefore, it is proposed to estimate the true cyclic frequency recursively. For this purpose, two recursive algorithms based on gradient ascent and greedy search are proposed.

The gradient ascent algorithm is based on the fact that the main lobe of the sinc function is concave and can be maximized by moving in the direction of the gradient. The resulting algorithm has a linear complexity in terms of the number of samples being used. However, the performance of this algorithm depends on the adaptation step size being chosen. It is observed that a small step size leads to a better estimate of the true cyclic frequency at the cost of convergence time. Whereas, a larger step size will result in faster convergence but will result in an increased variance of the final estimate. A proper choice of the step

size parameter may mitigate the loss due to CFO by more than 8 dB.

The greedy search algorithm divides the received signal samples into blocks. Here, the cyclic frequency maximizing the cyclic autocorrelation function is selected for each block. A smaller block size leads to more precise estimates at the cost of computation time. The complexity of this algorithm is $\mathcal{O}(M^2)$ for M samples. This provides an additional 4 dB gain over the gradient ascent algorithm for a successful detection rate of 90%. As compared with the algorithm in [103], the greedy search algorithm provides a gain of nearly 6 dB and the gradient ascent algorithm a gain of more than 1 dB for a 90% rate of successful detection at a 1% probability of false alarm. Similar trends are observed for fading channels as well.

In the seventh chapter, the problem of CFO in the adaptation stage of a FRESH filter-based spectrum sensor is studied. The derived results show that a CFO in the adaptation stage will result in the optimal weight vector being a null vector. This results in a degraded performance for both the energy and the cyclostationarity detectors. The greedy search algorithm developed in the previous chapter is, therefore, modified to estimate the true cyclic frequency of the adaptation stage of a FRESH filter-based spectrum sensor. It is shown via simulation that the loss due to CFO in a FRESH filter-based sensor followed by an energy detector is reduced to 2 dB from 8 dB and for a cyclostationarity detector it is reduced from 16 dB to 1 dB.

8.2 Directions for Future Work

In this thesis, we have used the energy detector and the cyclostationarity detector for FRESH filter-based spectrum sensing. However, it is possible to use other detectors as well. The estimator correlator introduced in [69] is one such detector. Here, the cross correlation of the output of the FRESH filter with the input signal can be used as a test statistic. It is to be noted that due to the absence of spectral coherence in the ambient noise, the mean value of this test statistic under the null hypothesis will be zero. However, this will take a non-zero value under the alternative hypothesis.

Alternatively, a non-parametric detector, comparing the ratio of the energy of the filtered signal to that of the unfiltered signal may also be developed. It was shown in the fourth chapter that the energies of the filtered signal and the unfiltered signal will be approximately equal when the primary user signal is absent. However, the energy of the filtered signal will be much greater than that of the unfiltered signal in case a primary user signal is present. Therefore, a detector using the ratio of the energies of the filtered and the unfiltered signal may as well be developed. It may also be interesting to look at the energy of the filtered signal in terms of the eigenvalues of the covariance matrix of the sensed signal. The performance of this detector can then be compared with other non-parametric detectors based on the eigenvalues of the received signal covariance matrix.

It was mentioned in the fourth chapter that the detection performance may be improved if the correlation structure of the primary signal and hence the optimal weights are known. In case these weights are known ,a FRESH filter-bank-based detector similar to the approach in [38] may be developed to detect the presence of a primary user signal. Further, a sequential detection approach based on the FRESH filter-bank-based detector may also be developed. The sequential detector may use energy detection, cyclostationary detection, the estimator correlator or the non-parametric detector discussed above.

Appendix A

Derivation of the C2LMS algorithm

The function to be minimized, as given in (3.69), may be written in the form

$$\begin{aligned} J(\mathbf{w},\mathbf{h}) &= \mathbf{h}^H\mathbf{R}_{xx}\mathbf{h} - \mathbf{h}^H\mathbf{R}_{xu}\mathbf{w} - \mathbf{w}^H\mathbf{R}_{ux}\mathbf{h} \\ &\quad +\mathbf{w}^H\mathbf{R}_{uu}\mathbf{w} + \lambda\left\{\|\mathbf{h}\|_2^2 - g^2\right\} \end{aligned} \tag{A.1}$$

and it may be shown that

$$\nabla_{\mathbf{h}} J = 2\left\langle \mathbf{x}[\mathbf{n}](\mathbf{e}^*(\mathbf{n}))\right\rangle + 2\lambda\mathbf{h} \tag{A.2}$$

$$\nabla_{\mathbf{w}} J = 2\left\langle \mathbf{u}[\mathbf{n}](-\mathbf{e}^*(\mathbf{n}))\right\rangle \tag{A.3}$$

Using the method of steepest descent, the update equations for the weight vectors may be written as

$$\begin{aligned} \mathbf{h}[n+1] &= \mathbf{h}[\mathbf{n}] - \tfrac{\mu}{\mathbf{2}}\nabla_{\mathbf{h}}\mathbf{J} \\ &= \mathbf{h}[n] - \mu\langle \mathbf{x}[n]e^*[n]\rangle - \mu\lambda\mathbf{h}[n] \\ &= (1-\mu\lambda)\mathbf{h}[n] - \mu\langle \mathbf{x}[n]e^*[n]\rangle \end{aligned} \tag{A.4}$$

$$\begin{aligned} \mathbf{w}[n+1] &= \mathbf{w}[\mathbf{n}] - \tfrac{\mu}{\mathbf{2}}\nabla_{\mathbf{w}}\mathbf{J} \\ &= \mathbf{w}[n] + \mu\langle \mathbf{u}[n]e^*[n]\rangle \end{aligned} \tag{A.5}$$

Replacing the deterministic gradient in the above equations with the stochastic gradient, the following update equations are obtained.

$$\mathbf{h}[n+1] = (1-\mu\lambda)\mathbf{h}[n] - \mu\mathbf{x}[n]e^*[n] \tag{A.6}$$

$$\mathbf{w}[n+1] = \mathbf{w}[n] - \mu\mathbf{u}[n]e^*[n] \tag{A.7}$$

Invoking the constraint $\|\mathbf{h}[n+1]\|_2 = g$, we have

$$\|(1-\mu\lambda)\mathbf{h}[n] - \mu\mathbf{x}[n]e^*[n]\|_2^2 = g^2 \tag{A.8}$$

or

$$(1-\mu\lambda)^2 - 2*(1-\mu\lambda)\mu\Re\{e^*[n]y[n]\} + \mu^2\|\mathbf{x}[n]\|_2^2|e[n]|^2 - g^2 = 0 \tag{A.9}$$

By substituting

$$\begin{aligned} z &= (1-\mu\lambda) \\ b &= \mu\Re\{e^*[n]y[n]\} \\ c &= \mu^2\|\mathbf{x}[n]\|_2^2|e[n]|^2 - g^2 \end{aligned} \tag{A.10}$$

the above equation reduces to a quadratic equation yielding two solutions $z = b \pm \sqrt{b^2 - c}$. Using only the solution corresponding to $z = b + \sqrt{b^2 - c}$ the adaptation algorithm, as described in Chapter 3, may be obtained.

Appendix B

Equivalence of the MMSE and the Maximum Correlation Solutions

Assume that a zero-mean cyclostationary signal $s[n]$ is incident on a K-antenna array from a direction θ such that the signal received vector $\mathbf{x}[n]$ is given as

$$\mathbf{x}[n] = \mathbf{a}(\theta)s[n] + \boldsymbol{\nu}[n]$$

where $\mathbf{a}[\theta]$ is the array response vector for the direction θ and $\boldsymbol{\nu}[n]$ the zero mean additive noise noise vector. It is known that the signal of interest (SOI) exhibits non-conjugate spectral coherence at frequencies $\mathcal{A} = \{\alpha_1, \alpha_2, \ldots, \alpha_{M_1}\}$ and conjugate spectral coherence at $\mathcal{B} = \{\beta_1, \beta_2, \ldots, \beta_{M_2}\}$, $M1 + M2 = M$.

The signal $\mathbf{x}[n]$ will, therefore exhibits spatial, temporal and spectral correlation. That is, if we define

$$u_{km}[n-l] = [x_k[n-l]]^{(*)} e^{-j2\pi\alpha_m n}$$

with an optional conjugation and $\alpha_m \in \mathcal{A} \cup \mathcal{B}$; then by virtue of these properties, any element $x_p[n]$ of $\mathbf{x}[n]$ may be expressed as

$$x_p[n] = c_{kpml} u_{km}[n-l] + \eta_{kpml}[n]$$

where c_{kpml} is the regression coefficient and $\eta_{kpml}[n]$ is the innovation component. Each element of $\mathbf{u}[\mathbf{n}]$ may, hence, be expressed as a linear combination of time and frequency shifted version of all the elements of $\mathbf{u}[\mathbf{n}]$.
Now, if we define

$$u_{km}[n] = [x_k[n]]^{(*)} e^{-j2\pi\alpha_m n}$$

then,

$$\mathbf{u}_{km}[n] = [u_{km}[n], u_{km}[n-1], u_{km}[n-2], \ldots, u_{km}[n-L+1]]^T$$

and

$$\mathbf{u}_k[n] = [\mathbf{u}_{u1}^T[n], \mathbf{x}_{u2}^T[n], \ldots, \mathbf{u}_{kM}^T[n]]^T$$

$$\mathbf{u}[n] = [\mathbf{u}_1^T[n], \mathbf{u}_2^T[n], \ldots, \mathbf{u}_K^T[n]]^T$$

then there exist nonzero vectors $\mathbf{w}, \mathbf{h}$ such that

$$\mathbf{w}^H\mathbf{u}[n] = \mathbf{h}^H\mathbf{x}[n] + \eta[n]$$

Defining

$$r[n] = \mathbf{h}^H\mathbf{x}[n]$$

and

$$y[n] = \mathbf{w}^H\mathbf{u}[n]$$

we may find the weight vectors $\mathbf{w}_o$ and $\mathbf{h}_o$ such that mean square error defined as

$$J(\mathbf{w}, \mathbf{h}) = \mathbb{E}\left[|\mathbf{w}^H\mathbf{u}[n] - \mathbf{h}^H\mathbf{x}[n]|^2\right]$$

is minimized.

Also, there will exist vectors $\mathbf{w'_o}, \mathbf{h'_o}$ that will maximize the cross-correlation coefficient of $y[n]$ and $r[n]$, defined as

$$F(\mathbf{w}, \mathbf{h}) = \frac{[\mathbb{E}[y[n]r^*[n]]]^2}{E[|y[n]|^2]E[|r[n]|^2]} \tag{B.1}$$

In the following sections we show that the solutions to these two problems take identical forms.

B.1 Solution to the MMSE Problem

The MMSE problem for the objective function $J(\mathbf{w}, \mathbf{h})$ may be written as,

$$\begin{aligned}
[\mathbf{w_o}, \mathbf{h}_o] &= \arg\min_{\mathbf{w},\mathbf{h}} J(\mathbf{w}, \mathbf{h}) \\
&= \arg\min_{\mathbf{w},\mathbf{h}} [\mathbf{w}^H\mathbf{x}[n] - \mathbf{h}^H\mathbf{u}[n]][\mathbf{w}^H\mathbf{x}[n] - \mathbf{h}^H\mathbf{u}[n]]^* \qquad \text{(B.2)} \\
&= \arg\min_{\mathbf{w},\mathbf{h}} [\mathbf{w^H R_{uu} w} - \mathbf{w^H R_{ux} h} - \mathbf{h^H R_{xu} w} + \mathbf{h^H R_{xx} h}
\end{aligned}$$

Differentiating this separately w.r.t $\mathbf{w}$ and $\mathbf{h}$ [2], we have

$$\nabla_{\mathbf{w}} J = \mathbf{R}_{uu}\mathbf{w} - \mathbf{R}_{ux}\mathbf{h} \tag{B.3}$$

and

$$\nabla_{\mathbf{h}} J = \mathbf{R}_{xx}\mathbf{h} - \mathbf{R}_{xu}\mathbf{h} \tag{B.4}$$

where $\mathbf{R}_{ux} = \mathbf{R}_{ux}^H$. Now, the objective function will be minimized in terms of $\mathbf{w}$ and $\mathbf{h}$ when equations (B.3) and (B.4) are, respectively, equated to zero.

Equating (B.3) to zero, we have

$$\nabla_{\mathbf{w}} J = \mathbf{R}_{xx}\mathbf{w} - \mathbf{R}_{xu}\mathbf{h} = 0$$

or

$$\mathbf{R}_{uu}\mathbf{w} = \mathbf{R}_{ux}\mathbf{h}$$

Therefore,

$$\mathbf{w}_o = \mathbf{R}_{uu}^{-1}\mathbf{R}_{ux}\mathbf{h} \tag{B.5}$$

Similarly

$$\mathbf{h}_o = \mathbf{R}_{xx}^{-1}\mathbf{R}_{xu}\mathbf{w} \tag{B.6}$$

B.2 Solution to the Maximum Cross Correlation Problem

This solution has been presented by Schell and Gardner in [2]. Looking at (B.1) it may be observed that the two weight vectors should be selected such that the cross correlation coefficient of $y[n]$ and $r[n]$ is maximized. That is,

$$\begin{aligned} [\mathbf{w}'_o, \mathbf{h}'_o] &= \arg\max_{w,h} F(\mathbf{w}, \mathbf{h}) \\ &= \arg\max_{w,h} \frac{\left[\mathbf{w^H R_{xu}[n]h}\right]^2}{[\mathbf{w^H R_{xu}[n]h}][\mathbf{h^H R_{ux}[n]w}]} \end{aligned} \tag{B.7}$$

For the objective function F, we may define F_N and F_D as

$$F_N = \left[\mathbf{w^H R_{ux}[n]h}\right]^2 = \mathbf{w^H R_{ux}[n]hh^H R_{xu}[n]w}$$

$$F_D = \left[\mathbf{w^H R_{uu}[n]w}\right]\left[\mathbf{h^H R_{xx}[n]h}\right]$$

We may write $F = \frac{F_N}{F_D}$ therefore

$$\nabla_{\mathbf{w}} F = \frac{\nabla_{\mathbf{w}} F_N . F_D - \nabla_{\mathbf{w}} F_D . F_N}{F_D^2}$$

and

$$\nabla_{\mathbf{h}} F = \frac{\nabla_{\mathbf{h}} F_N . F_D - \nabla_{\mathbf{h}} F_D . F_N}{F_D^2}$$

Equating the numerators of these terms to zero, we get

$$\nabla_{\mathbf{w}} F_N . F_D - \nabla_{\mathbf{w}} F_D . F_N = 0 \tag{B.8}$$

$$\nabla_{\mathbf{h}} F_N . F_D - \nabla_{\mathbf{h}} F_D . F_N = 0 \tag{B.9}$$

Now

$$\nabla_{\mathbf{w}} F_N = \mathbf{R_{ux}[n]hh^H R_{xu}[n]w}$$

$$\nabla_{\mathbf{h}} F_N = \mathbf{R_{xu}[n]ww^H R_{ux}[n]h}$$

$$\nabla_{\mathbf{w}} F_D = \mathbf{R_{uu}[n]wh^H R_{xx}[n]h}$$

$$\nabla_{\mathbf{h}} F_D = \mathbf{R_{xx}[n]hw^H R_{uu}[n]w}$$

Substituting these values into (B.8) and (B.9), we have

$$\begin{aligned} [\mathbf{R_{ux}[n]hh}^H\mathbf{R_{ux}[n]w}][\mathbf{w}^H\mathbf{R_{ux}[n]h}]\left[\mathbf{h}^H\mathbf{R_{xu}[n]w}\right] &= \mathbf{R_{uu}[n]wh}^H\mathbf{R_{xx}[n]h} \\ &\quad \mathbf{w^H R_{ux}[n]hh^H R_{xu}[n]w} \end{aligned} \tag{B.10}$$

Or

$$[\mathbf{R_{ux}[n]h}][\mathbf{w^H R_{uu}w}] = \mathbf{w^H R_{ux}hR_{uu}w}$$

and

$$[\mathbf{R_{xx}[n]h}][\mathbf{h}^H\mathbf{R_{xu}w}] = \mathbf{h}^H\mathbf{R_{xx}hR_{xu}w}$$

It may be observed that for optimal weight vectors, $[w^H R_{xu} h]$ will correspond to the largest singular value of the matrix $\mathbf{R_{xu}}$.
The equations thus reduce to

$$\mathbf{w'}_o = d_1 \mathbf{R}_{xx}^{-1} \mathbf{R}_{xu} \mathbf{h} \tag{B.11}$$

and similarly

$$\mathbf{h'}_o = d_2 \mathbf{R}_{uu}^{-1} \mathbf{R}_{ux} \mathbf{w} \tag{B.12}$$

It may be observed that the solutions to the two problems are scaled versions of each other.

Bibliography

[1] A. Agarwal and A. Jagannatham, "Distributed estimation in homogenous poisson wireless sensor networks," *IEEE Wireless Communications Letters*, vol. 3, no. 1, pp. 90–93, February 2014.

[2] B. Agee, S. Schell, and W. Gardner, "Spectral self-coherence restoral: a new approach to blind adaptive signal extraction using antenna arrays," *Proceedings of the IEEE*, vol. 78, no. 4, pp. 753 –767, April 1990.

[3] S. Althunibat, R. Palacios, and F. Granelli, "Performance optimisation of soft and hard spectrum sensing schemes in cognitive radio," *IEEE Communications Letters*, vol. 16, no. 7, pp. 998–1001, July 2012.

[4] S. Astaneh and S. Gazor, "Cooperative spectrum sensing over mixture-nakagami channels," *IEEE Wireless Communications Letters*, vol. 2, no. 3, pp. 259–262, June 2013.

[5] E. Axell and E. Larsson, "A bayesian approach to spectrum sensing, denoising and anomaly detection," in *IEEE Intl. Conf. Acoustics, Speech and Signal Processing, 2009. ICASSP 2009.*, April 2009, pp. 2333 –2336.

[6] ——, "Spectrum sensing of orthogonal space-time block coded signals with multiple receive antennas," in *IEEE Intl. Conf. Acoustics Speech and Signal Processing (ICASSP), 2010*, Mar. 2010, pp. 3110 –3113.

[7] ——, "Multiantenna spectrum sensing of a second-order cyclostationary signal," in *4th IEEE Intl. Workshop on Computational Advances in Multi-Sensor Adaptive Processing (CAMSAP), 2011*, Dec. 2011, pp. 329 –332.

[8] ——, "Optimal and sub-optimal spectrum sensing of ofdm signals in known and unknown noise variance," *IEEE J. Selected Areas in Communications*, vol. 29, no. 2, pp. 290 –304, Feb. 2011.

[9] E. Axell, G. Leus, E. Larsson, and H. Poor, "Spectrum sensing for cognitive radio : State-of-the-art and recent advances," *IEEE Signal Processing Magazine*, vol. 29, no. 3, pp. 101 –116, May 2012.

[10] K. Ben Letaief and W. Zhang, "Cooperative communications for cognitive radio networks," *Proceedings of the IEEE*, vol. 97, no. 5, pp. 878 –893, May 2009.

[11] D. Bhargavi and C. Murthy, "Performance comparison of energy, matched-filter and cyclostationarity-based spectrum sensing," in *IEEE Eleventh International Workshop on Signal Processing Advances in Wireless Communications (SPAWC), 2010*, June 2010, pp. 1–5.

[12] J. Bingham, "Multicarrier modulation for data transmission: an idea whose time has come," *IEEE Communications Magazine*, vol. 28, no. 5, pp. 5–14, May 1990.

[13] S. Bokharaiee, H. Nguyen, and E. Shwedyk, "Blind spectrum sensing for ofdm-based cognitive radio systems," *IEEE Transactions on Vehicular Technology*, vol. 60, no. 3, pp. 858–871, March 2011.

[14] H. Bolcskei, A. Paulraj, K. Hari, R. Nabar, and W. Lu, "Fixed broadband wireless access: state of the art, challenges, and future directions," *IEEE Communications Magazine*, vol. 39, no. 1, pp. 100–108, Jan 2001.

[15] R. Boyles and W. Gardner, "Cycloergodic properties of discrete- parameter nonstationary stochastic processes," *IEEE Transactions on Information Theory*, vol. 29, no. 1, pp. 105–114, Jan 1983.

[16] D. Cabric, S. Mishra, and R. Brodersen, "Implementation issues in spectrum sensing for cognitive radios," in *Signals, Systems and Computers, 2004. Conference Record of the Thirty-Eighth Asilomar Conf.*, vol. 1, Nov. 2004, pp. 772 – 776 Vol.1.

[17] F. Cattivelli and A. Sayed, "Diffusion lms strategies for distributed estimation," *IEEE Transactions on Signal Processing*, vol. 58, no. 3, pp. 1035–1048, March 2010.

[18] ——, "Diffusion strategies for distributed kalman filtering and smoothing," *IEEE Transactions on Automatic Control*, vol. 55, no. 9, pp. 2069–2084, Sept 2010.

[19] ——, "Distributed detection over adaptive networks using diffusion adaptation," *IEEE Transactions on Signal Processing*, vol. 59, no. 5, pp. 1917–1932, May 2011.

[20] M. Chakraborty and H. Sakai, "Convergence analysis of a complex lms algorithm with tonal reference signals," *IEEE Transactions on Speech and Audio Processing*, vol. 13, no. 2, pp. 286–292, March 2005.

[21] M. Chakraborty, R. Shaik, and M. H. Lee, "A block-floating-point-based realization of the block lms algorithm," *IEEE Transactions on Circuits and Systems II: Express Briefs*, vol. 53, no. 9, pp. 812–816, Sept 2006.

[22] M. Chakraborty, H. So, and J. Zheng, "New adaptive algorithm for delay estimation of sinusoidal signals," *IEEE Signal Processing Letters*, vol. 14, no. 12, pp. 984–987, Dec 2007.

[23] V. Chakravarthy, A. Nunez, J. Stephens, A. Shaw, and M. Temple, "Tdcs, ofdm, and mc-cdma: a brief tutorial," *IEEE Communications Magazine*, vol. 43, no. 9, pp. S11 – S16, Sept. 2005.

[24] J.-F. Chamberland and V. Veeravalli, "Decentralized detection in sensor networks," *IEEE Transactions on Signal Processing*, vol. 51, no. 2, pp. 407–416, Feb 2003.

[25] S. Chaudhari, V. Koivunen, and H. Poor, "Autocorrelation-based decentralized sequential detection of ofdm signals in cognitive radios," *IEEE Trans. Signal Processing*, vol. 57, no. 7, pp. 2690–2700, Jul. 2009.

[26] S. Chaudhari, J. Lunden, V. Koivunen, and H. Poor, "Cooperative sensing with imperfect reporting channels: Hard decisions or soft decisions?" *IEEE Trans. Signal Processing*, vol. 60, no. 1, pp. 18 –28, Jan. 2012.

[27] H.-S. Chen, W. Gao, and D. Daut, "Signature based spectrum sensing algorithms for ieee 802.22 wran," in *IEEE Intl. Conf. Communications, 2007.*, Jun. 2007, pp. 6487–6492.

[28] Y. Chen, "Improved energy detector for random signals in gaussian noise," *IEEE Trans. Wireless Communications,*, vol. 9, no. 2, pp. 558 –563, Feb. 2010.

[29] C. Cordeiro, M. Ghosh, D. Cavalcanti, and K. Challapali, "Spectrum sensing for dynamic spectrum access of tv bands," in *2nd Intl. Conf. Cognitive Radio Oriented Wireless Networks and Communications, 2007. CrownCom 2007.*, Aug. 2007, pp. 225 –233.

[30] C. da Silva, B. Choi, and K. Kim, "Distributed spectrum sensing for cognitive radio systems," in *Information Theory and Applications Workshop, 2007*, Jan 2007, pp. 120–123.

[31] A. Dandawate and G. Giannakis, "Statistical tests for presence of cyclostationarity," *IEEE Trans. Signal Processing*, vol. 42, no. 9, pp. 2355–2369, Sep.

[32] M. Derakhshani, T. Le-Ngoc, and M. Nasiri-Kenari, "Efficient cooperative cyclostationary spectrum sensing in cognitive radios at low SNR regimes," *IEEE Trans. Wireless Communications*, vol. 10, no. 11, pp. 3754 –3764, Nov. 2011.

[33] F. Digham, M.-S. Alouini, and M. Simon, "On the energy detection of unknown signals over fading channels," in *IEEE Intl. Conf. Communications, 2003. ICC '03.*, vol. 5, May 2003, pp. 3575 – 3579 vol.5.

[34] D. Donoho, "Compressed sensing," *IEEE Trans. Information Theory,*, vol. 52, no. 4, pp. 1289 –1306, April 2006.

[35] K.-L. Du and W. H. Mow, "Affordable cyclostationarity-based spectrum sensing for cognitive radio with smart antennas," *IEEE Trans. Vehicular Technology*, vol. 59, no. 4, pp. 1877 –1886, May 2010.

[36] K. Du and M. Swamy, "A class of adaptive cyclostationary beamforming algorithms," *Circuits, Systems and Signal Processing*, vol. 27, no. 1, pp. 55 –63, Jan 2008.

[37] S. Dwivedi, A. Kota, and A. Jagannatham, "Optimal bartlett detector based sprt for spectrum sensing in multi-antenna cognitive radio systems," *IEEE Signal Processing Letters*, vol. 22, no. 9, pp. 1409–1413, Sept 2015.

[38] B. Farhang-Boroujeny, "Filter bank spectrum sensing for cognitive radios," *IEEE Trans. Signal Processing,*, vol. 56, no. 5, pp. 1801 –1811, May 2008.

[39] FCC, "Spectrum policy task force report," ET docket No, 02-155, Tech. Rep., 2002.

[40] J. Font-Segura, G. Vazquez, and J. Riba, "Multi-frequency glrt spectrum sensing for wideband cognitive radio," in *IEEE Intl. Conf. Communications (ICC), 2011*, June 2011, pp. 1 –5.

[41] J. Font-Segura and X. Wang, "Glrt-based spectrum sensing for cognitive radio with prior information," *IEEE Trans. Communications,*, vol. 58, no. 7, pp. 2137 –2146, Jul. 2010.

[42] M. Gandetto and C. Regazzoni, "Spectrum sensing: A distributed approach for cognitive terminals," *Selected Areas in Communications, IEEE Journal on*, vol. 25, no. 3, pp. 546–557, April 2007.

[43] W. Gardner, "Measurement of spectral correlation," *IEEE Trans. Acoustics, Speech and Signal Processing*, vol. 34, no. 5, pp. 1111 – 1123, Oct. 1986.

[44] ——, "Spectral correlation of modulated signals: Part i–analog modulation," *IEEE Trans. Communications*, vol. 35, no. 6, pp. 584 – 594, June 1987.

[45] W. Gardner, W. Brown, and C.-K. Chen, "Spectral correlation of modulated signals: Part ii–digital modulation," *IEEE Trans. Communications*, vol. 35, no. 6, pp. 595 – 601, June 1987.

[46] W. Gardner and L. Franks, "Characterization of cyclostationary random signal processes," *IEEE Trans. Information Theory*, vol. 21, no. 1, pp. 4 – 14, Jan. 1975.

[47] W. Gardner, "Exploitation of spectral redundancy in cyclostationary signals," *IEEE Signal Processing Magazine,*, vol. 8, no. 2, pp. 14 –36, April 1991.

[48] ——, "Cyclic wiener filtering: theory and method," *IEEE Trans. Communications*, vol. 41, no. 1, pp. 151 –163, Jan. 1993.

[49] W. A. Gardner, "Signal interception: a unifying theoretical framework for feature detection," *IEEE Transactions on Communications*, vol. 36, no. 8, pp. 897–906, Aug 1988.

[50] ——, *Statistical Spectral Analysis A Nonprobabalisitic Theory.* Prentice Hall,NJ, 1988.

[51] W. A. Gardner, A. Napolitano, and L. Paura, "Cyclostationarity: Half a century of research," *Signal Processing*, vol. 86, no. 4, pp. 639 – 697, 2006. [Online]. Available: http://www.sciencedirect.com/science/article/pii/S0165168405002409

[52] D. Gesbert, L. Haumonte, H. Bolcskei, R. Krishnamoorthy, and A. Paulraj, "Technologies and performance for non-line-of-sight broadband wireless access networks," *IEEE Communications Magazine*, vol. 40, no. 4, pp. 86–95, Apr 2002.

[53] A. Ghasemi and E. Sousa, "Collaborative spectrum sensing for opportunistic access in fading environments," in *2005 First IEEE Intl. Symposium on New Frontiers in Dynamic Spectrum Access Networks, 2005. DySPAN 2005.*, Nov. 2005, pp. 131 –136.

[54] ——, "Asymptotic performance of collaborative spectrum sensing under correlated log-normal shadowing," *IEEE Communications Letters*, vol. 11, no. 1, pp. 34–36, Jan 2007.

[55] ——, "Spectrum sensing in cognitive radio networks: requirements, challenges and design trade-offs," *IEEE Communications Magazine,*, vol. 46, no. 4, pp. 32 –39, April 2008.

[56] A. Gupta and S. Joshi, "Variable step-size lms algorithm for fractal signals," *IEEE Transactions on Signal Processing*, vol. 56, no. 4, pp. 1411–1420, April 2008.

[57] S. Gurugopinath, C. Murthy, and C. Seelamantula, "Zero-crossings based spectrum sensing under noise uncertainties," in *2014 Twentieth National Conference on Communications (NCC)*, Feb 2014, pp. 1–6.

[58] S. Gurugopinath, C. Murthy, and V. Sharma, "Error exponent analysis of energy-based bayesian spectrum sensing under fading channels," in *2011 IEEE Global Telecommunications Conference (GLOBECOM 2011),*, Dec 2011, pp. 1–5.

[59] S. Haykin, "Cognitive radio: brain-empowered wireless communications," *IEEE Journal on Selected Areas in Communications*, vol. 23, no. 2, pp. 201 – 220, Feb. 2005.

[60] S. Haykin, D. Thomson, and J. Reed, "Spectrum sensing for cognitive radio," *Proceedings of the IEEE*, vol. 97, no. 5, pp. 849 –877, May 2009.

[61] S. Haykin, *Adaptive Filter Theory*. Pearson Education, 2002.

[62] K. Hossain, B. Champagne, and A. Assra, "Cooperative multiband joint detection with correlated spectral occupancy in cognitive radio networks," *IEEE Trans. Signal Processing*, vol. 60, no. 5, pp. 2682 –2687, May 2012.

[63] Y. Huang and X. Huang, "Detection of temporally correlated signals over multipath fading channels," *IEEE Transactions on Wireless Communications*, vol. 12, no. 3, pp. 1290–1299, March 2013.

[64] C.-H. Hwang, G.-L. Lai, and S.-C. Chen, "Spectrum sensing in wideband ofdm cognitive radios," *Signal Processing, IEEE Trans.*, vol. 58, no. 2, pp. 709 –719, Feb. 2010.

[65] D. A. K., A. Garg, and A. Banerjee, "On primary user detection using energy detection technique for cognitive radio," in *2009 National Conference on(Communications (NCC),*, Jan 2009, pp. 1–5.

[66] S. S. Kalamkar and A. Banerjee, "Improved double threshold energy detection for cooperative spectrum sensing in cognitive radio," *Defence Science Journal*, vol. 11, no. 1, pp. 116 –130, quarter 2009.

[67] ——, "On the performance of generalized energy detector under noise uncertainty in cognitive radio," in *2013 National Conference on Communications (NCC),*, Feb 2013, pp. 1–5.

[68] S. M. Kay, *Fundamentals of Statistical Signal Processing, Volume I : Estimation Theory*. Prentice Hall, 1993.

[69] ——, *Fundamentals of Statistical Signal Processing, Volume II : Detection Theory*. Prentice Hall, 1998.

[70] S.-J. Kim and G. Giannakis, "Sequential and cooperative sensing for multi-channel cognitive radios," *IEEE Trans. Signal Processing*, vol. 58, no. 8, pp. 4239 –4253, Aug. 2010.

[71] J.-W. Lee, S.-E. Kim, W.-J. Song, and A. Sayed, "Spatio-temporal diffusion strategies for estimation and detection over networks," *IEEE Transactions on Signal Processing*, vol. 60, no. 8, pp. 4017–4034, Aug 2012.

[72] J.-H. Lee and Y.-T. Lee, "Robust adaptive array beamforming for cyclostationary signals under cycle frequency error," *IEEE Trans. Antennas and Propagation*, vol. 47, no. 2, pp. 233–241, 1999.

[73] J.-H. Lee, Y.-T. Lee, and W.-H. Shih, "Efficient robust adaptive beamforming for cyclostationary signals," *IEEE Trans. Signal Processing*, vol. 48, no. 7, pp. 1893 –1901, Jul. 2000.

[74] H. Li, H. Dai, and C. Li, "Collaborative quickest spectrum sensing via random broadcast in cognitive radio systems," in *IEEE Global Telecommunications Conference, 2009. GLOBECOM 2009.*, 30 2009-dec. 4 2009, pp. 1 –6.

[75] Z. Li, F. Yu, and M. Huang, "A distributed consensus-based cooperative spectrum-sensing scheme in cognitive radios," *IEEE Transactions on Vehicular Technology*, vol. 59, no. 1, pp. 383–393, Jan 2010.

[76] T. J. Lim, R. Zhang, Y. C. Liang, and Y. Zeng, "Glrt-based spectrum sensing for cognitive radio," in *IEEE Global Telecommunications Conference, 2008. IEEE GLOBECOM 2008.*, 30 2008-Dec. 4 2008, pp. 1 –5.

[77] C. Lopes and A. Sayed, "Incremental adaptive strategies over distributed networks," *IEEE Transactions on Signal Processing*, vol. 55, no. 8, pp. 4064–4077, Aug 2007.

[78] ——, "Diffusion least-mean squares over adaptive networks: Formulation and performance analysis," *IEEE Transactions on Signal Processing*, vol. 56, no. 7, pp. 3122–3136, July 2008.

[79] Z. Lu, Y. Ma, P. Cheraghi, and R. Tafazolli, "Novel pilot-assisted spectrum sensing for OFDM systems by exploiting statistical difference between subcarriers," *IEEE Trans. Communications*, vol. 61, no. 4, pp. 1264–1276, 2013.

[80] J. Lunden, S. Kassam, and V. Koivunen, "Robust nonparametric cyclic correlation-based spectrum sensing for cognitive radio," *IEEE Trans. Signal Processing*, vol. 58, no. 1, pp. 38 –52, Jan. 2010.

[81] J. Lunden and V. Koivunen, "Spatial sign and rank cyclic detectors," *IEEE Signal Processing Letters*, vol. 21, no. 5, pp. 595–599, May 2014.

[82] J. Lunden, V. Koivunen, A. Huttunen, and H. Poor, "Collaborative cyclostationary spectrum sensing for cognitive radio systems," *IEEE Trans. Signal Processing*, vol. 57, no. 11, pp. 4182 –4195, Nov. 2009.

[83] J. Ma, G. Zhao, and Y. Li, "Soft combination and detection for cooperative spectrum sensing in cognitive radio networks," *IEEE Trans. Wireless Communications,*, vol. 7, no. 11, pp. 4502 –4507, Nov. 2008.

[84] H. Mahmoud and H. Arslan, "Sidelobe suppression in ofdm-based spectrum sharing systems using adaptive symbol transition," *IEEE Communications Letters*, vol. 12, no. 2, pp. 133 –135, Feb. 2008.

[85] S. Maleki and G. Leus, "Censored truncated sequential spectrum sensing for cognitive radio networks," *IEEE Journal on Selected Areas in Communications,*, vol. 31, no. 3, pp. 364–378, March 2013.

[86] A. Mishra, A. Garg, and A. Banerjee, "Selection based detection method for spectrum sensing for cognitive radio," in *2010 International Conference on Signal Processing and Communications (SPCOM),*, July 2010, pp. 1–5.

[87] I. Mitola, J. and J. Maguire, G.Q., "Cognitive radio: making software radios more personal," *IEEE Personal Communications,*, vol. 6, no. 4, pp. 13 –18, Aug. 1999.

[88] F. Moghimi, A. Nasri, and R. Schober, "Adaptive lp norm spectrum sensing for cognitive radio networks," *IEEE Trans. Communications*, vol. 59, no. 7, pp. 1934 –1945, Jul. 2011.

[89] T. Nadkar, V. Thumar, G. Tej, S. Merchant, and U. Desai, "Distributed power allocation for secondary users in a cognitive radio scenario," *IEEE Transactions on Wireless Communications*, vol. 11, no. 4, pp. 1576–1586, April 2012.

[90] A. Napolitano, "Generalizations of cyclostationarity: A new paradigm for signal processing for mobile communications, radar, and sonar," *IEEE Signal Processing Magazine*, vol. 30, no. 6, pp. 53–63, Nov 2013.

[91] M. Oner and F. Jondral, "Cyclostationarity based air interface recognition for software radio systems," in *IEEE Radio and Wireless Conf., 2004*, Sept. 2004, pp. 263 – 266.

[92] ——, "Cyclostationarity-based methods for the extraction of the channel allocation information in a spectrum pooling system," in *IEEE Radio and Wireless Conf.*, Sept. 2004, pp. 279– 282.

[93] U. Pandya and U. Desai, "A novel algorithm for bluetooth ecg," *IEEE Transactions on Biomedical Engineering*, vol. 59, no. 11, pp. 3148–3154, Nov 2012.

[94] A. Papoulis, *Probability, Random Variables and Stochastic Processes.* Mc Graw Hill, 2002.

[95] A. Patel, B. Tripathi, and A. Jagannatham, "Robust estimator-correlator for spectrum sensing in mimo cr networks with csi uncertainty," *IEEE Wireless Communications Letters*, vol. 3, no. 3, pp. 253–256, June 2014.

[96] A. Paulraj and C. Papadias, "Space-time processing for wireless communications," *IEEE Signal Processing Magazine*, vol. 14, no. 6, pp. 49–83, Nov 1997.

[97] D. B. Percival and A. T. Walden, *Spectral Analysis for Physical Applications*, 1st ed. Cambridge University Press, Jun. 1993. [Online]. Available: http://www.worldcat.org/isbn/9780521435413

[98] S. Prasad and S. Joshi, "A new recursive pseudo least squares algorithm for arma filtering and modeling. i," *IEEE Transactions on Signal Processing*, vol. 40, no. 11, pp. 2766–2774, Nov 1992.

[99] ——, "A new recursive pseudo least squares algorithm for arma filtering and modeling. ii," *IEEE Transactions on Signal Processing*, vol. 40, no. 11, pp. 2775–2783, Nov 1992.

[100] J. G. Proakis, *Digital Communication*. Mc Graw Hill, 2000.

[101] Z. Quan, S. Cui, and A. Sayed, "Optimal linear cooperation for spectrum sensing in cognitive radio networks," *IEEE Journal of Selected Topics in Signal Processing*, vol. 2, no. 1, pp. 28–40, Feb 2008.

[102] Z. Quan, S. Cui, A. Sayed, and H. Poor, "Optimal multiband joint detection for spectrum sensing in cognitive radio networks," *IEEE Trans. Signal Processing*, vol. 57, no. 3, pp. 1128 –1140, Mar. 2009.

[103] E. Rebeiz, P. Urriza, and D. Cabric, "Optimizing wideband cyclostationary spectrum sensing under receiver impairments," *IEEE Trans. Signal Processing*, vol. 61, no. 15, pp. 3931–3943, Aug. 2013.

[104] H. Sadeghi, P. Azmi, and H. Arezumand, "Optimal multi-cycle cyclostationarity-based spectrum sensing for cognitive radio networks," in *19th Iranian Conf. on Electrical Engineering (ICEE), 2011*, May 2011, pp. 1 –6.

[105] H. Saggar, "Cyclostationary spectrum sensing techniques for cognitive radios," Master's thesis, Indian Institute of Technology Roorkee, 2011.

[106] G. Sanjeev, K. Chaythanya, and C. Murthy, in *2010 International Conference on Signal Processing and Communications (SPCOM),*.

[107] I. Schizas, G. Mateos, and G. Giannakis, "Distributed lms for consensus-based in-network adaptive processing," *IEEE Transactions on Signal Processing*, vol. 57, no. 6, pp. 2365–2382, June 2009.

[108] M. Shakir, A. Rao, and M.-S. Alouini, "Generalized mean detector for collaborative spectrum sensing," *IEEE Transactions on Communications*, vol. 61, no. 4, pp. 1242–1253, April 2013.

[109] A. Sharma and C. Murthy, "Group testing-based spectrum hole search for cognitive radios," *IEEE Transactions on Vehicular Technology*, vol. 63, no. 8, pp. 3794–3805, Oct 2014.

[110] G. Sharma, V. Ganwani, U. Desai, and S. Merchant, "Performance analysis of maximum likelihood detection for decode and forward mimo relay channels in rayleigh fading," *IEEE Transactions on Wireless Communications*, vol. 9, no. 9, pp. 2880–2889, September 2010.

[111] S. Sharma, S. Chatzinotas, and B. Ottersten, "Eigenvalue-based sensing and snr estimation for cognitive radio in presence of noise correlation," *IEEE Transactions on Vehicular Technology*, vol. 62, no. 8, pp. 3671–3684, Oct 2013.

[112] J.-C. Shen and E. Alsusa, "Joint cycle frequencies and lags utilization in cyclostationary feature spectrum sensing," *IEEE Transactions on Signal Processing*, vol. 61, no. 21, pp. 5337–5346, Nov 2013.

[113] L. Shen, H. Wang, W. Zhang, and Z. Zhao, "Multiple antennas assisted blind spectrum sensing in cognitive radio channels," *IEEE Communications Letters*, vol. 16, no. 1, pp. 92 –94, Jan. 2012.

[114] A. Singh, M. Bhatnagar, and R. Mallik, "Cooperative spectrum sensing in multiple antenna based cognitive radio network using an improved energy detector," *IEEE Communications Letters,*, vol. 16, no. 1, pp. 64 –67, Jan. 2012.

[115] F.-X. Socheleau, S. Houcke, P. Ciblat, and A. Assa-El-Bey, "Cognitive OFDM system detection using pilot tones second and third-order cyclostationarity," *Signal Processing*, vol. 91, no. 2, pp. 252–268, February 2011. [Online]. Available: http://www.sciencedirect.com/science/article/pii/S0165168410002884

[116] C. Stevenson, G. Chouinard, Z. Lei, W. Hu, S. Shellhammer, and W. Caldwell, "IEEE 802.22: The first cognitive radio wireless regional area network standard," *IEEE Communications Mag.*, vol. 47, no. 1, pp. 130–138, Jan. 2009.

[117] G. Strang, *Linear Algebra and Its Applications*, 4th ed. Cengage Learning, Feb. 2007.

[118] C. Sun, W. Zhang, and K. Letaief, "Cooperative spectrum sensing for cognitive radios under bandwidth constraints," in *IEEE Wireless Communications and Networking Conference, 2007.WCNC 2007.*, Mar. 2007, pp. 1 –5.

[119] H. Sun, A. Nallanathan, J. Jiang, D. Laurenson, C.-X. Wang, and H. Poor, "A novel wideband spectrum sensing system for distributed cognitive radio networks," in *2011 IEEE Global Telecommunications Conference (GLOBECOM 2011)*, Dec 2011, pp. 1–6.

[120] P. Sutton, K. Nolan, and L. Doyle, "Cyclostationary signatures in practical cognitive radio applications," *IEEE J. Selected Areas in Communications*, vol. 26, no. 1, pp. 13–24, Jan. 2008.

[121] R. Tandra, S. Mishra, and A. Sahai, "What is a spectrum hole and what does it take to recognize one?" *Proceedings of the IEEE*, vol. 97, no. 5, pp. 824–848, May 2009.

[122] R. Tandra and A. Sahai, "SNR walls for signal detection," *IEEE J. Selected Topics in Signal Processing*, vol. 2, no. 1, pp. 4–17, Feb. 2008.

[123] A. Tani and R. Fantacci, "A low-complexity cyclostationary-based spectrum sensing for uwb and wimax coexistence with noise uncertainty," *IEEE Trans. Vehicular Technology*, vol. 59, no. 6, pp. 2940 –2950, Jul. 2010.

[124] D. Thomson, "Spectrum estimation and harmonic analysis," *Proceedings of the IEEE*, vol. 70, no. 9, pp. 1055 – 1096, Sept. 1982.

[125] Z. Tian, "Cyclic feature based wideband spectrum sensing using compressive sampling," in *IEEE Intl. Conf. Communications (ICC), 2011*, June 2011, pp. 1 –5.

[126] Z. Tian and G. B. Giannakis, "A wavelet approach to wideband spectrum sensing for cognitive radios," in *1st Intl. Conf. Cognitive Radio Oriented Wireless Networks and Communications, 2006.*, June 2006, pp. 1 –5.

[127] Z. Tian, Y. Tafesse, and B. Sadler, "Cyclic feature detection with sub-nyquist sampling for wideband spectrum sensing," *IEEE Journal of Selected Topics in Signal Processing*, vol. 6, no. 1, pp. 58 –69, Feb. 2012.

[128] J. Tropp and S. Wright, "Computational methods for sparse solution of linear inverse problems," *Proceedings of the IEEE*, vol. 98, no. 6, pp. 948 –958, June 2010.

[129] S.-Y. Tu and A. Sayed, "Diffusion strategies outperform consensus strategies for distributed estimation over adaptive networks," *IEEE Transactions on Signal Processing*, vol. 60, no. 12, pp. 6217–6234, Dec 2012.

[130] V. Turunen, M. Kosunen, M. Vaarakangas, and J. Ryynanen, "Correlation-based detection of ofdm signals in the angular domain," *IEEE Trans. Vehicular Technology*, vol. 61, no. 3, pp. 951 –958, Mar. 2012.

[131] P. Urriza, E. Rebeiz, and D. Cabric, "Multiple antenna cyclostationary spectrum sensing based on the cyclic correlation significance test," *IEEE Transactions on Selected Areas in Communications*, vol. 31, no. 11, pp. 2185–2195, November 2013.

[132] M. Vu and A. Paulraj, "Mimo wireless linear precoding," *IEEE Signal Processing Magazine*, vol. 24, no. 5, pp. 86–105, Sept 2007.

[133] D. Vucic, M. Oradovic, and O. D., "Spectral correlation of ofdm signals related to their plc applications," in *6th Int. Symp. on Power Line Communications (ISPLC '02)*, Mar 2002, pp. 329 –332.

[134] Q. Wu and K. M. Wong, "Blind adaptive beamforming for cyclostationary signals," *IEEE Trans. Signal Processing*, vol. 44, no. 11, pp. 2757 –2767, nov 1996.

[135] O. Yeste Ojeda and J. Grajal, "Adaptive-fresh filters for compensation of cycle-frequency errors," *IEEE Trans. Signal Processing*, vol. 58, no. 1, pp. 1 –10, Jan. 2010.

[136] T. Yucek and H. Arslan, "Spectrum characterization for opportunistic cognitive radio systems," in *IEEE Military Communications Conference, 2006. MILCOM 2006.*, Oct. 2006, pp. 1 –6.

[137] ——, "A survey of spectrum sensing algorithms for cognitive radio applications," *IEEE Communications Surveys and Tutorials*, vol. 11, no. 1, pp. 116 –130, quarter 2009.

[138] A. Zahedi-Ghasabeh, A. Tarighat, and B. Daneshrad, "Spectrum sensing of OFDM waveforms using embedded pilots in the presence of impairments," *IEEE Trans. Vehicular Technology*, vol. 61, no. 3, pp. 1208–1221, Mar. 2012.

[139] F. Zeng, C. Li, and Z. Tian, "Distributed compressive spectrum sensing in cooperative multihop cognitive networks," *IEEE Journal of Selected Topics in Signal Processing*, vol. 5, no. 1, pp. 37 –48, Feb. 2011.

[140] Y. Zeng and Y. chang Liang, "Eigenvalue-based spectrum sensing algorithms for cognitive radio," *IEEE Trans. Communications*, vol. 57, no. 6, pp. 1784 –1793, June 2009.

[141] ——, "Eigenvalue-based spectrum sensing algorithms for cognitive radio," *IEEE Trans. Communications*, vol. 57, no. 6, pp. 1784 –1793, June 2009.

[142] Y. Zeng and Y.-C. Liang, "Maximum-minimum eigenvalue detection for cognitive radio," in *IEEE 18th Intl. Symposium on Personal, Indoor and Mobile Radio Communications, 2007. PIMRC 2007.*, Sept. 2007, pp. 1 –5.

[143] ——, "Spectrum-sensing algorithms for cognitive radio based on statistical covariances," *IEEE Trans. Vehicular Technology*, vol. 58, no. 4, pp. 1804 –1815, May 2009.

[144] Y. Zeng, Y.-C. Liang, and T.-H. Pham, "Spectrum sensing for OFDM signals using pilot induced auto-correlations," *IEEE J. Selected Areas in Communications*, vol. 31, no. 3, pp. 353–363, 2013.

[145] J. Zhang, K. Wong, Q. Jin, and Q. Wu, "A new kind of adaptive frequency shift filter," in *1995 Intl. Conf. Acoustics, Speech, and Signal Processing, 1995. ICASSP-95.,*, vol. 2, May 1995, pp. 913 –916 vol.2.

[146] J. Zhang, K. Wong, Z.-Q. Luo, and P. Ching, "Blind adaptive fresh filtering for signal extraction," *IEEE Transactions on Signal Processing*, vol. 47, no. 5, pp. 1397–1402, May 1999.

[147] W. Zhang, Y. Guo, H. Liu, Y. Chen, Z. Wang, and J. Mitola, "Distributed consensus-based weight design for cooperative spectrum sensing," *IEEE Transactions on Parallel and Distributed Systems*, vol. 26, no. 1, pp. 54–64, Jan 2015.

[148] W. Zhang and K. Letaief, "Cooperative spectrum sensing with transmit and relay diversity in cognitive radio networks - [transaction letters]," *IEEE Transactions on Wireless Communications*, vol. 7, no. 12, pp. 4761–4766, December 2008.

[149] W. Zhang, R. Mallik, and K. Letaief, "Optimization of cooperative spectrum sensing with energy detection in cognitive radio networks," *IEEE Transactions on Wireless Communications*, vol. 8, no. 12, pp. 5761–5766, December 2009.

[150] X. Zhao and A. Sayed, "Performance limits for distributed estimation over lms adaptive networks," *IEEE Transactions on Signal Processing*, vol. 60, no. 10, pp. 5107–5124, Oct 2012.

[151] X. Zhou, J. Ma, G. Li, Y. H. Kwon, and A. Soong, "Probability-based combination for cooperative spectrum sensing," *IEEE Transactions on Communications*, vol. 58, no. 2, pp. 463–466, February 2010.

[152] Q. Zou, S. Zheng, and A. Sayed, "Cooperative sensing via sequential detection," *IEEE Trans. Signal Processing,*, vol. 58, no. 12, pp. 6266 –6283, Dec. 2010.